THE ROLE OF TPL2 IN PREVENTING IMMUNOPATHOLOGY DURING INFLUENZA A VIRUS INFECTION

by

KRISHNA LATHA

(Under the Direction of WENDY T. WATFORD)

ABSTRACT

Tumor progression locus 2 (Tpl2, MAP3K8, COT) is a serine threonine kinase known to regulate inflammation in a variety of infections, cancers, and autoimmune diseases. During infection, Tpl2 responds in a cell type-specific manner by transducing signals downstream of various pathogen recognition receptors initiating induction of pro-inflammatory mediators, which regulate the recruitment of various cell types to the site of infection. Our lab has shown previously that *Tpl2*$^{-/-}$ mice succumb to influenza infection, however the root cause of morbidity and mortality have not yet been identified. The goal of this project is to determine the cellular and molecular mechanisms by which Tpl2 genetic ablation leads to exacerbation of disease during influenza infection. We observed that a heightened immune response rather than impaired viral control was primarily responsible for increased disease severity in *Tpl2*$^{-/-}$ mice. Specifically, over-expression of interferon-β (IFN-β), interferon-γ (IFN-γ) and CCL2 along with increased recruitment of inflammatory monocytes and neutrophils characterized the lungs of influenza-infected *Tpl2*$^{-/-}$ mice at 7 days post infection (dpi). We next examined the effect of Tpl2 ablation on the immune response to influenza in the absence of type I IFN (T1 IFN) signaling using *IFNAR*$^{-/-}$ (Interferon Alpha Receptor 1 knockout) mice to determine

if deregulated T1 IFN response in *Tpl2*$^{-/-}$ mice could be the sole cause of enhanced disease severity. However, the *IFNAR*$^{-/-}$*Tpl2*$^{-/-}$ mice succumbed to influenza infection by 7 dpi, earlier than either *IFNAR*$^{-/-}$ or *Tpl2*$^{-/-}$ mice. The enhanced morbidity and mortality in *IFNAR*$^{-/-}$*Tpl2*$^{-/-}$, was attributed to this switch from excessive monocyte recruitment in *Tpl2*$^{-/-}$ mice to excessive neutrophil recruitment in *IFNAR*$^{-/-}$*Tpl2*$^{-/-}$ mice, accompanied by excessive levels of IL-6, IL-1β, IFN-γ, IFN-λ and CXCL1. Further histological and clinical examination of *Tpl2*$^{-/-}$ mice revealed pulmonary edema and alveolar damage similar to the pathology seen in hospitalized influenza patients who develop Acute Respiratory Distress Syndrome (ARDS). Collectively, these studies demonstrate the importance of Tpl2 in preventing respiratory exacerbations caused by influenza infections by regulating the IFN response and the influx of inflammatory cells that induce pulmonary damage, which progresses to ARDS-like disease.

INDEX WORDS: TPL2, Influenza, Hypercytokinemia, Interferons, ARDS

THE ROLE OF TPL2 IN PREVENTING IMMUNOPATHOLOGY DURING INFLUENZA A VIRUS INFECTION

by

KRISHNA LATHA

Integrated MSc.(with BSc.), Savitribai Phule Pune University, India, 2015

A Dissertation Submitted to the Graduate Faculty of The University of Georgia in Partial Fulfillment of the Requirements for the Degree

DOCTOR OF PHILOSOPHY

ATHENS, GEORGIA

2021

TO IDENTIFY THE ROLE OF TPL2 IN PREVENTING IMMUNOPATHOLOGY DURING INFLUENZA INFECTIONS

by

KRISHNA LATHA

Major Professor: Wendy Watford
Committee: Biao He
Kimberly Klonowski
Karen Norris
Balazs Rada

Electronic Version Approved:

Ron Walcott
Vice Provost for Graduate Education and Dean of the Graduate School
The University of Georgia
December 2021

With love and gratitude

To my parents

For persevering through the hard times and celebrating the good ones,

now and always

ACKNOWLEDGEMENTS

My sincerest thanks to Dr. Wendy Watford for accepting me in her lab and also for providing constant support and training. Her guidance was invaluable to my growth as a scientist. I am also thankful to my doctoral committee members, Drs. Balazs Rada, Biao He, Kim Klonowski and Karen Norris for their time, support and advice throughout my PhD program.

I would like to thank the members of Watford lab - Kara Wyatt, Chris Slade, Denise Fahey, Jocelyn Sotolongo-Gomez for their help with the science and being great listeners. I would like to thank Katelyn Jamison, Yesha Patel and Sanjana Rao for letting me experience mentorship while contributing so much towards this thesis. Special thanks to Kaori Sakamoto and Denise Fahey for all their help with experiments. I would also like to express my gratitude to Jamie Barber, Julie Nelson, Lynette Rowe, Safije Bakalli, Julia Flores-Rivera as well as staff at College of Veterinary Medicine Central Animal Facility, Coverdell Rodent Vivarium and UGA Diagnostic lab, who have aided my dissertation work on multiple occasions.

An important part of my life has been the support for my friends here, who never let me feel too far from home. First and foremost, I would like to thank Kimberly Oliva for all her help especially when I was struggling with animal work, being my first friend here and suffering together through tough coursework. I am very grateful to Alicer Andrews, Nicole Williams, Mariel Pfeifer, Carly Duffy, Chelsea Gunderson, Ben Hoffman, Edwin Pierre Louis and Rachel LoPilato for being my support and motivation through the ups & downs of this journey.

As a part of the Graduate Research Assistants Diversifying STEM, I also met and worked with wonderful folks like Yohana Bernadette-White, Shibu Xu, Andrea Sweigart, Judy Milton, Kat Milligan-Myrhe, Ana Porras and so many more who inspired me to face the obstacles in my choices of this career path. Also thanks to UGA, I got to experience teaching both college and school kids, which gave me the strength to hang on during the rough times of troubleshooting research, with a special thanks to Zoe Morris for showing me that teaching is actually fun if done with heart. Getting to experience events like STEMzone, 3 Minute Thesis, Outbreak Simulation, being on the Eboard of Experiential Profession Development, Research communication, and so much more, was a privilege that I am grateful to UGA for and all the involved parties. It has made this graduate experience that much more endearing and enriching.

Lastly, but in no way lesser than the above, I am grateful to have in my life supportive family and friends from India. They have been the reason I was able to recharge and face all my obstacles so far away from home. It was their belief in me that got me to even attempt a PhD and persevere through it.

TABLE OF CONTENTS

LIST OF FIGURES

CHAPTER 1

INTRODUCTION

INFLUENZA VIRUS AND THE INFECTION CYCLE

Influenza virus belongs to the Orthomyxoviridae family of viruses and has an enveloped genome of negative sense single-stranded RNA[1]. While there are currently 7 known genera in this family with 9 species of virus, only viruses from A and B genera infect humans[2]. The genome for the genera A and B is comprised of 8 segments encoding 11 proteins. While Influenza B virus also causes seasonal infections in humans and is included in annual vaccines[3], this review will focus on the Influenza A Viruses (IAV).

Structurally, the virus has in the innermost a nucleocapsid comprised of the RNA genome coated with the Nucleoprotein (NP) and the heterotrimeric RNA-directed RNA polymerase composed of Polymerase Basic protein 1 (PB1), Polymerase Basic protein 2 (PB2) and Polymerase Acidic protein (PA)[4,5]. This capsid along with nuclear export protein (NEP), is then encapsulated by the matrix protein (M1)[6,7]. Finally, the outermost layer is made of glycoproteins Hemagglutinin (HA) and Neuraminidase (NA) embedded into the host derived lipid bilayer envelope, along with Matrix (M2) Ion Channels[1,8].

HA interaction with the Salic acid on the host cell allows for attachment of the virion and further receptor mediated endocytosis for the virus to enter the cell[8,9] (Figure 1.1). While the endosome continues towards the nucleus, the acidic environment of the endosome induces opening of the M2 channels and dissociation of M1 with the nucleocapsid[10,11]. NEP allows for the capsid to translocate into the host's nucleus where genome replication and transcription occur using the host machinery[7,12]. Initially the mRNA (+strand) is made from the viral RNA template to transcribe more viral proteins. Meanwhile, further viral RNA templates are synthesized complementary to the mRNA strand, to be the genetic material for progeny viruses[13,14]. Nuclear export signals are utilized to facilitate translocation from the nucleus into the cytoplasm for packaging, assembly and the progeny virions bud the surface of the host cell, within a portion of the lipid bilayer[14].

SEASONAL AND PANDEMIC INFLUENZA VIRUSES

IAV are further classified into subtypes based on the combination of HA and NA proteins on their surface. There are 18 known HA subtypes and 11 known NA subtypes, of which H1N1 (ie. HA 1 protein and NA 1 protein) and H3N2 are the most common seasonal variants in humans[15].

Bar two subtypes, most of the subtypes are found infecting bird species[16,17]. As birds are the natural reservoir of influenza A viruses, they are the basis of classifying the infectivity of the avian strains that can have economic or health impact on humans. Most viruses only cause disease in their primary avian host, either wild or domesticated poultry, and are called Low Pathogenic Avian Influenza viruses (LPAI)[18,19]. However, when circulating within poultry certain LPAI can mutate and become more infectious and resurface as Highly Pathogenic Avian Influenza viruses (HPAI) that are capable of killing 90-100% of the flock and also cause epidemics in livestock that necessitates trade restrictions[20,21]. Avian viruses do not easily infect humans, but it can occur occasionally when the virus gets close to the mucosal surface in the human hosts mouth, eyes or nose. Virus transmission can occur from one infected individual to another susceptible person through aerosols or respiratory fomites[22,23]. With LPAI, the infections usually do not transmit from one infected person to another, with only 1 human case known so far[24]. When we consider influenza strains that have caused major health disasters for humans classified as pandemics, there have been 4 namely, 1918 H1N1 avian based influenza pandemic, two pandemics in 1957 and 1968 that were caused by avian based influenza strains of H3N2 lineage and finally, the 2009 pandemic caused a new H1N1 virus from swine origin called (H1N1) pdm09[25]. Comparatively, the HPAI strain of H5N1 has been involved in 850 cases with 50-60% case fatality, mostly due to the strain lacking the ability for human-human transmission[3], suggesting that not all HPAI strains have the potential to affect human health on a pandemic scale. However seasonally we have various stains (not necessarily avian in origin) that significantly impact human health.

Influenza disease worldwide results in 3 to 5 million cases of severe illness, and about 290,000 to 650,000 respiratory deaths annually according to WHO estimates[26]. While immune memory of infections and vaccinations do help to combat the seasonal infection, there are several factors that hamper this protection. Vaccinations are made based on predictions of the strains expected to predominate in a season based on antigenic shift and drift. Antigenic drift refers to the events where point mutations are introduced in the influenza genome (similar to general virus evolution)[27]. However, added variation is also introduced due to antigenic shift. Antigenic shift is the byproduct of having extensive and overlapping host reservoirs, wherein co-infection of a single host's cells with two different viruses allows for rearrangement/exchange of entire gene segments[27].

CLINICAL PRESENTATION OF INFLUENZA INFECTION

The clinical presentation of seasonal influenza infections can vary from asymptomatic to severe disease leading to death. Viral titers and clinical symptoms usually peak 2-3 days post infection; virus shedding returns to baseline by 6-7 days post infection (dpi), whereas clinical symptoms typically subside by 8-9 dpi[28]. Seasonal influenza is potentially more detrimental for individuals below 6 years of age and above 60 years, as well as for people with other risk factors like smoking, genetic predisposition to interferonopathies, heart disease, chronic pulmonary disease, pregnancy, immune response alterations due to sex steroid treatment and obesity[29–34]. The most common symptoms associated with influenza include fever, headache, myalgia, cough, and sore throat[29]. While specific testing for influenza antigens is required to start antiviral treatment for drugs like amantadine (Symmetrel), rimantadine (Flumadine), zanamivir, and oseltamivir (Tamiflu). Treatment with amantadine and rimantadine is most effective when initiated within 48 hours of symptom development[35]. However, in cases of severe influenza, the disease progresses rapidly to hospitalization, pneumonia, acute respiratory distress and death, especially in people with comorbidities[36].

In severe cases, it can affect the respiratory gas exchange in the lung due to obstruction of the airways, loss of the alveolar structure, epithelial damage due to virus mediated cytopathic effects or excessive inflammation leading to destruction of the lung structure or degradation of the extra cellular matrix[37,38]. 30-40% of the patients hospitalized for influenza are susceptible to bacterial pneumonia and that has a higher likelihood to lead to Acute Respiratory Distress Syndrome (ARDS)[37]. Hence it is not surprising that the most common viral causative agent for ARDS is influenza A[39]. While diagnosis of ARDS in its early stages is hard, detection of it early enough allows for treatment with high flow oxygen while preventing exacerbation of the pulmonary edema (fluid management), pharmacology and antiviral therapy[40,41].

Thus, we see that influenza infection, even on a seasonal basis and involving strains that are not classified HPAI, are able to induce severe clinical cases. This maybe in part due to co-morbidity, secondary infection or a multitude of factors that can cause a condition like ARDS and require rigorous treatment on time to prevent death. Understanding the immune response to influenza is one of the ways to predict, prevent, diagnose, and treat such a disease progression.

THE KINETICS OF THE IMMUNE RESPONSE TO INFLUENZA

Influenza is a virus that primarily colonizes the upper respiratory track, before making its way down to the lung, wherein the epithelium is the primary target of replication. There are also other lung resident cells that capable of being infected like the alveolar macrophages[42]. These resident cells are equipped with the mechanisms to induce pro-inflammatory cytokines and chemokines that allow for recognition of the infection site and anti-viral responses that control the infection[43,44]. Dendritic cells, inflammatory monocytes and neutrophils are cells of the myeloid origin that are resident or recruited to the site of infection in the earlier stages of infection[45,46]. They try to control the infection further, limit the viral spread and prime the cells that are involved in ultimate stages of infection. Natural killer cells, T cell and B cells are prominently recruited in the later stages of infection and are specially equipped to clear out the virus from the lungs of the mice[47,48]. Along with clearance of virus, the lungs also initiate mechanisms that repair the damage to return the system to homeostasis. This includes myofibroblasts replacing the damaged epithelium, restructuring of the vasculature and other factors that allow for resolution of the damage[49,50]. While a well-balanced and timed immune response is critical towards resolving the infection, issues at any step of this process would lead to lung damage due to uncontrolled virus induced damage, cytokine storm leading to excessive inflammation induced damage or delayed inflammation control leading to issues during repair/rebuilding of the lungs (Figure 1.2). This process is discussed in detail in the subsequent sections in order to shed light on all aspects that contribute to a finely tuned and effective immune response to influenza.

PRIMARY INFECTION AND SENSING OF INFLUENZA

Pulmonary epithelial cells are the primary target cell of influenza because the outer NA protein recognizes Salic acid (SA) residues abundant on the epithelium. Influenza viruses have two common cellular receptors which differ in their attachment to galactose: SA α-2,3 galactose (SAα-2,3-Gal) and SA α-2,6 galactose (SAα-2,6-Gal)[48]. Human influenza viruses prefer SA α-2,6-Gal residues found on the upper respiratory tract of humans, whereas avian and swine influenza viruses prefer SA α-2,3-Gal residues are found in birds, pigs and even the lower respiratory tract of humans. This explains how HPAI viruses of avian or swine origin can cause human pandemics. Human viruses (like H1N1,H3N2) are therefore more likely to cause tracheobronchitis, whereas the avian viruses (like H5N1) that are able to infect the lower respiratory tract of humans instead cause severe pneumonia and alveolar damage[51].

Another major target for infection, apart from the varied epithelial cells, are alveolar macrophages (AM). AM are resident lung cells monitor the homeostasis in the lung. They are derived from yolk monocytes, differentiate and repopulate by self-renewal throughout the lifetime (except in cases of infection induced severe depletion, wherein renewal is dependent on the bone marrow derived monocytes)[52,53]. While these macrophages can become infected with influenza virus, it was previously believed that the virus was unable to propagate from the infection[54]. However, recent studies have demonstrated that certain IAV strains, particularly those expressing HA5, are able to replicate fully in macrophages[55]. The primary function of AM is phagocytosis. They also secrete cytokines like IL-6, TNF, MCP-1, RANTES, and TGF-β, however they produce less pro-inflammatory cytokines in response to infection compared with peripheral blood-derived macrophages and are thought to serve a tolerogenic function[56,57]. In addition, they are vital for promoting tissue repair in response to infection-induced inflammation and express suppressors or cytokine signaling proteins, SOCS1 and SOCS3, to silence transcription of inflammatory mediators, particularly the interferons (IFN). Other than the resident macrophage population in the lung that are exposed to the influenza infection there are lesser known and understood population of interstitial macrophages as well. They generally express MHCII or CXCR3, are more involved in antigen presentation, expression of IL10 and have anti-fibrotic activities[58]. While interstitial macrophages are functional in response to bacterial stimulation, so far influenza infection is not known to stimulate them[59].

Pathogen associated Molecular patterns are parts of the virus (or any microbial intrusion) that the infected host cells can recognize and then elicit an immune response against. For RNA viruses like influenza, the primary component to be recognized is the RNA of the virus either in its double stranded form; or single stranded RNA with the presence of 5′-triphosphate (5′ppp) or a 5′-diphosphate (5′pp) group at various stages of its life cycle (Figure 1.1). On entry of the virus via endosome mediated endocytosis, both the double-stranded RNA viral replication intermediates (if present) and single-stranded viral genomic RNA are recognized within endosomes by TLR3[60,61] and TLR7[62,63], respectively. TLR7-mediated recognition of viral RNA is believed to be most prominent in the plasmacytoid dendritic cells (pDC) to induce interferon production[64]. Negative-stranded viruses have a short dsRNA duplex formed due to complementary ends of the viral genome, a structure like a panhandle. This structure serves as the viral promoter region, but is also most widely recognized by the Retinoic acid-inducible gene I (RIG-I) receptor[65]. Additionally, RIG-I is able to recognize the presence of 5′-triphosphate (5′ppp) or a 5′-diphosphate (5′pp) group of the viral genomic RNA, while it is being assembled into a progeny virion in the cytoplasm[66].However, compared to other RIG-I-Like receptors(RLRs), RIG-I is better at recognizing influenza that MDA-5, even though the both recognize dsRNA, as MDA-5 requires the duplex form of the dsRNA present in the pathogen to sense it[67,68]. The influenza NS1 also has evolved to prevent the activation by RIG-I through translational modifications like interfering with the ubiquitination[69], On activation, the PRRs are able to induce interferon and pro-inflammatory mediator expression[70].

The activation of the inflammasome complex is another major antiviral response against influenza especially by sensing of the PAMPs. The NLRP3 inflammasome complex consists of a sensor (NLRP3), an adaptor (ASC; also known as PYCARD) and an effector (caspase 1), of which all are involved in the sensing of influenza. On activation of NLRP3 (NOD-, LRR- and pyrin domain-containing protein 3) the pyrin domain interacts homotypically with the pyrin domain of the ASC and activates it. The ASC then interacts with the CARD domains of pro-caspase-1, then this allows for cleavage and activation of caspase-1. Meanwhile, the influenza infection induces the expression of pro-IL-1β and pro-IL-18 via activation of the NFκB pathway. These forms are then cleaved into mature IL-1β and IL-18 cytokines by the caspase-1. NLRP3 has not been shown to be directly activated by influenza viral RNA, but it is has been shown to be activated by the viral channel M2[71]. More prominently, it is believed that activation of the TLR/RIG-I by influenza allows for caspase-1 activation, thereby allowing for further activation of IL-1β and IL-18[72–74]. Especially in epithelial cells, sensing of the IAV nucleoprotein by myxoma resistance protein 1 (MxA) interacts with the ASC to trigger activation of the inflammasome[75]. Interferon-inducible protein Z-DNA binding protein 1 (ZBP1) senses the influenza NP and PB1 proteins and triggers the inflammasome, by activation of caspase 8[76]. Even without NLRP3 involvement, activation of Caspase-1 in adaptive T and B cells is able to activate the inflammasome[73]. However activation of the inflammasome in the later stages of infection, along with excessive cytokine expression, leads to increased damage in the lungs and mortality of the mice in question[77]. It was also interesting to note that the Influenza NS1 protein is able to restrict the expression of IFN, IL-1β and prevent inflammasome activation[73,78].

In this manner, both infected cellular targets (epithelial and alveolar macrophages) are able to express cytokines and present the virus to other immune cells for their activation. While the alveolar epithelial cells produce CXCL10(IP10), CCL5(RANTES), IFNβ and IL6 on infection with influenza virus, infection with HPAI leads to higher level of cytokine induction than other LPAI[79,80]. In studies of involving infection of human and mouse macrophages, expression cytokines including IFNβ/α IL-1α, IL-1β, IL-6, TNF-α, CXCL8, CCL2 (MCP-1), CCL3 (MIP-1α), CCL4 (MIP1-β), CXCL9 and CXCL10 have been observed[43,44,81–83].

In addition to activation of the other immune cells, the communication between the epithelium and alveolar macrophages themselves have been under scrutiny for their contribution in mitigating the influenza infection. The paracrine interaction between these cells, via the IAV induced- epithelial T1IFNs was found to prevent edema clearance due to reduction of the Na, K-ATPase, leading to ARDS[84]. However clinical trials of cytokine treatment/blocking did not yield the expected results, bringing other types of extra-cellular communication via extracellular vesicles to the forefront[85]. Recent studies have shown, a type of extracellular vesicle formed by budding of the plasma membrane called Microvesicles (MVs), are prominent in BALF post induction of hypoxia[86,87]. These MVs are produced mostly by the epithelial cells and are able to activate the alveolar macrophages, to regulate further inflammatory responses leading to lung injury. Additionally during LPS induced lung injury, MVs containing TNF produced by alveolar macrophages could induce ICAM-1 and pro-inflammatory cytokine expression from epithelial cells[88]. Thus the role of MVs facilitating epithelial- alveolar macrophage interactions in other lung injury models could also be considered for its role in influenza induced lung damage/ARDS.

CYTOKINE INDUCTION

The most predominant cytokines to be discussed in the context of a viral infection are the interferons (IFNs), which were so named due to their ability to 'interfere' with viral replication. There are 3 major classes of interferons, classified based on function, structural homology and receptor chain usage: Type I, II and III interferons[89].

Type I Interferons (T1 IFN), including a single IFNβ protein and 13 IFNα proteins, are the primary cytokines released post influenza infection[89,90]. T1 IFNs are induced by recognition of the RNA component of the virus by the RIG I receptors[91], which leads to activation of TANK-binding kinase 1 (TBK1). TBK1 then activates IFN-regulatory factor 3 (IRF3) or TGFβ-activated kinase 1 (TAK1) to activate NFκB[89,90]. These transcription factors then translocate to the nucleus to induce the primary interferons IFNβ and IFNα4. Once secreted, they bind to the cell surface Interferon Alpha Receptor (IFNAR) comprised of two receptor chains, IFNAR1 and IFNAR2[90]. Ligand binding results in a conformational change in the cytoplasmic tails of the receptor chains that leads to phosphorylation of the Janus kinase 1 and 2 (JAK1 and JAK2) proteins, that in turn phosphorylate and activated the signal transducers and activators of transcription 1 and 2 (STAT1 and STAT2)[89,92]. STAT1 and STAT2 in complex with along with IRF9 forms the Interferon Stimulated Gene Factor 3 (ISGF3) complex. This complex translocates to the nucleus where it stimulates the expression of the transcription factor IRF7, which is required for expression of all other subtypes of IFNα (except IFNα4)[93]. T1IFNs further induce other Interferon Stimulated Genes (ISGs) that collectively mediate an anti-viral response. These ISGs can mediate a variety of the functions. For example, IFITM3 prevents viral egress by altering endosomal pH[94]; MxA activates the NLPR3 inflammasome by sensing viral proteins[75].; OasL mimics polyubiquitination to enhance the RIG-I recognition of viral RNA[95,96]. and ISG15 is involved in the prevention of systemic inflammatory cytokine response[97]. Along with TNFα, IFNβ is able to stimulate the epithelial cells to secrete higher levels of CCL2, CCL5, CXCL8 and CXCL10 as well as stimulate the IRF and NFκB signaling pathway further[81,98]. Prominent among these is the T1 IFN induction of chemokine Monocyte Chemoattractant Protein 1 (MCP1 or CCL2) that, as its name suggests, is responsible for the recruitment of monocytes to the site of infection[99–101].

Interferon Lambdas or the T3 IFNs comprise four subtypes in humans, IFNλ1-4, that signal from a heterodimeric receptor distinct from the T1 and T2 IFNs [102]. The IFNλR has two subunits: the α-subunit (IL-28RA) and the β-subunit (IL-10RB)[103]. IFN-λs are expressed in the early stages of influenza infection[91]. Although they were discovered in 2003, it has been difficult to define unique functions for IFN-λ that are distinct from the T1 IFNs, as they have overlapping functions with largely redundant transcriptional signatures[104,105]. However, one key difference is that IFN-λ is not as inflammatory as the T1 IFNs[106], potentially due to restricted cellular expression[107–109]. Along with T1 IFNs, IFNλ has been shown to be involved in viral control, especially in reducing the spread of virus from upper respiratory system to the lungs and transmission to a naïve host[110,111]. One of the reasons it is hard to delineate the T1IFN independent function of IFN-λ, is believed to be due to the restricted IFN-λ receptor expression on the epithelial cells, neutrophils and dendritic cells[107–109]. It was recently shown the IFN-λ expression allowed for better viral control from both epithelium and neutrophils, moreover that IFN-λ was able to induce the antiviral response of neutrophils better than T1IFN during influenza infection[109]. It is able to promote the migration and function of the DCs that helps prime the T cells, thereby even allowing for heterosubtypic immunity development, or immunity of host to another subtype of the viral strain that infected them initially[107].

Interferon gamma (or Type II Interferon) is also induced in a manner similar to that of the T1 IFNS, but with heterodimerization of the IFNGR (Interferon Gamma Receptors) to induce the JAK-STAT pathway and subsequent gene expression[112]. IFN-γ is produced first by NK cells and then later by T cells during influenza infection[91]. Infection in the absence of IFN-γ leads to higher influx of neutrophils; however other responses such as induction of cytokines like IL-1β, TNF, IL-6, chemokines like CCL2, CXCL1, CXCL10, recruitment of monocytes and T cell-mediated inflammation was dependent on virus strain and dose in *Ifng*$^{-/}$ mice[-99,113,114]. Additionally, treatment with IFN-γ in the early stages of influenza infection protected mice from lethal infection by allowing for higher proliferation of NK cells, and prevented exacerbation of T cell recruitment into the lungs in the later stages of infection[115]. Thus, all interferons have protective functions against influenza infection when induced in a certain balance, however they do not function solely by themselves and are expressed in tandem with other proinflammatory cytokines to work in a cohesive manner.

IL-1β, IL-6 and TNF are other pro-inflammatory cytokines upregulated early during infection. Notably, IL-1β given intraperitonially reproduced the same weight loss and pathogenesis as the infection, itself, suggesting a prominent role for IL-1β in pathogenesis associated with influenza[116]. However, infection of *IL-1R*$^{-/-}$ mice paradoxically showed that the absence of IL-1β responsiveness reduced survival in influenza-infected mice due to reduced recruitment of neutrophils from 3-7 dpi; with reduced CD4 T cells, CD8 T cells and IgM antibodies 7 to 10 dpi[117]. Interestingly when considering the source of cytokines like IL-1β, it was found that endothelial as well as epithelial cells on infection with H1N1 induced higher levels of IL-1β, IL6, TNF, IL-18 and CCL5[118]. Collectively, these data demonstrate that a balanced IL-1β response is required for host protection upon influenza infection, as either too much or too little IL-1β signaling is detrimental.

IL-6 is a marker for severe infection which is noted for higher levels in lung and serum during infection with pandemic strain H1N1[119]. *IL-6*$^{-/-}$ mice showed increased susceptibility, more weight loss, higher IFNα and TNFα expression, less monocyte recruitment to the lungs, and increased apoptosis of the lung epithelium on influenza infection[120,121]. Thus, IL-6 activity during infection might be allowing for reduced fibroblast accumulation, epithelial damage and macrophage recruitment for virus phagocytosis[120]. IL-6 causes weight loss via muscle destruction on infection, and it acts via the STAT3-Foxp3-atrogin1 pathway[122]. Additionally, it was also found that influenza induces expression of the STAT3 suppressor SOCS3, thereby repressing STAT3 and IL-6 signaling. Moreover, infection of SOCS3-deficient mice led to attenuated lung injury, better survival and lower viral load, showing the critical role that the IL6-STAT3-SOCS3 axis plays in influenza infections[123].

CELLULAR RESPONSES TO VIRAL INFECTION

Neutrophils are often the first responders at any site of infection/ inflammation. They are recruited from the blood stream into the tissue by a particular sequence of events involving rolling, arrest, adhesion strengthening, crawling through the intraluminal spaces, protrusion through the endothelial junctions and finally interstitial migration to the destination[124]. Once they reach the site of inflammation, they affect change by phagocytosis, degranulation, reactive oxygen species (ROS) and Neutrophil Extracelluar traps (NETs)[125–127]. Neutrophils are not necessary for protection against mild influenza infections. However lesser neutrophil recruitment than required to mitigate an infection, can have detrimental consequences leading to severe infections[128]. On the other hand,excessive recruitment and activation of neutrophils can also cause tissue damage by release of cytokines, proteases and other factors from their granules[129,130].

Monocytes are the second innate responders to be recruited post an infection from the peripheral blood phagocyte subsets[131]. Functional subsets of monocytes can be differentiated based on their expression of Ly6C in mice. Ly6C^{hi} monocytes are more antimicrobial in function[132], express higher levels of CCR2[133] and are recruited to the inflammatory tissues based on the CCL2 expression along with other factors[134,135]. In contrast, Ly6C low monocytes are patrolling monocytes that provide immune surveillance to the tissues[136]. In infections involving Highly pathogenic influenza viruses or infections of juvenile mice, it has been observed that excessive recruitment of inflammatory monocytes is due to overproduction of the chemokine MCP-1 (CCL2) which is detrimental to the mice, leading to mortality[101,137]. Additionally, it has been shown using *IFNAR*$^{-/-}$ mice and in other studies, that the MCP-1 dependent recruitment of monocytes is due to T1 IFN signalling[100,101]. When considering the factors allow for monocytes to mediate pathology/damage, Nitric Oxide and TNF Receptor Apoptosis Inducing Ligand have been reported to be active in influenza and related bacterial co-infections[101,138].

Dendritic cells are cells that specialize in processing and presenting antigens to the immune cells that predominate the adaptive arm of the immune response, the T cells[139,140]. The CD103+DCs are able to present the antigen on MHC I receptor to the T cells in a process called as cross presentation[141,142]. They are able to prime the T cells at the mucosal sites of infection and also maintain a steady state stimulation of T cells in secondary lymphoid organs like spleen and mediastinal lymph nodes[143,144] A subset of the DCs, that are a relatively smaller population are called Plasmacytotid DCs (pDCs). They are the major producers of IFNα, found mainly in blood and secondary lymphoid tissues, but are recruited to the sites of infection within hours of infection[92]. Myeloid DCs are susceptible to infection but pDCs are not. However infection reduces the ability of DCs to cross present to T cells[145]. PDCs are not as efficient at antigen presentation unlike the conventional dendritic cells for T cells, however they are better at priming B cells[142,146,147].

Natural Killer cells are mediators of innate immunity that have natural cytotoxicity, produce cytokines and prime the T cell response[148] as their primary functions. Their recruitment is dependent on the expression of the ligands for CXCR3 and CCR5 in the lung, along with viral dose[149]. Moreover the NK cell cytotoxicity and IFN-γ production directly correlates with the cytotoxicity of T lymphocytes[148]. NK cell receptor NKp46 can recognize healthy cells by their expression of the MHC I marker[150]. Therefore, when influenza downregulates the host cell MHC-I expression toevade the CD8T cell mediated killing[151], this makes the infected cells more susceptible to recognition by NK cells. To mitigate this, Influenza tries to overexpress MHC I on epithelial cells[152], however NKp46 is also able to recognize the HA virus protein on an infected cell, which then activates the NK cell cytotoxicity and also induces cytokine production[153,154].

B cells are the primary antibody producers in the body. In the initial stages of infection, follicular B cells from the mediastinal lymph nodes are activated in an interferon dependent manner to produce antibodies against influenza[155]. At this stage the antibody secreted is mostly IgM or membrane bound. After this, the further development of antigen specific B cells can be via CD4T cell help in germinal centers of secondary lymphoid organs, or without CD4T cell help into extrafollicular plasmablasts[156]. However the extrafollicular plasmablasts are likely to last only 3-5 days and more prominent in the innate response[157,158]. On the other hand the geminal center B cells are more likely to last longer with high affinity antibodies and develop into circulating memory B cells[159]. The quality of the antibodies is much better when they come from the germinal center B cells because they have undergone somatic hypermutation. They are functionally more tailored to the virus infection because of the isotype switching that also occurs in the T-dependent responses[160]. Of the types of antibodies generated the major antigens focused are against HA, NA and integral proteins like M2 that are exposed on the external surface of the virus. The HA neutralizing antibodies generated naturally are focused on the head region that is the most exposed and most variable (due to antigenic drift)[161,162], than stalk region that evolves much more slowly (due to inaccessibility)[163]; thus current vaccine efforts are trying to focus on generating more antibodies focusing the stalk as it more conserved across subtypes and slower to mutate[163,164]. Meanwhile, the antibodies to NA are protective as they prevent virus egress but produced in lower amounts than those against HA[165]; M2 antibodies, while attractive target due to the conservation of epitopes, are also not abundant potentially due to low level of protein expression[166–168] and the magnitude/effectivity of antibodies against internal proteins are still an ongoing examination [169–171].

T cells are critical for influenza control because of their ability to enhance humoral immunity and to destroy infected cells[172]. Of the alpha beta T cells are of two major subsets namely CD4 and CD8T cells. Antigen specific CD8 T cells recognize infected cells by the MHC-1 antigen presentation on their surface[173–175], lyse infected cells by releasing their granular content (perforin/granzyme)[176], and also express TNFα, FASL, TRAIL to induce death in the recipient infected cell[177–179] There are various subsets of CD4 T cells based on their primary cytokine response in retaliation to an infection based on the pathogen type. TH1 CD4 T cells are predominantly producers of pro-inflammatory cytokines like IFN-γ, IL-12 that are involved in the influenza response[180,181]. These cells are also responsible for helping the B cells develop antibodies in response. Influenza specific CD4 T cells and CD8 T cells that are long lived in the system as memory cells also require IL-6 for their recall. IL-6 is helpful here as it is able to suppress the virus specific Treg cells[182](another CD4T cell subset, that is more anti-inflammatory in nature) that would otherwise hamper the function of the memory CD8T (Th1) cells. Additionally IL6 is also required for the development of heterosubtypic immunity of CD8 T cells, wherein the cells are able to protect against a different subsequent viral subtype infection[121].

Furthermore, after successfully recovering from one viral infection, the T and B cells recall the insult and such memory cells are present as a small population in circulation (and tissue site) to expand once the same or similar virus infects again[42].

LUNG REPAIR POST VIRAL CLEARANCE

After the damage of the influenza infection, the membranes sustain heavy damage and require fast repair of the epithelium-capillary interface to allow for reestablishment of the gaseous exchange interface in the lung. The process of repair involves spreading of the neighboring epithelial cells to cover the destructed area and then migration, proliferation and transformation of the progenitor cells to replace the lost epithelium[183–185]. Post infection the tissue repair is assisted by IL1β and TNFα support the proliferation of the remaining Type II epithelial cells that can then contribute to the alveolar regeneration[186]. TGFβ is another growth factor secreted by epithelial cells, macrophages and fibroblasts during the repair phase post the infection induced damage is resolved. TGFβ is associated with lung injury and ARDS development (with higher expression in the BALF of ARDS patients)[187,188] through the formation of edema and over-activation of the procollagen-1[120]. Other cytokines with a decisive role in the repair are IL22 and IL33. Il22 is required for prevention from secondary bacterial infection and activation of the anti-apoptotic proteins in the pulmonary epithelium[189–191]. IL-33 expression by the epithelium, alveolar macrophages or innate lymphoid cells allows for a tightly regulated pro-fibrotic phase that rebuilds the matrix of the epithelium-endothelium via induction of factors like amphiregulin[192–194]. Other such growth factors secreted by the macrophages, innate lymphoid cells and fibroblasts are also upregulated in the process of tissue repair, thereby inducing fibrosis and higher deposition of the extracellular matrix to repair the lung[194–197]. Interestingly, it was recently found that expression of certain interferons like IFN-λ during the late stages of influenza infection prevented epithelium repair by activation of apoptosis inducing p53 that then prevented epithelial cell proliferation for repair[198].

IMMUNOMODULATION BY TUMOR PROGRESSION LOCUS 2

Tumor Progression Locus 2 (Tpl2) is a serine-threonine kinase that of the MAP kinase family, also known as MAP3K8 and Cancer Osaka Thyroid (*Cot*)[199]. TPL2 is expressed in multiple organs like the spleen, thymus, lung, endometrium, liver, intestine; as outlined with various disease models of cancer or inflammation [200–203]. The TPL2 protein is expressed at steady state in two forms, both containing the kinase domain[204]. The truncated Tpl2 protein is proteosomally degraded from the full length protein at (aa 435-457) and at steady state the truncated form is expressed at 2.6 folds higher with 3.8 fold higher kinase activity than the full length protein[205]. The stimulation of the various receptors, including TLRs[206,207], TNF Family Receptors[208,209], Interleukin 1 Receptor[210] and some G protein-coupled receptors (GPCR)[211], leads to Tpl2 activation downstream of the IKK complex (Figure 1.3). The IKK complex is made up of the IKKα, IKKβ, and IKKγ[212]. Prior to activation, Tpl2 is in a complex with NFκB inhibitory protein-1 (NFκB-1) p105 and ABIN-2 (A20-binding inhibitor of NF-κB 2). As Tpl2 is complexed with the p105 at a C terminal conserved helical domain (residues 497-539), it is believed to stabilize the protein from truncation as well[213]. When the IKK is activated, the p105 is phosphorylated, it triggers the ubiquitination and thereby causes the proteasomal degradation, leading to the release of Tpl2[214]. This leads to Tpl2 phosphorylation at multiple sites, of which the following are the most well characterized: T290 phosphorylation leads to disassociation from P105[199,215,216], S400 is an auto/trans phosphorylation site for response to LPS[217–219] and phosphorylation at S62 is more important for IL-1β stimulation rather than LPS[210]. It is now able to phosphorylate and activate MEK, leading to downstream activation of MEK, ERK, p38[206–209,220,221].

Tpl2 being the intermediary between the receptor stimulation to induce/activate downstream signaling of NFκB, IRF, ERK, JNKs and p38[207,213,221], raised the question of how it would really function in physiological conditions, until the first study involving *Tpl2*$^{-/-}$ mice showed that the ablation did not affect the size, lifespan and immune cell development[206]. Further studies have shown how this is due to the Tpl2 regulation of cytokine signaling being stimulus and cell specific, whichwill be discussed in detail further.

The impact of Tpl2 deficiency has been examined for the type of PRR activation involving RIG-I, TLR7/8 in *Tpl2*$^{-/-}$ macrophages[222,223] and pDCs[222] as well as LPS activation in *Tpl2*$^{-/-}$ neutrophils[224] and BMDMs[225–227]. In cellular stimulations such as the ones referenced above, the absence of Tpl2 leads to decreased production of pro-inflammatory mediators such as TNF[194,208,220,227], IL-1β[117,227], IL-10[228] and CCL2[225] increased production of IL-12p70[225,226], and cell type-specific effects on type I IFNs[222,225,229]. Specifically, *Tpl2*$^{-/-}$ macrophages and dendritic cells over-produce type I IFNs compared to WT cells, whereas *Tpl2*$^{-/-}$ pDCs have abrogated type I IFN production[222,225,229].

While immune cells develop in the *Tpl2*$^{-/-}$ mice, there are functional differences in cytokine expression as we see above for various stimulations. Additionally depending on the inflammation/cancer model that the cellular function is being examined, other functions also differ from model to cell type being considered. In a model of zymosan treatment, *Tpl2*$^{-/-}$ mice showed lesser neutrophil recruitment and reduction in myeloperoxidase activity[230]; meanwhile *Tpl2*$^{-/-}$ neutrophils show reduced reactive oxygen species production when stimulated with various TLR ligands[226]. Additionally in a model of thioglycolate induced sterile stimulation, *Tpl2*$^{-/-}$ macrophages showed defective trafficking to the peritoneal cavity[225], and in a model of High Fat Diet induced obesity there were lesser macrophages recruited to the adipose tissue in the absence of Tpl2 signaling[231]. However in a model of tuberculosis infection, higher bacterial colony forming units (cfu) load and IFN expression was seen in *Tpl2*$^{-/-}$ mice, which was reverted to WT levels using *IFNAR*$^{-/-}$/*Tpl2*$^{-/-}$ mice; thereby suggesting that Tpl2 is responsible for controlling the inflammation via suppression of the T1 IFNs[228]. In a T cell lymphoma model, the lack of Tpl2 allowed for enhancement of T cell receptor signals and higher T cell proliferation by blocking a CTLA4 feedback loop[221]. On the other hand, in *Toxoplama gondii* infection model, the T cells lacking Tpl2 had impaired IFN-γ production[232] and we observed lower antigen specific T cells in influenza infection model[222]. In a *Citrobacter rodentium* infection model, T cells produced higher IFN-γ and IL-17 on infection in a mixed bone marrow chimera, but at the same time showed reduced monocyte and neutrophil recruitment[233]. Overall, these data suggest that there is not a consensus on how a cell type would react in the absence of Tpl2 and it depends on a variety of factors involved.

It is easier to identify the differential immune activation and explain the excessive disease burden involved in infections with pandemic strains/HPAI strains compared to milder seasonal influenza infection strains. Annually, in just the USA, seasonal influenza infections result in around 400,000 cases of hospitalizations[234]. Several factors can predispose an individual (even from moderately pathogenic strains of) seasonal influenza to severe disease such as age, smoking, heart disease, obesity, chronic pulmonary disease, pregnancy, genetic predisposition to interferonopathies and immune response alterations due to sex steroid treatment[29–34]. Furthermore the damage resulting from the influenza infection can also predispose the person to bacterial co-infection, especially post long-term mechanical ventilation or in patients older than 65 years of age[235–237]. Therefore, while highly pathogenic influenza infections have their own signature immune/clinical profile, seasonal infections do not have such identifiers of severe disease and moreover can have multitude of factors that also facilitate this progression. With the difficulty in identifying the underlying immune and pathological responses that can make a seasonal influenza infection progress to hospitalization or even death, the immune system functionality needs to be examined in depth to predict/diagnose a deteriorating condition and treat it better. Herein lies the significance of examining the role of the immune response to such a moderate strain of influenza such as the x31, as it recapitulates a model of seasonal influenza.

The immune response is initiated by the sensing of the influenza infection and subsequent activation of the PRRs. Upon the activation of PRRs, MAP kinases like Tpl2 regulate antiviral responses by induction of the pro-inflammatory cytokines. Hence, the previous study examined the effect of Tpl2 ablation on the induction of the primary antiviral cytokines namely the IFNs. Both IFN-λ and IFN-α are early response cytokines that initiate a cascade of signaling and cellular recruitment to limit the spread of influenza[111,238]. While we did not see differences in the levels of the various T1 IFNs examined, the transcriptional levels of ISGs such as Ifitm3, Oasl2 and Isg15 were downregulated in the lungs of *Tpl2*$^{-/-}$ mice at 1dpi[222]. IFN-λ was also downregulated in the lungs at 1dpi and the BALF at 3dpi for the *Tpl2*$^{-/-}$ mice. Moreover the *Tpl2*$^{-/-}$ pDCS (early cytokine responders) also showed downregulated levels of IFN-λ on in-vitro infection, along with reduced expression of T1 IFNs and IFN-λ on in-vitro stimulation with the TLR7 ligand R848[222]. Therefore establishing that the ablation of Tpl2 results in dampening of the early T1 IFN and IFN-λ responses in the influenza infected mice. Clinically the *Tpl2*$^{-/-}$ mice showed higher weight loss from 7i to 9dpi and all mice succumbing to the infection approximately by 10dpi[222]. The early downregulation of the IFN response could not explain the late stage differential weight loss and why the mice succumbed to infection only by 9dpi.

Moreover, despite significantly increased viral titers in the *Tpl2*$^{-/-}$ mice throughout the course of infection, the titers consistently reduce over the course of the infection and appear unable to explain the mortality seen at 9 dpi. The phenotype of morbidity and mortality, however, was similar to mice succumbing to infection with a lethal influenza strain[239], obesity[240], juvenile age[137] or those with a dysregulated immune response[137,241,242]. We know that Tpl2 is a major regulator in the balance between beneficial and pathologic immune cell activity via the regulation of various cytokines and chemokines. Thus our hypothesis was that, it could be a long term effect or a specific, timed functionality of the Tpl2 ablation post infection with influenza,that progresses to a dysregulated immune response

Hence chapter 2 will focus on the role of Tpl2 in regulating the immune response during influenza by initially examining the contribution of virus versus cytokines to the morbidity in the *Tpl2*$^{-/-}$ mice at later time points of the infection, corresponding to the clinical symptoms. We will also explore the cytokine expression and concomitant cellular recruitment to classify the immune response in depth. Similar to tuberculosis, influenza is a pathogen that elicits a strong interferon response, so chapter 3 will focus on the regulation of IFNs by Tpl2 for the contribution to the morbidity (seen in the *Tpl2*$^{-/-}$ mice) and by examination of the gene expression, cytokine secretion and cellular recruitment profile. Finally, in chapter 4 we will examine the influenza infected *Tpl2*$^{-/-}$ mice histopathologically to access how Tpl2 ablation clinically leads to pulmonary damage and mortality.

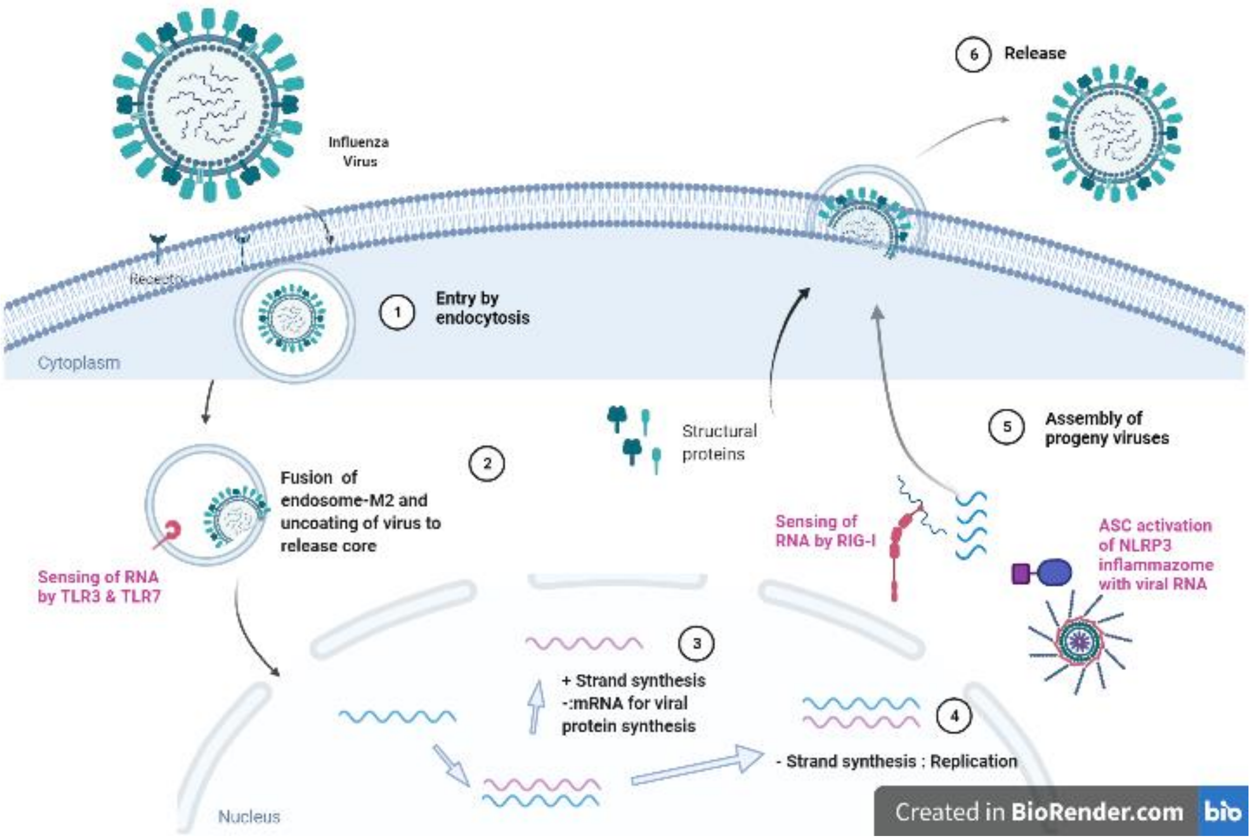

Figure 1.1: Summary of Influenza Virus infection and Immune sensing checkpoints

On influenza virus infection, HA interacts with the Salic acid on the host cell and enters via receptor mediated endocytosis. The acidic environment of the endosome induces dissociation of the nucleocapsid, which then translocates to the nucleus the host's nucleus. First, the mRNA (+strand) is made from the viral RNA template to transcribe more viral proteins. Meanwhile during viral replication, further viral RNA templates are synthesized complementary to the mRNA strand, to generate the genetic material for progeny viruses. Nuclear export signals are utilized to facilitate translocation from the nucleus into the cytoplasm for packaging, assembly and the progeny virions bud the surface of the host cell, within a portion of the lipid bilayer. Herein the viral ssRNA sensing by the TLRs occur inside the endosome, while the RNA with the 5’ppp hang is sensed at the end stages by the cytoplasmic RIG-I. Inflammasome mediated viral particle sensing is also done in the later stages of the viral assembly with the components in the cytoplasm.

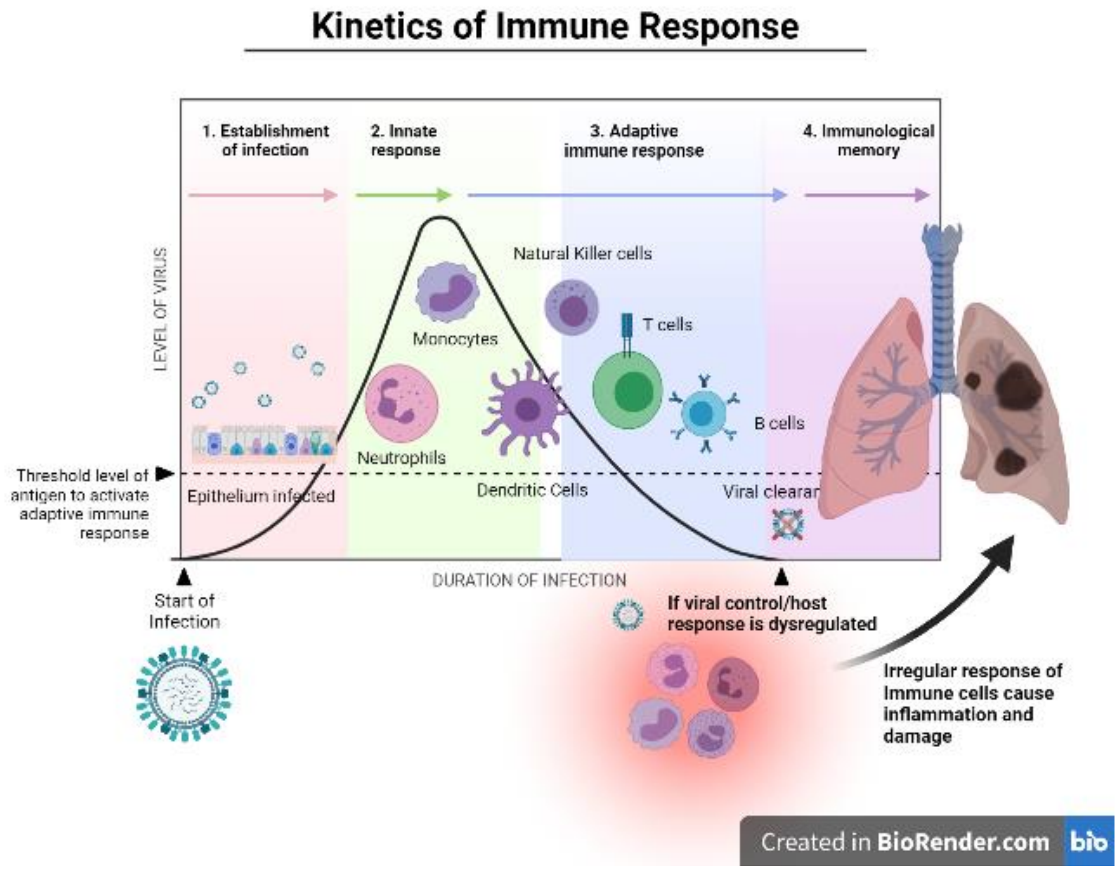

Figure 1.2: Kinetics of Influenza infection

Influenza virus primarily infect the pulmonary epithelium and other resident cells like alveolar macrophages. They induce pro-inflammatory cytokines and chemokines that allow for recognition of the infection site. Dendritic cells, inflammatory monocytes and neutrophils are cells of the myeloid origin that are resident or recruited to the site of infection in the earlier stages of infection, generally referred to as the innate immune response. They try to control the infection further, limit the viral spread and prime the cells that are involved in ultimate stages of infection. Natural killer cells, T cell and B cells are prominently recruited in the later stages of infection and are specially equipped to clear out the virus from the lungs of the mice, as part of the adaptive response phase. While a well-balanced and timed immune response is critical towards resolving the infection, issues at any step of this process would lead to lung damage due to uncontrolled virus induced damage, cytokine storm leading to excessive inflammation induced damage or delayed inflammation control leading to issues during repair/rebuilding of the lungs. Thus it is important to understand what contributes towards a finely tuned and effective immune response to influenza.

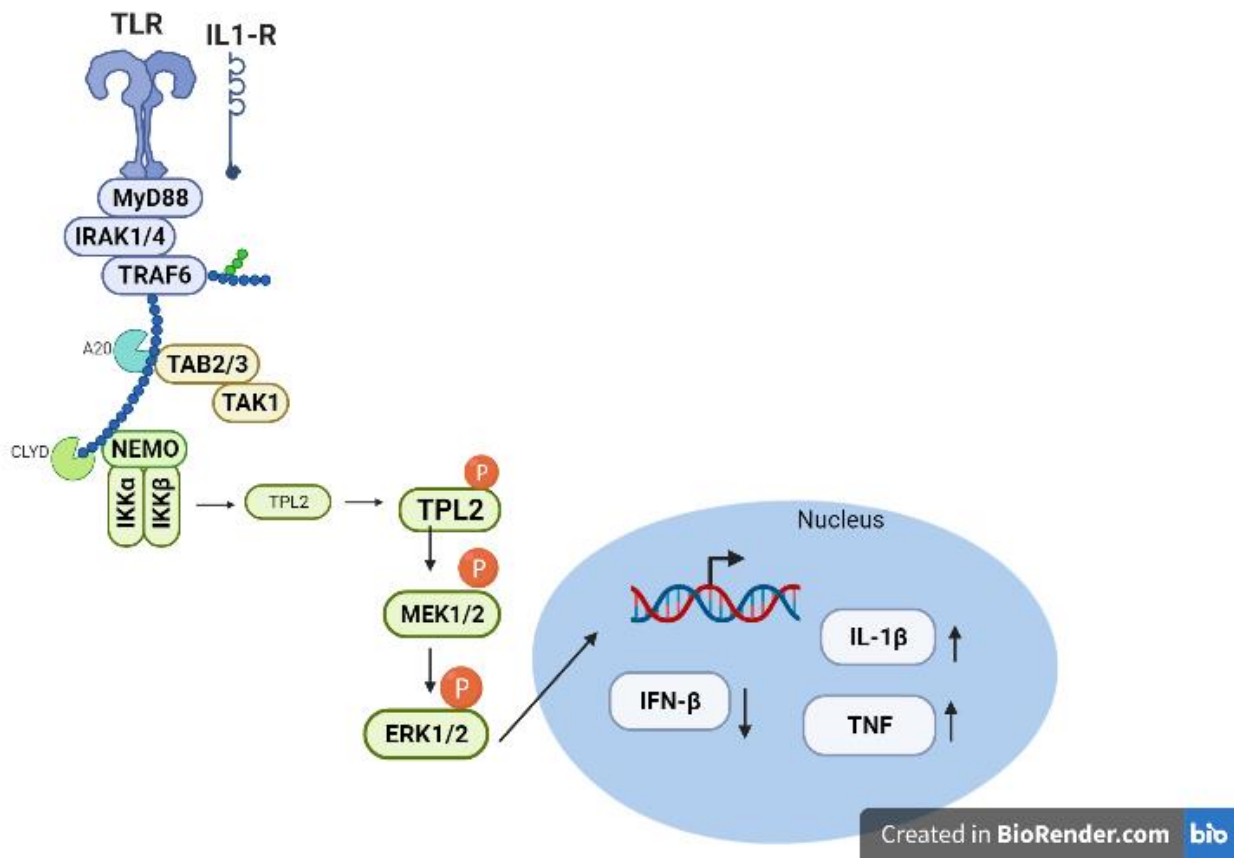

Figure 1.3: TLR, IL-1βR simulation leading to Tpl2 activation and signaling

The stimulation of the various receptors, including TLRs and Interleukin 1 Receptor, leads to Tpl2 activation downstream of the IKK complex. The IKK complex is made up of the IKKα, IKKβ, and IKKγ. Prior to activation, Tpl2 is in a complex with NFκB inhibitory protein-1 (NFκB-1) p105 and ABIN-2 (A20-binding inhibitor of NF-κB 2). When the IKK is activated, the p105 is phosphorylated, it triggers the ubiquitination and thereby causes the proteasomal degradation, leading to the release of Tpl2. This leads to Tpl2 phosphorylation at multiple sites, and is now able to phosphorylate and activate MEK, leading to downstream activation of ERK, that then has a cell and stimulus specific activation of various cytokines. In this representative macrophage cell, Tpl2 activation upregulates IL1-β, TNF, while downregulating IFN responses.

CHAPTER 2

TPL2 ABLATION LEADS TO HYPERCYTOKINEMIA AND EXCESSIVE CELLULAR INFILTRATION TO THE LUNGS DURING LATE STAGES OF INFLUENZA INFECTION.

Latha, K, Jamieson, K.F., Watford, W.T, Published in *Front. Immunol.* 12: 3919. 2021. Reprinted here with permission of publisher

ABSTRACT

Tumor progression locus 2 (Tpl2) is a serine-threonine kinase known to promote inflammation in response to various pathogen-associated molecular patterns (PAMPs), inflammatory cytokines and G-protein-coupled receptors and consequently aids in host resistance to pathogens. We have recently shown that *Tpl2*$^{-/-}$ mice succumb to infection with a low-pathogenicity strain of influenza (x31, H3N2) by an unknown mechanism. In this study, we sought to characterize the cytokine and immune cell profile of influenza-infected *Tpl2*$^{-/-}$ mice to gain insight into its host protective effects. Although *Tpl2*$^{-/-}$ mice display modestly impaired viral control, no virus was observed in the lungs of *Tpl2*$^{-/-}$ mice on the day of peak morbidity and mortality suggesting that morbidity is not due to virus cytopathic effects but rather to an overactive antiviral immune response. Indeed, increased levels of interferon-β (IFN-β), the IFN-inducible monocyte chemoattractant protein-1 (MCP-1, CCL2), Macrophage inflammatory protein 1 alpha (MIP-1α; CCL3), MIP-1β (CCL4), RANTES (CCL5), IP-10 (CXCL10) and Interferon-γ (IFN-γ) was observed in the lungs of influenza-infected *Tpl2*$^{-/-}$ mice at 7 days post infection (dpi). Elevated cytokine and chemokines were accompanied by increased infiltration of the lungs with inflammatory monocytes and neutrophils. Additionally, we noted that increased IFN-β correlated with increased CCL2, CXCL1 and nitric oxide synthase (NOS2) expression in the lungs, which has been associated with severe influenza infections. Bone marrow chimeras with Tpl2 ablation localized to radio-resistant cells confirmed that Tpl2 functions, at least in part, within radio-resistant cells to limit pro-inflammatory response to viral infection. Collectively, this study suggests that Tpl2 tempers inflammation during influenza infection by constraining the production of interferons and chemokines which are known to promote the recruitment of detrimental inflammatory monocytes and neutrophils.

INTRODUCTION

Seasonal influenza A virus (IAV) infections account for approximately $11.2 billion in total economic burden to the healthcare system[243], 500,000 hospitalizations and 40,000 deaths per yearc. While vaccination does prevent severe disease, the efficacy of each seasonal vaccine is variable. Factors such as the inaccurate prediction of the seasonal strains, poor immunogenicity of the vaccination, vaccine production issues and public vaccination non-compliance all contribute to suboptimal influenza vaccine efficacy each season[244]. Treatment options for influenza are adamantane drugs that inhibit the M2 inner protein and inhibitors that target the neuraminidase surface protein[245]. However, with the high rate of viral mutation, rapid development of resistance to these antivirals has been observed, with approximately 45% of IAV strains worldwide already resistant to adamantanes as of 2013[246] and growing resistance against neuraminidase inhibitors[247]. Despite these available interventions, influenza infections still account for 3.4% of critical illness hospitalizations, even during moderate seasons[248].

Many factors contribute to influenza-associated hospitalizations and deaths, such as underlying medical problems, secondary bacterial pneumonia and congestive heart failure. A common feature of severe disease progression in many patients with such comorbidities is hypercytokinemia, the over-production of soluble host-derived pro-inflammatory mediators initially intended to restrict local virus spread but whose dysregulation leads to systemic inflammation and potentially life-threatening complications[249]. Hypercytokinemia is more prevalent in cases of avian influenza or lethal pandemics[250,251] compared to season influenza, correlating the higher cytokine levels with severe disease progression[252–254].

Cytokines are secreted in response to influenza infection of target cells that possess cellular sensors for viral components. For example, RIG-I-like receptors (RLRs) and Toll-like receptors (TLRs) recognize viral genomic RNA and initiate a signaling cascade, via NF-κB, MAPKs and interferon regulatory factors (IRFs) that leads to the production of pro-inflammatory cytokines and interferons (IFNs). These, in turn, induce an anti-viral response in neighboring cells to limit viral spread. Complex signaling networks further lead to cytokine release by neighboring cells[255]. Proinflammatory cytokines and chemokines direct the rapid recruitment of innate immune cells, comprising neutrophils, natural killer (NK) cells, and inflammatory monocytes[256] which home to the site of infection. CXCL1 promotes neutrophil recruitment, whereas CCL2 recruits inflammatory monocytes[257,258]. Neutrophils and inflammatory monocytes are responsible for early viral control, but their dysregulation can also inadvertently damage host tissues and cause severe immunopathology systemically.

In cases of severe influenza disease, as with highly pathogenic avian influenza (HPAI), hypercytokinemia promotes excessive recruitment of neutrophils and inflammatory monocytes through overproduction of IFNs, IL-6, IL-1β, CCL2, CCL3, TNF, and IP-10[251,253,254,259]. These cells have been shown to contribute to pathology through the expression of effector molecules that promote viral clearance but also contribute of host immunopathology, including inducible nitric oxide synthase (iNOS), myeloperoxidase (MPO) and TNF-α Related Apoptosis Inducing Ligand (TRAIL). Because of potentially deadly consequences of hypercytokinemia during influenza and other viral infections, it is critical that we gain a better understanding of its regulation including factors that shift the balance from a beneficial towards a pathological response and *vice versa*.

These molecules represent potential therapeutic targets for patients with known comorbidities or those who otherwise develop severe influenza disease.

Tumor progression locus 2 (Tpl2, also known as COT or MAP3K8) has been shown to regulate the immune response to a variety of intracellular pathogens including *T. gondii*, *L. monocytogenes*, *M. tuberculosis*, and influenza virus[222,228,229,232]. Tpl2 is a serine-threonine kinase that is expressed in various cell types with functions that differ depending on cell type and stimulus[222,260,261]. Tpl2 is most widely recognized for its role in the mitogen-activated protein kinase (MAPK) pathway. For example, Tpl2 transmits signals downstream of TLRs and RLRs via activation of MEK1/2, ERK1/2, and p38[262–264]. Tpl2 exists in an inactive complex with p105 and ABIN2.[265] Upon activation by IKK phosphorylation, p105 is proteolyzed to p50 dimers, releasing Tpl2 and enabling it to initiate downstream signaling of the ERK pathway[218,260,266]. Consequently, Tpl2 promotes the expression of pro-inflammatory cytokines such as IL-6[267], TNF[260,206] and IL-1β[268] and constrains the expression of IL-12[232] and type I IFNs[228,229,269]. Notably, these Tpl2-regulated cytokines have been implicated in severe influenza disease. We previously demonstrated that *Tpl2*$^{-/-}$ mice show more severe disease in response to low pathogenicity influenza infection and succumb to infection by 10 days post infection (dpi)[222]. In this study, we sought to characterize the cytokine and immune cell profile of influenza-infected *Tpl2*$^{-/-}$ mice to gain insight into its host protective effects.

Despite modestly increased viral titers in the *Tpl2*$^{-/-}$ mice throughout the course of infection, the titers consistently decreased over time to undetectable levels by 9 dpi, confirming that impaired viral clearance failed to explain the observed mortality in *Tpl2*$^{-/-}$ mice. Instead, we demonstrate that Tpl2 ablation disrupts the balance between beneficial and pathologic immune cell activity, leading to excessive accumulation of inflammatory monocytes, neutrophils, and NOS2 production in *Tpl2*$^{-/-}$ mice by 7 dpi. This imbalance is attributed to an excessive type I IFN signature observed in the lung tissue of *Tpl2*$^{-/-}$ mice late in the course of infection. Tpl2 deficiency partly recapitulates the severe immunopathology observed in human HPAI infections, including excessive monocyte and neutrophil recruitment. Therefore, understanding how Tpl2 regulates the IFN-β and downstream late-stage responses to influenza may lead to better interventions for viral-induced lung immunopathology.

MATERIALS AND METHODS

Mice and Viruses

Wild type (WT) C57BL/6 mice were purchased from the Jackson Laboratory. *Tpl2*$^{-/-}$ mice backcrossed 10 generations onto the C57BL/6 strain were kindly provided by Dr. Philip Tsichlis (32). Animals were housed in micro-isolator cages in the Coverdell Rodent Vivarium, UGA. Both male and female mice were used in experiments to evaluate sex as a biological variable.

Embryonated, specific pathogen-free chicken eggs were purchased from Poultry Diagnostics and Research Center, UGA. Influenza virus A/HKx31 (H3N2; hereafter x31) stocks were propagated in the allantoic cavity of 9- to 11-day-old, embryonated, specific pathogen-free (SPF) chicken eggs at 37°C for 72 hours, and viral titers were enumerated by plaque assays. Madin Darby Canine Kidney (MDCK) cells were cultured and plated on a 12-well plate at a concentration of $5x10^5$ cells/ well. After 24 hours the well is generally confluent, and 100 ml of serially diluted sample was added to the well, along with 200 ml of the Infection Media (Minimal Essential Media containing 1 µg/ml TPCK treated typsin and lacking serum). The sample was allowed to incubate with the cells for an hour at 37°C to promote infection of the monolayer, followed by the addition of 2.4% Avicel in Overlay Media (Infection Media with 40 mM HEPES, 4 mM L-gutamine, 200 U/ml penicillin, 200 U/ml streptomycin and 0.15% Sodium Bicarbonate) to facilitate localized viral infection and plaque formation. After 72 hours, wells were washed with PBS, cells were fixed with 60% acetone: 40% methanol, and plaques were stained with crystal violet (made by mixing one volume of 0.0012 w/v of crystal violet powder in 5% Methanol, 11.1% Formaldehyde, 60% H_2O with one volume of PBS) for visualization and enumeration.

Influenza Infection of Mice

Age-matched, 6- to 8-week-old, WT and *Tpl2*$^{-/-}$ mice were anesthetized with approximately 250 mg/kg of 2% weight/volume Avertin (2,2,2- Tribromoethanol, Sigma) followed by intranasal instillation of 50 µl PBS containing 10^4 pfu of influenza A/HKX31 (H3N2, hereafter referred to as x31). The mice were studied for their susceptibility to infection by measuring daily weight loss and clinical scores according to the following index: piloerection, 1 point; hunched posture, 2 points; rapid breathing, 3 points. Mice with a cumulative score of 5 or that had lost 30% of their initial weight were humanely euthanized.

Tissue Collection

Mice were sacrificed at 7 to 9 dpi. Blood was collected from the heart by cardiac puncture into serum collection tubes, centrifuged at 9000 x *g* for 5 min, and the sera were stored at -80°C until cytokine analysis. Bronchoalveolar lavage fluid (BALF) was obtained from the lungs prior to harvest using

1 ml of PBS instilled twice into the lungs. The BALF was centrifuged at 500 x *g* for 5 min, and the cell-free BALF was stored at -80°C until cytokine analysis; the cellular pellet was lysed in TRK lysis buffer (E.Z.N.A Omega Bio-Tek, Inc. Norcross, GA, USA) for quantitation of gene

expression. The lungs were perfused with 10 ml of PBS injected directly into the right ventricle of the heart. Lungs were harvested into 1 ml of PBS and homogenized in a bead mill homogenizer (Qiagen Tissue Lyser II) at 25 hz for 2-4 min. The homogenate was centrifuged at 500 x *g* for 5 min, and the pre-cleared homogenate was either: (1) directly aliquoted for viral titer assessment, (2) lysed in TRK tissue lysis buffer for RNA extraction, or (3) centrifuged at 5000 x *g* for 5 min to clarify the homogenate for cytokine analysis by ELISA. For mice sacrificed at 9 dpi, whole lungs were processed without perfusion or BALF harvesting.

Cytokine Analysis

Cytokine quantitation in the blood, BALF, and clarified lung homogenates was performed using the Mouse Inflammation Cytometric Bead Array (CBA) (IL-6, IFN-γ, MCP-1, TNF, IL- 10 and IL-12p70, Becton Dickenson), Mouse ProcartaPlex 9-plex (RANTES, IP-10, MIP-1α, MIP-1β, IL-1α, IL-1β, IL-28, G- CSF, Invitrogen), Standard murine ABTS ELISA Development kit (CXCL1 & IFN-γ, Peprotech) and Lumikine express kits (IFN-b, Invivogen).

Cellular Analysis

At 4 and 7 dpi, the following protocol was used to assess the BALF and lung cellular composition after the BALF harvesting and lung perfusion as noted above. The lungs were harvested into Hyclone RPMI media (15-040-CV, Corning, Manassas, VA) containing 10% FBS and 2 mM L-glutamine (Invitrogen, Grand Island, NY). Lungs were minced with razor blades, and incubated in EDTA solution [RPMI 1640 containing 0.01 M HEPES (Lonza, Walkersville, MD),

1.25 mM EDTA (Fisher Bioreagents, Fair Lawn, NJ),] for 1 hour at 37°C in an incubator shaking at 250 RPM. The tissue was centrifuged at 350 x *g* for 10 min and then digested with 10 mL of collagenase solution [RPMI 1640 containing 1 mM $CaCl_2$, 0.01 M HEPES (Lonza, Walkersville, MD), 2 mM L-glutamine (Invitrogen, Grand Island), 100 U/ml penicillin, 100 U/ml streptomycin, 5% FBS, 0.2 μg/mL Gentamicin, and 150 U/ml collagenase (Sigma- Aldrich C2139)] for 30 min at 37°C in an incubator shaking at 350 RPM. The digested tissue was passed through a 70 μm cell strainer, and the cell suspension was centrifuged at 350 x *g* for 10 min, resuspended in 44% Percoll, and layered on top of 67% Percoll. The gradients were spun at 900 x *g* for 20 min (without brake), and the enriched leukocytes were recovered from the interface. The cells were washed with PBS at 350 x *g* for 10 min and enumerated using an automated cell counter (Cell Countess, Life Technologies).

Cells were stained at 4°C for 20 min with fluorescently-labeled antibodies against the following cell surface markers in the presence of Fc blocker (eBioscience, San Diego, CA location): Siglec F, CD11b, CD11c, Ly6C, Ly6G, CD45.2 (Stain 1); TCR αβ, TCR γδ, CD4, CD8, DX5, CD45.2 (Stain 2). The cells were fixed with 1% formalin and analyzed on the LSR II flow cytometer (BD Biosciences). CD45.2-gated hematopoietic-derived leukocyte populations were characterized as follows: inflammatory monocytes (Siglec F^-, $CD11b^{high}$, $CD11c^{low}$, $Ly6C^+$), neutrophils (Siglec F^-, $CD11b^{high}$, $CD11c^{low}$, $Ly6G^+$), alveolar macrophages (Siglec F^{high}, $CD11b^{int}$), eosinophils (Siglec F^{high}, $CD11b^{high}$), NK cells (αβ TCR^-, $DX5^+$), CD4 T cells (αβ TCR^+, $CD4^+$), CD8 T cells (αβ TCR^+, $CD8^+$), and γδ T cells (αβ TCR^-, γδ TCR^+). The gating strategy is shown in Supplementary Figure 2.10.

Analysis of Gene Expression

Messenger RNA was extracted from lung homogenates using the E.Z.N.A. Total RNA kit (Omega Bio-Tek, Inc. Norcross, GA, USA) and converted into cDNA using a High Capacity RNA-to-cDNA kit (Thermo Fisher, Waltham, MA) according to the manufacturer's protocol. Relative expression of various genes was assessed using Sensifast Probe Hi-ROXkit(BIO-82020 Bioline, Taunton, MA) and probes sourced from Applied Biosystems (Beverly, MA) using a StepOne Plus instrument

(Applied Biosystems, Beverly, MA). Results are expressed relative to the actin internal control and the WT or untreated sample using the DDC_T method. The probes used are as follows: IFNβ1(Mm00439552), IFNα1(Mm03030145), IFNα4(Mm00833969), IFN-γ (Mm0116813), IL-6(Mm00446190), IL 1 β(Mm00434228), CCL2(Mm00441242), CXCL1 (Mm04207460), CCL5(Mm01302427), TNFSF10(Mm01283606), NOS2(Mm00440502), MPO(Mm01298424), STAT1 (Mm00439518), SOCS1(Mm01342740), IL-10(Mm01288386), SOCS3 (Mm01249143), S OCS 4 (Mm00439518) and STAT4(Mm00448890).

Chimera Experiments

WT and *Tpl2*$^{-/-}$ mice were irradiated at 1100 Rads after reaching adulthood (> 6 weeks of age) and then injected with bone marrow from C57BL/6 mice at 3 x 10^6 cells in 200 µl PBS. The mice were then maintained on acidified water (pH 2.5) for 2 months to allow forreconstitution of the hematopoietic compartment with WT cells. The resulting chimeras were infected with 10^4 pfu x31 virus, andbody weights were measured over a period of 8 to 10 days, at which times the mice were euthanized to assess the cytokine profiles on days with varying pathologies.

Statistical Analysis

P values were calculated with GraphPad PRISM software version 9.2.0(332) using (one-way ANOVA with Tukey's multiple comparisons test. Differences were considered statistically significant if $p \leq 0.05$. Data represent means ± SEM. Survival data are graphed as Kaplan-Meier plots using GraphPad PRISM software, and *p* values were determined by Mantel-Cox test. Gaussian Correlation was performed to calculate the coefficient based on Pearson's Correlation test with a two-tailed test. Simple Linear Regression analysis was also performed to analyze the best fit value or the slope and intercept to see if the two variables being compared for a particular genotype correlated or not (as seen by the straight dashed line). Additionally, the confidence interval was set at 95% (as seen by the curved dashed line).

RESULTS

Tpl2$^{-/-}$ mice succumb to influenza approximately 9 days post infection

We have previously observed that *Tpl2*$^{-/-}$ mice are more susceptible than WT mice to influenza A virus infection using a low pathogenicity strain (x31; H3N2)[222]. We reasoned that increased morbidity in the *Tpl2*$^{-/-}$ mice was likely due to impaired or delayed viral clearance or to an excessive anti-viral immune response. To distinguish between these possibilities, we infected wild type and *Tpl2*$^{-/-}$ mice with x31 and monitored viral titers and inflammatory cytokine production as functions of morbidity and mortality late during the disease course. WT mice showed signs of disease from 1 to 7 dpi, at which time they began to recover as evidenced by weight gain and decreasing clinical scores (Figure 2.1 A-C). In contrast, *Tpl2*$^{-/-}$ mice displayed progressive weight loss and increasing clinical symptoms from 7 to 9 dpi (Figure 2.1A-C). Notably, the weight loss and clinical symptoms were not different between male and female mice after 7 dpi with influenza (Supplementary Figure 2.8 A-D). Importantly, despite severe clinical symptoms in *Tpl2*$^{-/-}$ mice, no virus was observed in either WT or *Tpl2*$^{-/-}$ mice at peak morbidity and mortality (9 dpi; Figure 2.1D), demonstrating that both strains had successfully cleared the virus by this time point. As expected from these findings, there was no correlation between morbidity as measured by weight loss and viral titers (Figure 2.1E), confirming that the morbidity observed in influenza-infected *Tpl2*$^{-/-}$ mice was not due to increased viral loads.

Hypercytokinemia is widely reported in severe influenza-infected patients that eventually succumb to disease[250,254]. It is characterized by significantly increased levels of interferons (IFNs), IL-6, TNF, IL-12, IL-1β and various chemokines such as CCL2, MIP-1α, MIP-1β, RANTES, and IP-10[250,254]. Therefore, the pro-inflammatory cytokine profile of lung homogenates from influenza-infected WT or *Tpl2*$^{-/-}$ mice was assessed using a multiplex protein assay. Significantly increased levels of IFN-β, CCL2, IFN-γ, CCL3, CCL4, CCL5 and CXCL10 were observed in the lung tissue of influenza-infected *Tpl2*$^{-/-}$ mice compared to WT (Figure 2.2A-C, 2I-L); increased levels of IFN-β, IL-6 and IL-10 were observed in the air spaces of *Tpl2*$^{-/-}$ mice (Supplementary Figure 2.9H, K, N); and increased levels of IFN-γ were observed in the blood of *Tpl2*$^{-/-}$ mice at 7 dpi (Supplementary Figure 2.9C). These data demonstrate that *Tpl2*$^{-/-}$ mice display increased levels of pro-inflammatory cytokines and chemokines typically observed in human patients with influenza-induced hypercytokinemia[249–252]. Notably, increased weight loss at 7 dpi correlated with high levels of IFN-β in the lungs of the *Tpl2*$^{-/-}$ mice (Figure 2.2Q). However, there was no correlation between weight loss and viral load in the tissue at 7 dpi (Figure 2.2R), as was the case at 9 dpi (Figure 2.1E). These data demonstrate that the morbidity in *Tpl2*$^{-/-}$ mice is due to the overexuberant immune response in *Tpl2*$^{-/-}$ mice at the late stage of influenza infection rather than impaired viral control.

Tpl2*$^{-/-}$ *mice are characterized by excessive inflammatory infiltration of the lungs at 7 days post influenza infection

We next assessed the cellular composition of the lung tissue and alveolar air spaces to identify cells that would be consequently recruited due to the hypercytokinemia and could contribute to tissue damage in the lungs and mortality. Mice were infected with influenza, and bronchoalveolar lavage fluid (BALF) and lung tissue were harvested at 7 dpi for analysis of cellular composition by flow cytometry (Supplementary Figure 2.10). The total cellularity of the lungs was significantly increased in *Tpl2*$^{-/-}$ mice. Higher numbers of cells were present in the perfused and lavaged lung tissue of the *Tpl2*$^{-/-}$ mice (Figure 2.3A). Furthermore, *Tpl2*$^{-/-}$ mice had significantly increased absolute numbers of inflammatory monocytes and neutrophils compared to WT mice at 7 dpi (Figure 2.3B-C). An increase in frequency of inflammatory monocytes and neutrophils was also noted (Supplementary Figure 2.11A-B), however no differences in total alveolar macrophages, NK cells, CD4 or CD8 αβ T cells or even γδ T cells were observed (Figure 2.3D-H). Therefore, it is the numerical increase in inflammatory monocytes and neutrophils that account for the higher total cellular infiltrates observed in infected *Tpl2*$^{-/-}$ mice. Typically, innate immune cells are recruited early during influenza infection to phagocytose or endocytose infected cells[270]; therefore, it was unexpected to see such high numbers of them late in the infection in *Tpl2*$^{-/-}$ mice. Because Tpl2 deficiency has been demonstrated to impair monocyte, macrophage and neutrophil recruitment in response to inflammatory stimuli[224,225,228,233,271], we further assessed the kinetics for the paradoxically increased monocytes and neutrophils in the lung tissue of influenza-infected *Tpl2*$^{-/-}$ mice. Therefore, we characterized the cellular composition of lungs at an earlier time point (4 dpi) with uninfected mice as negative controls. Although we noted influenza infection-induced recruitment of both inflammatory monocytes and neutrophils by 4 dpi, there was no difference between the WT and *Tpl2*$^{-/-}$ mice (Figure 2.3I-J). This was also true of all the other cell types examined (Supplementary Figure 2.11E-F). These data suggest a late acting effect of Tpl2, possibly in limiting the amplitude of the response or in promoting resolution of inflammation.

NOS2 is overexpressed in the lungs of influenza-infected Tpl2$^{-/-}$ mice

Highly pathogenic influenza viruses induce exaggerated immune responses that cause immunopathology via damage to the pulmonary epithelium by the recruited immune cells and their effector molecules[101,258]. A study of juvenile mice that exhibit severe disease in response to influenza infection revealed recruitment of inflammatory monocytes with high expression of inducible nitric oxide synthase (NOS2)[137], which induces apoptosis of epithelial cells. Another mediator of influenza-associated lung injury is myeloperoxidase (MPO), which is predominantly secreted by neutrophils during cases of severely pathogenic influenza infections[272]. Neutrophil Elastase (ELANE) is an inflammatory mediator of neutrophils that is predictive of development of acute lung injury (ALI) or acute respiratory distress syndrome (ARDS) , however its role in influenza infections is debatable[130,273–275] TNF-α receptor-induced apoptosis ligand (TRAIL), released by NK cells and inflammatory monocytes, interacts with death receptors on the surface of epithelial cells to induce apoptosis[138]. Given that Tpl2 ablation leads to increased recruitment of inflammatory monocytes and neutrophils to the lungs, we next assessed the lung expression of pro-inflammatory cytokines and chemokines that recruit these cells as well as their effector molecules that could potentially damage the pulmonary epithelium and compromise lung function. Consistent with protein data, we noted overexpression of various pro-inflammatory cytokine mRNAs in lung tissue from influenza-infected *Tpl2*$^{-/-}$ mice at 7 dpi, including IFN-β, IFN-γ and IL-6, as well as overexpression of chemokines CCL2, CXCL1, CCL5 and CXCL10 which are collectively involved in recruitment of inflammatory monocytes and neutrophils (Figure 2.4A-J). We also examined the level of CXCL2, another neutrophil recruiting chemokine[276] known to be active in bacterial infection models and found no difference between WT and *Tpl2*$^{-/-}$ lung tissue (Figure 2.4K). On testing for various inflammatory mediators, including NOS2, MPO, ELANE and TNFRSF10 (the gene encoding TRAIL), we observed upregulation of only NOS2 in the lungs of *Tpl2*$^{-/-}$ mice at 7 dpi (Figure 2.4M-P), suggesting that elevated NOS2 secretion by the increased numbers of inflammatory monocytes or neutrophils may contribute to morbidity. Notably, we observe that the IFN-β mRNA expression correlates with CCL2 mRNA expression (Figure 2.4S), and NOS2 mRNA expression in the lungs of the *Tpl2*$^{-/-}$ mice correlates with both CCL2 and IFN-β expression (Figure 2.4T-U), supporting the hypothesis that over-expression of IFN-β in *Tpl2*$^{-/-}$ mice stimulates increased production of the IFN-inducible gene, CCL2, which is responsible for the recruitment of NOS2-expressing monocytes that contribute to the damage of the pulmonary epithelium. Additionally, CXCL1 mRNA expression positively correlates with both IFN-β and NOS2 mRNA expression in the lungs of *Tpl2*$^{-/-}$ mice (Figure 2.4V-W), even though CXCL1 was not upregulated by protein expression at 7 dpi.

Because IFN-γ protein and mRNA expression were very high in influenza-infected *Tpl2*$^{-/-}$ mice (Figure 2.2C and 2.4D) & has been reported to induce damage via NOS2[277], we also examined whether IFN-γ correlated with NOS2 mRNA expression and did not find any correlation (Figure 2.4X). To further address the source of the high levels of IFN-γ, *Tpl2*$^{-/-}$ mice and *Tpl2*$^{-/-}$*Rag1*$^{-/-}$ mice were infected with influenza, and IFN-γ protein levels in lung homogenates were assessed at 7 dpi. Both *Tpl2*$^{-/-}$ and *Tpl2*$^{-/-}$/*Rag*$^{-/-}$ mice that lack T cells, produced similar levels of IFN-γ protein (Supplementary Figure 2.12A), suggesting that T cells are not the source of IFN-γ overproduction. Collectively, these significant correlations support the hypothesis that the expression of NOS2 is linked to the recruitment of inflammatory monocytes and neutrophils under the influence of IFN-β overexpression and the most likely cause of the morbidity seen in the *Tpl2*$^{-/-}$ mice.

Influenza-infected Tpl2$^{-/-}$ mice exhibit an increased interferon response that cannot be adequately controlled by SOCS1-mediated regulation

The IFNs signal primarily via activation of the JAK/STAT pathway, with STAT1 playing a central role for both Type I and II interferons[278]. Furthermore, interferons participate in a feed-forward loop with IFN-β amplifying the signal through Interferon Alpha Receptor 1 (IFNAR1) by inducing multiple IFNαs and other interferon-stimulated genes (ISGs), such as CCL2[278,279]. Finally, resolution of this pathway is mediated in large part by the IFN-mediated induction of suppressors of cytokine signaling 1 (SOCS1), which downregulates interferon expression and signaling via STAT1[280]. Because *Tpl2*$^{-/-}$ mice show higher recruitment of inflammatory monocytes and neutrophils as the infection progresses, we hypothesized that Tpl2 either limits the amplitude or promotes resolution of the antiviral IFN response. To address the regulation of the IFN pathway by Tpl2 in response to influenza infection, we first measured the expression of both STAT1 and SOCS1, which serve as positive and negative regulators of the IFN pathway, respectively. At the peak of morbidity in *Tpl2*$^{-/-}$ mice at 9 dpi, STAT1 was markedly downregulated in the lungs of *Tpl2*$^{-/-}$ mice (Figure 2.5A). In order to determine the cause of STAT1 downregulation, we assessed expression of the various SOCS genes and found that SOCS1 was overexpressed by 7 dpi (Figure 2.4R) and remained elevated through 9 dpi (Figure 2.5B). Notably, the IFNs and ISGs were no longer upregulated at a transcriptional level in *Tpl2*$^{-/-}$ mice at 9 dpi, suggesting that elevated SOCS1 is suppressing the IFN response (Figure 2.5F-O). Additionally, in *Tpl2*$^{-/-}$ mice, SOCS1 is upregulated at 9 dpi while all IFNs and ISGs decline to WT levels by 9 dpi, providing further evidence of SOCS1-mediated transcriptional repression of the interferon response. Overexpression of SOCS1 in *Tpl2*$^{-/-}$ lung tissue was associated with increased levels of IL-10 protein in the lungs (Figure 2.5R), indicative of a reparative response. However, despite elevated SOCS1 and decreased NOS2 mRNA expression in *Tpl2*$^{-/-}$ mice at 9 dpi (Figure 2.5B, N), CCL2 protein levels remained elevated (Figure 2.5Q) and were accompanied by trending higher levels of other pro-inflammatory cytokines, including IFN-γ and IL-6 (Figure 2.5S-V). Cxcl1 levels were not different (Figure 2.5W), consistent with protein levels observed at 7 dpi (Figure 2.2H).Therefore, we conclude that inefficient regulation of the IFN/STAT1 pathway via SOCS1 permitted persistently elevated levels of CCL2, the chemokine recruitment signal for monocytes, in *Tpl2*$^{-/-}$ mice at the peak of morbidity (9 dpi). Collectively, these findings suggest that dysregulation of the IFN pathway in *Tpl2*$^{-/-}$ mice promotes excessive and prolonged influx of inflammatory cells that contribute to lung damage and morbidity observed in influenza-infected *Tpl2*$^{-/-}$ mice.

In chimeras with Tpl2 ablation restricted to radio resistant cells, hypercytokinemia is suppressed

In an effort to localize Tpl2 functions that regulate hypercytokinemia in late stages of influenza infection, we generated chimeras using WT or *Tpl2*$^{-/-}$ recipient mice that were given WT donor bone marrow post irradiation, ensuring that hematopoietic cells would be of WT origin post recovery (as outlined in Figure 2.6A). Differential weight loss was observed in the *Tpl2*$^{-/-}$ chimeras from 7 to 8 dpi (Figure 2.6B), after which the mice recovered. Upon examination of the cytokines in the lungs, CCL2, IFN-γ and IL-6 were all upregulated in *Tpl2*$^{-/-}$ chimeras (Figure 2.6 C-E) at 8 dpi, whereas the levels of other pro-inflammatory cytokines such as TNF, IL-12, IL-10 and CXCL1 were not affected (Figure 2.6 F-I). Upregulation of CCL2, IFN-γ and IL-6 at 8 dpi in *Tpl2*$^{-/-}$ chimeras suggests that the cytokine dysregulation is partially attributed to Tpl2 deficiency in radio-resistant cells, such as epithelial[79,80] or stromal cells[281]. Importantly, the regulation of these cytokines normalized in *Tpl2*$^{-/-}$ chimeras by 10 dpi, at which time the Tpl2 chimeras fully recovered. This overall phenotype is unlike the prolonged cytokine dysregulation and progressive weight loss seen in germline *Tpl2*$^{-/-}$ mice at 9 dpi (Figure 2.1A), suggesting that *Tpl2*$^{-/-}$ chimera recovery is mediated by suppression of hypercytokinemia by WT hematopoietic cells. As alveolar macrophages are also part of the lung resident immune cell population and are radioresistent[282], we considered the possibility that the source of the dysregulated cytokines at 7 dpi was the alveolar macrophages rather than the epithelial or stromal cells. However, we found no differences in the gene expression for CCL2, IL-6, IFN-γ or IFN-β at 7 dpi in sorted alveolar macrophages from WT and *Tpl2*$^{-/-}$ lungs (Supplementary Figure 2.13A-D).

DISCUSSION

Tpl2$^{-/-}$ mice exhibit enhanced morbidity and mortality to influenza infection with deteriorating clinical symptoms from 7 to 9 dpi. Live virus was undetectable by 9 dpi, confirming complete, albeit delayed, viral clearance in the *Tpl2*$^{-/-}$ mice as noted in our previous study[222]. Despite viral clearance, the *Tpl2*$^{-/-}$ mice showed hypercytokinemia and influx of inflammatory cells, specifically inflammatory monocytes and neutrophils, by 7 dpi. Increased inflammatory monocyte and neutrophil recruitment in *Tpl2*$^{-/-}$ mice coincided with increased expression of type I interferons and the inflammatory mediator NOS2 (Figure 2.7).These findings demonstrate that Tpl2 serves a regulatory role during influenza infection by tempering the production of type I interferons and IFN-stimulated chemokines that leads to excessive recruitment of inflammatory cells known to cause physical trauma to the pulmonary epithelium[101,251,258,283].

ınfection of mice with virulent strains of influenza leads to increased expression of IFNs and concomitant overexpression of CCL2, which induces excessive recruitment of inflammatory monocytes and immunopathology[100,101,137,258]. Consistent with these studies, severe weight loss in

Tpl2$^{-/-}$ mice was associated with increased expression IFN-β. High IFN-β expression correlated with increased CCL2 and NOS2 expression, supporting IFNβ-CCL2-NOS2 as an axis of monocyte-mediated recruitment and inflammation in *Tpl2*$^{-/-}$ mice. Importantly, IFN-β and CCL2 were also both overproduced at the protein level in influenza-infected *Tpl2*$^{-/-}$ mice, further supporting this mechanism of regulation. Although high CXCL1 correlated with elevated IFN-β and NOS2 at the mRNA level in *Tpl2*$^{-/-}$ mice, lack of CXCL1 protein overexpression at 7 dpi suggests translational control of this chemokine in the *Tpl2*$^{-/-}$ mice despite high mRNA levels, questioning the contribution of this pathway in cellular recruitment. Other chemokines elevated in influenza-infected *Tpl2*$^{-/-}$ mice, including CXCL10, CCL5, CCL3 and CCL4, are also overexpressed in human cases of lethal influenza infections[249,252] and recognized for recruitment of inflammatory monocytes and neutrophils[251]. Notably, CCL3 (MIP1α) has also been recognized as a neutrophil recruiter[284], and CCL3 was increased in the *Tpl2*$^{-/-}$ at the protein level at 7 dpi (Figure 2.2K). Importantly, IL-6 and chemokines like CCL3, CCL4 and CCL5, which are not classically induced by IFNs, are also upregulated in *Tpl2*$^{-/-}$ mice, indicative of a generalized inflammatory response. However, overexpression of IFNs (IFN-β/IFN-γ) and IFN-inducible chemokines, like CCL2[100,279] and CXCL10[285], suggest a more pronounced alteration of these IFN pathways. According to multiple lines of evidence[249,250,286], targeted dysregulation in these pathways is sufficient to cause the excessive recruitment of the inflammatory monocytes and neutrophils, consistent with the phenotype of influenza-infected *Tpl2*$^{-/-}$ mice at 7 dpi.

It is important to note that the excessive recruitment of monocytes and neutrophils in *Tpl2*$^{-/-}$ mice reported herein during influenza infection was unexpected based upon the recruitment phenotypes observed in *Tpl2*$^{-/-}$ mice using other inflammatory models. Multiple studies have shown that Tpl2 ablation leads to *decreased* recruitment of both macrophages and neutrophils in response to inflammation induced by zymosan, acetaminophen, caerulein or thioglycollate administration[225,267,271,287,288]. However, these studies have focused on the acute effects (within 72 hours) of Tpl2 ablation unlike the later phenotype assessed herein. In this regard, we previously noted similar levels of IFN-β at 1 and 3 dpi with influenza[222], consistent with similar cellular recruitment profiles at 4 dpi (Figure 2.3I-J), suggesting an important kinetic component. Another important distinction in the models is the differential expression of type I IFNs, which are known for their immunomodulatory effects. Influenza infections are characterized by high levels of type I IFNs compared to the acute inflammatory models used to assess innate immune cell recruitment in *Tpl2*$^{-/-}$ mice[225,267,271,287,288]. Infection of *Tpl2*$^{-/-}$ mice with *Mycobacterium tuberculosis* results in a high type I IFN signature that impairs antibacterial functions via induction of IL-10, reminiscent of the present findings[228]; however, potential effects of Tpl2 on pulmonary recruitment of monocytes and neutrophils was not assessed in this model[228]. Collectively, these studies emphasize the importance of kinetic regulation of cytokines and chemokines in promoting inflammation. Furthermore, they suggest that stimuli that promote strong type I IFN responses are likely to elicit uncontrolled inflammation in *Tpl2*$^{-/-}$ mice.

The use of bone marrow chimeras revealed important information about the source of the Tpl2-dependent immunoregulation during influenza infection. We observe upregulation of the IFN response in later stages of the infection in germline *Tpl2*$^{-/-}$ mice as well as chimeras, although this was not sustained in the chimeras. Transient IFN overexpression resolved by 10 dpi, corresponding with complete recovery of *Tpl2*$^{-/-}$ chimeras. These findings indicate that Tpl2 ablation in radioresistant cells like the pulmonary epithelium or endothelium leads to an initial cytokine dysregulation and overexpression at 7 dpi. The full recovery of *Tpl2*$^{-/-}$ chimeras compared to the high morbidity of germline *Tpl2*$^{-/-}$ mice further suggests that Tpl2 also functions to some extent within the non-hematopoietic compartment to limit influenza-induced inflammation. Overall, these findings suggest that the source of hypercytokinemia is an interplay between Tpl2-dependent effects in both radioresistant stromal cells and radiosensitive hematopoietic cells.

The most prominent radioresistant lung cell populations that are susceptible to influenza infection are the Type 1 and Type 2 airway epithelial cells as well as alveolar macrophages. While the alveolar macrophages are susceptible to infection, they express lower levels of cytokines than peripheral blood monocyte derived macrophages[57]. Furthermore, the similar expression levels of IFNβ and CCL2 (among others) by alveolar macrophages isolated from influenza-infected WT and *Tpl2*$^{-/-}$ mice suggest that dysregulated cytokine responses in influenza-infected *Tpl2*$^{-/-}$ mice likely originate from other cellular sources, like the pulmonary epithelial cells that are primary targets and replicative niches for influenza. Cell-type specific regulation of the type I interferons by Tpl2 has been characterized in multiple immune cell types, including macrophages, DCs and pDCs. However, evidence of Tpl2-dependent regulation of epithelial cell functions is sparse. One study of intestinal inflammation using the DSS model has demonstrated that Tpl2 is essential for intestinal homeostasis, with Tpl2-deficient mice showing extensive intestinal inflammation characterized by focal ulceration, loss of Goblet cells and loss of crypts [289].The protective role for Tpl2 in that study was shown to be intrinsic to intestinal myofibroblasts that sense epithelial damage and signal homeostatic responses via a Tpl2-COX-2-Prostaglandin E2 pathway. Another study demonstrated that Tpl2 signals ERK1/2 activation in response to *Pseudomonas* antigens and several purified TLR ligands via TAK1 and IKK-β in BEAS-2B immortalized human bronchial epithelial cells, and Tpl2 inhibitor treatment resulted in decreased *Pseudomonas*-induced IL-6 and

IL-8 secretion[290]. A follow-up study from the same group showed that Tpl2 also promoted IL-33 expression in response to *Pseudomonas aeruginosa* via the same pathway in airway epithelial cells expressing a Cystic Fibrosis mutation (CFTRdelF508)[261]. Unfortunately, none of these studies provides insight into whether or how Tpl2 regulates type I interferon production in pulmonary epithelial cells. Ongoing studies are addressing the Tpl2-dependent regulation of antiviral responses specifically within pulmonary epithelial cells. However, the current findings suggest that overall Tpl2 functions as a negative regulator of type I IFNs late during influenza infection, which is consistent with the negative regulation observed in macrophages and dendritic cells [222,229].

Antiviral IFNs are potent inhibitors of viral spread, but they also stimulate strong inflammatory responses, including antigen presentation by dendritic cells and T cell differentiation and activation, and their dysregulation can lead to immunopathologies [99,291,292]. The necessarily tight control over IFN signaling is achieved, in part, by the actions of a family of eight SOCS proteins that inhibit JAK/STAT signaling. Not only did we observe overexpression of IFNs and ISGs such as STAT1, CCL2 and IFN-γ at 7 dpi, but we also observed a striking induction of SOCS1 in the lungs of the *Tpl2*$^{-/-}$ mice. SOCS1 is an ISG induced during influenza infection to inhibit the expression of IFNs and their downstream signaling by inhibiting STAT1 or JAK1, which are required for signaling via this pathway[280,293]. Moreover SOCS1 can be stimulated in response to influenza by a wide range of pathways including RIG-I, MAVS and the IFNAR1 pathway and can concomitantly downregulate other ISGs including STAT1, IFN-β and IRF-3[280]. SOCS3 is another ISG that has been found to downregulate similar ISGs as SOCS1 and impacts the regulation of IL-6 via the STAT3 pathway independent of the IFN signaling pathway[123,280,294]. Additionally, *Socs4*$^{-/-}$ mice are highly susceptible to influenza infections due to elevations in key inflammatory cytokines such as IL-6, IFN-γ and CCL2 with impaired trafficking of virus specific CD8 T cells to the lungs, highlighting the importance of SOCS4 mediated regulation of the influenza response[295]. Among the various SOCS family members, we observed consistently upregulated levels of SOCS1 in *Tpl2*$^{-/-}$ mice from 7 to 9 dpi. This increase in SOCS1 in *Tpl2*$^{-/-}$ mice presumably assisted in the downregulation of STAT1 and other ISGs such as NOS2 by 9 dpi. Despite the downregulation of CCL2 mRNA at 9 dpi, corresponding reductions at the protein level were delayed, and overexpression of CCL2 and IL-10 proteins were still evident at 9 dpi. Therefore, negative regulation of the interferon pathway is operative in the *Tpl2*$^{-/-}$ mice, although delayed such that CCL2 protein levels are inefficiently suppressed at 9 dpi, potentiating cellular infiltration in *Tpl2*$^{-/-}$ mice late during infection.

Nitric oxide synthase 2 (NOS2) is one of the inflammatory mediators shown to cause epithelial cell damage and thereby lead to morbidity in influenza-infected mice that present with hypercytokinemia[137,283]. NOS enzymes catalyze the production of nitric oxide (NO) from L-arginine. Notably, NOS and NO have previously been implicated in damage to the pulmonary epithelium. First, higher expression of NO has been observed in mice infected with highly pathogenic avian influenza strains compared to seasonal strains, and antibody blockade of NO led to increased survival[283]. Second, *NOS2*$^{-/-}$ mice survived infection with a low pathogenicity virus strain via an IFNγ-dependent anti-viral mechanism, demonstrating that NOS2 contributed more to influenza-mediated pneumonitis rather than viral control in WT mice[277]. Although NO expression is not restricted to either inflammatory monocytes or neutrophils[283], NO expression by other sources such as the epithelium is low and transient[296]. Similarly, NO expression by alveolar macrophages is also restricted, being stimulated by IFNγ only from macrophages that are in contact with type II alveolar epithelial cells[296,297]. Importantly, during influenza infection, the primary source of NOS2 has been demonstrated to be inflammatory monocytes[137,258]. NOS2 is also expressed to a lesser extent by neutrophils, which were also increased in *Tpl2*$^{-/-}$ mice (Figure 2.3C). However, failure to detect coincident elevations in MPO expression (Figure 2.5L, 6O), a hallmark neutrophil effector molecule, in *Tpl2*$^{-/-}$ mice suggests that neutrophils are not a dominant mediator of pulmonary damage in this model or they are working in concert with inflammatory monoctyes[257,298,299]. Therefore, it is likely that the numerically increased inflammatory monocyte pool, with additional neutrophil contribution in the *Tpl2*$^{-/-}$ mice induces lung pathology via their expression of NOS2 and NO.

Analyses of peripheral blood during influenza infection in humans has demonstrated upregulation of Tpl2 expression at days 4 and 6 post infection[300]. We show that Tpl2 tempers severe immunopathology during influenza infection in mice via suppression of late-stage cytokine regulation. Future studies should examine the correlation of Tpl2 expression with influenza outcomes, as Tpl2 expression may represent a diagnostic tool in the prediction of severe immunopathology during influenza infection. Furthermore, a better understanding of immunoregulation of influenza infections by Tpl2 could also guide the discovery of immunotherapies for cases of hypercytokinemia.

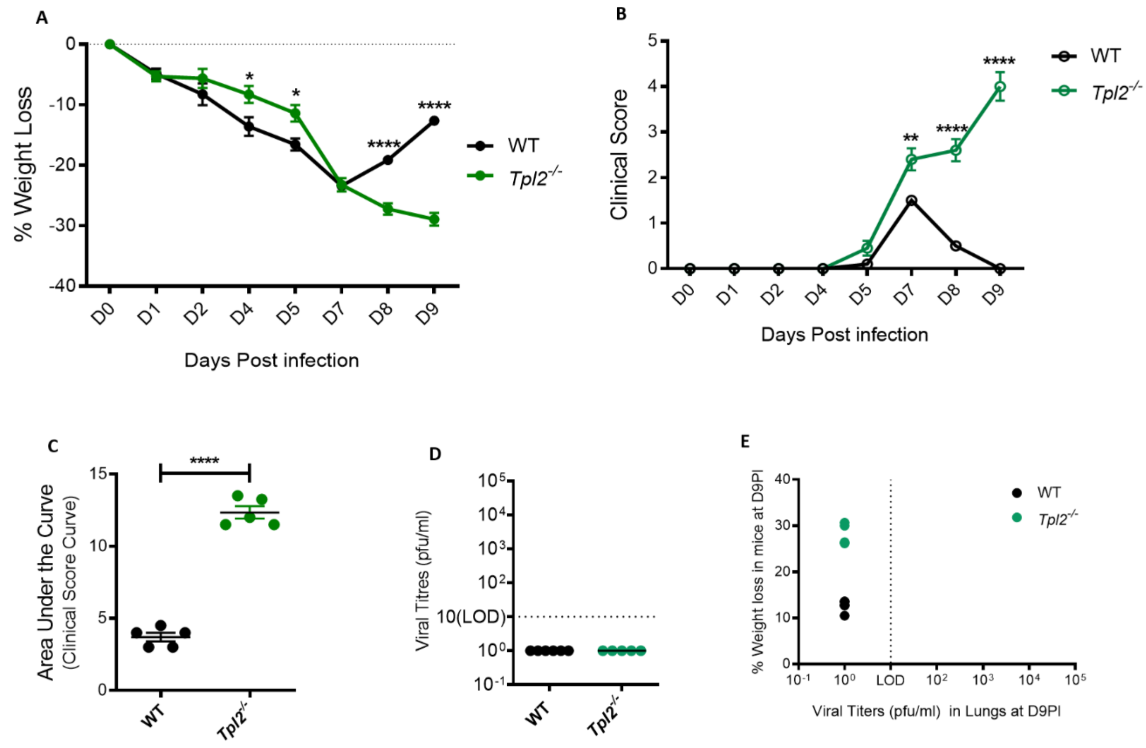

Figure 2.1: Severe pathology in influenza-infected *Tpl2*$^{-/-}$ mice does not correlate with viral load. (A) Percent weight change of WT (n=5) versus *Tpl2*$^{-/-}$ (n=5) mice 9 dpi with 10^4 pfu influenza A virus strain x31. Data are representative of 5 experiments Unpaired student's *t*-test; *p<0.05, **p<0.01, ****p<0.0001 (B) Progression of clinical symptoms including lethargy, piloerection, and hunching is shown throughout the course of infection with Data are representative of 5 experiments Unpaired student's *t*-test; *p<0.05, **p<0.01, ****p<0.0001 (C) Area under the curve statistics. Data are representative of 5 experiments, Area Under the Curve analysis was performed per genotype in Prism and then compared statistically by Unpaired student's *t*-test; ****p<0.0001 (E) Lung viral titers (pfu/ml) were quantitated at 9 dpi. Baseline represents the limit of detection (LOD = 10 pfu/ml). Undetectable virus loads were assigned a value of 1. (F) Correlation of viral titers with weight loss at 9 dpi. Data are representative of 2 experiments. Two tailed Pearson's Correlation test was performed

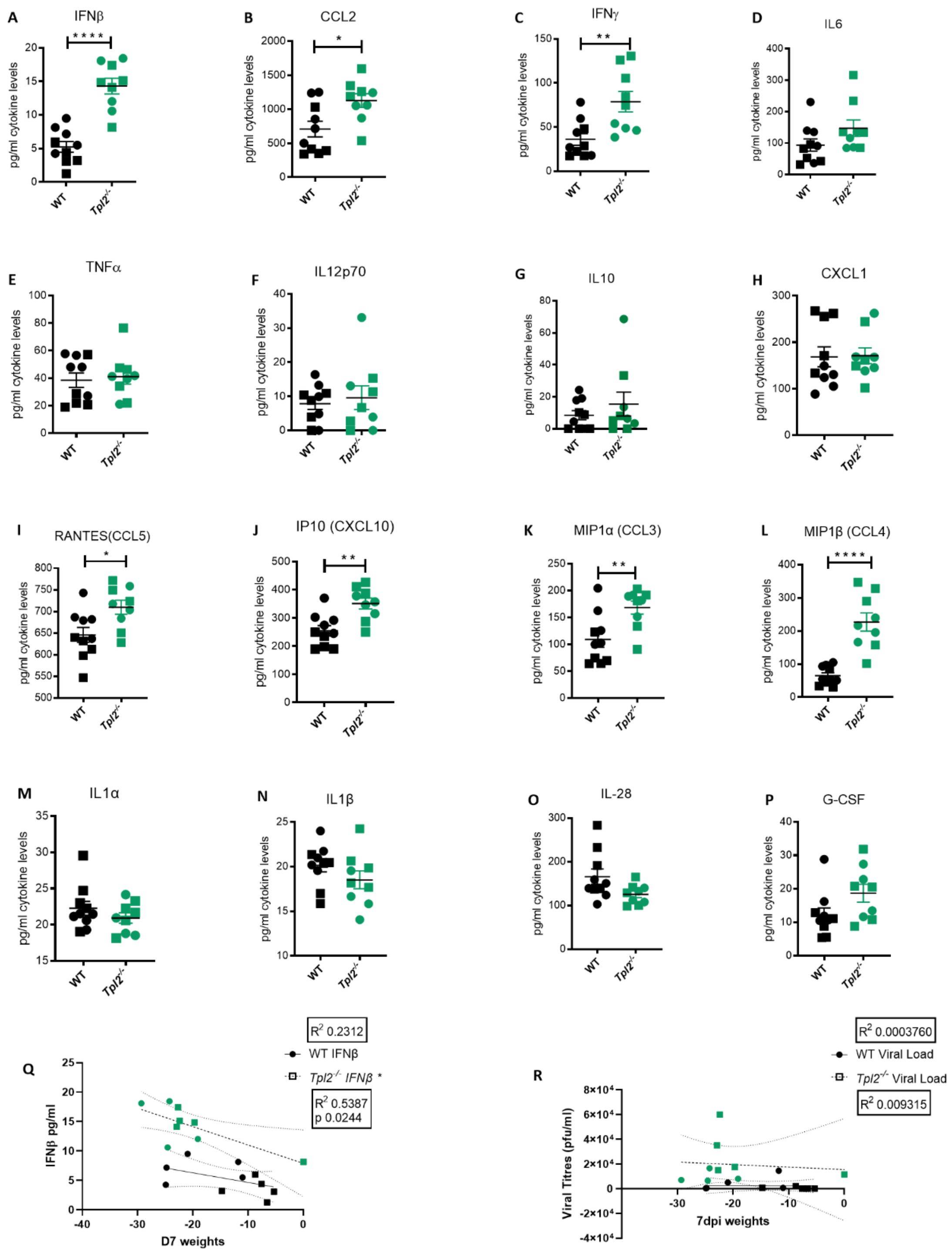

Figure 2.2. Excessive IFN cytokine signature is observed in influenza-infected *Tpl2*$^{-/-}$ mice at 7 dpi. WT (n=10) and *Tpl2*$^{-/-}$ (n=9) mice were infected intranasally with 10^4 pfu of influenza x31

and euthanized at 7 dpi. (A-P) The lungs were homogenized for analysis of cytokine expression. Squares represent male mice, and circles represent female mice. Data are representative of 2 experiments. Unpaired student's *t*-test*p<0.05, **p<0.01, ***p<0.001, ****p<0.0001. (Q) Correlation of Interferon levels in the perfused and lavaged lungs with weight loss at 7 dpi. (R) Correlation of viral titers in the perfused and lavaged lungs with weight loss at 7 dpi. Data are representative of 2 experiments. Two tailed Pearson's Correlation test was performed *p<0.05,

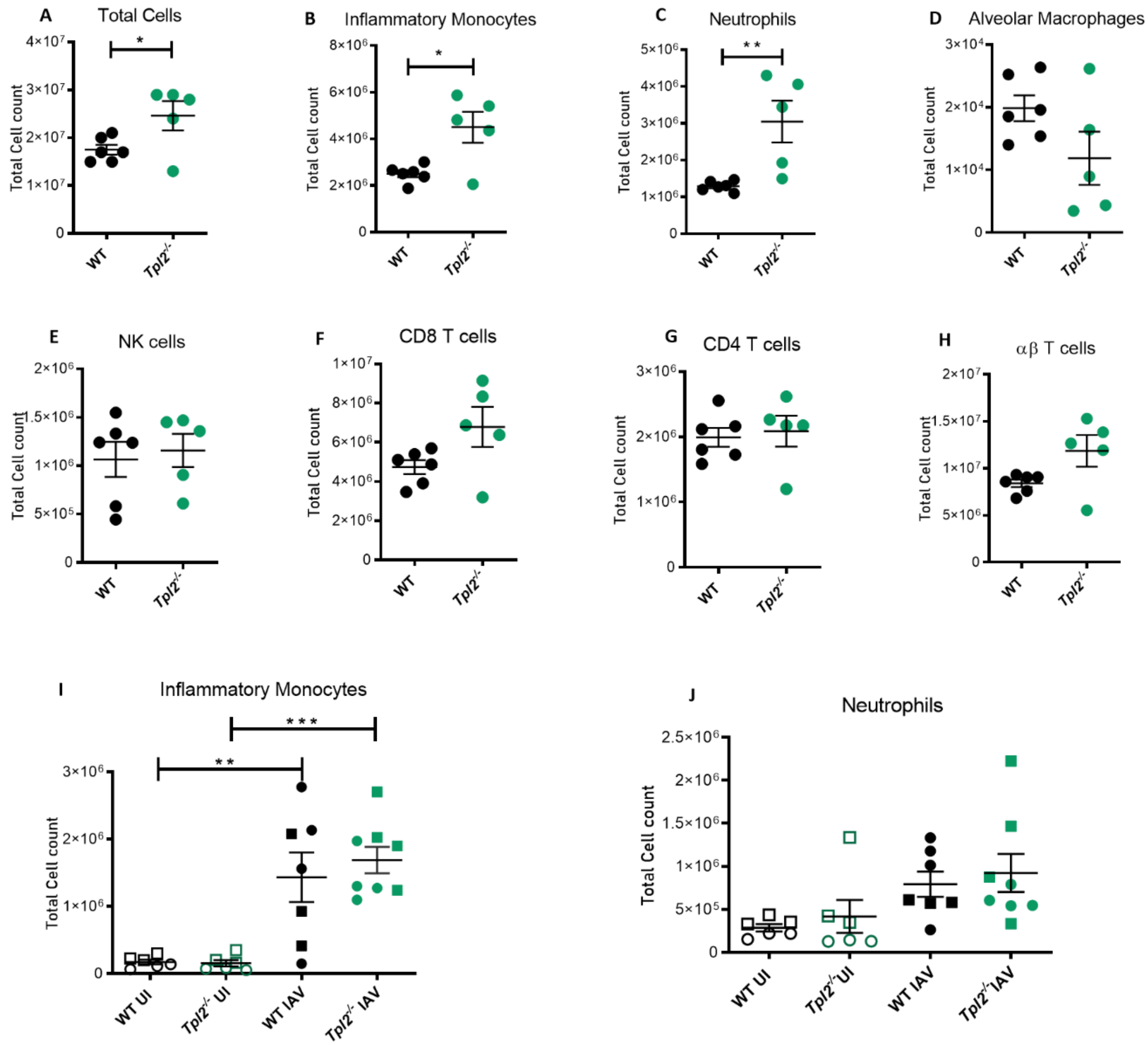

Figure 2.3. Excessive cellular influx of inflammatory monocytes and neutrophils in *Tpl2*$^{-/-}$ mice infected with influenza. WT and *Tpl2*$^{-/-}$ mice were infected intranasally with 10^4 pfu of influenza x31 and euthanized at 7 dpi. The lungs were lavaged, perfused with PBS, digested with collagenase, and interstitial leukocytes were enriched by Percoll density gradient centrifugation (A-H). Cell populations of infected WT (n=6) and *Tpl2*$^{-/-}$ (n=5) mouse lungs (post lavage, perfusion and digest) at 7 dpi are shown. Data are representative of 3 experiments. (I-J) Infiltrating cell populations were also assessed for wild type (n=7) and *Tpl2*$^{-/-}$ (n=8) mice at 4 dpi (post lavage, perfusion and digest), including uninfected controls (UI). Data are representative of 3 experiments.

Unpaired student's *t*-test*p<0.05, **p<0.01, ***p<0.001. Squares represent male mice, and circles represent female mice.

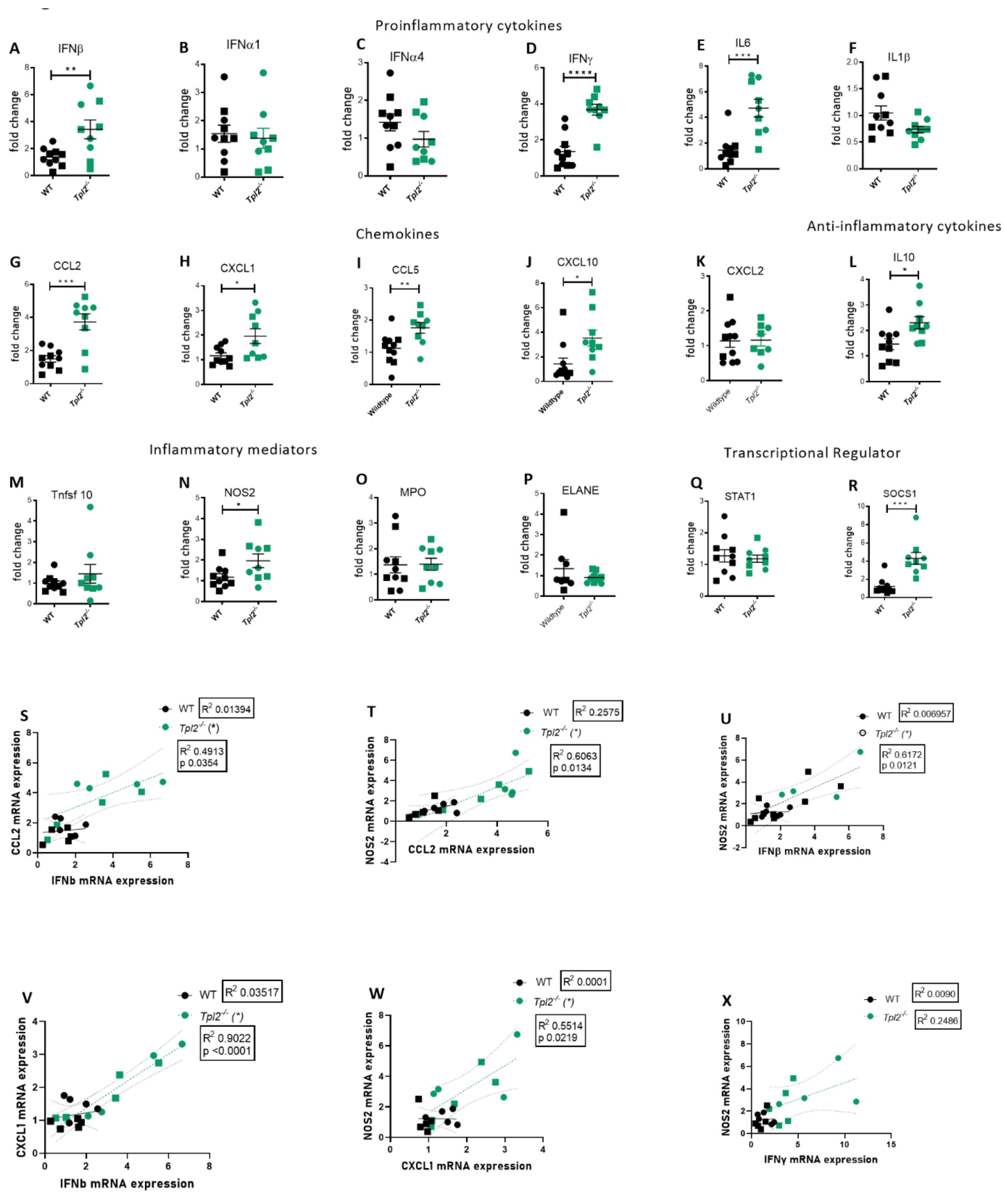

Figure 2.4. Increased mRNA expression of proinflammatory mediators in lungs of influenza-infected *Tpl2*$^{-/-}$ mice at 7 dpi. (A-R) WT (n=10) and *Tpl2*$^{-/-}$ (n=9) mice were infected intranasally

with 10^4 pfu of influenza X-31 and euthanized at 7 dpi. The lungs were homogenized, and RNA was extracted and analyzed for gene expression by real-time PCR for pro-inflammatory cytokines (A-F), chemokines (G-K), anti-inflammatory cytokine (L), inflammatory mediators (M-P) and transcriptional regulators (Q-R). Unpaired student's *t*-test*p<0.05, **p<0.01, ***p<0.001, ****p<0.0001. (S) Pearson's correlation of CCL2 mRNA versus IFN-β mRNA on day 7. *p<0.05 (T) Pearson's correlation of NOS2 mRNA versus CCL2 mRNA on day 7. *p<0.05 (U) Pearson's correlation of NOS2 mRNA versus IFNβ mRNA on day 7. *p<0.05 (V) Pearson's correlation of CXCL1 mRNA versus IFNβ mRNA on day 7. *p<0.05 (W) Pearson's correlation of NOS2 mRNA versus CXCL1 mRNA on day 7. *p<0.05 (X) Pearson's correlation of NOS2 mRNA versus IFN-γ mRNA on day 7. *p<0.05 Data are representative of 2 experiments. Squares represent male mice, and circles represent female mice.

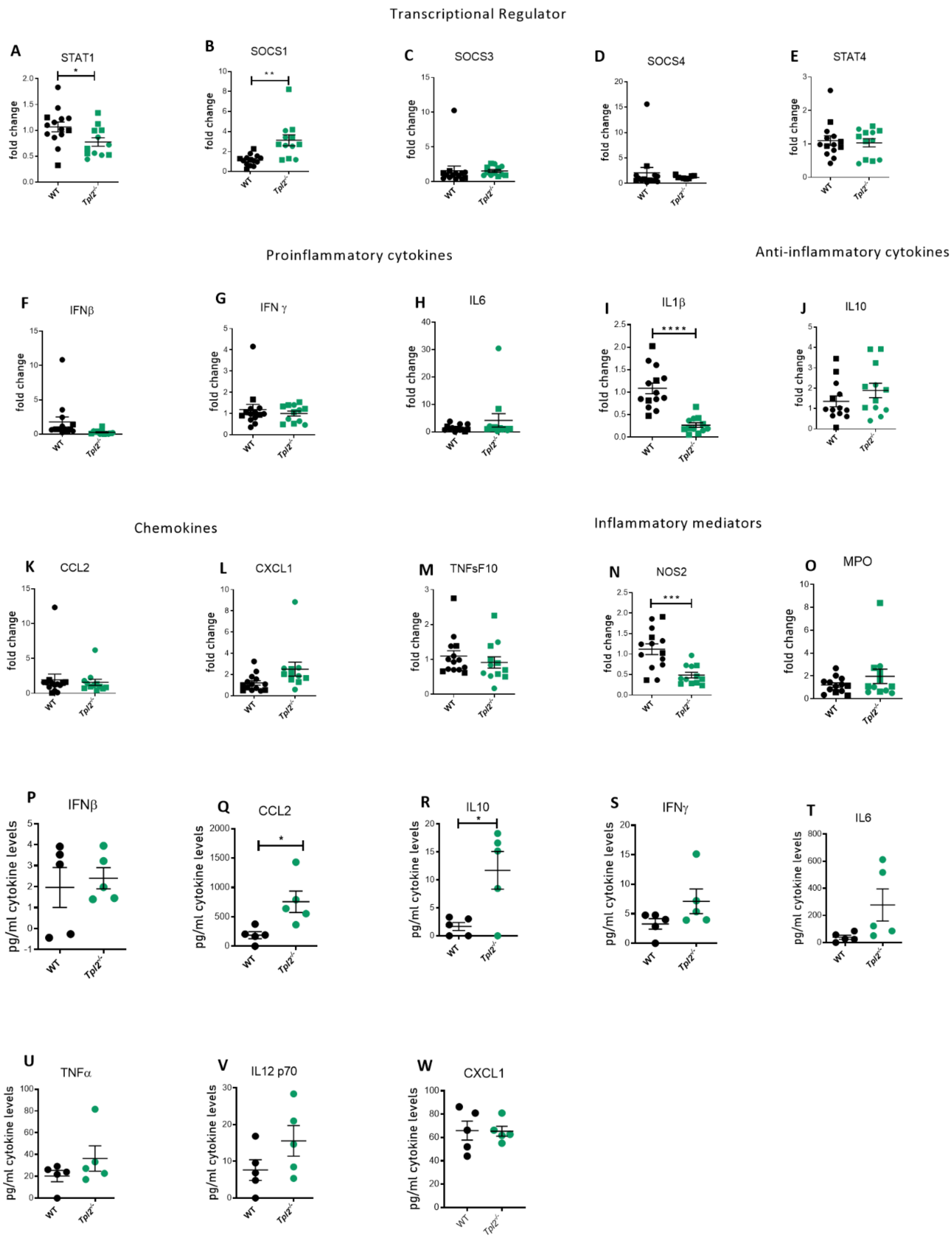

Transcriptional Regulator
A STAT1
B SOCS1
C SOCS3
D SOCS4
E STAT4
Proinflammatory cytokines
Anti-inflammatory cytokines
F IFNβ
G IFN γ
H IL6
I IL1β
J IL10
Chemokines
Inflammatory mediators
K CCL2
L CXCL1
M TNFsF10
N NOS2
O MPO
fold change
P IFNβ
Q CCL2
R IL10
S IFNγ
T IL6
U TNFα
V IL12 p70
W CXCL1
pg/ml cytokine levels
WT
Tpl2-/-

Figure 2.5. Ineffective suppression of CCL2 protein levels despite transcriptional repression in influenza-infected *Tpl2*$^{-/-}$ mice at 9 dpi. WT (n=5) and *Tpl2*$^{-/-}$ (n=5) mice were infected intranasally with 10^4 pfu of influenza x31 and euthanized at 9 dpi. (A-O) WT (14) & *Tpl2*$^{-/-}$ (11) lungs were homogenized and analyzed for gene expression for transcriptional regulators (A-E), pro-inflammatory cytokines (F-I), anti-inflammatory cytokines (J), chemokines (K-L) and inflammatory mediators (M-O). (P-W) The lungs were homogenized and assessed for cytokine protein levels. Squares represent male mice, and circles represent female mice. Data are representative of 2 experiments. Unpaired student's *t*-test *p<0.05, **p<0.01, ***p<0.001, ****p<0.0001.

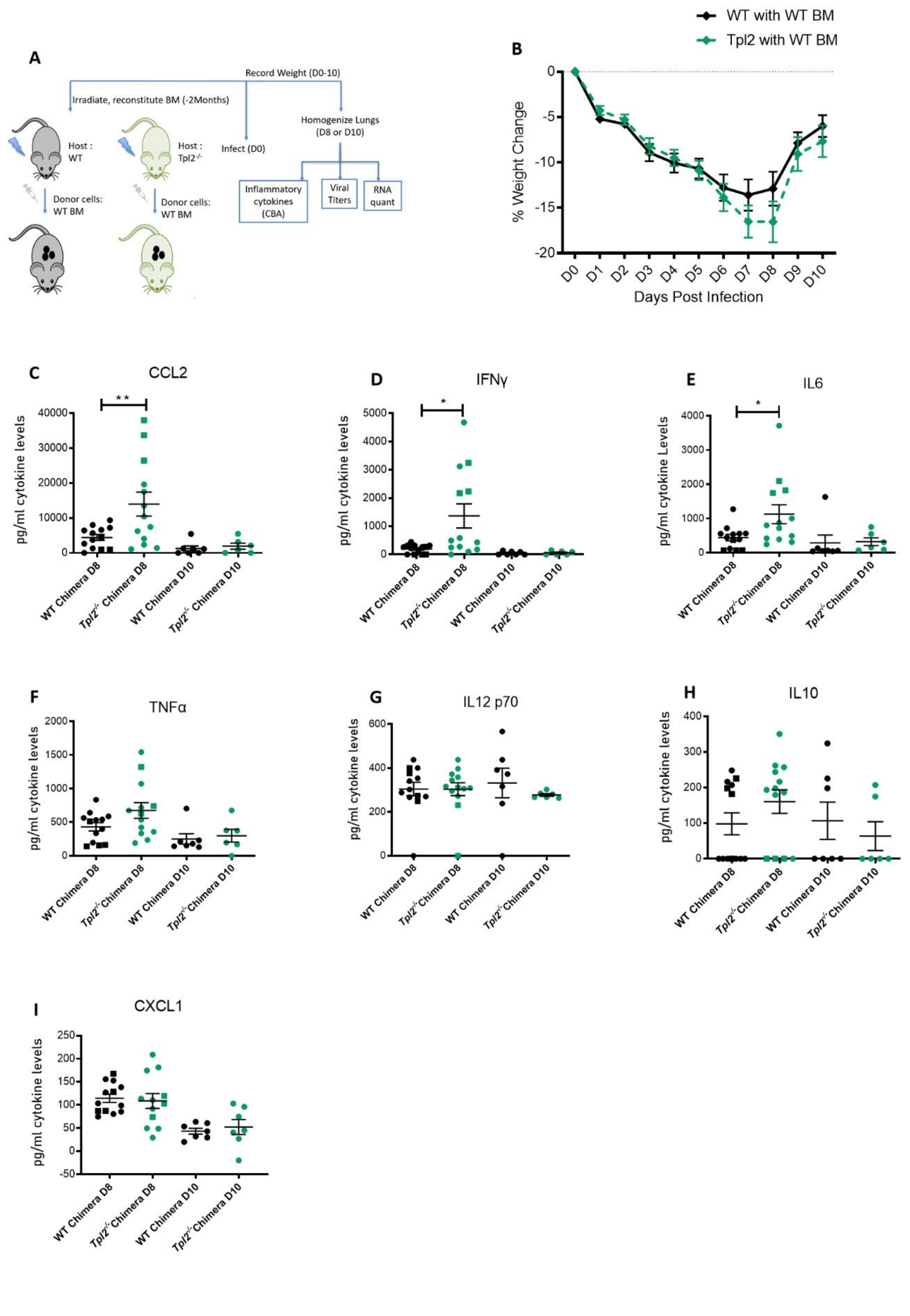
A
Record Weight (D0-10)
Irradiate, reconstitute BM (~2Months)
Host : WT
Host : Tpl2-/-
Donor cells: WT BM
Infect (D0)
Homogenize Lungs (D8 or D10)
Inflammatory cytokines (CBA)
Viral Titers
RNA quant
B
WT with WT BM
Tpl2 with WT BM
% Weight Change
Days Post Infection
C
CCL2
D
IFNγ
E
IL6
F
TNFα
G
IL12 p70
H
IL10
I
CXCL1
pg/ml cytokine levels
WT Chimera D8
Tpl2-/- Chimera D8
WT Chimera D10
Tpl2-/- Chimera D10

Figure 2.6. Tpl2 ablation in the radioresistant cells allows for an initial cytokine burst at 8 dpi, but they recover by 10 dpi. (A) Experimental outline for infection of chimeras WT or *Tpl2*$^{-/-}$ mice were irradiated and given WT bone marrow to reconstitute for 2 months. They were then infected and studied for 8-10 days for clinical outcome & cytokine examination on Day 8 or Day 10 post infection. (B) Weight loss curve shows that the *Tpl2*$^{-/-}$ chimeras show greater weight loss by day 8, but are able to recover their weights by day 10 post infection. Diamonds are used to represent that the data points are averaged for males and females (C-I) Cytokine expression at day 8 or day 10 post infection. Unpaired student's *t*-test *p<0.05, **p<0.01.

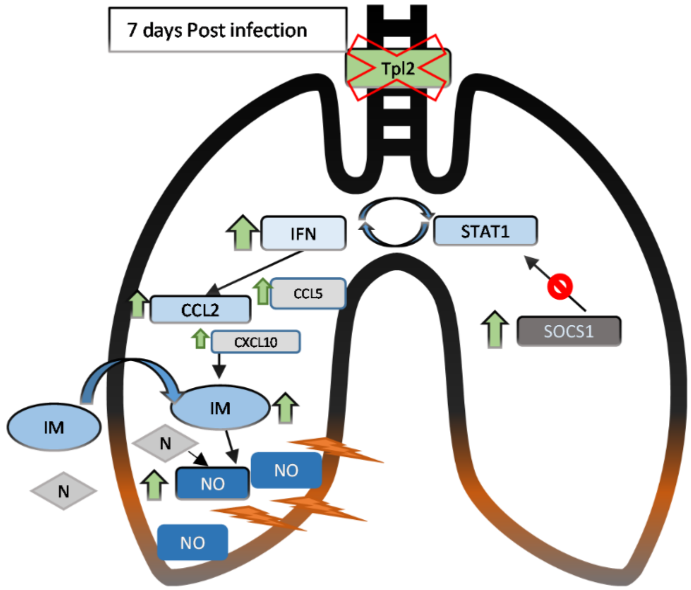

Figure 2.7: Tpl2 regulation of the Immune response for late stages of Influenza infection. In the lungs of influenza-infected *Tpl2*$^{-/-}$ mice at 7 dpi, upregulation (green arrows) of the IFNs and chemokines leads to recruitment and retention of inflammatory monocytes (IM, circles) and neutrophils (N, boxes) that lead to lung damage likely via nitric oxide (NO). IFN signaling also activates the SOCS1 transcriptional repressor, that suppresses STAT1 mRNA levels to limit further IFN signaling by 9 dpi. However, inefficient SOCS1-mediated repression in *Tpl2*$^{-/-}$ mice allows persistent CCL2 overexpression and inflammation, progressing to morbidity and mortality.

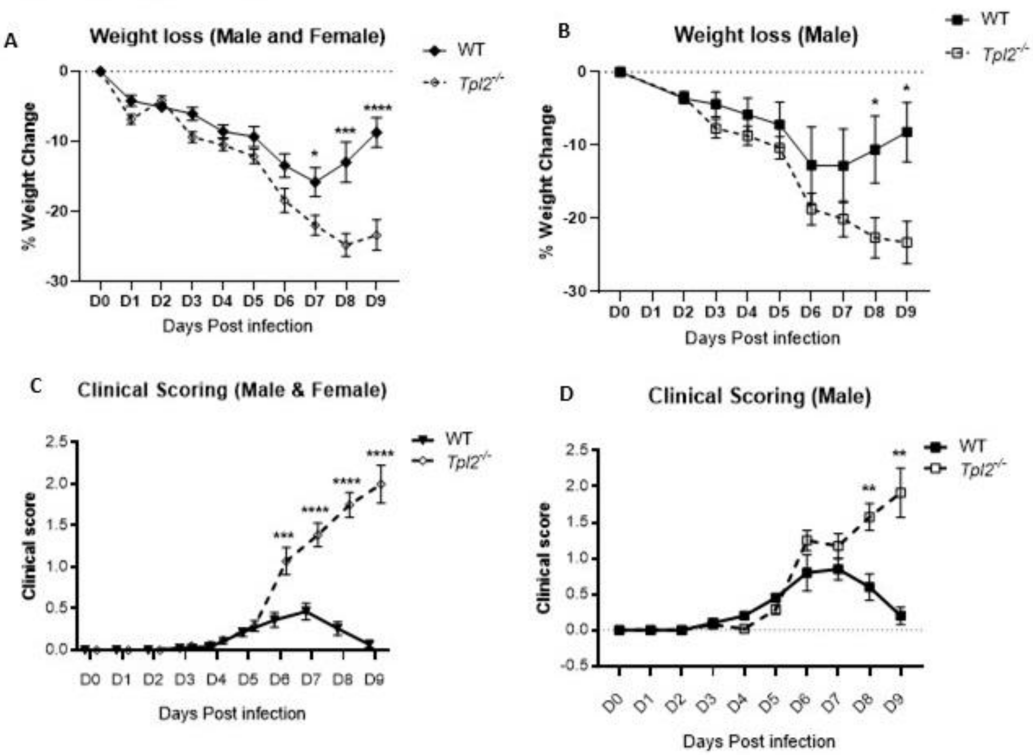

Supplementary Figure 2.8. Male mice show similar weight loss and clinical scores as female mice in response to influenza A virus. (A) Percent weight change of both female and male WT (n=21) versus *Tpl2*$^{-/-}$ (n=30) mice 9 dpi with 10^4 pfu influenza A virus strain x31. Data are representative of 5 experiments. Unpaired student's *t*-test; *p<0.05, **p<0.01, ***p<0.001, ****p<0.0001 (at each dpi). (B) Percent weight change of male WT (n=5) versus male *Tpl2*$^{-/-}$ (n=14) mice 9 dpi with 10^4 pfu influenza A virus strain x31. Data are representative of 3 experiments. (C-D) Progression of clinical symptoms including lethargy, piloerection, and hunching is shown throughout the course of infection for both sexes (C) with data representative of 5 experiments and for males only (D) with data representative of 3 experiments. Unpaired student's *t*-test; *p<0.05, **p<0.01, ***p<0.001, ****p<0.0001. Diamonds denote the inclusion of both males and female data points in the average; squares represent male data points only included in averages.

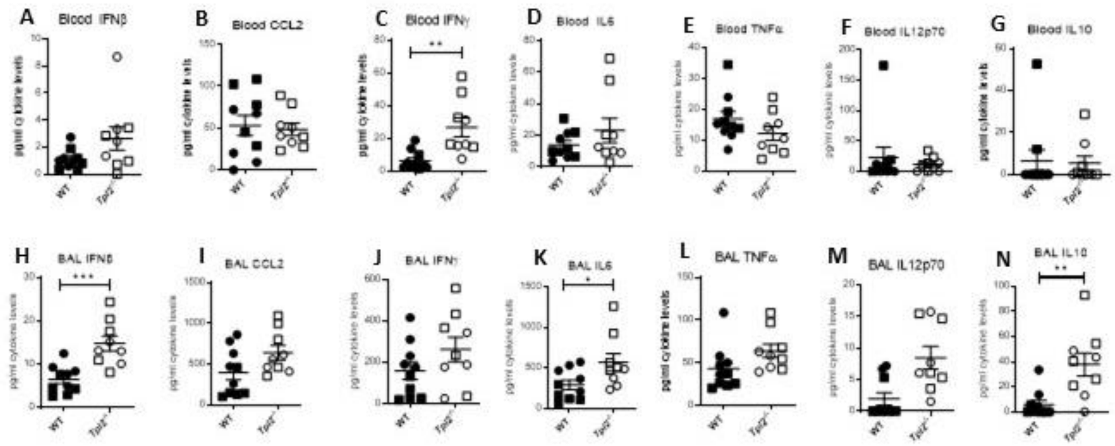

Supplementary Figure 2.9. Increased blood and BAL cytokines in influenza-infected *Tpl2$^{-/-}$* mice at 7 dpi. Wild type (n=10) and *Tpl2$^{-/-}$* (n=9) mice were infected intranasally with 10^4 pfu of influenza x31 and euthanized at 7 dpi. **(A-G)** The Blood was collected by cardiac puncture to analyze the cytokine expression**. (H-N)** PBS was intratrachially injected into the Bronchio-Alveolar spaces to collect the BAL fluid and then used to analyze cytokine expression. Squares represent male mice, and circles represent female mice. Data are representative of 2 experiments. Unpaired student's *t*-test *p<0.05, **p<0.01, ***p<0.001.

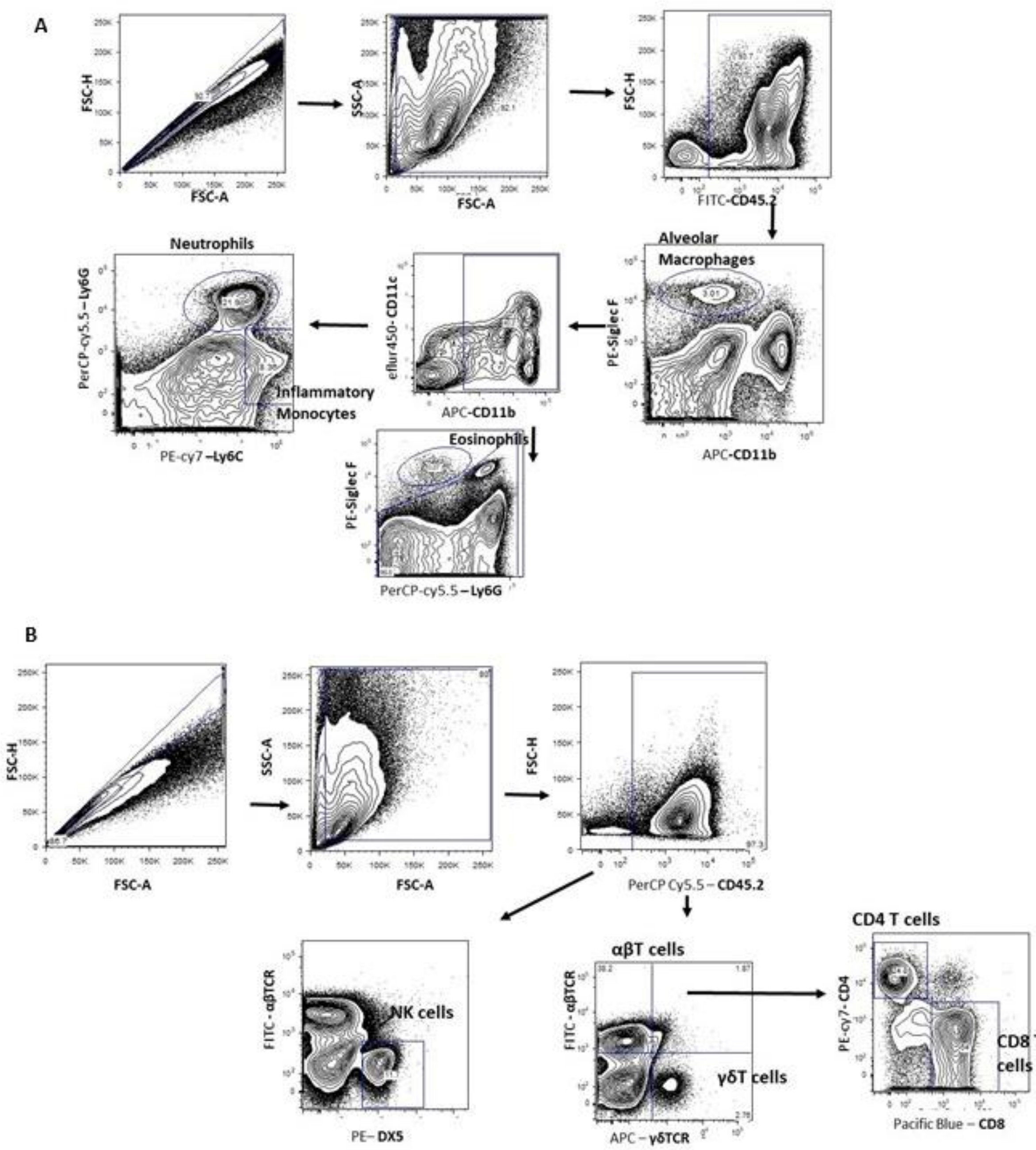

Supplementary Figure 2.10. Flow cytometry gating strategy used to differentiate populations. (A) Siglec F, CD11b, CD11c, Ly6C, Ly6G, CD45.2 (Stain 1); **(B)** TCRαβ, TCRγδ, CD4, CD8, DX5, CD45.2 (Stain 2).

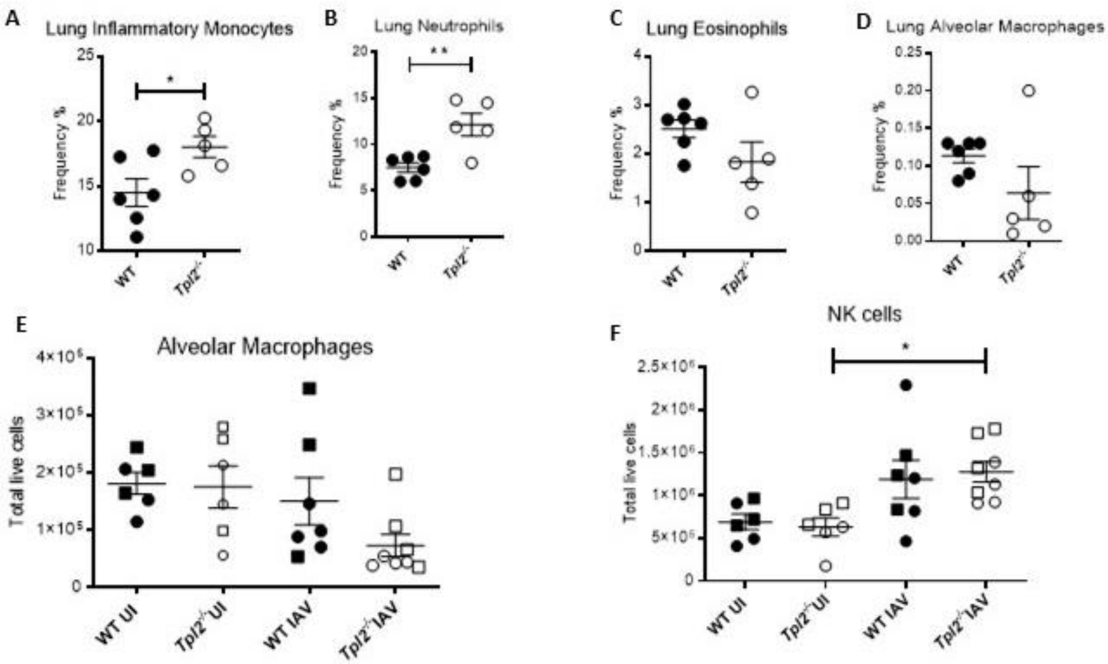

Supplementary Figure 2.11. Additional cellular profiling at 4pi and 7dpi. WT (n=6) and *Tpl2*$^{-/-}$ mice (n=5) were infected intranasally with 10^4 pfu of influenza x31 and euthanized at 7 dpi. The lungs were lavaged, perfused with PBS, digested with collagenase, and interstitial leukocytes were enriched by Percoll density gradient centrifugation. Squares represent male mice, and circles represent female mice. (A-D) lung cell frequencies(post lavage, perfusion and digest) are shown. (E-F) Total cell numbers in Lung(post lavage, perfusion and digest) at 4 dpi were determined by flow cytometry as specified in *Materials and Methods*. Data are representative of 3 experiments. Unpaired student's *t*-test *p<0.05, **p<0.01.

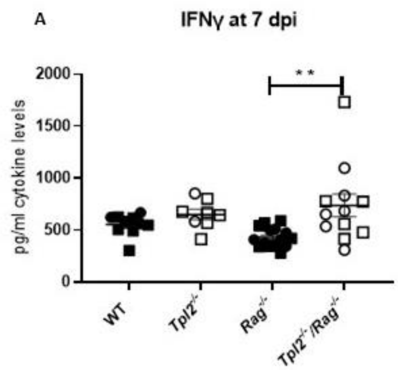

Supplementary Figure 2.12. Interferon γ levels are not affected in the absence of T cells in *Tpl2$^{-/-}$/Rag$^{-/-}$* mice compared to *Tpl2$^{-/-}$* infected mice at 7dpi. WT (n=10), *Tpl2$^{-/-}$* mice (n=8), *Rag$^{-/-}$* (n=15) & *Tpl2$^{-/-}$/Rag$^{-/-}$* (n=12) were infected intranasally with 10^4 pfu of influenza x31 and euthanized at 7 dpi. (A) IFNy levels in the homogenized lungs (not perfused or lavaged) assayed by Peprotech ELISA from infected mice at 7 dpi. Data includes 2 representative experiments. Squares represent male mice, and circles represent female mice. Unpaired student's *t*-test *p<0.05, **p<0.01.

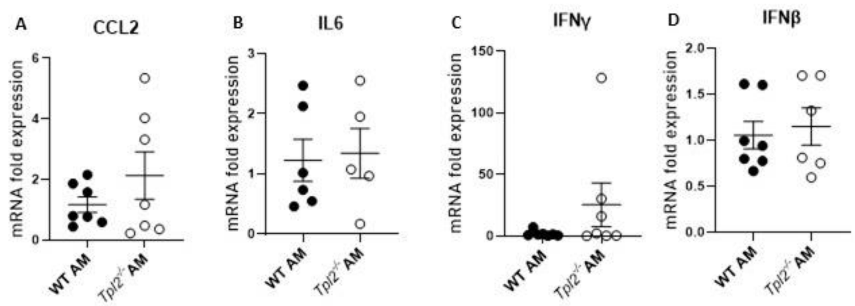

Supplementary Figure 2.13. No difference in cytokine expression between WT and *Tpl2*$^{-/-}$ alveolar macrophages for CCL2, IL-6 and IFN-γ. WT(n=7) and *Tpl2*$^{-/-}$(n=7) mice were infected intranasally with 10^4 pfu of influenza x31 and euthanized at 7 dpi. Their lungs were digested with collagenase and leukocytes were sorted out based on the flow gating strategy in Supplementary Figure 3 for Alveolar Macrophages (AM). (A-D) The cells were lysed in TRK lysis buffer, and the RNA was extracted, converted to cDNA and analyzed by qPCR using the respective Taqman probe and normalized to their WT counterparts, which was designated a value of 1. Data are representative of 2 experiments. Unpaired student's *t*-test was used to compare between WT and *Tpl2*$^{-}$ *p<0.05, **p<0.01, ***p<0.001, ****p<0.0001. Female mice were used for these experiments.

CHAPTER 3

TPL2 ABLATION INDUCES OVEREXPRESSION OF INTERFERON λ, CXCL1 AND NEUTROPHIL RECRUITMENT IN THE ABSENCE OF TYPE I INTERFERON REGULATION DURING INFLUENZA INFECTION

Latha K, Patel Y, Rao S and Watford WT. *Submitted to Scientific Reports*

ABSTRACT

Tumor progression locus 2 (Tpl2) is a serine-threonine kinase known to promote inflammation in response to various infectious agents. We have previously shown that *Tpl2*$^{-/-}$ mice succumb to infection with a normally low-pathogenicity strain of influenza (x31, H3N2). *Tpl2*$^{-/-}$ mice expressed increased levels of Interferon-β (IFN-β), chemokine CCL2 (Monocyte chemoattractant protein/MCP-1) and IFN-γ, which were accompanied by excessive pulmonary influx of monocytes and neutrophils. The goal of the current study is to evaluate the contribution of these mediators to morbidity and mortality in *Tpl2*$^{-/-}$ mice. Since Type 1 Interferons (T1 IFNs) are known to induce CCL2 during influenza, we examined the phenotype of *IFNAR1*$^{-/-}$*Tpl2*$^{-/-}$ mice to determine if increased morbidity and mortality were due solely to the Tpl2-dependent overexpression of IFN-β. In the absence of T1 IFN signaling, Tpl2 deficiency did not lead to increased CCL2 expression or monocyte recruitment, confirming that Tpl2 normally constrains influenza-induced inflammatory monocyte recruitment via inhibition of the T1 IFN/CCL2 axis. Unexpectedly, we observed excessive recruitment of neutrophils as early as 4 days post infection (dpi) in both *IFNAR1*$^{-/-}$ and *IFNAR1*$^{-/-}$*Tpl2*$^{-/-}$ mice compared to control mice, demonstrating a generalized inhibition of neutrophil recruitment via IFNAR1 signaling. However, among *IFNAR1*$^{-/-}$ strains, neutrophil recruitment was significantly increased in *IFNAR1*$^{-/-}$*Tpl2*$^{-/-}$ compared to *IFNAR1*$^{-/-}$ mice by 7 dpi, revealing a secondary pathway of neutrophil recruitment during influenza infections that is active in the absence of type I IFN signaling and inhibited by Tpl2. In addition to the neutrophil recruitment, the cytokines IL-6, IFN-γ, IL-1β, and G-CSF were upregulated in both the *IFNAR1*$^{-/-}$ and *IFNAR1*$^{-/-}$*Tpl2*$^{-/-}$ strains, but IFN-λ and CXCL1 was overexpressed only in the *IFNAR1*$^{-/-}$*Tpl2*$^{-/-}$ mice at 7 dpi. These findings highlight a role for Tpl2 in restricting the expression of IFN-λ, CXCL1 and pulmonary recruitment of neutrophils during influenza infection, independent of T1

IFN regulation. This information positions Tpl2 for potential host-targeted therapies to treat severe cases of influenza which are typically associated with excess type I IFNs and robust inflammatory monocyte recruitment.

INTRODUCTION

Influenza disease worldwide results in 3 to 5 million cases of severe illness, and about 290,000 to 650,000 respiratory deaths annually, by WHO estimates[26]. While annual vaccinations help to combat seasonal infections by generating immunologic memory, there are several factors that hamper this protection, including failed predictions of prevalent circulating strains and poor public compliance. The available antiviral treatment is most effective when initiated 48 hours post onset of symptoms[301,302], however specific testing for influenza antigens is required to start treatment[36,303,304]. Additionally, development of drug resistance strains also is an impediment to successful treatment[305–307]. Furthermore even seasonal infections can lead to severe disease in certain cases, progressing rapidly to hospitalization, pneumonia, acute respiratory distress and death, especially in people with comorbidities[36,308].The groups at higher risk for severe influenza include individuals below 6 years of age and above 60 years, as well as people with other risk factors like smoking, heart disease, obesity, chronic pulmonary disease, pregnancy, genetic predisposition to interferonopathies and immune response alterations due to sex steroid treatment[29–34]. In addition, the disease is generally more severe in epidemics involving highly pathogenic strains like the avian H1N5 strain or the swine pandemic strain, H1N1[309–312].

Influenza viruses belong to the Orthomyxoviridae family and have an enveloped genome of negative sense single-stranded RNA[1]. Infected host cells sense influenza infection via recognition of pathogen-associated molecular patterns (PAMPs) such as viral RNA, by host pathogen recognition receptors (PRRs). The primary PRRs involved in influenza recognition include the RIG-I-like receptor family, Toll-Like receptors (TLRs) and the inflammasome complex, of which RIG-I activation is the predominant inducer of antiviral interferons (IFNs)[70]. RIG-I is able to recognize the presence of 5′-triphosphate (5′ppp) or a 5′-diphosphate (5′pp) group of the viral genomic RNA, while it is being assembled into a progeny virion in the cytoplasm[66].

One of the most prominent and early anti-viral responses is the production of the Type 1 interferons (T1 IFN), including a single IFN-β and thirteen IFN-α subtypes[89,90]. Upon recognition of viral components by RIG-I, induction of T1 IFNs[91] leads to activation of TANK-binding kinase 1 (TBK1). TBK1 activates IFN-regulatory factor 3 (IRF3) or TGFβ-activated kinase 1 (TAK1) to ultimately activate NFκB[89,90]. Collectively, this leads to IRF3-mediated nuclear transcription of the primary interferons, IFN-β and IFN-α4[313]. Once secreted, they bind to the heterodimeric Interferon Alpha Receptor (IFNAR1 and IFNAR2) on the cell surface[90]. This leads to phosphorylation of the Janus Kinases 1 and 2 (JAK1 and JAK2) proteins that, in turn, phosphorylate and activate the Signal Transducers and Activators of Transcription 1 and 2 (STAT1 and STAT2)[89,92]. STAT1 and STAT2 together with IRF9, form the Interferon Stimulated Gene Factor 3 (ISGF3) complex. This complex translocates to the nucleus where it stimulates the expression of the transcription factor interferon regulatory factor 7 (IRF7), which is required for expression of all other IFN-α subtypes[93]. T1 IFNs also induce other IFN-stimulated genes (ISGs) that collectively mediate the antiviral response. For example, IFITM3 prevents viral egress by altering endosomal pH[94]; MxA activates the NLPR3 inflammasome by sensing viral proteins[75].; OasL mimics polyubiquitination to enhance the RIG-I recognition of viral RNA[95,96]. and ISG15 is involved in the prevention of systemic inflammatory cytokine response[97]. IFN-β stimulates epithelial cells to secrete higher levels of TNF, chemokines CCL2, CCL5, CXCL8 and CXCL10

[81]. These chemokines collectively recruit monocytes and natural killer (NK) cells to the site of infection[99–101].

One host regulator of the T1 IFN response is the serine-threonine kinase Tumor Progression Locus 2 (Tpl2), also known as MAP3K8 and Cancer Osaka Thyroid (*Cot*)[199]. TPL2 is a member of the MAP kinase family that is prominently expressed in multiple organs, including the spleen, thymus, lung, endometrium, liver and intestine[200–203]. Prior to activation, Tpl2 is in a complex with NFκB inhibitory protein-1 (NFκB-1) p105 and ABIN-2 (A20-binding inhibitor of NF-κB-2)[213]. Stimulation of various receptors, including TLRs[206,207], TNF family receptors[208,209], IL-1 receptor[210] and some G protein-coupled receptors (GPCR)[211], leads to Tpl2 activation downstream of the IKK complex. The IKK complex is made up of the IKKα, IKKβ, and IKKγ[212] Specifically, IKK activation leads to NFκBp105 phosphorylation, ubiquitination and limited proteosomal degradation, resulting in the release of Tpl2 from its negative regulation[214]. Tpl2 kinase activity is subsequently triggered by IKK-mediated phosphorylation [214]. Active Tpl2 mediates downstream signaling via multiple pathways, including NFκB, IRFs, ERK, JNK and p38[207,213,221].

Tpl2 promotes host immunity to a variety of intracellular pathogens including *Toxoplasma gondii*, *Listeria monocytogenes*, *Mycobacterium tuberculosis*, Group B Streptococcus and influenza A virus[222,228,232,314] Notably, impaired host resistance to both *Mycobacterium tuberculosis* and Group B Streptococcus was associated with alterations in the T1 IFN response. Infection of *Tpl2*$^{-/-}$ mice with *Mycobacterium tuberculosis* significantly increased T1 IFN responses, and susceptibility of *Tpl2*$^{-/-}$ mice to *M. tuberculosis* could be rescued by simultaneously interrupting T1 IFN signaling in *IFNAR1*$^{-/-}$*Tpl2*$^{-/-}$ mice[228]. Conversely, increased susceptibility to Group B Streptococcus was associated with decreased T1 IFN response[314]. On examination of T1 IFN regulation by Tpl2 on a cellular scale, we note that*Tpl2*$^{-/-}$ macrophages and dendritic cells over-produce TI IFNs compared to WT cells, whereas *Tpl2*$^{-/-}$ pDCs display significantly reduced TI IFN production[222,225,229]. Thus, we see that Tpl2 regulation of T1 IFN responses are regulated in a cell type- and stimulus-specific manner.

We have previously shown that *Tpl2*$^{-/-}$ mice exhibit enhanced morbidity and mortality to influenza infection, with deteriorating clinical symptoms from 7 to 9 dpi[315]. Live virus was undetectable by 9 dpi, confirming complete, albeit delayed, viral clearance in the *Tpl2*$^{-/-}$ mice as noted in our previous study. Despite viral clearance, *Tpl2*$^{-/-}$ mice showed hypercytokinemia and excessive pulmonary influx of inflammatory monocytes and neutrophils by 7 dpi. Increased inflammatory monocyte and neutrophil recruitment in *Tpl2*$^{-/-}$ mice correlated with increased expression of T1 IFN and the inflammatory mediator, nitric oxide synthase 2 (NOS2). These findings demonstrate that Tpl2 serves a regulatory role during influenza infection by tempering the production of T1 IFNs and IFN-stimulated chemokines. In this way, Tpl2 ablation leads to excessive pulmonary accumulation of inflammatory cells known to cause physical trauma to the respiratory tract[101,251,283]. The goal of the current study is to determine whether enhanced morbidity and mortality in *Tpl2*$^{-/-}$ mice can be alleviated by the absence of T1 IFN signaling and to gain additional insight into increased neutrophil recruitment observed in *Tpl2*$^{-/-}$ mice.

MATERIALS AND METHODS

Ethics Statement

All animal experiments were performed in accordance with “The Guide for Care and Use of Laboratory Animals” and were approved by the University of Georgia Institutional Animal Care and Use Committee (IACUC).

Mice and influenza infections

Wild type (WT) C57BL/6 and *Rag1*$^{-/-}$ mice were purchased from the Jackson Laboratory and bred in-house. *Tpl2*$^{-/-}$ mice backcrossed 10 generations onto the C57BL/6 strain were kindly provided by Dr. Philip Tsichlis[206]. Animals were housed in microisolator cages in the Central Animal Facility of the College of Veterinary Medicine. *IFNAR1*$^{-/-}$ mice were kindly provided by Dr. Biao He (University of Georgia).

Age-matched, 6- to 8-week-old WT, *Tpl2*$^{-/-}$, *IFNAR1*$^{-/-}$ and *IFNAR1*$^{-/-}$*Tpl2*$^{-/-}$ mice were anesthetized with approximately 250 mg/kg of 2% weight/volume Avertin (2,2,2-Tribromoethanol, Sigma) followed by intranasal instillation of 50 µl PBS containing 10^4 pfu of influenza A/HKX31 (H3N2, hereafter referred to as x31). The stock virus was propagated in specific pathogen free eggs (Poultry Diagnostics and Research Center, UGA) and then tittered as described previously[315].

Mice were studied for their susceptibility to infection by measuring daily weight loss and clinical scores according to the following index: piloerection, 1 point; hunched posture, 2 points; rapid breathing, 3 points. Mice with a cumulative score of 5 or that had lost 30% of their initial body weight were humanely euthanized.

Tissue collection and analysis for virus titers, cytokine, and gene expression

Mice were sacrificed at 7 dpi. The lungs were lavaged with 1ml of PBS instilled twice into the lungs and then perfused with 10 ml of PBS injected directly into the right ventricle of the heart. Alternatively, some whole lungs were homogenized without lavage or perfusion, where noted. Lungs were harvested into 1 ml of PBS and homogenized in a bead mill homogenizer (Qiagen

Tissue Lyser II) at 25 hz for 2-4 min. The homogenate was centrifuged at 500 x *g* for 5 min, and the pre-cleared homogenate was: (1) directly aliquoted for viral titer assessment with the titration protocol described previously[315], (2) lysed in TRK tissue lysis buffer (E.Z.N.A Omega Bio-Tek) for analysis of gene expression or (3) further centrifuged at 5000 x *g* for 5 min to clarify the homogenate for cytokine analysis by ELISA. For gene expression analysis, RNA was extracted, converted to cDNA using a High Capacity RNA-to-cDNA kit (Thermo Fisher) and assessed for gene expression. Sensifast Probe Hi-ROX kit (BIO-82020 Bioline) and the following probes (Applied Biosystems) were used: IFN-β1 (Mm00439552), IFN-γ (Mm0116813), IFN-λ3 (Mm00663660), IFITM3 (Mm00847057), IL-6 (Mm00446190), IL-1β (Mm00434228), ISG15 (Mm01705338), CCL2 (Mm00441242), CXCL1 (Mm04207460), TNFSF10 (Mm01283606), NOS2 (Mm00440502), MPO (Mm01298424) and SOCS1 (Mm01342740). The qPCR was run on StepOne Plus instrument (Applied Biosystems) and gene expression performed using the $\Delta\Delta C_T$ method as describe previously[315] relative to an internal actin control and normalized to the WT samples set to a value of 1. Cytokine quantitation was performed using a Mouse Inflammation Cytometric Bead Array (CBA, analytes IL-6, IFN-γ, MCP-1, TNF, IL-10 and IL-12p70, Becton Dickenson), Mouse ProcartaPlex (analytes IL-1β, IL-28, GM-CSF, Invitrogen), Standard murine ABTS ELISA Development kit (CXCL1, IFN-γ, IL-6, CCL2 and IL-1β, Peprotech) and LumiKine Xpress kits (IFN-β, Invivogen).

Cellular Analysis

At 4 and 7 dpi, the following protocol was used to assess lung cellular composition. After the Bronchoalveolar Lavage Fluid (BALF) harvesting and lung perfusion as noted above, the lungs were harvested, minced with razor blades and incubated in EDTA solution[315] for 1 hour at 37^0C with shaking at 250 RPM. Post centrifugation, the tissue was further digested in collagenase solution[315] for 30 min at 37°C in a shaking incubator at 350 RPM. The digested tissue was passed through a 70 µm cell strainer, and cells were centrifuged at 350 x g for 10 min, resuspended in 44% Percoll (GE Healthcare) and layered on top of 67% Percoll. After density gradient centrifugation at 900 x g for 20 min (without brake), the cells were recovered from the interface, washed and counted for staining as detailed previously[315].

Cells were stained at 4°C for 20 min with fluorescently labeled antibodies against the following cell surface markers: Siglec F, CD11b, CD11c, Ly6C, Ly6G, CD45.2 (Stain 1); TCRαβ, TCRγδ, CD4, CD8, DX5, CD45.2 (Stain 2). The cells were fixed with 1% formalin and analyzed on the LSR II flow cytometer (BD Biosciences). CD45.2-gated hematopoietic-derived leukocyte populations were characterized as follows: inflammatory monocytes (IM; Siglec F^- $CD11b^{high}$, $CD11c^{low}$ $Ly6C^+$), neutrophils (Siglec F^- $CD11b^{high}$, $CD11c^{low}$ $Ly6G^+$), alveolar macrophages (AM; Siglec F^{high} $CD11b^{int}$), eosinophils (Siglec F^{high} $CD11b^{high}$), NK cells (αβ TCR^- $DX5^+$), CD4 T cells (αβ TCR^+ $CD4^+$), CD8 T cells (αβ TCR^+ $CD8^+$), and γδ T cells (αβ TCR^- γδ TCR^+).

Cellular Sort for Gene Expression Analysis

At 7 dpi, lungs from all four genotypes of mice were harvested, digested and single cell suspensions were generated as described above. Cells were stained with Stain 1 above, and inflammatory monocytes, neutrophils and alveolar macrophages were isolated by fluorescence-activated cell sorting (FACS) using the same gating strategy on a MoFlo Astrios (BD Biosciences). Sorted populations of cells were lysed in TRK lysis buffer, RNA was extracted and converted into cDNA. Gene expression was quantified as described above with the results expressed relative to the actin internal control and the WT sample for each cell type set to 1 using the $\Delta\Delta C_T$ method.

Alternatively, to facilitate comparisons across cell types, gene expression was also calculated relative to the actin internal control and the WT alveolar macrophages (AM) as the baseline.

Therapeutic Antibody Interventions to Treat Influenza

Age-matched, 6- to 8-week-old, WT, *Tpl2*$^{-/-}$, *IFNAR1*$^{-/-}$ and *IFNAR1*$^{-/-}$*Tpl2*$^{-/-}$ mice were infected intranasally with 10^4 pfu of x31 mouse-adapted influenza virus. On days 5 and 7 post infection, the mice were administered intraperitoneally (i.p.) either 200 µg isotype control antibody (clone 2A3#BE0089, BioXCell), 200 µg anti-Ly6G antibody (clone 1A8 #BE0075-1, BioXCell) or 2.5 µg anti-IFN-λ antibody (clone 244716 #MAB17892, R&D Systems). Mice were weighed and scored for clinical symptoms throughout the course of infection and treatment.

Statistical Analysis

P values were calculated with GraphPad PRISM software version 9.2.0(332) using One-way ANOVA with Tukey's multiple comparisons test. Data represent means ± SEM. Survival data are graphed as Kaplan-Meier plots using GraphPad PRISM software, and *p* values were determined by Mantel-Cox test. Differences were considered statistically significant if $p \leq 0.05$.

RESULTS

Tpl2-deficient mice display increased disease severity to influenza, independent of T1 IFN signaling

In order to assess the contribution of T1 IFN signaling to severe disease in influenza-infected *Tpl2*$^{-/-}$ mice, *Tpl2*$^{-/-}$ mice were intercrossed with *IFNAR1*$^{-/-}$ mice to generate *IFNAR1*$^{-/-}$*Tpl2*$^{-/-}$ mice. WT, *Tpl2*$^{-/-}$, *IFNAR1*$^{-/-}$ and *IFNAR1*$^{-/-}$*Tpl2*$^{-/-}$ mice were infected with 10^4 pfu influenza A virus strain x-31 (IAV x31; H3N2), and their weight loss, clinical symptoms and survival were monitored over the course of disease (Fig 3.1A-C). Clinical symptoms are plotted only through day 9 when peak morbidity and mortality occurred, because loss of the severely ill mice subsequently biased the average clinical scores (Fig 3.1C). Similar to what we observed previously[315], WT mice displayed transient weight loss and mild clinical symptoms at 7 dpi and recovered by 9 dpi. In contrast, *Tpl2*$^{-/-}$ mice showed significantly greater weight loss and more severe clinical symptoms compared to WT mice between 7 and 9 dpi, at which time approximately 60% of *Tpl2*$^{-/-}$ mice met the humane endpoints of the study (Figure 3.1A-C). *IFNAR*$^{-/-}$*/Tpl2*$^{-/-}$ mice showed similarly poor outcomes to influenza infection as *Tpl2*$^{-/-}$ mice in terms of weight loss, clinical symptoms and had modest increase in mortality by difference of 1 day for median survival compared to *Tpl2*$^{-/-}$ mice (Figure 3.1C). Notably, *IFNAR*$^{-/-}$ mice showed trending differences in mortality compared to the *IFNAR*$^{-/-}$ *Tpl2*$^{-/-}$ mice, with significantly less weight loss and clinical scores compared to both *IFNAR1*$^{-/-}$ *Tpl2*$^{-/-}$ and *Tpl2*$^{-/-}$mice at 9 dpi (Figure 3.1A-B). *IFNAR1*$^{-/-}$ mice that survived beyond 7 dpi, recovered their weights similar to WT mice (Figure 3.1A). These data demonstrate that interferon signaling blockade is insufficient to reverse the morbidity and mortality in influenza-infected *Tpl2*$^{-/-}$ mice.

When we assessed each sex separately to evaluate sex as a biological variable, we found that both males and females of either genotype showed the same trends, with higher weight loss and clinical scores for the *Tpl2*$^{-/-}$and *IFNAR1*$^{-/-}$*/Tpl2*$^{-/-}$ mice during the later stages of infection. However, we did note slightly more points of significance in the female weight loss and clinical comparison (Supplementary Figure 3.8 A-D).

Increased inflammatory monocyte recruitment to lungs of influenza-infected *Tpl2*$^{-/-}$ mice is dependent on type I IFN signaling.

To gain insight into the contribution of T1 IFN signaling to cellular recruitment, we first assessed monocyte recruitment in all four strains of mice. Consistent with our previous study[315], we observed excessive influx of monocytes to the lungs of *Tpl2*$^{-/-}$ mice, and this phenotype was reversed in both *IFNAR1*$^{-/-}$ strains(Figure 3.2A), demonstrating that increased T1 IFN signaling in influenza-infected *Tpl2*$^{-/-}$ mice is responsible for the increased monocyte recruitment to the lungs. Cytokine and gene expression profiling surprisingly showed that IFN-β protein and mRNA levels were highest in the lungs of *IFNAR1*$^{-/-}$*Tpl2*$^{-/-}$ (Figure 3.2B, D). However, analysis of the IFN-inducible chemokine CCL2 (MCP-1) showed the highest protein and mRNA levels in lungs of *Tpl2*$^{-/-}$ mice (Figure 3.2C, E). Likewise, mRNA expression of ISGs including ISG15, IFITM3 as well as the inducible negative regulator of T1 IFN signaling, SOCS1, are all overexpressed only in *Tpl2*$^{-/-}$ mice at 7 dpi (Figure 3.2F-H), reflecting the inability of the *IFNAR1*$^{-/-}$ strains to transduce T1 IFN signals. These data demonstrate that blockade of T1 IFN signaling prevents the excessive monocyte recruitment seen within *Tpl2*$^{-/-}$ mice. Therefore, it was unclear why the *IFNAR1*$^{-/-}$*Tpl2*$^{-/-}$ mice remained severely ill. We also assessed viral titers in the various strains, because T1 IFN signaling is known to mediate viral control. Consistent with our previous study[222], viral titers were modestly increased in *Tpl2*$^{-/-}$ mice compared to WT mice at 7 dpi (Supplementary Figure 3.9A). Importantly, viral titers were only increased in the *IFNAR1*$^{-/-}$ background if Tpl2 was also ablated, demonstrating that viral loads were higher in the absence of Tpl2, irrespective of IFNAR signaling (Supplementary Figure 3.9A-C) The only difference noted here was that of the viral titers upregulated in the intact lungs(Supplementary Figure 3.9A), the tissue had the predominant viral load in the *IFNAR1$^{-/-}$Tpl2$^{-/-}$* mice(Supplementary Figure 3.9B) whereas the BALF contained the excessive viral load of the *Tpl2$^{-/-}$* mice(Supplementary Figure 3.9C)

IFNAR1$^{-/-}$Tpl2$^{-/-}$ mice display increased neutrophil recruitment at 7 dpi accompanied by overexpression of CXCL1 and IFN-λ

Cellular profiling revealed that the only other cell type that was differentially recruited to the lungs of these mouse strains was neutrophils (Supplementary Figure 3.10A-D), with the highest recruitment seen in the *IFNAR1$^{-/-}$Tpl2$^{-/-}$* mice at 7 dpi (Figure 3.3A). Along with this enhanced influx of neutrophils, we observe increased expression of cytokines and chemokines previously implicated in neutrophil recruitment[99,121,257,298,316,317], including IFN-γ, IL-6, IL-1β, and G-CSF in both *IFNAR1$^{-/-}$* and *IFNAR1$^{-/-}$Tpl2$^{-/-}$* mice (Figure 3.3B-E), with similar trends noted at the mRNA level (Supplemental Figure 3.11A-F). Notably, IFN-λ was the only cytokine upregulated solely in the *IFNAR1$^{-/-}$Tpl2$^{-/-}$* mice (Figure 3.3F). Although we did not see any differences in protein expression of the chemokine CXCL1 in the perfused and lavaged lungs of infected mice (Figure 3G), it was solely upregulated by mRNA expression in the *IFNAR1$^{-/-}$Tpl2$^{-/-}$* mice at 7 dpi (Supplemental Figure 3.11F). Since CXCL1 has previously been reported to recruit neutrophils in the absence of interferon signaling during influenza infection[100], we also examined protein expression in intact lungs (without lavage or perfusion) and noted that the expression of CXCL1 is significantly upregulated solely in the lungs of *IFNAR1$^{-/-}$Tpl2$^{-/-}$* mice (Figure 3.3H), with no alterations noted for IFN-γ, IL-6 or CCL2 (Figure 3.3I-K).

Neutrophils are excessively recruited to the lungs of IFNAR1$^{-/-}$ mouse strains as early as 4 dpi via upregulation of CXCL1 expression in the absence of T1 IFN signaling

At 7 dpi, we have observed the overexpression of IFN-λ and CXCL1 along with enhanced pulmonary recruitment of neutrophils, which are normally involved in the early response to influenza infection[318,319]. In order to distinguish whether this recruitment was altered only by 7 dpi or if it occurred earlier, during innate immune response, and persisted through day 7 post infection, we examined the cellular recruitment profile of the lungs at 4 dpi. Inflammatory monocytes were not differentially recruited to the lungs at 4 dpi (Figure 3.4A). By contrast, neutrophils were excessively recruited in both *IFNAR1*$^{-/-}$ and *IFNAR1*$^{-/-}$*Tpl2*$^{-/-}$ mice by 4 dpi (Figure 3.4B). Examination of the cytokine profile of whole lung homogenates, showed that CXCL1 expression was significantly upregulated at 4 dpi in the *IFNAR1*$^{-/-}$*Tpl2*$^{-/-}$ mice (Figure 3.4C), with no significant changes noted in the other neutrophil-recruiting cytokines (IFN-γ, IL-6, IFN-λ, GCS-3); assessed at the protein level (Figure 3.4D-F) or by transcriptional expression (Figure 3.4G-H). Notably, a significant decrease in the expression of the monocyte-recruiting chemokine, CCL2, was noted in both *IFNAR1*$^{-/-}$ strains compared to *Tpl2*$^{-/-}$ mice, corresponding to the block in inflammatory monocyte recruitment in those strains (Figure 3.4F). However, IFN-β expression was upregulated in the *Tpl2*$^{-/-}$ mice at 4 dpi compared to all other strains (Figure 3.4I). Consequently, increased expression of the type I IFN-inducible chemokine CCL2 (MCP-1) was also observed in *Tpl2*$^{-/-}$ compared to both *IFNAR1*$^{-/-}$ *and IFNAR1*$^{-/-}$*Tpl2*$^{-/-}$ strains, confirming an active IFN-β-CCL2 pathway at 4 dpi (Figure 3.4I, J). Collectively, these data suggest that the excessive neutrophil recruitment observed in both *IFNAR1*$^{-/-}$ and *IFNAR1*$^{-/-}$*Tpl2*$^{-/-}$ mice at 4 dpi is triggered by the induction of CXCL1 in the absence of active T1 IFN signaling.

NOS2 is overexpressed in IFNAR1$^{-/-}$Tpl2$^{-/-}$ mice, with inflammatory monocytes and neutrophils redundantly contributing to expression

To gain insight into potential drivers of morbidity in influenza-infected *Tpl2*$^{-/-}$ and *IFNAR1*$^{-/-}$*Tpl2*$^{-/-}$ mice, we examined the lung expression levels of NOS2, MPO and TRAIL as previously examined in *Tpl2*$^{-/-}$ mice[315] (Figure 3.5A-C). Nitric oxide is expressed in lungs of humans[320,321], mice[137,283] and even chicken[322] on infection with highly pathogenic influenza viruses. Hence on observing that NOS2 expression was upregulated in both the *IFNAR1*$^{-/-}$ and *IFNAR1*$^{-/-}$*Tpl2*$^{-/-}$ mouse strains that are characterized by excessive neutrophil recruitment, suggested that the neutrophils may contribute to severe pathology in *IFNAR1*$^{-/-}$*Tpl2*$^{-/-}$mice via their NOS2 expression (Figure 3.5B). However, because both monocytes and neutrophils have been shown to express NOS2[101,283,323,324], we next examined sorted populations of innate immune cell types to determine both the source of the pro-inflammatory mediators as well as the identity of any other Tpl2- or T1 IFN-regulated inflammatory mediators expressed within each population, focusing on cytokines and chemokines known to be involved in monocyte and neutrophil recruitment. All four strains of mice were infected with x31 for 7 days, and innate immune cell populations, including alveolar macrophages, neutrophils and inflammatory monocytes, were isolated from digested lungs by fluorescence-activated cell sorting for analysis of gene expression. Gene expression was first normalized to the WT genotype within each cell type, so that a fold-change attributed to genotype could be determined. Compared to the other genotype, CCL2 has a higher fold expression in *Tpl2*$^{-/-}$ monocytes as well as neutrophils, with no differential expression noted in alveolar macrophages (Figure 3.5D, H, L). This expression is consistent with the increased CCL2 expression observed in lungs of *Tpl2*$^{-/-}$ mice (Figure 3.2C, E). There were no differences in the expression fold-change of the neutrophil-recruiting chemokine CXCL1 across genotypes all three cell types examined

(Figure 3.5E, I, M). Both the alveolar macrophages and inflammatory monocytes from the *IFNAR1*$^{-/-}$*Tpl2*$^{-/-}$ mice expressed higher fold-change levels of IL-1β than those from *Tpl2*$^{-/-}$ mice (Figure 3.5F, J, N). No differences were noted across genotypes for the inflammatory mediator NOS2 in either alveolar macrophages or neutrophils (Figure 3.5G, K). However, *IFNAR1*$^{-/-}$ and *IFNAR1*$^{-/-}$*Tpl2*$^{-/-}$ inflammatory monocytes expressed a higher fold-change of NOS2 expression compared to WT or *Tpl2*$^{-/-}$ inflammatory monocytes (Figure 3.5O). Collectively, these data show an overexpression of CCL2 in within the *Tpl2*$^{-/-}$ genotype of both inflammatory monocytes and neutrophils, whereas the induction of IL-1β and NOS2 were more pronounced in *IFNAR1*$^{-/-}$*Tpl2*$^{-/-}$ mice in inflammatory monocytes (and alveolar macrophages for IL-1β).

When the relative expression is computed with the WT alveolar macrophages as the baseline set to 1 to allow comparison across all cell types, there is a relatively even contribution of the different cell types to the overall CCL2 expression. We note increased CCL2 expression noted in *Tpl2*$^{-/-}$ neutrophils and a trending increase in the *Tpl2*$^{-/-}$inflammatory monocytes (Supplementary Figure 3.12A). Alveolar macrophages contribute slightly more to the lung CXCL1 expression (Supplementary Figure 3.12B). Surprisingly, neutrophils express significantly more IL-1β than either alveolar macrophages or inflammatory monocytes, particularly in the WT and *Tpl2*$^{-/-}$ strains (Supplementary Figure 3.12C). Notably, NOS expression, appears to be equally derived from both neutrophils and inflammatory monocytes, with neither playing a predominant role (Supplementary Figure 3.12D). Collectively, these data do not implicate a single cell type in the expression of the prominent pro-inflammatory mediator, NOS2, but rather suggest that monocytes and neutrophils exhibit overlapping and redundant expression of NOS2.

Neutrophil depletion reduced disease severity for IFNAR1$^{-/-}$Tpl2$^{-/-}$ compared to Tpl2$^{-/-}$ mice and anti-IFN-λ treatment increased survival of influenza-infected Tpl2$^{-/-}$ mice.

Because neutrophil recruitment to the lungs was dramatically increased in *IFNAR1*$^{-/-}$*Tpl2*$^{-/-}$ mice compared to *Tpl2*$^{-/-}$ mice and neutrophils contributed to the expression of NOS2, we hypothesized that a switch from monocyte to neutrophil recruitment induced by *IFNAR1* ablation could underlie the severe phenotype (rather than a rescue) of influenza-infected *IFNAR1*$^{-/-}$*Tpl2*$^{-/-}$ mice. Therefore, we tested whether preventing the excessive neutrophil accumulation using the neutrophil-depleting anti-Ly6G antibody administered intraperitoneally would ameliorate severe disease in the *IFNAR1*$^{-/-}$*Tpl2*$^{-/-}$ mice. Treatment at 5 and 7 dpi were selected based on the dysregulated cytokine profile and increased morbidity specifically observed in *IFNAR1*$^{-/-}$*Tpl2*$^{-/-}$ mice beginning at 7 dpi (Figure 3.1C, 3.3H), and reasoned that treatment 2 days prior, at 5 dpi may be sufficient to alter the disease outcome. This approach led to an increase in median survival time of *IFNAR1*$^{-/-}$*Tpl2*$^{-/-}$ by 2.5 days compared to isotype control treatment in the same genotype (Figure 3.6E). *IFNAR1*$^{-/-}$*Tpl2*$^{-/-}$ exhibited more variable weight loss (Figure 3.6D) and lower clinical scores compared to *Tpl2*$^{-/-}$ mice receiving the same treatment (Figure 3.6F) However on comparison with any other antibody treatment in the same group, Ly6G treatment on *IFNAR1*$^{-/-}$*Tpl2*$^{-/-}$ showed the best clinical response (Figure 3.6C, F, I). While a modest improvement, Ly6G treatment was not able to significantly reverse the mortality (Figure 3.6E). So, we then examined the effect of anti-IFN-λ treatment in the hyperimmune response observed in the *IFNAR1*$^{-/-}$*Tpl2*$^{-/-}$ mice with the same treatment days. While the *IFNAR1*$^{-/-}$*Tpl2*$^{-/-}$ mice do not show an improvement with the IFN-λ treatment, the *Tpl2*$^{-/-}$ mice have reduced weight loss, better clinical scores and improved survival, similar to WT and *IFNAR1*$^{-/-}$mice (Figure 3.6G-I) even compared to the isotype control treated

Tpl2$^{-/-}$mice (Figure 3.6A-C). This suggests that IFN-λ has a detrimental effect in *Tpl2*$^{-/-}$ infected mice beyond day 5 post infection.

DISCUSSION

In a previous study of *Tpl2*$^{-/-}$ mice infected with *Mycobacterium tuberculosis*, the authors observed overexpression of IFN-β similar to what we have previously reported in influenza-infected *Tpl2*$^{-/-}$ mice[228]. During *M. tuberculosis* infection, T1 IFNs are known to impair bacterial control[325]. This axis was further assessed in *IFNAR1*$^{-/-}$*Tpl2*$^{-/-}$mice, which resulted in efficient bacterial control despite the absence of Tpl2 when T1 IFN signaling is also blocked[228]. Therefore, our initial hypothesis was that *IFNAR1*$^{-/-}$*Tpl2*$^{-/-}$ mice would show better outcomes than the *Tpl2*$^{-/-}$ mice in the absence of the excessive T1 IFN seen in *Tpl2*$^{-/-}$, as in the case *M. tuberculosis* infection.

Using *IFNAR1*$^{-/-}$*Tpl2*$^{-/-}$, mice we addressed genetically whether increased T1 IFN expression exacerbated disease in *Tpl2*$^{-/-}$ mice by enhancing the recruitment of inflammatory monocytes and neutrophils. Unexpectedly, *IFNAR1*$^{-/-}$*Tpl2*$^{-/-}$ mice experienced similar, or even more severe disease with faster progression to morbidity, than *Tpl2*$^{-/-}$ mice. Importantly, the increased disease severity could not simply be attributed to loss of viral control in the absence of T1 IFN signaling, as there was no difference between the viral load in WT and *IFNAR1*$^{-/-}$ mice. Follow-up cellular studies demonstrated that while recruitment of inflammatory monocytes was reversed in *IFNAR1*$^{-/-}$*Tpl2*$^{-/-}$ mice, a switch from primarily monocytic to neutrophilic pulmonary infiltration occurred in *IFNAR1*$^{-/-}$*Tpl2*$^{-/-}$ mice. This switch was triggered by the absence of early interferon signaling (at 4 dpi), leading to higher protein levels of the neutrophil-recruiting chemokine CXCL1[100]. Furthermore, by 7 dpi, increased IFN-γ, IL-6, IL-1β, G-CSF and IFN-λ were observed in the lung tissue, with IFN-λ (and CXCL1) being upregulated only in the absence of both Tpl2 and T1 IFN signaling (Figure 3.7).

While upregulation of IFN-γ, IL-6, IL-1β and G-CSF are observed in *IFNAR1*$^{-/-}$ mice at 7 dpi, *IFNAR1*$^{-/-}$ mice maintain a higher survival rate, reduced weight loss and clinical scores compared to *IFNAR1*$^{-/-}$*Tpl2*$^{-/-}$ mice. Despite the excessive neutrophil recruitment induced by the absence of T1 IFN signaling in both *IFNAR1*$^{-/-}$ and *IFNAR1*$^{-/-}$*Tpl2*$^{-/-}$ mice at 4 dpi, by 7 dpi it is highest in the *IFNAR1*$^{-/-}$*Tpl2*$^{-/-}$ mice, along with CXCL1 expression. This suggests that other Tpl2-dependent and IFNAR1-independent cytokines may also play vital roles in the morbidity observed at later stages in *Tpl2*$^{-/-}$ and *IFNAR1*$^{-/-}$*Tpl2*$^{-/-}$ *mice*. Conversely, the consequence of the upregulated cytokines at 7 dpi and early influx of neutrophils could be what drives the 40% mortality observed in the *IFNAR1*$^{-/-}$ strains. Hence, it hard to pinpoint a clear role for these IFN independent inflammation seen in the *IFNAR1*$^{-/-}$ mice.

One aspect of inflammation that this study highlights is the role of overactive IFN signaling in *Tpl2*$^{-/-}$ mice that promotes inflammatory monocyte recruitment directly via the IFN-β/CCL2 axis. The upregulation of IFN-β at both the protein and mRNA levels in the *IFNAR1*$^{-/-}$ strains (Figure 2B, D) may initially appear paradoxical. However, unlike other IFN-αs and ISGs, IFN-β does not require feedback through the IFNAR1 for its expression[313,326,327]. Accordingly, none of the other ISGs were upregulated in the absence of IFNAR1, confirming that T1 IFN signaling was abrogated in the *IFNAR1*$^{-/-}$ strains. Moreover, similar to our previous study wherein IFN-β was overexpressed in *Tpl2*$^{-/-}$ mice at 7 dpi[315], IFN-β is also upregulated in *IFNAR1*$^{-/-}$*Tpl2*$^{-/-}$ mice compared to *IFNAR1*$^{-/-}$ mice, further confirming that Tpl2 negatively regulates IFN-β production during influenza infection.

CXCL1 has been shown to be upregulated and to stimulate neutrophil recruitment in the absence of IFNAR signaling during influenza infection[100]. However, due to the multitude of cytokines expressed in the absence of T1 IFN signaling and CXCL1 expression at 7dpi being upregulated only in the *IFNAR1$^{-/-}$Tpl2$^{-/-}$* mice, increased CXCL1 expression could be an indirect by-product of regulation by IFN-γ, IL-6, IL-1β G-CSF or IFN-λ [99,109,257,316,317]. To address this possibility, we examined the lung cytokine profile at 4 dpi, with an emphasis on whole lungs without lavage or perfusion, the conditions under which CXCL1 over-expression was noted in *IFNAR1$^{-/-}$Tpl2$^{-/-}$* mice at 7 dpi. At this time point, CXCL1 was only over-expressed in the absence of T1 IFN signaling in *IFNAR1$^{-/-}$* strains. Notably, overexpression of CXCL1, but none of the other neutrophil-recruiting cytokines under consideration at 4 dpi, led us to conclude that increased CXCL1 is the initial driving force for enhanced neutrophil recruitment in *IFNAR1$^{-/-}$Tpl2$^{-/-}$* mice. However, at 7dpi, considering that there is over-expression of IFN signaling in the absence of Tpl2, it could lead to further suppression of the CXCL1 expression at 7dpi. This hypothesis explains why *IFNAR1$^{-/-}$Tpl2$^{-/-}$* mice have an upregulation in CXCL1 at 7dpi exclusively in this strain.

Interferon λ is the only cytokine that is solely upregulated in the *IFNAR1$^{-/-}$Tpl2$^{-/-}$* mice. Primarily known for being one of the early response cytokines[319], it is interesting that IFN-λ was upregulated in the late stages of acute influenza infection, similar to IFN-β. Along with T1 IFNs, IFN-λ expression has been shown to be involved in viral control, especially in reducing the spread of virus from upper respiratory tract to the lungs and transmission to a naïve host[110,111]. Indeed, IFN-λ expression has been shown to promote optimal antiviral responses from neutrophils, prevent excessive inflammation and induce better viral control from the epithelium during influenza infection[109]. In another study, overexpression of IFN-λ induced higher proliferation of mature NK cells in spleen, lung and lymph nodes that were better able to defend against lethal influenza infection[328]. Although T1 IFNs and IFN-λ share an overlapping infection-induced transcriptional signature[329], IFN-λ appears to have more anti-inflammatory functions. In a previous study by our lab we observed downregulated levels of IFN-λ in both bronchoalveolar lavage fluid and lung homogenates in the absence of Tpl2 at 3 dpi, irrespective of T1 IFN signaling[222]. IFN-λ expression was also downregulated in *Tpl2*$^{-/-}$ pDCs, which are early contributors of IFN-λ. This could contribute to the dysregulation of viral control seen from the very early stages in *Tpl2*$^{-/-}$ strains[222], as other studies have shown the importance of IFN-λ expression in early viral control[109,111]. In the current study, there is no significant difference in the transcriptional expression of IFN-λ across all strains, suggesting normalizing of the IFN-λ response by this time point.

Notably, recent studies have highlighted a new role pro-inflammatory role for IFN-λ in later stages of influenza infection via inhibition of lung tissue repair[198]. Therefore, it is possible that late-stage expression of IFN-λ contributes to the excessive morbidity and mortality observed in *IFNAR1*$^{-/-}$*Tpl2*$^{-/-}$ mice, by preventing lung tissue repair, although we did not see any effect of the blocking of IFN-λ treatment in the *IFNAR1*$^{-/-}$*Tpl2*$^{-/-}$ mice to support this idea. It is interesting to note, however, that this treatment did reduce clinical symptoms and increase survival in *Tpl2*$^{-/-}$ mice. Thus, there could be a role for interferon λ in promoting morbidity in *Tpl2*$^{-/-}$ mice in conjunction with interferon signaling.

In order to examine the cellular source of the various inflammatory proteins examined here, alveolar macrophages, neutrophils and inflammatory monocytes were selected. While inflammatory monocytes and neutrophils selection was based on their higher recruitment numbers, alveolar macrophages were considered as they are radio-resistant sources of cytokines (as mentioned in the previous study)[315] and are potent producers of T1 IFN during influenza infection[330]. While CCL2 expression is upregulated in both *Tpl2*$^{-/-}$ inflammatory monocytes and neutrophils; NOS2 is upregulated in the *IFNAR1*$^{-/-}$ inflammatory monocytes despite their lower recruitment numbers. Both these results suggest that neutrophils and inflammatory monocytes might share a plurality of function, especially when the lack Tpl2 or T1 IFN. This is also seen in other studies involving *IFNAR1*$^{-/-}$ mice, wherein in the absence of *IFNAR1*$^{-/-}$ signaling, multiple mononuclear subsets (of Ly6C^{hi} and Ly6C^{lo} monocytes) subsets expressed higher levels of NOS2[99]. Furthermore it also could explain why in the absence of IFNAR signaling the recruitment switches form monocytes to neutrophils[99,100], in order to ensure that the cells of the system that respond to the infection are able to clear virus equally. In the case of only Tpl2 ablation, while sensing of the over-active IFN signaling in the *Tpl2*$^{-/-}$ mice leads to SOCS1 activation and concomitant dampening of the immune response (albeit inefficient)[315], granting the mice slower morbidity. In comparison in the *IFNAR1*$^{-/-}$*Tpl2*$^{-/-}$ mice, the lack of interferon signaling mediates the neutrophil recruitment from 4dpi (with increment at 7dpi), exacerbates IFN-λ that was kept in check (in the presence of T1 IFN) and has no active cytokine regulator to dampen the signal, the combined effect explains the earlier mortality in the mice at 7-8 dpi. Hence when we consider the effect that Ly6G treatment had wherein it allowed for slower morbidity in the *IFNAR1*$^{-/-}$*Tpl2*$^{-/-}$ mice compared to Isotype or IFN-λ treatment but was unable to constructively reduce the damage in these mice and thereby prevent death. Additionally, when we consider the redundancy in function of the monocytes and neutrophils, in the *IFNAR1*$^{-/-}$*Tpl2*$^{-/-}$ mice, the lower numbers of higher NOS2 expressing monocytes could also be major contributors for NOS2. In this case the depletion of the neutrophils using the Ly6G antibody, could have also not prevented morbidity.

IL-1β has been implicated in neutrophil recruitment[316] and was therefore also examined. Unexpectedly, IL-1β was significantly overexpressed in influenza-infected *IFNAR1*$^{-/-}$*Tpl2*$^{-/-}$ mice. This was unexpected, because IL-1β expression was not observed in influenza-infected *Tpl2*$^{-/-}$

mice at 7 dpi in our previous study[315]. Furthermore, IL-1β expression has been shown to be Tpl2-dependent *in vitro* in LPS-stimulated macrophages and *in vivo* in response to *Listeria monocytogenes* infection[227]. IL-1β overexpression in *IFNAR1*$^{-/-}$*Tpl2*$^{-/-}$ mice in the current study suggests that T1 IFN overexpression in *Tpl2*$^{-/-}$ mice may normally suppress IL-1β expression.

Overall, this study highlights the complex network of regulation of cytokines, chemokines and cellular recruitment under the control of Tpl2. Prominent among these is the negative regulation of the T1 IFNs, which in turn positively and negatively regulate CCL2 and CXCL1 expression, respectively. This dichotomy leads to a T1 IFN-induced switch from the pathologic increase in pulmonary recruitment of inflammatory monocytes in *Tpl2*$^{-/-}$ mice to neutrophils in *IFNAR1*$^{-/-}$*Tpl2*$^{-/-}$ mice. Inflammation is likely further exacerbated by dysregulated IFN-λ as noted above. Future studies will aim to apply this information towards preventing severe influenza cases by examining Tpl2-regulated pathways as potential predictors of potentially severe influenza progression and using influenza-infected *Tpl2*$^{-/-}$ mice as a preclinical model to test for intervention strategies.

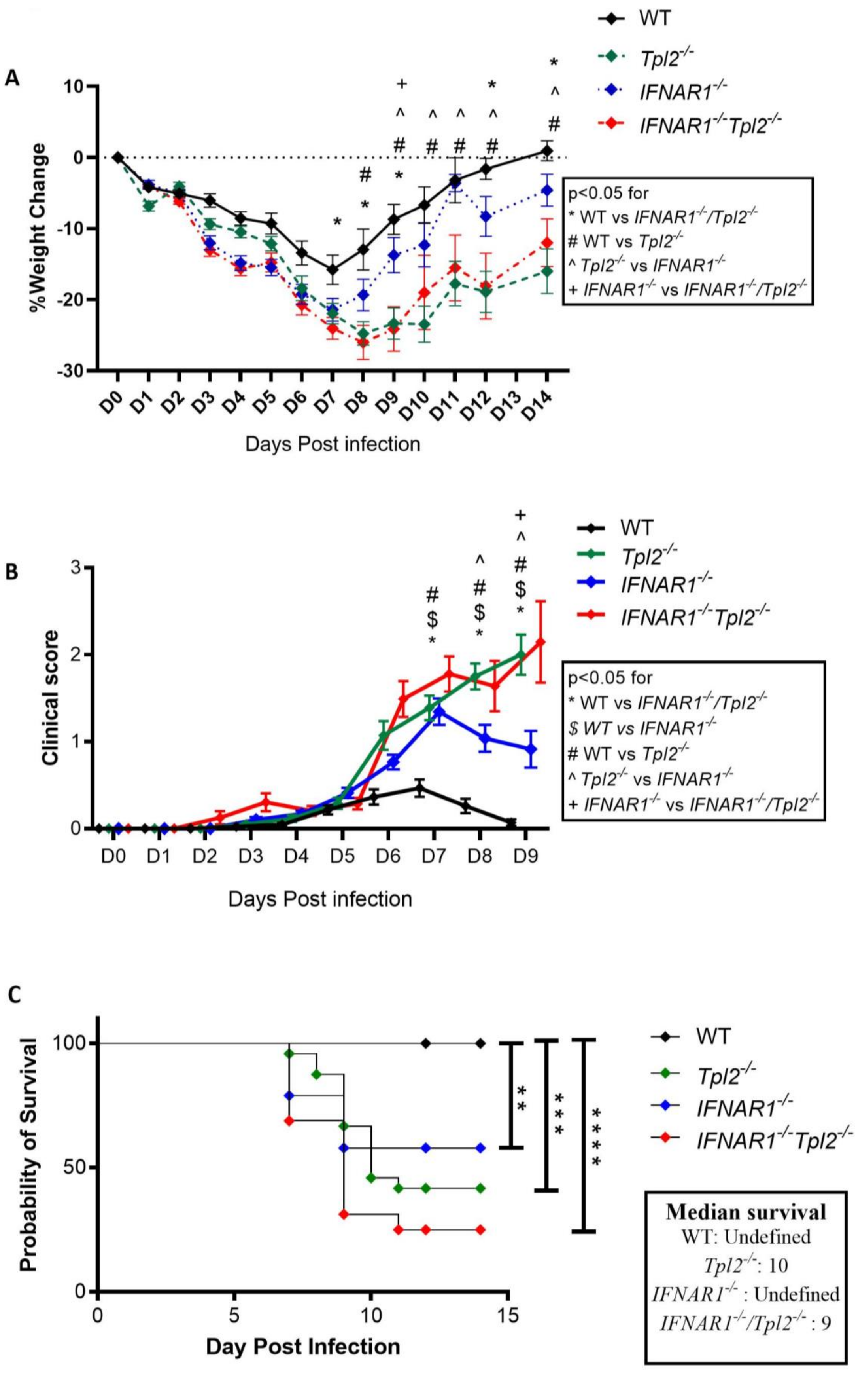
A
WT
Tpl2-/-
IFNAR1-/-
IFNAR1-/-Tpl2-/-
%Weight Change
Days Post infection
D0 D1 D2 D3 D4 D5 D6 D7 D8 D9 D10 D11 D12 D13 D14
p<0.05 for
* WT vs IFNAR1-/-/Tpl2-/-
# WT vs Tpl2-/-
^ Tpl2-/- vs IFNAR1-/-
+ IFNAR1-/- vs IFNAR1-/-/Tpl2-/-
B
WT
Tpl2-/-
IFNAR1-/-
IFNAR1-/-Tpl2-/-
Clinical score
Days Post infection
p<0.05 for
* WT vs IFNAR1-/-/Tpl2-/-
$ WT vs IFNAR1-/-
# WT vs Tpl2-/-
^ Tpl2-/- vs IFNAR1-/-
+ IFNAR1-/- vs IFNAR1-/-/Tpl2-/-
C
WT
Tpl2-/-
IFNAR1-/-
IFNAR1-/-Tpl2-/-
Probability of Survival
Day Post Infection
Median survival
WT: Undefined
Tpl2-/-: 10
IFNAR1-/- : Undefined
IFNAR1-/-/Tpl2-/- : 9

Figure 3.1: Enhanced susceptibility of *Tpl2*$^{-/-}$ mice to influenza infection is independent of T1 IFN signaling. (A) Percent weight change and **(B)** progression of clinical symptoms of WT (n=22), *Tpl2*$^{-/-}$ (n=29), *IFNAR1*$^{-/-}$ (n=40) and *IFNAR1*$^{-/-}$*Tpl2*$^{-/-}$ (n=28) mice infected with 10^4 pfu influenza A virus strain x31 through 14 dpi. Data are representative of 5 experiments. One-way ANOVA with Tukey's multiple comparison test was performed for each day post infection, with $p<0.05$ considered statistically significant. Symbols denote significant differences among groups as noted. **(C)** Survival curve for 14 dpi. Data are representative of 5 experiments. Significance determined with Log-rank Mantel-cox test; $^*p<0.05$, $^{**}p<0.01$ $^{***}p< 0.001$ and $^{****}p<0.0001$. Group averages of combined male and female mice are shown.

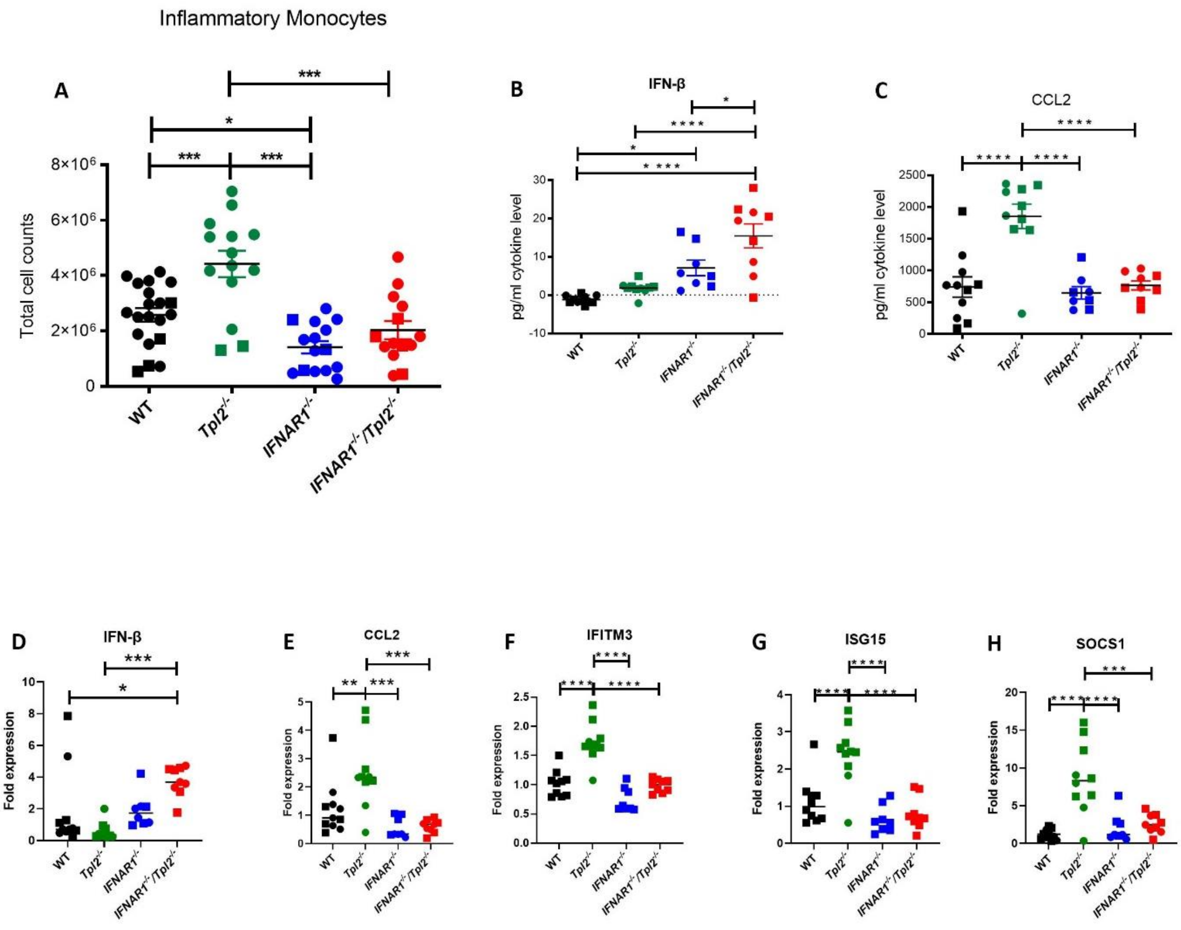

Figure 3.2. Enhanced recruitment of inflammatory monocytes and induction of interferon stimulated genes (ISGs) in influenza-infected *Tpl2*$^{-/-}$ mice is dependent on IFNAR1 signaling at 7 dpi. (A) WT (n=20), *Tpl2*$^{-/-}$ (n=14), *IFNAR1*$^{-/-}$ (n=15) and *IFNAR1*$^{-/-}$/ *Tpl2*$^{-/-}$ (n=14) mice were infected intranasally with 10^4 pfu of influenza x31 and euthanized at 7 dpi. The lungs were lavaged, perfused with PBS, digested with collagenase, and interstitial leukocytes were enriched by Percoll density gradient centrifugation. Inflammatory monocytes (Siglec F$^-$, CD11b^{high}, CD11c^{low}, Ly6C$^+$) at 7 dpi in the tissue of infected mice are shown. Data are representative of 3 experiments. Males are represented as squares and females as circles. One way ANOVA with

Tukey's multiple comparison test was performed with *p<0.05, **p<0.01 and ***p<0.001. WT (n=22), *Tpl2*$^{-/-}$ (n=13), *IFNAR1*$^{-/-}$ (n=19) and *IFNAR1*$^{-/-}$/ *Tpl2*$^{-/-}$ (n=21) mice were infected intranasally with 10^4 pfu of influenza x31 and euthanized at 7 dpi. The lungs were homogenized (perfused & lavaged prior to extraction) for analysis of cytokine protein levels for **(B)** IFN-β and **(C)** CCL2. Furthermore, the same homogenate was also used for RNA was extraction and analysis of gene expression by real-time PCR for **(D)** IFN-β and **(E-H)** IFN-stimulated genes (ISGs). Squares represent male mice, and circles represent female mice. Data are representative of 2 experiments. One way ANOVA with Tukey's multiple comparison test was performed with *p<0.05, **p<0.01, ***p<0.001 and ****p<0.0001.

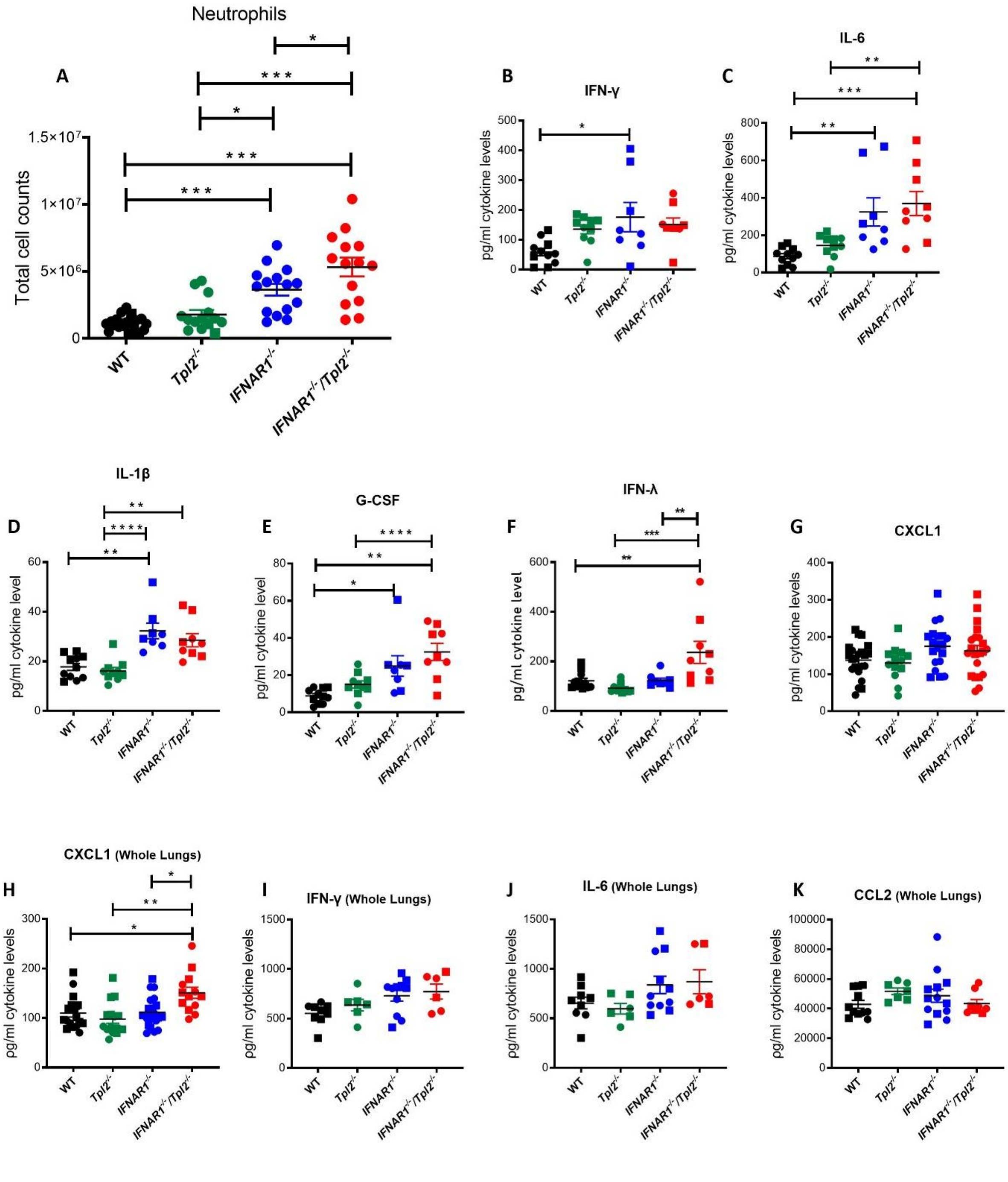

Figure 3.3. *IFNAR1*$^{-/-}$*Tpl2*$^{-/-}$ mice show the highest recruitment of neutrophils and unique overexpression of IFN-λ and CXCL1 at 7 dpi. (A) WT (n=20), *Tpl2*$^{-/-}$ (n=14), *IFNAR1*$^{-/-}$ (n=15) and *IFNAR1*$^{-/-}$*Tpl2*$^{-/-}$ (n=14) mice were infected intranasally with 10^4 pfu of influenza x31 and

euthanized at 7 dpi. The lungs were lavaged, perfused with PBS, digested with collagenase, and interstitial leukocytes were enriched by Percoll density gradient centrifugation. Neutrophils (Siglec F^- $CD11b^{high}$ $CD11c^{low}$ $Ly6G^+$) in the tissue of infected mice at 7 dpi are shown. Data are representative of 3 experiments. Males are represented as squares, and females are represented as circles. One way ANOVA with Tukey's multiple comparison test was performed with *p<0.05, **p<0.01 and ***p<0.001. WT (n=22), *Tpl2*$^{-/-}$ (n=13), *IFNAR1*$^{-/-}$ (n=19) and *IFNAR1*$^{-/-}$*Tpl2*$^{-/-}$ (n=21) mice were infected intranasally with 10^4 pfu of influenza x31 and euthanized at 7 dpi. The lungs were perfused lavaged prior to extraction and then homogenized for analysis of cytokine expression for **(B)** IFN-γ, **(C)** IL-6, **(D)** IL-1β, **(E)** G-CSF **(F)** IFN-λ and **(G)** CXCL1. Squares represent male mice, and circles represent female mice. Data are representative of 2 experiments. One way ANOVA with Tukey's multiple comparison test was performed with *p<0.05, **p<0.01, ***p<0.001 and ****p<0.0001. WT (n=17), *Tpl2*$^{-/-}$ (n=16), *IFNAR1*$^{-/-}$ (n=21) and *IFNAR1*$^{-/-}$*Tpl2*$^{-/-}$ (n=13) mice were infected intranasally with 10^4 pfu of influenza x31 and euthanized at 7 dpi. Whole lungs (without perfusion or lavage) were homogenized for analysis of cytokine expression for **(H)** CXCL1, **(I)** IFN-γ, **(J)** IL-6 and **(K)** CCL2. Squares represent male mice, and circles represent female mice. Data are representative of 2 experiments. One way ANOVA with Tukey's multiple comparison test was performed with *p<0.05 and **p<0.01.

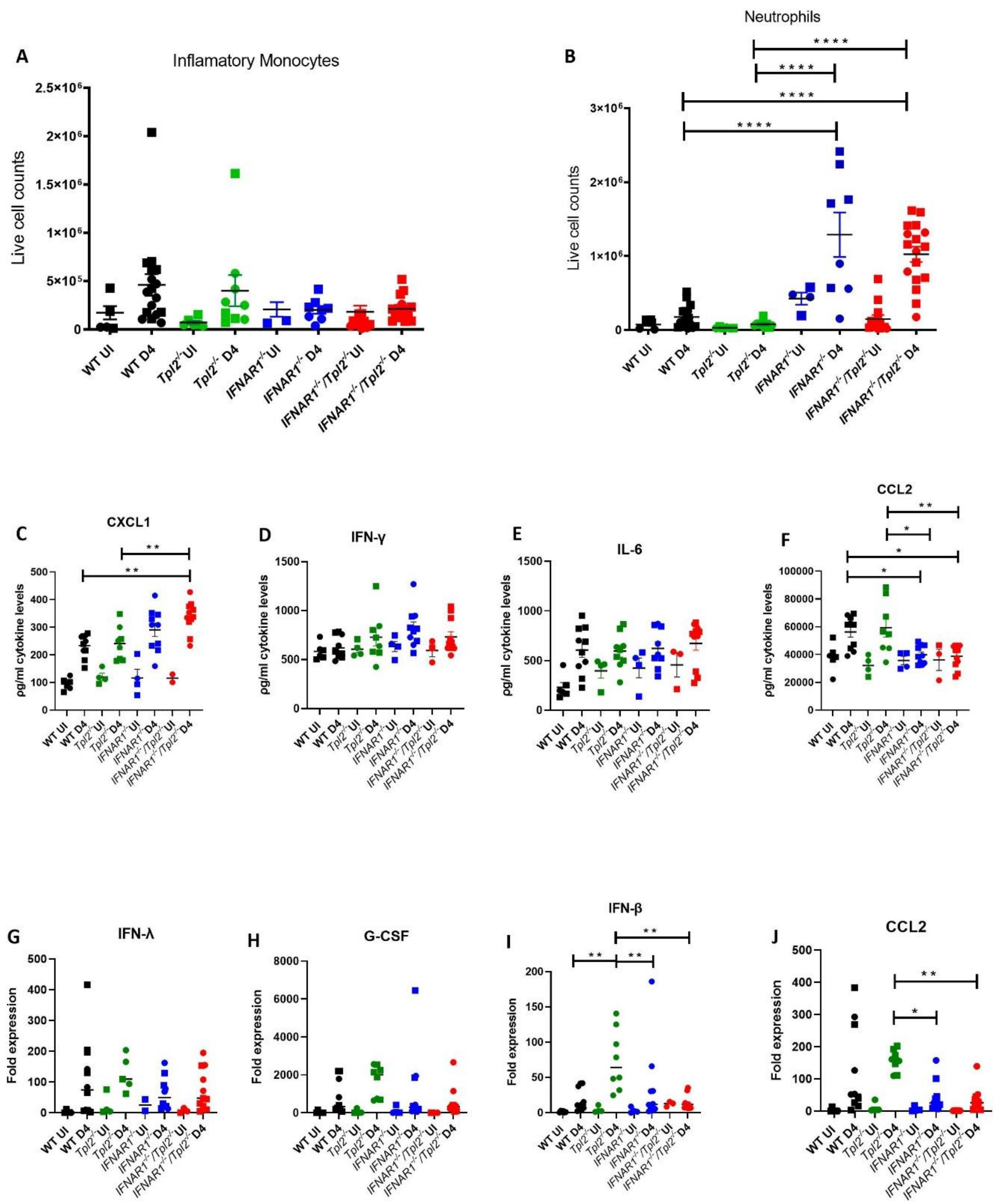

Figure 3.4. Neutrophils are excessively recruited to the lungs of *IFNAR1$^{-/-}$* mouse strains at 4 dpi with upregulation of CXCL1 expression in the absence of T1 IFN signaling. WT (n=17),

Tpl2$^{-/-}$ (n=9), *IFNAR1*$^{-/-}$ (n=8) and *IFNAR1*$^{-/-}$*Tpl2*$^{-/-}$ (n=17) mice were infected intranasally with 10^4 pfu of influenza x31 and euthanized at 4 dpi, along with uninfected controls. The lungs were lavaged, perfused with PBS, digested with collagenase, and interstitial leukocytes were enriched by Percoll density gradient centrifugation. **(A)** Inflammatory monocytes and **(B)** neutrophils were examined at 4 dpi along with uninfected controls. Data are representative of 3 experiments. Males are represented as squares, and females are represented as circles. One-way ANOVA with Tukey's multiple comparison test was performed. *p<0.05, **p<0.01 and ***p<0.001. WT (n=10), *Tpl2*$^{-/-}$ (n=8), *IFNAR1*$^{-/-}$ (n=10) and *IFNAR1*$^{-/-}$*Tpl2*$^{-/-}$ (n=11) mice were infected intranasally with 10^4 pfu of influenza x31 and euthanized at 4 dpi with uninfected controls. The intact lungs were homogenized for analysis of cytokine expression for **(C)** CXCL1, **(D)** IFN-γ, **(E)** IL-6 and **(F)** CCL2. Furthermore, the same homogenate was also used for RNA was extraction and analysis of gene expression by real-time PCR of **(G)** IFN-λ, **(H)** G-CSF **(I)** IFN-β and **(J)** CCL2. Squares represent male mice, and circles represent female mice. Data are representative of 2 experiments. One way ANOVA with Tukey's multiple comparison test was performed with *p<0.05, **p<0.01, ***p<0.001 and ****p<0.0001.

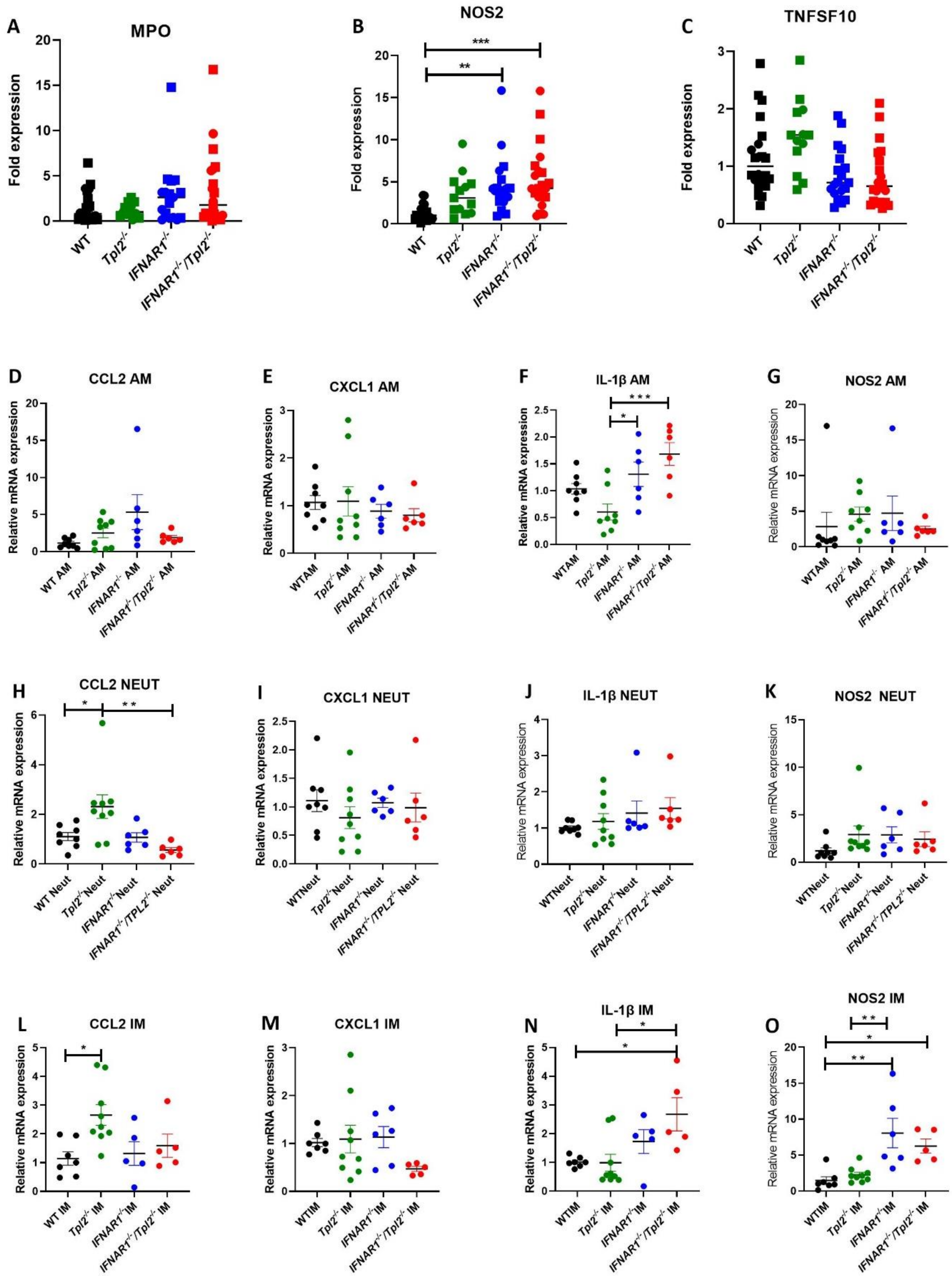
A
MPO
B
NOS2
C
TNFSF10
D
CCL2 AM
E
CXCL1 AM
F
IL-1β AM
G
NOS2 AM
H
CCL2 NEUT
I
CXCL1 NEUT
J
IL-1β NEUT
K
NOS2 NEUT
L
CCL2 IM
M
CXCL1 IM
N
IL-1β IM
O
NOS2 IM

Figure 3.5. NOS2 is overexpressed in the lungs in *IFNAR1$^{-/-}$Tpl2$^{-/-}$* *mice,* with neutrophils and inflammatory monocytes redundantly contributing to expression. WT (n=22), *Tpl2$^{-/-}$* (n=13), *IFNAR1$^{-/-}$* (n=19) and *IFNAR1$^{-/-}$Tpl2$^{-/-}$* (n=21) mice were infected intranasally with 10^4 pfu of influenza x31 and euthanized at 7 dpi. The lungs were homogenized for RNA extraction and analysis of gene expression by real-time PCR for **(A)** MPO, **(B)** NOS2 and **(C)** TNFSF10. Squares represent male mice, and circles represent female mice. Data are representative of 2 experiments. One way ANOVA with Tukey's multiple comparison test was performed with *p<0.05, **p<0.01, ***p<0.001, and ****p<0.0001. WT (n=8), *Tpl2$^{-/-}$* (n=9), *IFNAR1$^{-/-}$* (n=6) and *IFNAR1$^{-/-}$Tpl2$^{-/-}$* (n=6) mice were infected intranasally with 10^4 pfu of influenza x31 and euthanized at 7 dpi. Their lungs were digested with collagenase, and leukocytes were sorted as **(D-G)** alveolar macrophages (AM; Siglec F^{high} CD11b^{int}), **(H-K)** neutrophils (Neut; Siglec F^{-} CD11b^{high} CD11c^{low} Ly6G^{+}) and **(L-O)** inflammatory monocytes (IM; Siglec F^{-} CD11b^{high} CD11c^{low} Ly6C^{+}). Gene expression was analyzed by qPCR and data were normalized for each cell type relative to the actin endogenous control and the WT strain for a given cell type as baseline, which was designated a value of 1. Data are representative of 3 experiments. One-way ANOVA with Tukey's multiple comparison test was performed. *p<0.05 and **p<0.01. Female mice were used for these experiments.

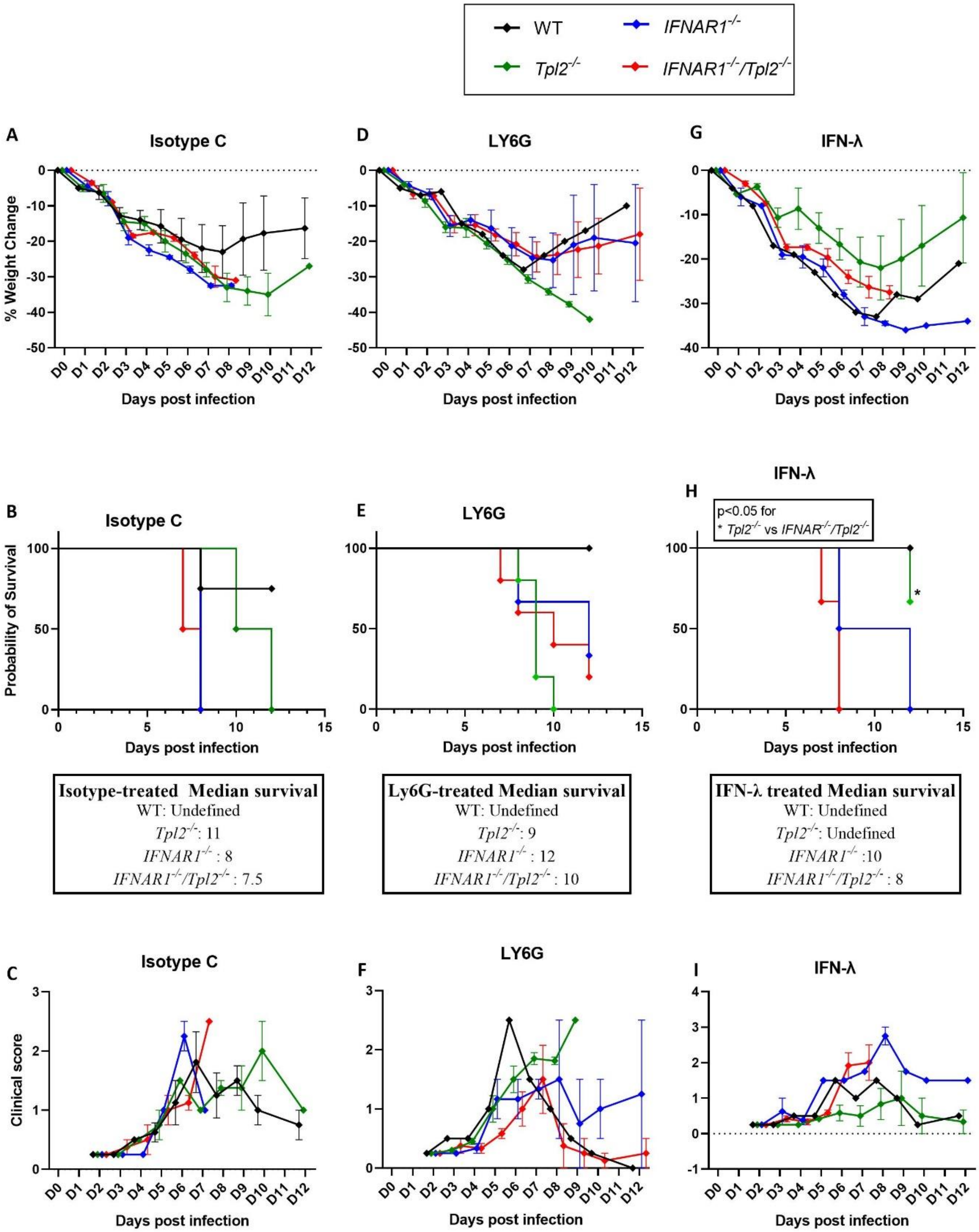
WT
IFNAR1-/-
Tpl2-/-
IFNAR1-/-/Tpl2-/-
A
Isotype C
% Weight Change
Days post infection
D
LY6G
Days post infection
G
IFN-λ
Days post infection
B
Isotype C
Probability of Survival
Days post infection
E
LY6G
Days post infection
IFN-λ
H
p<0.05 for
* Tpl2-/- vs IFNAR-/-/Tpl2-/-
Days post infection
Isotype-treated Median survival
WT: Undefined
Tpl2-/-: 11
IFNAR1-/- : 8
IFNAR1-/-/Tpl2-/- : 7.5
Ly6G-treated Median survival
WT: Undefined
Tpl2-/-: 9
IFNAR1-/- : 12
IFNAR1-/-/Tpl2-/- : 10
IFN-λ treated Median survival
WT: Undefined
Tpl2-/-: Undefined
IFNAR1-/- :10
IFNAR1-/-/Tpl2-/- : 8
C
Isotype C
Clinical score
Days post infection
F
LY6G
Days post infection
I
IFN-λ
Days post infection

Figure 3.6. Ly6G blocking of neutrophils is partially beneficial for *IFNAR1$^{-/-}$Tpl2$^{-/-}$* mice and Interferon λ treatment increases the survival of *Tpl2$^{-/-}$* infected mice compared to *IFNAR1$^{-/-}$/ Tpl2$^{-/-}$*. Mice were infected intranasally with 10^4 pfu of influenza x31. Following which they were administered 200 µg of an isotype control antibody **(A-C)**, anti-Ly6G depleting antibody **(D-F)** or anti-IFN-λ neutralizing antibody **(G-I)** intraperitoneally in 200 µl on days 5 and day 7 post infection. Their weight change **(A, D, G)** and **(B, E, H)** clinical scores were recorded daily. Survival **(C, F, I)** was assessed through 12 dpi. Numbers of mice: A-C, WT (n=4), *Tpl2$^{-/-}$* (n=5), *IFNAR1$^{-/-}$* (n=3) and *IFNAR1$^{-/-}$Tpl2$^{-/-}$* (n=5) mice. D-F, WT (n=1), *Tpl2$^{-/-}$* (n=5), *IFNAR1$^{-/-}$* (n=3) and *IFNAR1$^{-/-}$Tpl2$^{-/-}$* (n=5) mice; G-I, WT (n=1), *Tpl2$^{-/-}$* (n=3), *IFNAR1$^{-/-}$* (n=2) and *IFNAR1$^{-/-}$Tpl2$^{-/-}$* (n=3) mice. Data are representative of 2 two independent experiments. Log-rank Mantel-cox test was used for statistics. *p<0.05. Data averaged from males and female mice are represented by diamonds.

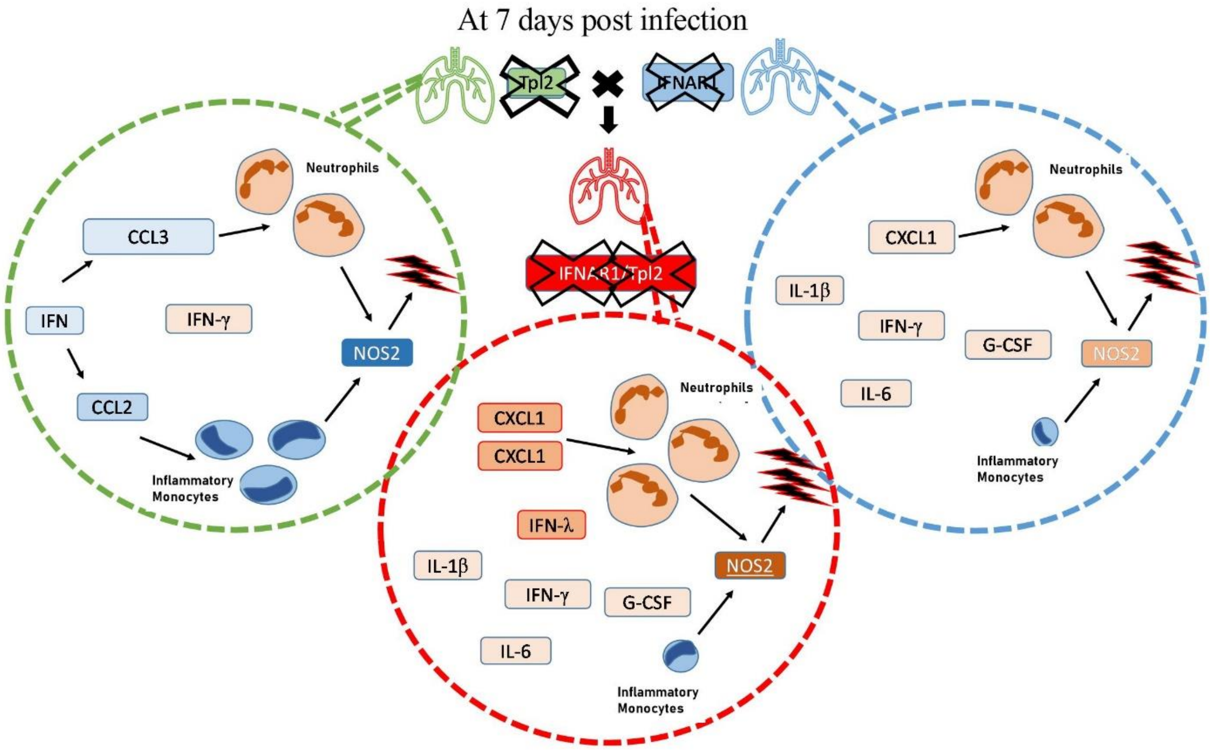

Figure 3.7. Tpl2 and TI IFN co-regulate IFN-λ, CXCL1 and neutrophil recruitment in late stage Influenza infection. In the lungs of influenza-infected *Tpl2*$^{-/-}$ mice at 7 dpi, upregulation of the IFNs and chemokines (CCL2, CCL3) leads to recruitment and retention of inflammatory monocytes and neutrophils, respectively that lead to lung damage likely via nitric oxide (NOS2). Meanwhile, in influenza-infected *IFNAR*$^{-/-}$ mice at 7dpi, we see overexpression of various cytokines along with higher recruitment of neutrophils. Along with the lower numbers of inflammatory monocytes (that express higher levels of NOS2), we see that the lung damage is still mediated by NOS2. However in the *IFNAR1*$^{-/-}$/ *Tpl2*$^{-/-}$ mice at the same time point we see the highest recruitment of neutrophils, and overexpression of CXCL1 and IFN-λ, along with the cytokines dysregulated due to lack of IFNAR signaling, all contributing towards inflammation.

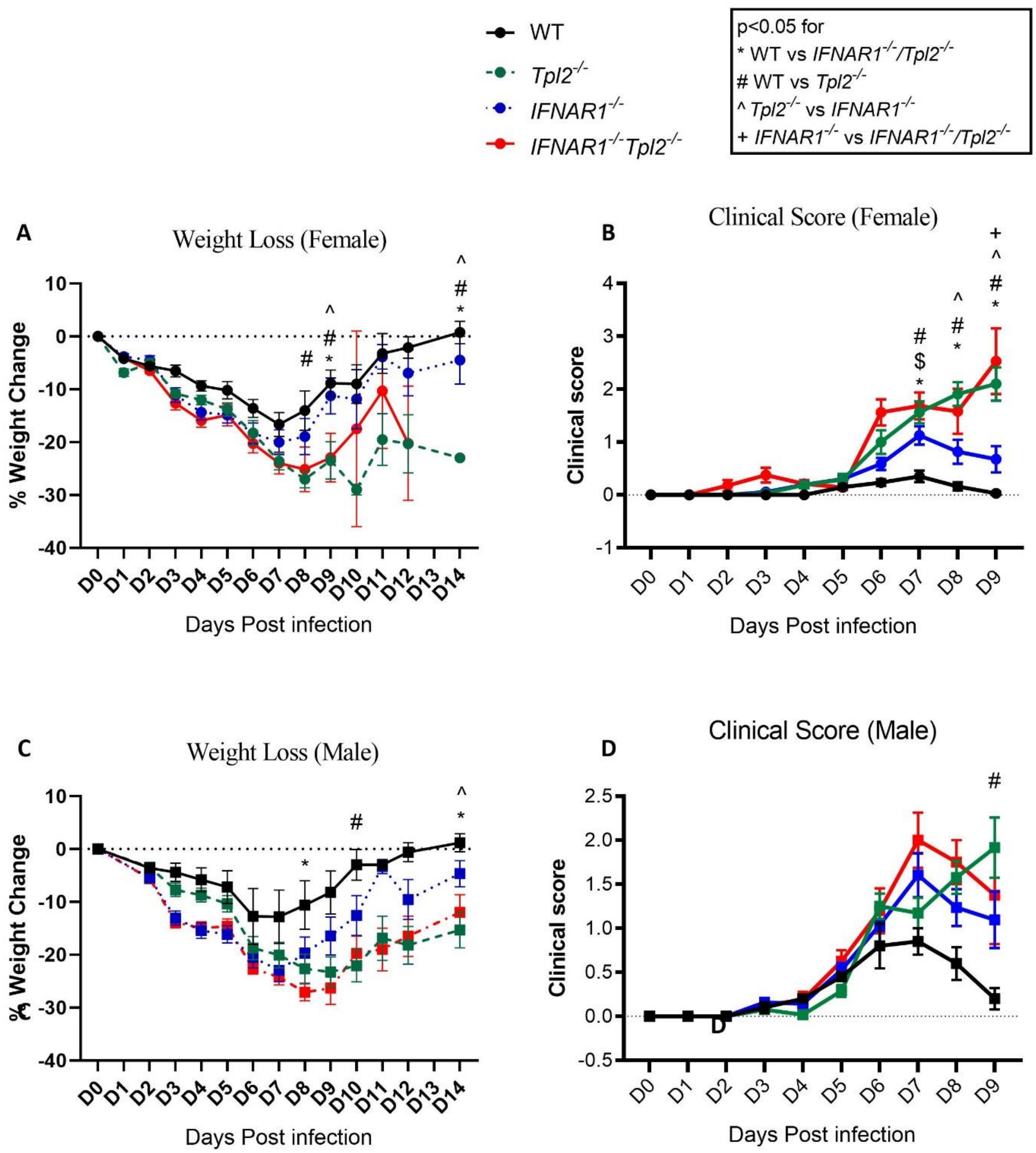

Supplementary Figure 3.8. Similar disease course observed in influenza-infected female and male mice. **(A)** Percent weight change and **(B)** progression of clinical symptoms for WT (n=17), *Tpl2*$^{-/-}$ (n=16), *IFNAR1*$^{-/-}$ (n=21) and *IFNAR1*$^{-/-}$*Tpl2*$^{-/-}$ (n=20) female mice (circle symbol) infected with 10^4 pfu influenza A virus strain x31 through 14 dpi. Data are representative of 4 experiments **(C)** Percent weight change and **(D)** progression of clinical symptoms for WT (n=4), *Tpl2*$^{-/-}$ (n=13), *IFNAR1*$^{-/-}$ (n=19) and *IFNAR1*$^{-/-}$*Tpl2*$^{-/-}$ (n=8) male mice (square symbols) infected with 10^4 pfu influenza A virus strain x31 through 14 dpi. Data are representative of 2 experiments. One-way ANOVA with Tukey's multiple comparison test was performed. *$p<0.05$, for each day post infection and is represented between the groups it is significant for, with the respective symbol, as shown above.

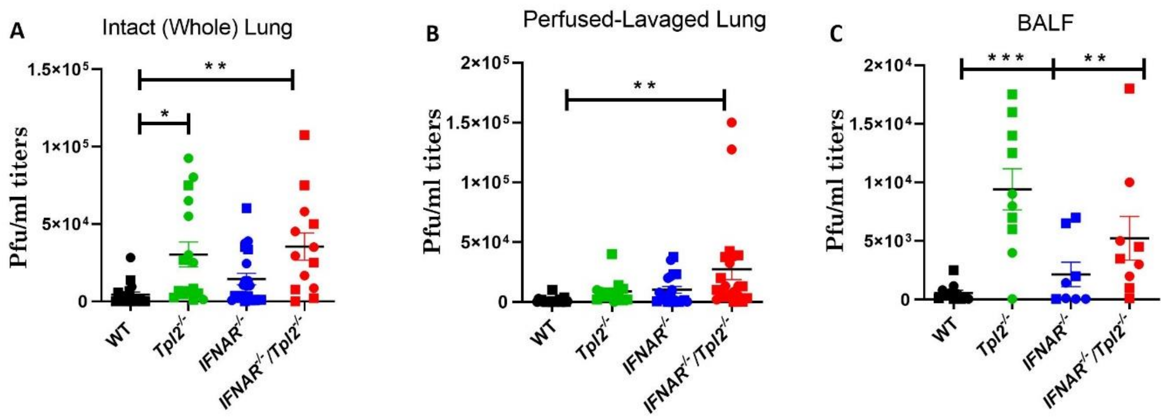

Supplementary Figure 3.9. Viral loads were higher in the absence of Tpl2, irrespective of IFNAR signaling. Viral titers represented as pfu/ml for all infected groups at 7 dpi from **(A)** intact lungs without lavage or perfusion prior to homogenization from WT (n=17), *Tpl2*$^{-/-}$ (n=16), *IFNAR1*$^{-/-}$ (n=21) and *IFNAR1*$^{-/-}$/ *Tpl2*$^{-/-}$ (n=13) prior to homogenization and **(B)** perfused & lavaged lung tissue or **(C)** BALF of WT (n=22), *Tpl2*$^{-/-}$ (n=13), *IFNAR1*$^{-/-}$ (n=19) and *IFNAR1*$^{-/-}$/ *Tpl2*$^{-/-}$ (n=21) infected mice is shown. Data are representative of 2 experiments. Males are represented as squares and females as circles. One way ANOVA with Tukey multiple comparison test was performed with *p<0.05 and **p<0.01.

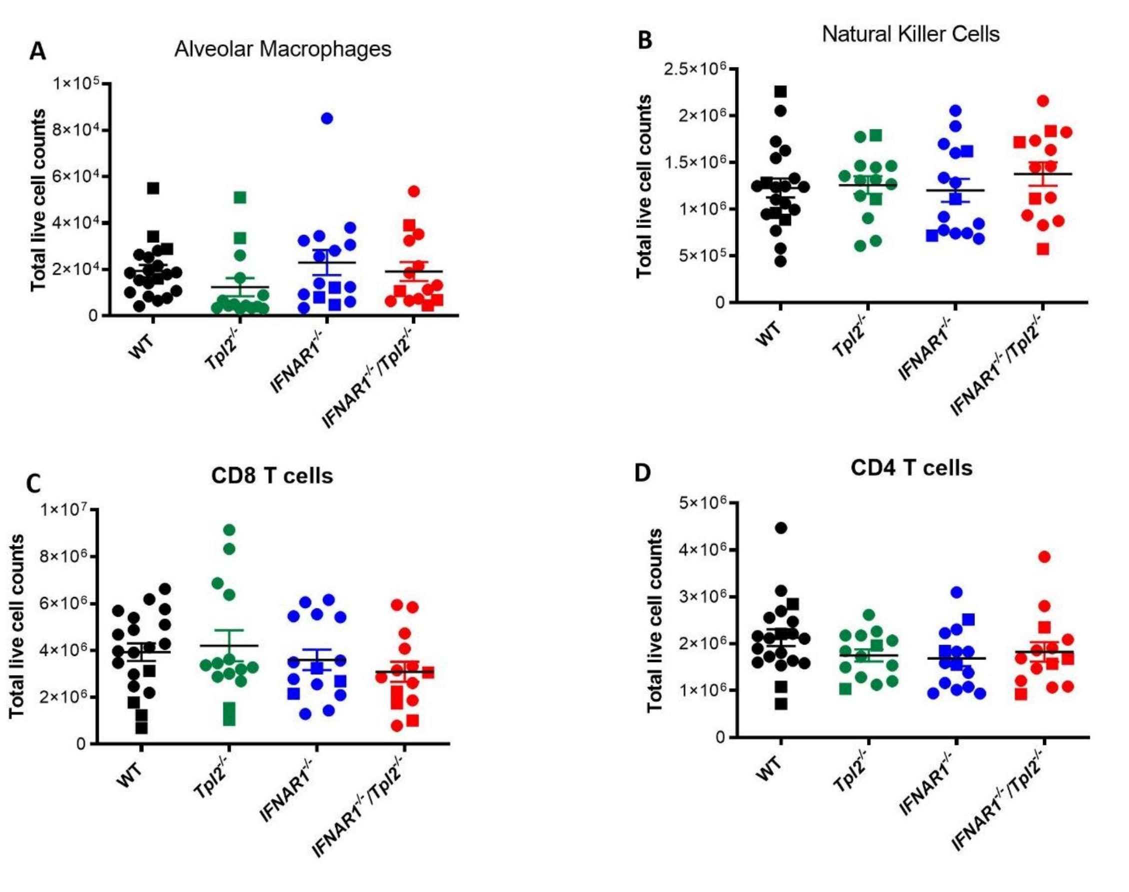

Supplementary Figure 3.10. Similar lung cellularity was observed for alveolar macrophages, NK cells and T cells. WT (n=17), *Tpl2*$^{-/-}$ (n=9), *IFNAR*$^{-/-}$ (n=8) and *IFNAR*$^{-/-}$/ *Tpl2*$^{-/-}$ (n=17) mice were infected intranasally with 10^4 pfu of influenza x31 and euthanized at 7 dpi. The lungs were lavaged, perfused with PBS, digested with collagenase, and interstitial leukocytes were enriched by Percoll density gradient centrifugation. **(A)** Alveolar Macrophages, **(B)** Natural Killer cells, **(C)** CD8T cells and **(D)** CD4 T cells were examined at 7dpi. Data are representative of 3 experiments. Males are represented as squares, and females are representated as circles. One way ANOVA with Tukey's multiple comparison test was performed with *p<0.05, **p<0.01 and ***p<0.001.

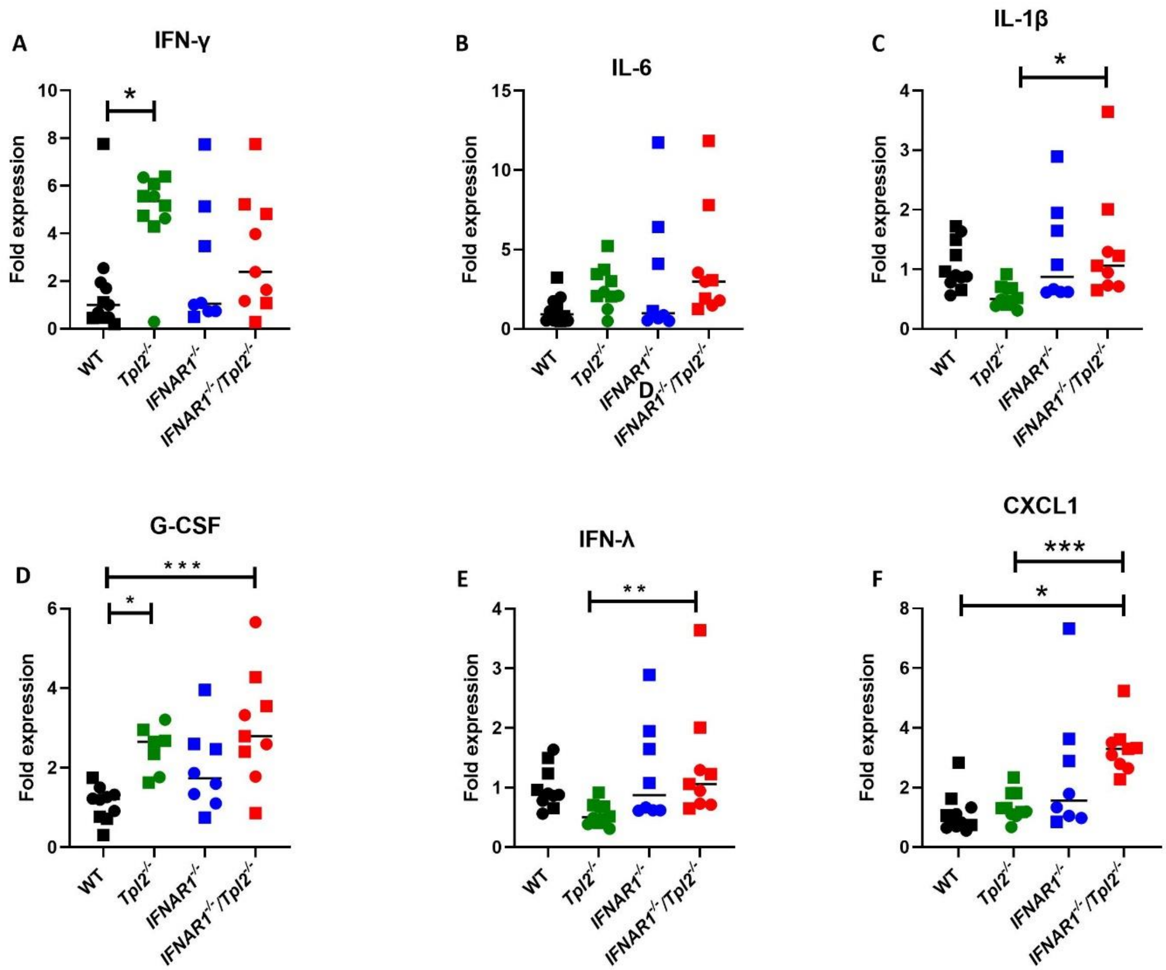

Supplementary Figure 3.11. Cytokine mRNA expression is similar to the protein expression seen at 7 dpi. WT (n=22), *Tpl2*$^{-/-}$ (n=13), *IFNAR*$^{-/-}$ (n=19) and *IFNAR*$^{-/-}$*Tpl2*$^{-/-}$ (n=21) mice were infected intranasally with 10^4 pfu of influenza x31 and euthanized at 7 dpi. The lungs were perfused and lavaged prior to extraction and then homogenized. RNA was extracted and analyzed for gene expression by real-time PCR for **(A)** IFN-γ, **(B)** IL-6, **(C)** IL-1β, **(D)** G-CSF **(E)** IFN-λ and **(F)** CXCL1. Squares represent male mice, and circles represent female mice. Data are representative of 2 experiments. One way ANOVA with Tukey's multiple comparison test was performed with *p<0.05, **p<0.01 and ***p<0.001.

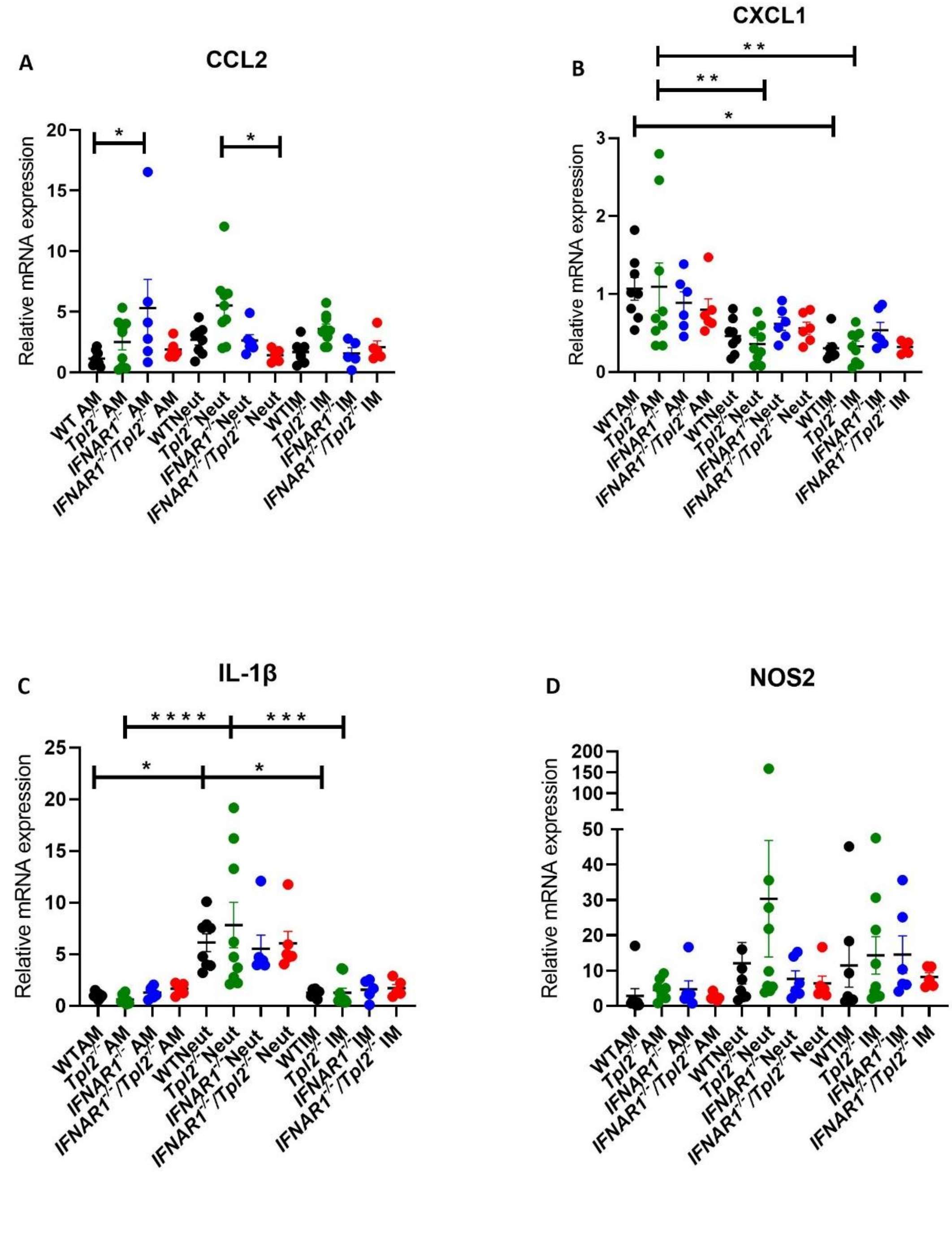

Supplementary Figure 3.12. Gene expression analysis of alveolar macrophages, neutrophils and inflammatory monocytes suggest functional redundancies in gene expression. WT (n=8), *Tpl2*$^{-/-}$ (n=9), *IFNAR1*$^{-/-}$ (n=6) and *IFNAR1*$^{-/-}$*Tpl2*$^{-/-}$ (n=6) mice were infected intranasally with 10^4

pfu of influenza x31 and euthanized at 7 dpi. Their lungs were digested with collagenase and leukocytes were sorted by flow cytometry as in Figure 5. Gene expression was analyzed by qPCR and normalized across all cell types and genotypes to the WT AM sample, which was designated a value of 1 to allow for comparisons across cell types. Data are representative of 3 experiments. One-way ANOVA with Tukey's multiple comparison test was performed. *p<0.05, **p<0.01, ***p<0.001 and ****p<0.0001. Female mice were used for these experiments.

CHAPTER 4

INFLUENZA A VIRUS INFECTION INDUCES AN ACQUIRED RESPIRATORY DISTRESS SYNDROME-LIKE PHENOTYPE IN TPL2-DEFICIENT MICE

Latha K, Rao S, Sakamoto K and Watford WT. *Submitted to American Journal of Respiratory Cell and Molecular Biology*

ABSTRACT

Excessive inflammation in patients with severe influenza disease may lead to acute lung injury that results in a clinical syndrome called Acute Respiratory Distress Syndrome (ARDS). ARDS is associated with alveolar damage and pulmonary edema that severely impairs gas exchange function leading to hypoxia. With no existing FDA-approved treatment for ARDS, the only option for treatment is invasive mechanical ventilation, which still results in high mortality. Therefore, it is important to understand the factors that lead to ARDS development in order to better prevent, diagnose and treat it. We have previously shown that *Tpl2*$^{-/-}$ mice succumb to infection with a normally low-pathogenicity strain of influenza (x31, H3N2) and that an overactive immune response rather than impaired viral control correlates with enhanced morbidity and mortality in *Tpl2*$^{-/-}$ mice. The goal of the current study is to evaluate *Tpl2*$^{-/-}$ mice clinically and histopathologically to gain insight into disease mechanisms, including the development of ARDS features. Histopathologically, we observed prominent signs of alveolar septal necrosis, pleuritis and higher lactate dehydrogenase (LDH) levels in the lungs of influenza-infected *Tpl2*$^{-/-}$ mice compared to WT mice from 7 to 9 dpi. Notably, WT mice showed signs of regenerating epithelium that were reduced in *Tpl2*$^{-/-}$ mice. Furthermore, biomarkers associated with human ARDS cases were upregulated in *Tpl2*$^{-/-}$ mice at 7 dpi, suggesting an ARDS-like phenotype in *Tpl2*$^{-/-}$ mice in response to influenza infection. Thus, this study highlights how Tpl2 regulation of hypercytokinemia and inflammation plays a role in preventing the development of ARDS like clinical syndrome induced by influenza and the utility of this model in investigation of diagnosis, prevention and treatment of ARDS.

INTRODUCTION

Acute Respiratory Distress Syndrome (ARDS) is a form of lung injury induced by a variety of insults, like sepsis, pneumonia, severe traumatic injury, and aspiration of gastric contents, that leads to both hypoxia (lack of oxygen) and edema (fluid in the lung)[331,332]. 30-40% of the patients hospitalized for influenza develop bacterial pneumonia, which has a higher likelihood of developing ARDS. Therefore, it is not surprising that the most common viral causative agent for ARDS is influenza A[39]. Regardless of the underlying cause, ARDS is characterized by the acute onset of non-cardiogenic pulmonary edema leading to increased work of breathing and acute hypoxemic respiratory failure[333]. Patients that do survive typically have lasting impairments, including persistent pulmonary dysfunction, cognitive impairment and muscle weakness[334,335]. Risk factors that lead to higher probability of developing ARDS include advanced age[336–338], female gender[339–341] and surgery[342,343].

One barrier to ARDS management is the difficulty in its diagnosis. In an ARDS study canvassing 50 countries in which the physician diagnoses of ARDS were based on the Berlin definition[344], the clinical diagnosis was less than 40%, with severe cases extending the probability of diagnosis to only 80%[345]. Contributing to failure of ARDS diagnosis is the fact that the measurement of the oxygen levels via ratio of arterial oxygen partial pressure to fractional inspired oxygen (PaO2/FiO2) is not always performed[346] or can vary on a patient-to-patient basis[347]. While diagnosis of ARDS in its early stages is difficult, detection of it early enough allows for treatment with high flow oxygen while avoiding the increase of pulmonary edema (optimal fluid management) , pharmacological and antiviral therapies[40,41]. Considering that ARDS remains a difficult disease to diagnose and manage, it is vital to understand the disease etiology and progression to better prevent, diagnose and treat it.

The general pathological features of ARDS are typically described as passing through three overlapping phases: (1) an inflammatory or exudative phase, (2) a proliferative phase and (3) a fibrotic phase[348,349]. The exudative phase is marked with alveolar damage due to necrosis of the epithelium, along with signs of inflammation, including cytokine secretion and associated inflammatory cell recruitment[333]. The proliferative phase is marked by recovery of the epithelium by replacement with fibroblasts and type II pneumocytes[349,350]. Moreover, this phase sees the transition from inflammatory cell-derived mediators of lung injury to anti-inflammatory macrophage- and fibroblast-derived growth factors that facilitate repair. The last stage is end-stage fibrosis, characterized by extensive thickening of the interstitium by fibrosis that compromises alveolar gas exchange, and hypoxia sets in[332,348]. At this stage, the only option for treatment is mechanical ventilation, however recovery depends on many factors including the level of care received and other treatments[351]. ARDS typically results in nearly 40% mortality, even with aggressive treatment[345,352–355]. Furthermore, it is harder to treat influenza-induced ARDS, due to both virus cytopathic effects and inflammation-induced lung damage.[356,357]

Inflammation in influenza-induced ARDS is generally associated with cytokines IL-6, IL-10, G-CSF, IL-1β, IL-8, MCP-1 and IL-12[358–361] and the recruitment and function of macrophages, neutrophils and monocytes[274,362–365]. The damage resulting from the influenza infection can predispose the person to bacterial co-infection, especially post long-term mechanical ventilation or in patients older than 65 years of age[235–237]. Hence, we see that post influenza infection, due to the multivariate nature of the inflammation, multiple mechanisms can trigger/facilitate the progression to ARDS. Furthermore, when cases involving any respiratory distress, are examined by radiography it is hard to distinguish influenza-induced ARDS from ARDS triggered by other insults, or to differentiate damage caused by bacterial pneumonia from damage caused by prior viral infection[237,366]. Thus, we note that with difficulty in clinically diagnosing the cause, it is hard to predict which cases of influenza would progress to ARDS. Therefore, it is essential to evaluate the regulators of the immune response to influenza, for their role in ARDS development. Hence, we wished to examine if Tpl2 regulation of the immune response to influenza in the mouse model[315], would have any clinical similarities to ARDS development.

Tpl2$^{-/-}$ mice exhibit enhanced morbidity and mortality to influenza infection with deteriorating clinical symptoms from 7 to 9 dpi[222,233]. Live virus was undetectable in lungs by 9 dpi, confirming viral clearance, albeit delayed, in the *Tpl2*$^{-/-}$ mice[222]. Despite viral clearance, *Tpl2*$^{-/-}$ mice exhibited excessive influx of inflammatory cells, specifically inflammatory monocytes and neutrophils, by 7 dpi. Additionally, IFN-β expression directly correlated with chemokines CCL2 and CXCL1, both of which also correlated with NOS2 over-expression. These data suggested that the damage to *Tpl2*$^{-/-}$ lung tissue at 7 dpi was mediated by recruited inflammatory monocytes and neutrophils[222]. However, it is still unclear precisely how this enhanced inflammatory response leads to morbidity and mortality in *Tpl2*$^{-/-}$ mice.

The goal of the current study is to evaluate *Tpl2*$^{-/-}$ mice clinically and histopathologically to gain insight into disease mechanisms, including the potential development of ARDS features. Histopathologically, we observed prominent signs of alveolar septal necrosis, pleuritis and higher LDH levels in the lungs of influenza-infected *Tpl2*$^{-/-}$ mice compare to WT mice from 7 to 9 dpi. Notably, WT mice showed signs of regenerating epithelium that were significantly reduced in *Tpl2*$^{-/-}$ mice. Furthermore, influenza-infected *Tpl2*$^{-/-}$ mice displayed upregulation of biomarkers associated with human ARDS, including Receptor for Advanced Glycosylation End Products (RAGE), Vascular Endothelial Growth Factor α (VEGFα) and Actin Alpha 2, Smooth Muscle (ACTA) at 7 dpi. Therefore, we are able to characterize the pathology seen in influenza-infected

Tpl2$^{-/-}$ mice as ARDS-like. Influenza-infected *Tpl2*$^{-/-}$ mice may therefore represent a novel murine model for studying ARDS-like disease.

MATERIALS AND METHODS

Mice and viruses

Wild type (WT) C57BL/6 mice were purchased from Jackson Laboratory. *Tpl2*$^{-/-}$ mice backcrossed 10 generations onto the C57BL/6 strain were kindly provided by Dr. Philip Tsichlis[315]. Animals were housed in microisolator cages in the Central Animal Facility of College of Veterinary Medicine. All animal experiments were performed in accordance to the guidelines provided by "The Guide for Care and Use of Laboratory Animals". The Institutional Animal Care and Use Committee (IACUC) of the University of Georgia approved all animal experiments.

Embryonated specific pathogen-free eggs were purchased from Poultry Diagnostics & Research Center, UGA. Influenza virus A/HKX31 (H3N2) stocks were kindly provided by Dr. Mark Tompkins (University of Georgia). The virus was propagated in the allantoic cavity of 9- to 11-day-old embryonated specific pathogen free (SPF) chicken eggs at 37°C for 72 hours, and viral titers were enumerated by plaque assays as described[315].

Influenza infection of mice

Age matched 6-8 week-old WT and *Tpl2*$^{-/-}$ mice were anesthetized with 250 mg/kg of 2% weight/volume Avertin (2,2,2- Tribromoethanol, Sigma) followed by intranasal instillation of 50 µl PBS containing 10^4 pfu of influenza A/HKX31 (H3N2, hereafter referred to as x31). The mice were maintained post infection while being scored according to the following index: piloerection, 1 point; 20% weight loss, 1 point; 25% weight loss, 2 points; hunched posture, 2 points; labored breathing, 3 points; 30% weight loss, 5 points. Mice with a cumulative score of 5 were humanely euthanized.

Histology

Mice were infected with 10^4 pfu of influenza A virus (IAV, x31)) for 7 and 9 days, with uninfected controls for each genotype also included, and lungs were harvested and fixed with 10% neutral-buffered formalin. Fixed lungs were processed into 4 μm sections for hematoxylin and eosin (H&E) staining. The sections were then scored for histological features by a board-certified, veterinary pathologist in a blinded manner, according to the following criteria:

- Alveolar/Alveolar edema/Pleuritis score: focal lesion, 1 point; multifocal lesions, 2 points; multifocal to coalescing lesions, 3 points; majority of lobule affected, 4 points.
- Interstitial pneumonia score: alveolar septa infiltrated and thickened by 1 leukocyte layer, 1 point; 2 cells-thick layer infiltration of alveolar septa, 2 points; 3 cells-thick layer infiltration of alveolar septa, 3 points; 4 cells-thick layer infiltration of alveolar septa, 4 points.
- Bronchiolar score: focally affected bronchiole, 1 point; multifocal affected bronchioles, 2 points; majority of the bronchioles in a lobule affected, 3 points; bronchioles diffusely affected in a lobule, 4 points.
- Vasculitis score: infiltration of vessel wall by leukocytes, 1 point; infiltration and separation of smooth muscle cells in the vessel wall, 2 points; infiltration and fibrinoid change, 3 points.

Analysis of gene expression

Mice were sacrificed at 7 to 9 days post infection (dpi). Lungs were harvested into 1 ml of PBS and homogenized in a bead mill homogenizer (Qiagen Tissue Lyser II) at 25 hertz for 2-4 minutes in prechilled rotors. The homogenate was centrifuged at 500x*g* for 5 minutes, and the pre-cleared homogenate was lysed in TRK tissue lysis buffer (RNEasy, Omega Bio-Tek) for RNA extraction. Messenger RNA was extracted using the E.Z.N.A. RNA Extraction Total RNA kit I (Omega Bio-Tek) and converted into cDNA using a High-Capacity RNA-to-cDNA kit (Thermo Fisher) according to manufacturer's protocol. Relative expression of various genes was assessed using RT-PCR Sensifast Hi-ROX PCR Mastermix (Bioline) and probes sourced from Applied Biosystems) using a StepOne Plus instrument (Applied Biosystems). Results are expressed relative to the actin internal control and the WT or untreated sample using the $\Delta\Delta C_T$ method. The following probes were used in this process: ACTA (Mm01546133), AGER (Mm001134790), CD200 (Mm00487740), CD200R1 (Mm00491164), COX2 (Mm03294838), CXCL5 (Mm00436451), Paprg (Mm00440940), Pecam1 (Mm 01242584), Ptges2 (Mm00460181) and Vegfα (Mm00437306).

Serum Complete Blood Count and Lactate Dehydrogenase measurements

Mice were sacrificed at 7 to 9 dpi. Blood was collected by cardiac puncture or renal vein bleed into 1.1 ml Z Gel Micro tubes (Catlog #41.1378.005, Starstedt). Complete blood count (CBC) with automated differential was performed at the UGA-Athens Veterinary Diagnostic Laboratory. Lactate dehydrogenase (LDH) was measured with a QuantiChrom™ Lactate Dehydrogenase Kit (catalog# D2DH-100, VWR) using 3 μl of serum.

Chimeras

Different Host Bone Marrow Chimeras (DH) chimeras were made by irradiating adult (> 6 weeks of age) WT and *Tpl2*$^{-/-}$ mice with 1100 Rads followed the next day with injection of 3 x 10^6 bone marrow cells from WT donor mice in a volume of 200 µl PBS as mentioned previously[315]. Different Donor Bone Marrow Chimeras (DD) chimeras were made by irradiating adult (> 6 weeks of age) WT mice with 1100 Rads followed the next day with injection of 3 x 10^6 bone marrow cells from WT or *Tpl2*$^{-/-}$ donor mice in a volume of 200 µl PBS. Chimeras were maintained on acidified water (pH 2.5) in sterile caging for 2 months to allow for reconstitution of the hematopoietic compartment. The resulting chimeras were infected with 10^4 pfu x31 virus, and body weights were measured over a period of 8 to 10 days, at which times the mice were euthanized to assess the lung cytokine profile and ARDS marker expression on the day of expected peak clinical symptoms (i.e. weight loss).

Statistical Analysis

P values were calculated with GraphPad PRISM software version9.2.0(332) using Student's T test or one-way ANOVA with Tukey's multiple comparisons test, depending on the number of groups being compared. Differences were considered statistically significant if $p \leq 0.05$. Data represent means ± SEM.

RESULTS

Tpl2$^{-/-}$ *mice present with increased immunopathology upon influenza infection*

Influenza-infected *Tpl2*$^{-/-}$ mice show severe inflammation, as measured by cytokine expression by 7 dpi[315]. To gain further insight into the etiology of disease in influenza-infected *Tpl2*$^{-/-}$ mice, we assessed the lung tissue for pathological alterations at 7 dpi, because this was the clinically divergent time point at which WT mice show signs of recovery, whereas *Tpl2*$^{-/-}$ mice become progressively worse[315]. The lungs were scored by a board-certified veterinary pathologist blinded to the groups according to the scale defined in the *Materials and Methods*. Lung sections from *Tpl2*$^{-/-}$ mice showed a greater percent of the lung area affected by inflammation by 7 dpi (Figure 4.1A-B). Increased alveolar septal necrosis and inflammation of the pleura were also observed in *Tpl2*$^{-/-}$ lung sections (Figure 4.1A, C-D), indicating that increased epithelial and alveolar damage extended to the pleura in *Tpl2*$^{-/-}$ mice. While interstitial pneumonia was higher in WT mice, other indices, including bronchiolar, vasculitis, alveolar, and alveolar edema scores were similar between WT and *Tpl2*$^{-/-}$ mice (Figure 4.1E-I), suggesting that specific alterations and not wholesale inflammation were occurring. We also examined fibrosis with Masson's Trichrome staining and found no difference in fibrosis at 7 dpi between WT or *Tpl2*$^{-/-}$ mice (Figure 4.1J-L).

Biomarkers for ARDS increased in Tpl2 at day 7 post infection

We have previously noted the influx of excessive neutrophils and monocytes into the lungs of influenza-infected *Tpl2*$^{-/-}$ mice by 7 dpi, along with overexpression of the inflammatory enzyme NOS2[315]. In other mouse models of influenza-induced ARDS, neutrophils have been shown to contribute to the damage induced, with similar clinical signs of weight loss and morbidity at approximately 10 dpi[130,367,368]. Considering the epithelial damage observed histolopathologically in *Tpl2*$^{-/-}$ mice at 7 dpi along with inflammation noted in influenza-infected mice previously[315] and the similar clinical course and outcomes seen in the exudative phase of ARDS[333,349,369], we examined the expression of early ARDS biomarkers, in influenza-infected WT and *Tpl2*$^{-/-}$ mice at 7 dpi. Since ARDS manifests due to issues involving the epithelium, endothelium and other contributing cell types like alveolar macrophages, broadly representative biomarkers were selected. For examination, the lung tissue was either unprocessed, or perfused and lavaged prior to homogenization. The perfused-lavaged lung tissue, is important as it is the location of the hyperketonemia and cellular differences seen in the previous study[315], however the intact (unprocessed) lung was required to factor in the contribution from the blood & BAL (with focus on epithelium-endothelium interaction). We examined several widely accepted biomarkers of the exudative phase of ARDS, including Receptor for Advanced Glycosylation Endproducts (RAGE), Vascular Endothelial Growth Factor (VEGFα), CXCL5 (or ENA78, which has structural homology to IL-8), and Platelet and Endothelial Cell Adhesion Molecule 1 (PECAM-1)[369–372]. RAGE is expressed in epithelial cells, whereas VEGFα, PECAM-1, and CXCL5 are associated with endothelial activation during ARDS[373] linked with the restructuring of the endothelium to facilitate neutrophil adhesion[374–376] and angiogenesis of blood vessels[377–381]. Interestingly, RAGE (represented by the gene AGER), VEGFα, PECAM-1 and CXCL5 are upregulated in the *Tpl2*$^{-/-}$ intact/whole lungs but not in the *Tpl2*$^{-/-}$ perfused and lavaged lungs compared to WT (Figure 4.2A-H. During influenza infection, CD200 Receptor (CD200R) expression is upregulated on various myeloid cells, especially alveolar macrophages; concomitantly, CD200 is expressed by the epithelial, endothelial cells and to some extent B and T cells. CD200 interacts with the CD200R to suppress the inflammatory activity of alveolar macrophages[382]. Furthermore, *CD200*$^{-/-}$ mice developed ARDS in response to influenza infection, due to the increased pro-inflammatory macrophage function[382]. Likewise, intratracheal instillation of LPS reduced CD200 expression in mice in a model of LPS-induced ALI[383]. Therefore, reduced expression of CD200 has been associated with (mouse models of) ARDS, as it is then unable to suppress the inflammatory function of alveolar macrophages[382,383]. Interestingly, we observed upregulated levels of CD200 along with no difference in the expression of CD200R1 in both the intact and perfused/lavaged *Tpl2*$^{-/-}$ lungs at 7 dpi (Figure 4.2I-L). We also examined another biomarker, peroxisome proliferator- activated receptor *gamma* (PAPR-γ), to represent the interaction between the pulmonary epithelium and alveolar macrophages. PAPR-γ is a receptor expressed on alveolar macrophages that mediates anti-inflammatory effects by suppressing inflammatory products like MCP-1, MIP2, NOS2, COX2, ICAM, and P-selectin, as well as prevention of injury/edema[384,385]. PAPR-γ was not differentially expressed in either the intact or perfused/lavaged *Tpl2*$^{-/-}$ lungs at 7 dpi (Figure 4.2M-N). Finally, Actin Alpha 2 (ACTA), which is required for the movement of myofibroblasts in the early stages of the lung injury and has been shown to be upregulated in ARDS patients[386], was overexpressed in both the intact and perfused/lavaged *Tpl2*$^{-/-}$ lungs at 7 dpi (Figure 4.2O-P). Collectively, we found overexpression of AGER, VEGFα, PECAM-1, CXCL5 and ACTA, in influenza-infected *Tpl2*$^{-/-}$ mice at 7 dpi that correspond to ARDS biomarker profiles in human patients, with no difference in CD200R1 (along with over-expression of CD200) and PAPRγ in *Tpl2*$^{-/-}$ mice at 7dpi.

In our previous study, we observed that chimeric mice with Tpl2 ablation localized to the radio-resistant compartment showed differential weight loss compared to control WT chimeras on 8 dpi but recovered by 10 dpi. Moreover, they also exhibited cytokine dysregulation with overexpression of CCL2, IFN-γ and IL-6 at 8 dpi[315]. We examined these chimeras to localize the cellular contribution of Tpl2 to ARDS biomarker expression and only found a decrease in PECAM-1 expression (Supplementary Fig. 4.7A-E), contrary to the increase observed with global Tpl2 ablation (Figure 4.2E). We next generated Different Donor Bone Marrow (DD) chimeras, wherein WT mice were irradiated and given bone marrow from either WT or *Tpl2*$^{-/-}$ mice resulting in mice with Tpl2 ablation restricted to the radiosensitive compartment (Supplementary Figure 4.8A) to examine their contribution towards the phenotypic profile of global Tpl2 deficient mice. In these DD chimeras, there was no difference in influenza-induced weight loss, irrespective of Tpl2 ablation (Supplementary Figure 4.8B). However, there was increased expression of CCL2 in the DD *Tpl2*$^{-/-}$ chimeras (Supplementary Figure 4.8C), with no difference in IFN-γ or IL-6 levels (Supplementary Figure 4.7D-E), indicating that this was a much milder model of disease than observed in either mice with global Tpl2 ablation or DH chimeras[315]. Accordingly, examination of ARDS biomarkers in these chimeras showed no differential expression (Supplementary Figure 4.8F-J). Collectively, these data reveal that ARDS biomarker expression is dependent upon Tpl2 ablation in both radioresistant and radiosensitive compartments.

***Histopathological damage intensifies in influenza-infected Tpl2*$^{-/-}$ mice at 9 dpi.**

Tpl2$^{-/-}$ mice have histopathological indications of damage and early signs of ARDS by 7 dpi, which corresponds to the day that WT and *Tpl2*$^{-/-}$ mice clinically diverge. Since the *Tpl2*$^{-/-}$ mice succumb to the infection at approximately 10 dpi[315], we further examined both WT and *Tpl2*$^{-/-}$ mice at 9 dpi. At this time point, histology revealed prominent alveolar septal necrosis with the formation of a hyaline membrane (fibrin lining the septa; Figure 4.3A-C), which are histopathologic lesions seen in patients with pathogenic influenza infection or influenza-induced ARDS patients[38,239,387]. The representative images for the *Tpl2*$^{-/-}$ lung section to depict alveolar septal necrosis as well as the hyaline membrane, are from mice that naturally succumbed to the infection and as represented by their darker pink staining in contrast to the WT section. Inversely, signs of type 2 pneumocyte hyperplasia, which indicates regeneration of the epithelium post injury and characteristic of patients recovering from influenza[38,388], is higher in WT at 9 dpi compared to *Tpl2*$^{-/-}$ mice (Figure 4.3A, C), wherein visually we see that there are more of the darker, slightly bigger cells that are linking the alveoli at a more pronounced proportion than the *Tpl2*$^{-/-}$ lung section. Other lesion metrics, such as percent of lung affected and pleuritis, which were different at 7 dpi, and other scored lesions were not affected by Tpl2 ablation (Figure 4.3D-I), however alveolar edema appeared to be decreased in lungs of *Tpl2*$^{-/-}$ mice compared to WT mice at 9 dpi (Figure 4.3J). We also did not observe significant differences in fibrosis by histochemistry at 9 dpi (Figure 4.3K-M). ARDS biomarkers that were upregulated at 7 dpi, were no longer differentially expressed in *Tpl2*$^{-/-}$ mice at 9 dpi, suggesting that the disease had progressed beyond the peak transcriptional expression of these early-stage ARDS markers (Supplementary Figure 4.9A-E). Therefore, we examined the fibrotic response of the lung as a measure of the final fibrotic stage of ARDS focusing on Cyclooxygenase 2 (COX2) expression. COX2 is an inducible enzyme that allows for the resolution of lung injury by assisting prostaglandins and lipid mediators in limiting the pathobiological function of fibroblasts, and thereby limiting fibrosis[389,390]. Moreover, it was recently shown that alveolar macrophage-specific deletion of Tpl2 caused a reduction in COX2 expression and induced pulmonary fibrosis in a bleomycin-induced model of idiopathic pulmonary fibrosis (IPF)[391]. However, there was not a significant difference in the levels of COX2 between the *Tpl2*$^{-/-}$ or WT intact lungs at 9 dpi (Supplementary Figure 4.9F) nor at the earlier time point of 7 dpi (Supplementary Figure 4.9G).

CBC profiling shows more RBCs and platelets in *Tpl2*$^{-/-}$ mice, suggestive of injury and repair

With increased histopathological signs of lung damage in influenza-infected *Tpl2*$^{-/-}$ mice at 9 dpi (Figure 4.3A-B) and higher clinical scores in *Tpl2*$^{-/-}$ mice, involving hunching and dyspnea (or labored breathing)[315], we examined the complete blood profile at 9 dpi. Notably, anemia is linked to cases of severe influenza disease[392]. Higher red blood cell counts, hemoglobin content, hematocrit (HCT), and platelets were observed in circulation in *Tpl2*$^{-/-}$ mice compared to WT at 9 dpi (Figure 4.4A-C, I). However, no differences were observed for various other measures, including red cell distribution width (RDW), mean corpuscular hemoglobin concentration (MCHC), mean corpuscular volume (MCV), and mean corpuscular hemoglobin (MCH), which are primarily measured to assess anemia (Figure 4.4D-G). There was also no difference in white blood cell (WBC) counts or mean platelet volume (MPV) (Figure 4.4H, J).

Pulmonary edema and LDH overexpression in blood at day 9 suggests accumulating damage in *Tpl2*$^{-/-}$ mice.

Lactate Dehydrogenase (LDH) is the enzyme that converts pyruvate to lactate in the presence of NADH and is widely accepted to evaluate cellular damage for various pathological conditions, including influenza-induced apoptosis and COVID-19 severity prognosis[393–395]. We first examined LDH levels in the blood and BALF at 7 dpi and found that, while *Tpl2*$^{-/-}$ mice did not show any differences in LDH release in blood at 7 dpi (Figure 4.5A), we did observe increased LDH release in the BALF of the same mice (Figure 4.5B). By 9 dpi, LDH release was also observed in the blood (Figure 4.5C), consistent with progression of the disease by that time point. Pulmonary edema (fluid in the lungs) is a major component of ARDS and is often used to clinically define the condition[396,397]. Therefore, we examined pulmonary edema by measuring the wet/dry lung weights at 9 dpi. *Tpl2*$^{-/-}$ mice had significantly higher levels of pulmonary edema compared to WT mice at 9 dpi (Figure 4.5E), also consistent with increased morbidity in *Tpl2*$^{-/-}$ mice.

DISCUSSION

Our previous study established hypercytokinemia and increased pulmonary recruitment of inflammatory monocytes and neutrophils in influenza-infected *Tpl2*$^{-/-}$ mice at 7 dpi, when they start showing increased weight loss and clinical scores compared to WT mice. Accordingly, *Tpl2*$^{-/-}$ mice succumb to influenza infection by 9 dpi[315]. In this study, detailed examination of lung histopathology from 7 to 9 dpi revealed alveolar septal necrosis at 7 dpi that became more prominent in the *Tpl2*$^{-/-}$ mice by 9 dpi with formation of hyaline membranes. Conversely, WT mice showed signs of recovering and regenerating epithelium by 9 dpi, consistent with their full recovery. We also observed pleuritis and higher levels of LDH in the BALF of *Tpl2*$^{-/-}$ mice at 7 dpi, and in the blood at 9 dpi. Notably, increased morbidity in the *Tpl2*$^{-/-}$ mice was accompanied by increased pulmonary edema, a hallmark of ARDS, at 9 dpi. Assessment of ARDS biomarkers showed that *Tpl2*$^{-/-}$ mice showed differential expression of RAGE, VEGFα, PECAM-1, CXCL5, and ACTA, at 7 dpi in the *Tpl2*$^{-/-}$ mice, consistent with an ARDS-like phenotype (Figure 4.6).

The early stages of influenza-related acute alveolar injury are characterized by denudation of the alveolar epithelium that then progresses to widening of the alveolar septa due to fluid leakage from the vasculature, which along with fibrotic thrombi might be the cause for alveolar septal necrosis. The last stage of viral pneumonia is re-epithelialization of the alveolar septa and infiltration by leukocytes.[38,398] Moreover, the changes of influenza to the bronchioles are not long lasting and are mainly seen sub acutely as thickened epithelial linings primarily due to epithelial regeneration and bronchial inflammation, with signs of necrotizing bronchiolitis initially[398]. Additionally, in further review of the histology observed in various influenza patient lungs *post mortem*, the cases involving alveolitis (damage to the alveolar surfaces) were devoid of virus detection, whereas they showed regeneration of the epithelium within 5 dpi.[38] In the *Tpl2*$^{-/-}$ mice, we observed a higher occurrence of alveolar septal necrosis at 7 dpi, which becomes more prominent by 9 dpi. This was coupled with formation of the hyaline membrane and undetectable virus by 9 dpi[315]. These findings confirm that the pathology seen in *Tpl2*$^{-/-}$ mice results from a dysregulated immune response rather than viral replication.

Alveolar septal necrosis observed by 7 dpi is consistent with the diffuse alveolar damage characteristic of the early stages of ARDS[239,387]. The biomarkers overexpressed at 7 dpi, including AGER, VEGFα, PECAM-1 and CXCL5, are representative of the early/exudative phase of ARDS. Furthermore, on examination of intact versus perfused-lavaged lungs, we observed AGER, VEGFα, PECAM-1 and CXCL5 were all overexpressed with contribution from all components of the lung, whereas CD200 and ACTA were primarily overexpressed in the *Tpl2*$^{-/-}$ lung tissue compartment, suggesting a localization of the predominant expression for each marker. For example, CD200 being overexpressed in the perfused-lavaged lung tissue correlates with CD200 expression as an epithelial ligand[382]. CD200 is also an early phase marker, whose decreased expression typically leads to ARDS development. However, we noted instead that CD200 expression is increased in *Tpl2*$^{-/-}$ mice, perhaps as a compensatory mechanism to control excessive inflammation by suppressing the inflammatory functions of alveolar macrophages. This is similar to the SOCS1 overexpression in *Tpl2*$^{-/-}$ mice from 7 to 9 dpi to suppress the excessive T1 IFN signaling[315] (that is also predominantly associated with alveolar macrophages[56,57]). However, increased expression of CD200 and unchanged CD200R1 expression as early as 7dpi, along with no reduction in the PAPRγ levels suggests that the alveolar macrophages are not actively contributing towards ARDS development at later timepoints.

Another interesting aspect is that ACTA over-expression could be a sign of progression of the ARDS to the early proliferative phase, and that could also add to why it is so highly over-expressed. Especially when we consider the fact that none of the biomarkers are significant by mRNA expression at 9 dpi, it might be due to passage of the early-mid of the ARDS phase. Type 2 pneumocyte hyperplasia is a sign of previous alveolar damage that is being covered by regenerating epithelium, and has been found to be upregulated in patients with recovery post influenza[38]. Seeing this histologic characteristic upregulated in WT mice at 9 dpi is a sign of recovery of the mice post infection. Concomitantly seeing that it is not as upregulated in the *Tpl2*$^{-/-}$ mice could suggest that the mice are unable to progress past the early proliferation phase and hence we see the excessive RBCs and platelets in the blood at 9dpi as well.

When we examined the chimeras with Tpl2 ablation localized into radioresistant (DH chimeras) and radiosensitive compartments (DD chimeras), we see that while the chimeras overexpress CCL2 at day 7/8 post infection, they do not differentially express the ARDS markers, except for reduction of PECAM-1. This suggests that the chimeras are spared the extensive pulmonary damage that typically progresses to ARDS development. In the global *Tpl2*$^{-/-}$ mice, we observed differential ARDS biomarker expression at 7 dpi, which correlates to the peak of hypercytokinemia and differential weight loss in *Tpl2*$^{-/-}$ mice. In the DH chimeras, among the ARDS markers, only PECAM1 was differentially expressed at the peak of cytokine dysregulation, which was also less severe that in the global *Tpl2*$^{-/-}$ mice. The similar weight loss in DH chimeras confirm the less severe disease progression in these mice, consistent with rapid control of the cytokine dysregulation[315] and ARDS marker expression in this model. Similarly, in the DD chimeras, we do not observe differential ARDS biomarker expression at the time point with CCL2 dysregulation, and no differences in weight loss were noted. Considering that we examined markers that were more specific to interactions between alveolar macrophages and the epithelium, along with those specific for epithelial or endothelial damage, the similar ARDS biomarker expression in the chimeras suggests that even the early stages of ARDS development is a product of multiple interactions that are only facilitated by systemic Tpl2 ablation. Collectively, these data support that Tpl2 ablation in both radio-resistant and radiosensitive cells is required to cause the severe dysregulated and prolonged inflammation in response to influenza infection that then induces damage to develop into an ARDS-like phenotype.

Pulmonary edema has been associated with the endogenous activity of NOS2 (Nitric Oxide synthase 2) in various models and clinical cases of lung injury, including hypercalcemia, endotoxin treatment, influenza, and ARDS[399–402]. Additionally, NOS2 was found to be required for pathologic vascular changes in the lungs[403]. Indeed, we have observed increased NOS2 expression in the *Tpl2*$^{-/-}$ mice at 7 dpi[315]. The development of pulmonary edema is consistent with the dyspnea observed in *Tpl2*$^{-/-}$ late during the disease course, and ultimately explains the morbidity and mortality observed in *Tpl2*$^{-/-}$ mice via an ARDS-like mechanism. While reduced alveolar edema was noted in the *Tpl2*$^{-/-}$ mice by histology, this could be due to random sampling of less affected areas by histology. However, whole organ analysis by quantitation of lung wet:dry weight ratio clearly showed a significant increase in pulmonary edema in influenza-infected *Tpl2*$^{-/-}$ mice. The pulmonary edema observed by weight could explain the increased RBC, HgB, and HCT values in the *Tpl2*$^{-/-}$ mice secondary to dehydration due to loss of fluid into the alveolar compartment. Poor oxygenation could also be driving upregulation of RBC production in the *Tpl2*$^{-/-}$ mice. Increased platelet counts in the *Tpl2*$^{-/-}$ mice are consistent with the increased inflammation observed in this group. Furthermore, alveolar damage seen from 7 to 9 dpi by histologic examination has been associated with excessive inflammation mediated by inflammatory cells like neutrophils[387] in cases of ARDS caused by influenza and COVID-19[388,403,404]. In turn, the hypercytokinemia leading to the increased cellular influx in the *Tpl2*$^{-/-}$ mice by 7 dpi[315] is most likely caused by damage to the alveolar septa.

In studies examining the role of Tpl2 in lung injury induced by mechanical ventilation, genetic ablation and pharmacological Tpl2 inhibition before and after the ventilation reduced the severity of acute lung injury[405], whereas another study reported that Tpl2 kinase genetic inhibition was unable prevent ventilation-induced lung injury [406]. In contrast, our study is the first to show that Tpl2 serves a protective role during influenza-induced lung injury by preventing severe inflammation and ARDS development. Future studies will seek to further dissect the Tpl2-dependent host response to influenza infection within the different cellular compartments, including the epithelium, endothelium and alveolar macrophages requisite for severe influenza disease development and ARDS progression. Furthermore, the influenza-infected *Tpl2*$^{-/-}$ mouse model of influenza-induced ARDS development could enable us to better understand this aggressive disease and assist in the design of better diagnostics and treatments.

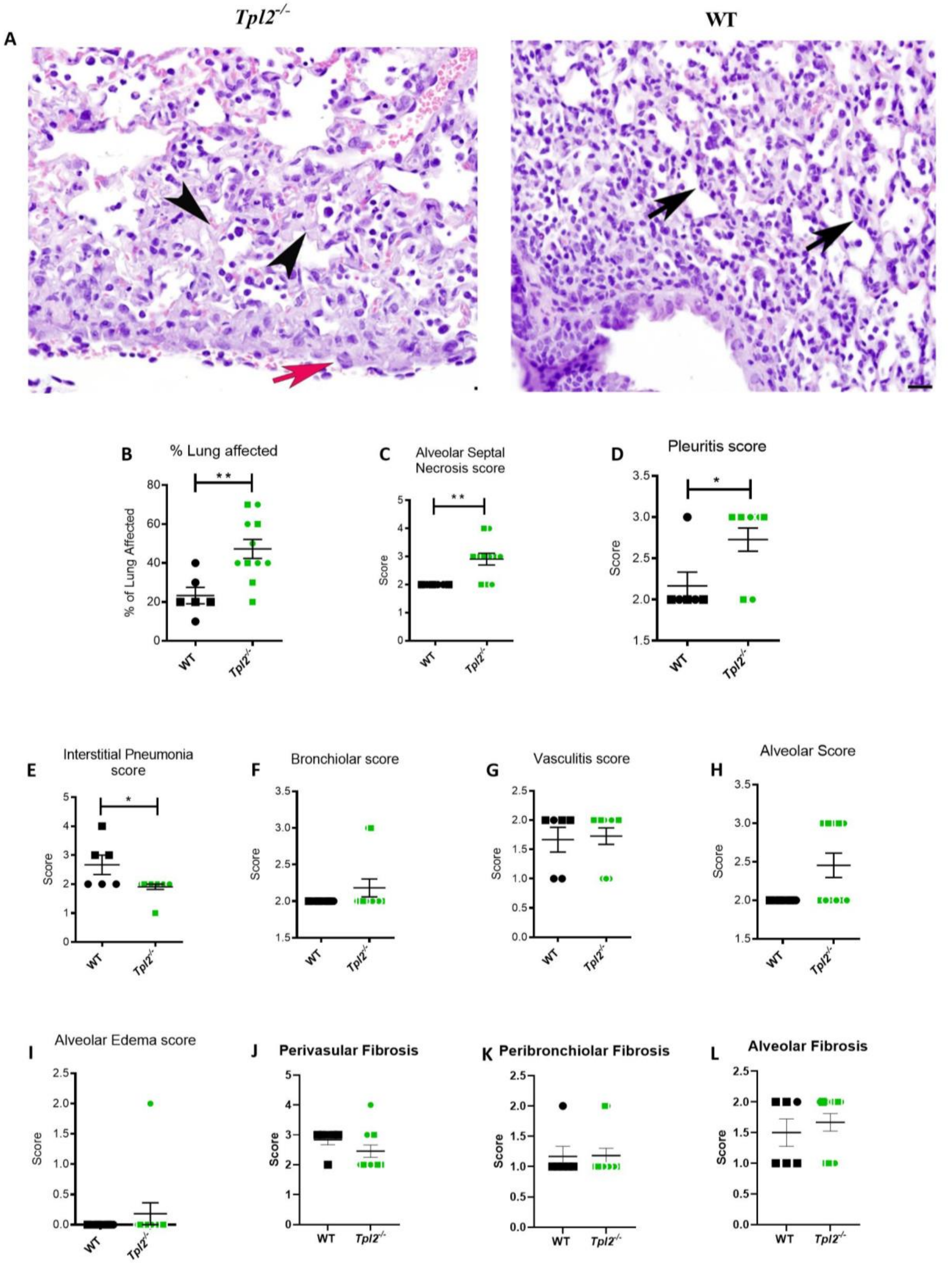

A
Tpl2-/-
WT
B
% Lung affected
% of Lung Affected
**
C
Alveolar Septal
Necrosis score
D
Pleuritis score
E
Interstitial Pneumonia
score
F
Bronchiolar score
G
Vasculitis score
H
Alveolar Score
I
Alveolar Edema score
J
Perivasular Fibrosis
K
Peribronchiolar Fibrosis
L
Alveolar Fibrosis
Score
WT
Tpl2-/-

Figure 4.1. Increased severity and distribution of some pulmonary lesions in *Tpl2*$^{-/-}$ mice at 7 dpi with influenza. WT (n=6) and *Tpl2*$^{-/-}$ (n=11) mice were infected intranasally with 10^4 pfu of influenza x31. At 7 dpi, the lungs were fixed in formalin, stained with H&E, and scored. **(A)** Representative images of *Tpl2*$^{-/-}$ (left) and WT (right) lungs to highlight the pleuritis, alveolar septal damage, and interstitial pneumonia. Black arrows indicate alveolar septal necrosis, arrowheads indicate interstitial pneumonia, and red arrows indicate pleuritis. **(B-I)** Pooled scores for all lungs in the two groups. **(J-L)** Separate sections of the same lungs were stained with Masson's Trichrome stain and scored for fibrosis. Squares represent male mice, and circles represent female mice. Unpaired student's *t*-test; *$p<0.05$, **$p<0.01$. Data are representative of 2 experiments.

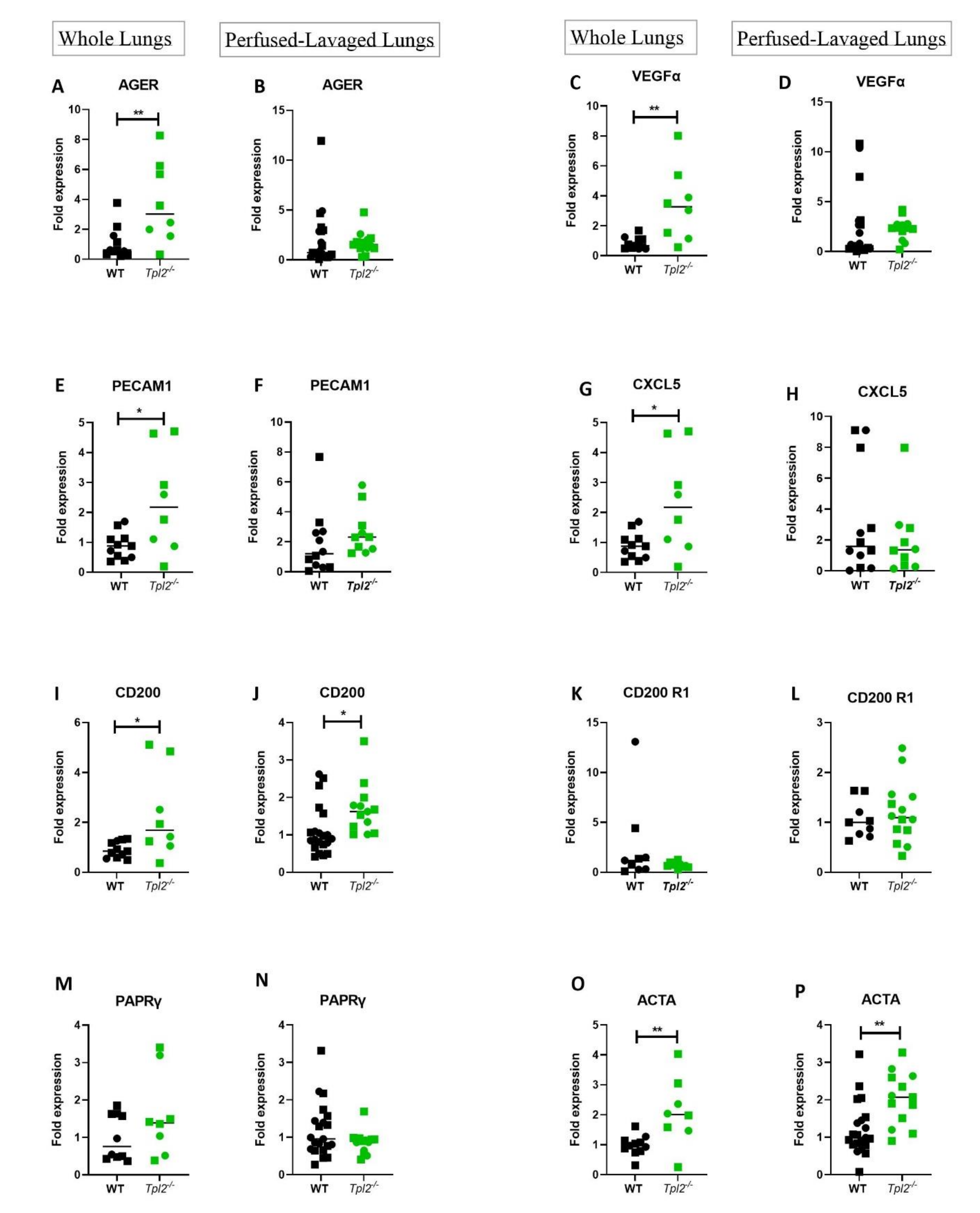

Figure 4.2. ARDS genes are overexpressed in lungs of influenza-infected *Tpl2*$^{-/-}$ mice at 7 dpi

in a tissue-specific manner. (A, C, E, G, I, K, M, O) WT (n=11) and *Tpl2*$^{-/-}$ (n=8) mice were infected intranasally with 10^4 pfu of influenza x31 for 7 days. The whole (intact) lungs were harvested without perfusion or lavage and homogenized for RNA extraction for gene expression analysis by real-time qPCR. Data are representative of 3 experiments. Squares represent male mice, and circles represent female mice. Unpaired student's *t*-test **p*<0.05, ***p*<0.01. **(B, D, F, H, J, L, N, M)** WT (n=19) and *Tpl2*$^{-/-}$ (n=10) mice were infected exactly as above, except that, prior to harvest and homogenization, lungs were perfused with 10 ml PBS prior and lavaged twice with the same 1 ml PBS. RNA was extracted, and real-time qPCR analysis was performed. Data are representative of 2 experiments. Squares represent male mice, and circles represent female mice. Unpaired student's *t*-test **p*<0.05, ***p*<0.01.

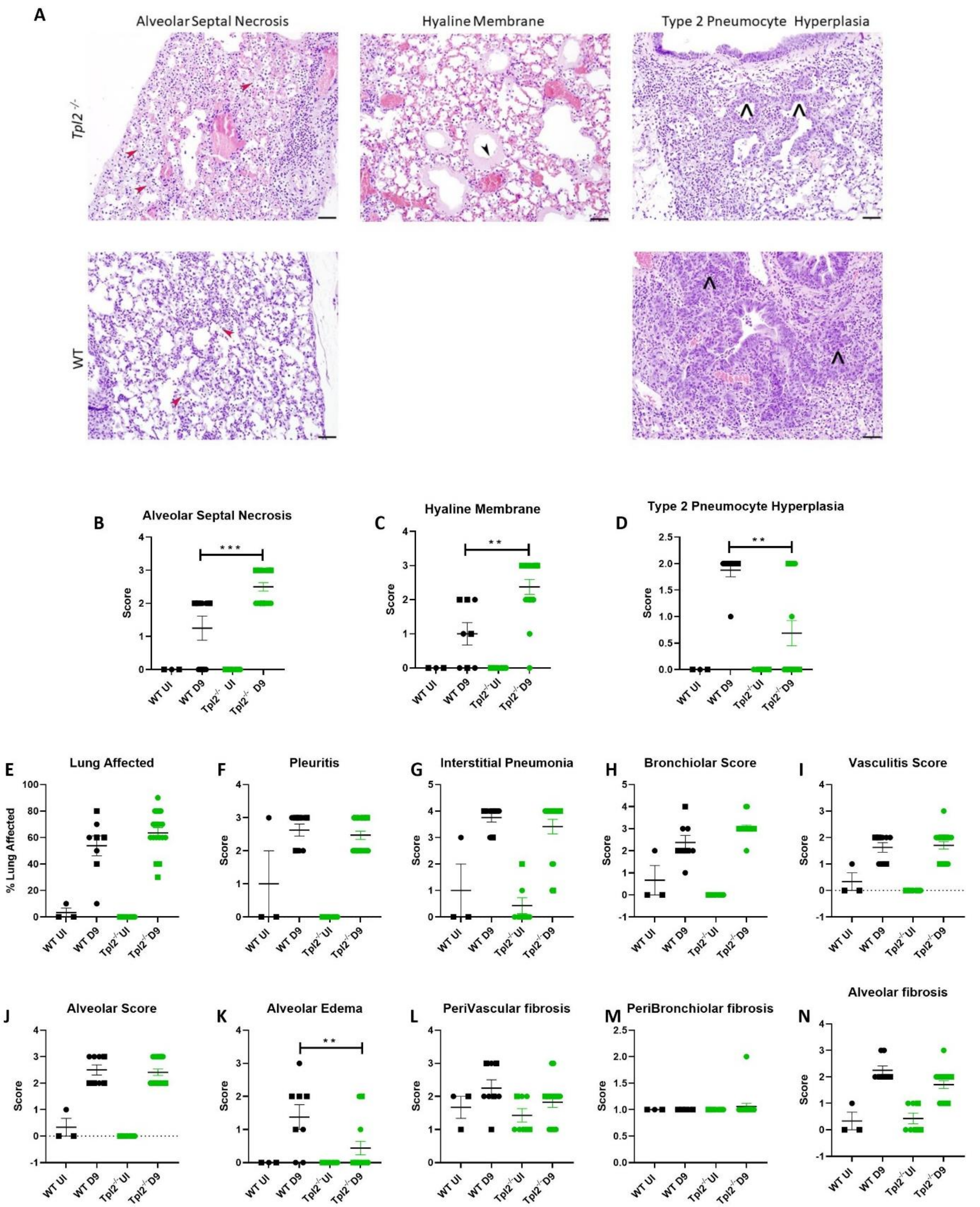
A
Alveolar Septal Necrosis
Hyaline Membrane
Type 2 Pneumocyte Hyperplasia
Tpl2 -/-
WT
B Alveolar Septal Necrosis
C Hyaline Membrane
D Type 2 Pneumocyte Hyperplasia
E Lung Affected
% Lung Affected
F Pleuritis
G Interstitial Pneumonia
H Bronchiolar Score
I Vasculitis Score
J Alveolar Score
K Alveolar Edema
L PeriVascular fibrosis
M PeriBronchiolar fibrosis
N Alveolar fibrosis
Score
WT UI
WT D9
Tpl2-/- UI
Tpl2-/- D9

Figure 4.3. Further increase in histopathologic damage in the *Tpl2$^{-/-}$* mice at 9 dpi. WT (n=8) and *Tpl2$^{-/-}$* (n=16) mice were infected intranasally with 10^4 pfu of influenza x31 with uninfected controls for WT (n=3) and *Tpl2$^{-/-}$* (n=7). At 9 dpi, the lungs were fixed in formalin, stained with H&E and scored. **(A)** Representative images of *Tpl2$^{-/-}$* (top) and WT (bottom) lungs to highlight the alveolar septal necrosis (ASN), hyaline membrane and Type II Pneumocyte Hyperplasia (T2PH). Red arrowheads indicate ASN, black arrowheads indicate the hyaline membrane, and black carrots indicate T2PH. **(B-K)** Pooled scores for all lungs in the two groups. **(L-N)** Additional sections of the same lungs were stained with Masson's Trichrome and scored for fibrosis. Squares represent male mice, and circles represent female mice. Data are representative of 2 experiments. One-way ANOVA with Tukey's multiple comparison test was performed. *p<0.05, **p<0.01, ***p<0.001.

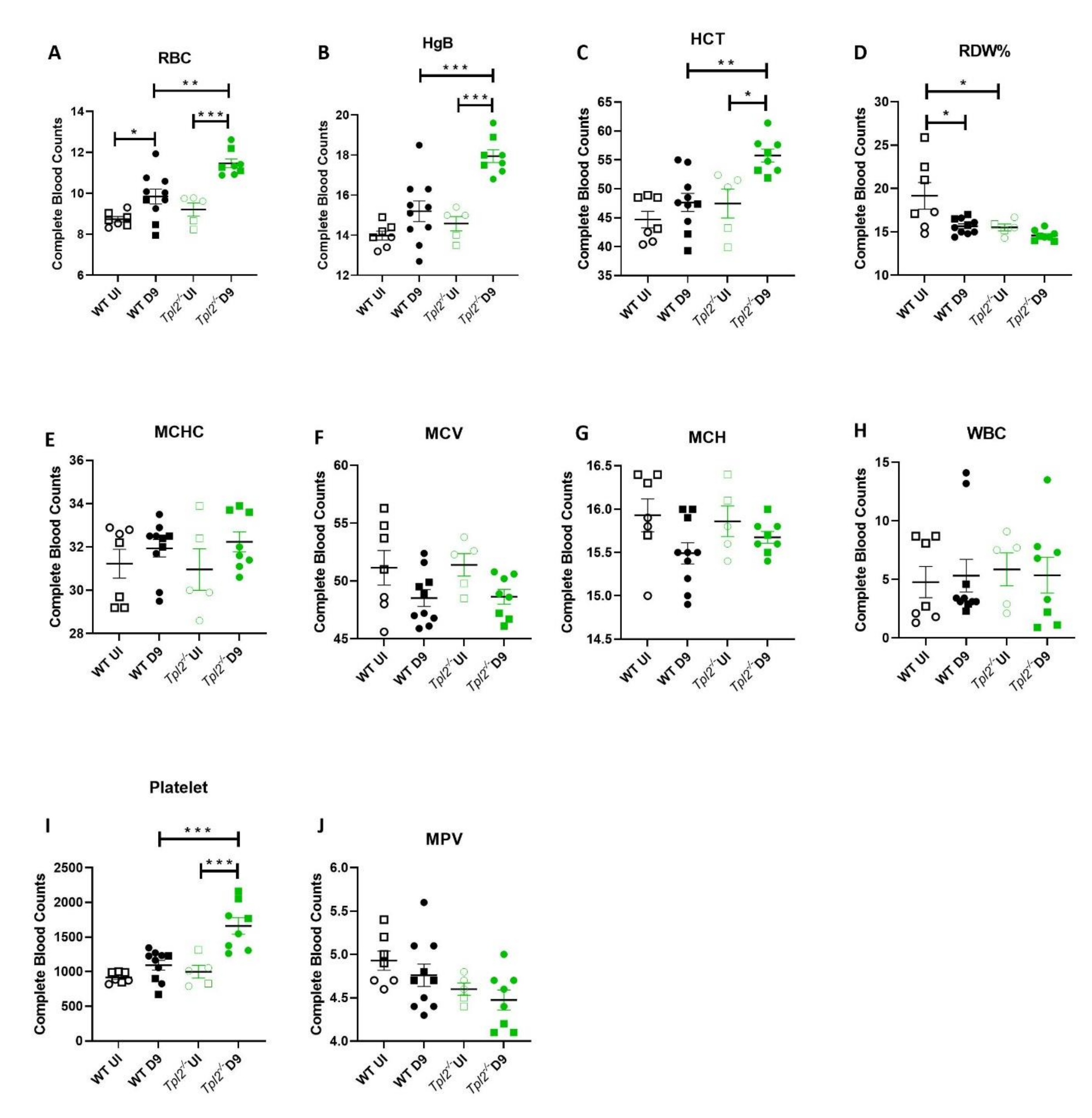

Figure 4.4. Blood counts indicate higher activity of cells involved in damage repair in *Tpl2$^{-/-}$* mice at 9 dpi. (A-J) WT (n=10) and *Tpl2$^{-/-}$* (n=8) mice were infected intranasally with 10^4 pfu of influenza A x31 with uninfected controls for WT (n=7) and *Tpl2$^{-/-}$* (n=5). At 9 dpi, blood was collected from the mice by cardiac puncture and assessed for complete blood counts. Data are

representative of 2 experiments. Squares represent male mice, and circles are female mice. One-way ANOVA with Tukey's multiple comparison test was performed. *$p<0.05$, **$p<0.01$, ***$p<0.001$.

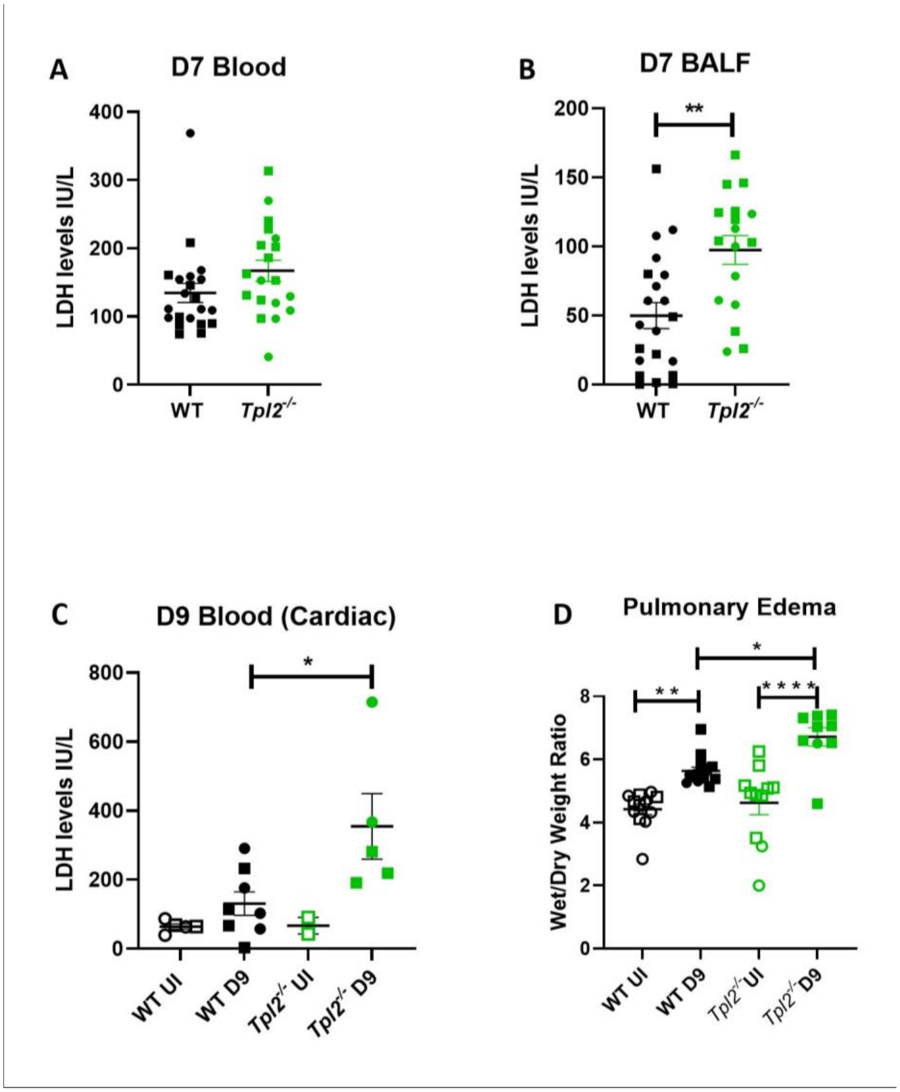

Figure 4.5. Increased lung injury and edema are observed in *Tpl2*$^{-/-}$ mice at 9 dpi. (A-B) WT (n=21) and *Tpl2*$^{-/-}$ (n=19) mice were infected intranasally with 10^4 pfu of influenza x31 for 7 days. Blood was collected by cardiac puncture **(A)**, and BALF was collected by intranasal instillation twice with the same 1 ml of PBS **(B)**. LDH was measured as described in *Materials and Methods*. Data are representative of 2 experiments. Unpaired student's *t*-test; **p*<0.05, ***p*<0.01, ****p*<0.001. Squares represent male mice, and circles represent female mice. **(C)** WT (n=8) and *Tpl2*$^{-/-}$ (n=5) mice were infected intranasally with 10^4 pfu of influenza x31 for 9 days with uninfected controls for WT (n=5) and *Tpl2*$^{-/-}$ (n=2). At 9 dpi, blood was collected by cardiac

puncture. **(C)** LDH release was assayed as in B. **(D)** WT (n=8) and *Tpl2*$^{-/-}$ (n=7) mice were infected intranasally with 10^4 pfu of influenza x31 with uninfected controls for WT (n=5) and *Tpl2*$^{-/-}$ (n=2). At 9 dpi, the lungs were collected, weighed, and dried for 7 days at 50°C before weighing again to calculate the pulmonary edema. One-way ANOVA with Tukey's multiple comparison test was performed with $*p<0.05$, $**p<0.01$, $***p<0.001$. Squares represent male mice; circles represent female mice.

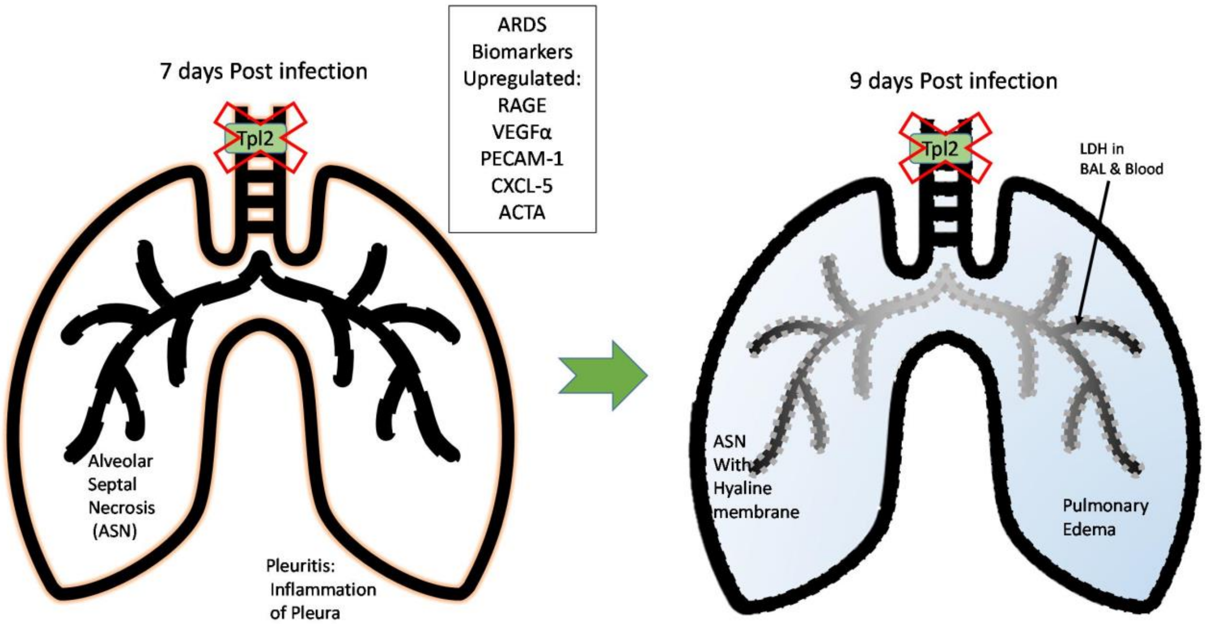

Figure 4.6. Influenza induced inflammation in *Tpl2*$^{-/-}$ mice results in damage that instigates the development of ARDS-like phenotype. In the lungs of influenza-infected *Tpl2*$^{-/-}$ mice at 7 dpi, histology shows signs of alveolar septal necrosis (ASN) (de-structured lines) and inflammation of the pleura cavity (orange outline of the lung), along with the upregulation of the ARDS biomarkers mentioned in the box. By 9dpi, the ASN progresses further with the formation of the hyaline membrane (wedged lines), LDH in the BAL and blood spaces and pulmonary edema (fluid in the lungs, represented by the blue gradient of the lungs) resulting in morbidity and mortality of the mice.

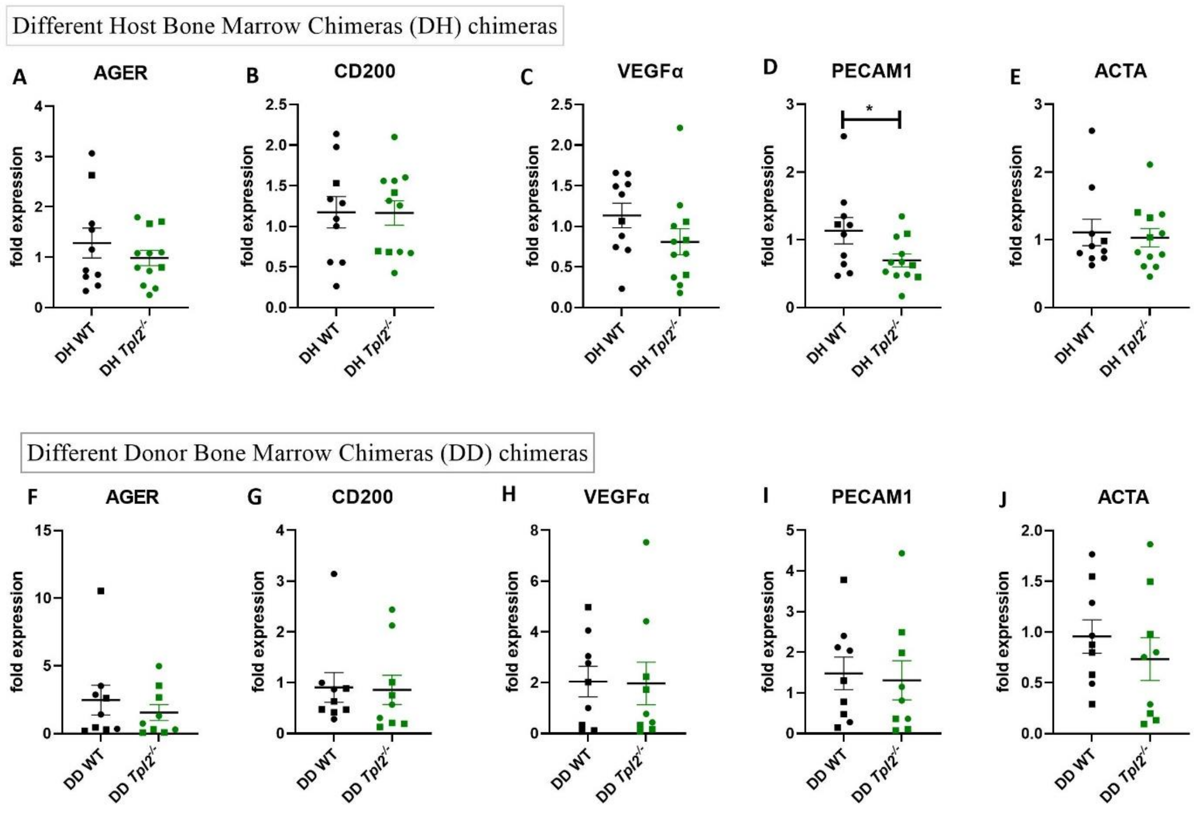

Supplementary Figure 4.7. ARDS biomarker expression is dependent upon Tpl2 ablation in both radio-resistant and radiosensitive cells. (A-E) WT (n=10) or *Tpl2*$^{-/-}$ (n=12) mice were lethally irradiated and reconstituted with WT bone marrow. After two months, chimeras were infected with influenza A x31, and 8 dpi the lungs were homogenized (without perfusion or lavage). RNA was extracted for qPCR analysis of ARDS biomarkers. **(F-J)** WT mice were lethally irradiated and reconstituted with WT (n=9) or *Tpl2*$^{-/-}$ (n=9) bone marrow to make DD chimeras. After two months, chimeras were infected with influenza A x31 for 7 days, and the whole lungs were homogenized without perfusion or lavage. RNA was extracted for qPCR analysis of ARDS markers by real-time qPCR. Data are representative of 2 experiments. Unpaired student's *t*-test **p*<0.05, ***p*<0.01. Squares represent male mice; circles represent female mice.

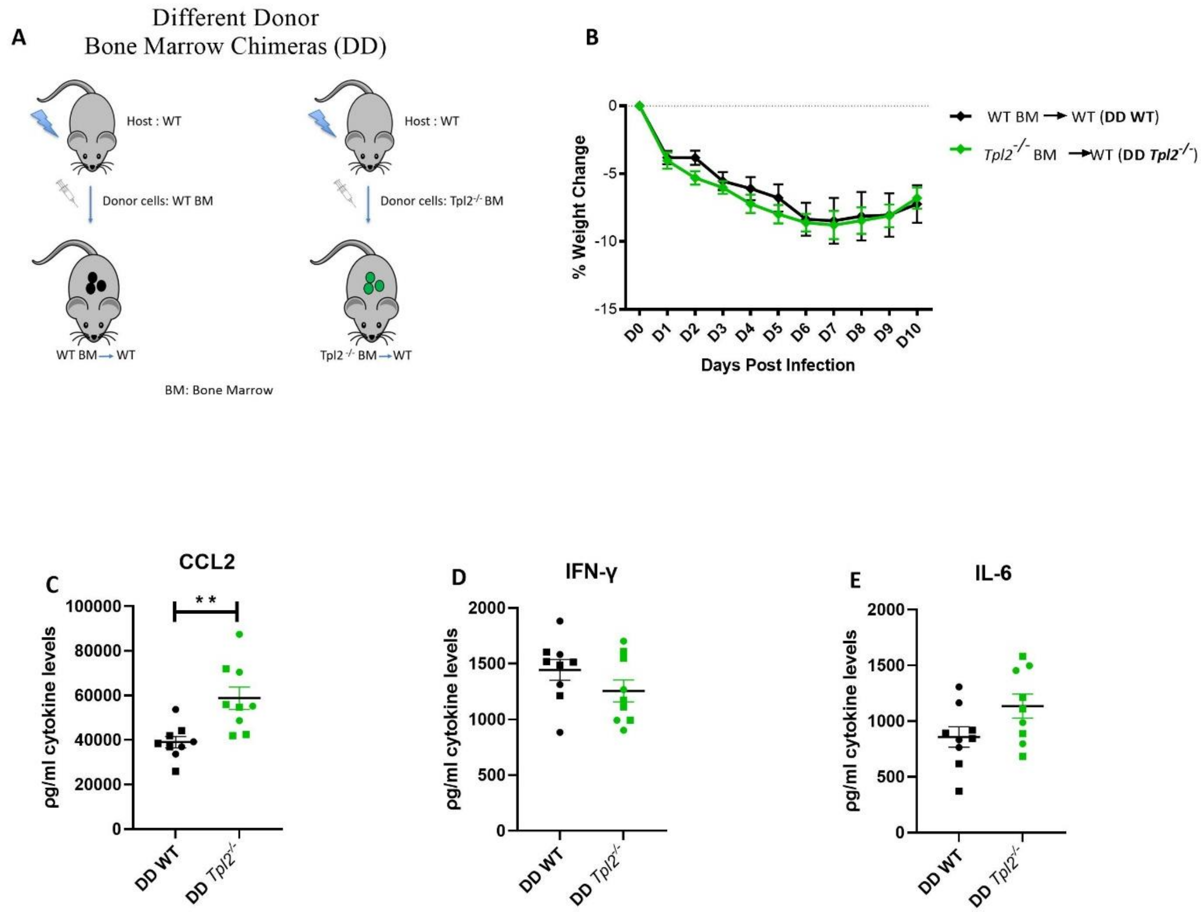

Supplementary Figure 4.8. Chimeras with Tpl2 ablation restricted to radiosensitive cells (DD) show no differences in influenza-induced weight loss despite higher CCL2 expression at 7 dpi. (A) Experimental schematic. WT mice were lethally irradiated and administered WT (n=9) or *Tpl2*$^{-/-}$ (n=9) mouse bone marrow the following day. After two months of reconstitution, chimeras were infected and studied for 10 days for clinical outcome and cytokine expression at 7 dpi. **(B)** Weight loss curve shows that the chimeras do not display differential weight loss at 7 dpi and fully recover their weights by 10 dpi. Diamonds are used to represent that the data points are averaged for males and females. Data are representative of 5 experiments. **(C-E)** Cytokine expression at 7 dpi. Data are representative of 2 experiments. Unpaired student's *t*-test **p*<0.05, ***p*<0.01. Squares represent male and circles are female mice.

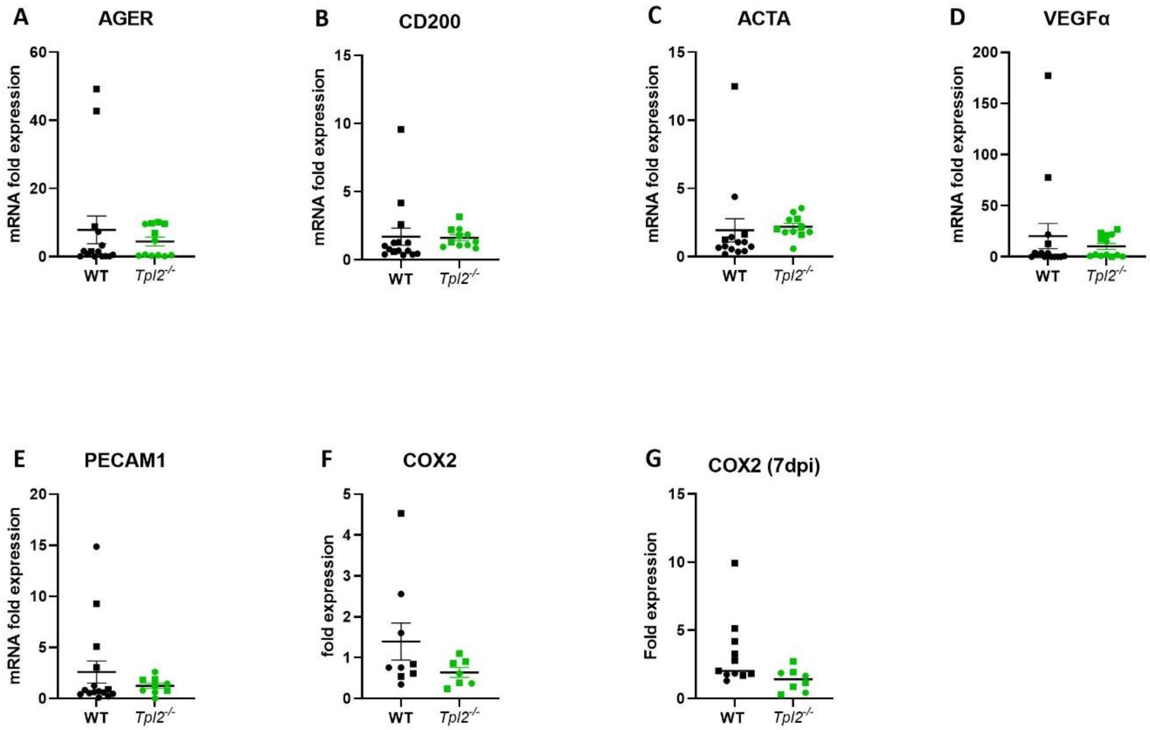

Supplementary Figure 4.9. ARDS biomarkers shows no overexpression for influenza infected *Tpl2*$^{-/-}$ mice at 9dpi.

WT (n=15) and *Tpl2*$^{-/-}$ (n=11) mice were infected intranasally with 10^4 pfu of influenza x31. At 9dpi, the whole (intact) lungs were harvested without perfusion or lavage and homogenized for RNA extraction for gene expression analysis by real-time qPCR. Data are representative of 2 experiments. Squares represent male mice, and circles represent female mice. Unpaired student's *t*-test **p*<0.05.

CHAPTER 5

CONCLUSION

Early days post the influenza infection of the *Tpl2*$^{-/-}$ mice showed that the Tpl2 ablation lead to reduced levels of IFNλ, ISG expression and IFN contribution from the pDCs[222]. While this impacted the viral titers (with delayed control), it could not explain the late appearance of the severely deteriorating clinical symptoms in the *Tpl2*$^{-/-}$ mice. On examination of influenza infected *Tpl2*$^{-/-}$ mice at 7dpi, when they commence to show differential weight loss compared to WT mice, we see excessive cytokine expression and cellular recruitment in the lungs of the *Tpl2*$^{-/-}$ mice[315]. While the IFN-β-CCL2 axis is responsible for the inflammatory monocyte recruitment, other chemokines like CCL3 and CXCL1(in the absence of T1 IFNs) are involved in the excessive neutrophil recruitment. Abolishment of the IFN signaling worsens the survival of infected *Tpl2*$^{-/-}$ mice, with a shift in the immune profile from monocytic to neutrophilic and increase in IFN-λ that might hamper repair. At the same time, the *Tpl2*$^{-/-}$ lungs show signs of alveolar septal necrosis, pleuritis, higher cellular damage in BALF and overexpression of various ARDS biomarkers, suggesting that the widespread clinical damage to the lungs is due to the hypercytokinemia

By 9dpi, IFN signaling pathway is being suppressed by SOCS1 activation, however it just slows down the inflammation and is unable to end it. At this point the *Tpl2*$^{-/-}$ lungs show worse alveolar septal necrosis with hyaline membrane formation, along with higher cellular damage, signs of dehydration and increased platelets (being recruited to repair) in blood. Furthermore, the inflammation induced damage at this point culminates in pulmonary edema, wherein the *Tpl2*$^{-/-}$ mice succumb to infection due to the development of ARDS.

Overall, the data shows us that Tpl2 is an important regulator of the inflammatory response at later timepoints post influenza infection. It also highlights the multifactorial role that Tpl2 plays in regulating IFN dependent and independent pathways, to then regulate various cytokines, chemokines, and downstream inflammatory cellular recruitment. This study is also the first to show that Tpl2 serves a protective role during influenza-induced lung injury by preventing severe inflammation and ARDS development. While we have defined the immune response and related clinical impact of influenza infection in *Tpl2*$^{-/-}$ mice, it also opens up several avenues to explore in order to adapt this knowledge into combating such infections.

Examination of the cytokine contribution from Tpl2 deficient radio-resistant versus radiosensitive compartments using chimera mouse models of infection, emphasized the contribution of both the compartments towards the hypercytokinemia seen in *Tpl2*$^{-/-}$ mice. Amongst the radio-resistant cells, on consideration of the source of the cytokine dysregulation, other studies in our lab have shown that Tpl2 deficient epithelial cells showed no cell intrinsic involvement in influenza infection (Wyatt, *et al*., unpublished) and we did not see any differential expression with alveolar macrophages (Supplementary Figure 2.13) at 7dpi. Meanwhile endothelial cells are known to express pro-inflammatory cytokines and mediators on influenza infection[407,408]/other diseases[409,410]. Furthermore, the differential SOCS1 expression (that dampens the inflammation) does not seem to be sourced from the alveolar macrophages (data not shown). However, we do not know if the source is the epithelium, after crosstalk with the of the alveolar macrophage via the microvesicles (or other programmed mechanisms). In addition, the ARDS biomarkers that were upregulated in influenza infected *Tpl2*$^{-/-}$ mice, were mostly epithelial and endothelial in origin. Therefore, future studies will seek to further dissect the Tpl2-dependent host response to influenza infection within the different cellular compartments including the epithelium, endothelium, and alveolar macrophages for their involvement towards severe influenza disease development and ARDS progression.

It is challenging to examine the contribution of the alveolar macrophages in late stage influenza immune responses as they are depleted by 90% by 7dpi[365]. When exploring mouse models in order to localize the Tpl2 deficiency within alveolar macrophages, there are a very few viable options. One of the defining markers for alveolar macrophages is Siglec F, however Siglec F knockout mouse models are prone to excessive eosinophilla, which might introduce more variability when examining the response post influenza[411]. While there are quite a few depletion models based on the linking of the alveolar macrophage markers (like CD11c) with diphtheria toxin to conditionally deplete macrophages[412], we need a system with viable macrophages lacking Tpl2. Blood monocytes, marked by CD115, were shown to replace the depleted alveolar macrophages, when injected into mice post depletion of the primary alveolar macrophage population in the CD11c-DTR system[413]. Hence, we could conditionally knockout Tpl2 within CD115 expressing cells using the cre-lox system, to obtain Tpl2 deficient blood monocytes. We then deplete the alveolar macrophages in the CD11C-DTR mice, inject the Tpl2 deficient blood monocytes and allow for the macrophage reconstitution. Thus, we can now examine the effect of influenza in Tpl2 deficient alveolar macrophages. In a similar fashion, conditional knockouts with markers specific for endothelial cells, could also be used to localize the Tpl2 deficiency within the endothelial cells to examine their contribution to hypercytokinemia and ARDS post influenza infection. An alternative approach to examine the interaction of epithelium and endothelium without contribution from alveolar macrophages, would be by generating *Tpl2*$^{-/-}$/CD11b-DTR DH chimera mice. First *Tpl2*$^{-/-}$/CD11b-DTR mice are generated by crossing *Tpl2*$^{-/-}$ mice with CD11b-DTR mice. Then these mice are irradiated along WT CD11b-DTR mice as controls. Both mice are given WT bone marrow post radiation, allowed to reconstitute their immune cells, and finally depleted of alveolar macrophages using the diphtheria toxin. If alveolar macrophages are dominating the immune response to infection until their depletion at 7dpi, infection of these chimeras should yield the same results at earlier timepoints comparable to what we see in *Tpl2*$^{-/-}$ mice by 7dpi. Identification of the source of the hypercytokinemia, might also narrow the search for identifying the PRR stimulant (such as replication defective virus particles, Damage associated Molecular Patterns (DAMPs), etc) that in turn induces the hypercytokinemia. This would allow for development of therapeutics that can inactivate/neutralize these stimulators. Furthermore, establishing a model system focused on the Tpl2 regulation of alveolar macrophage function could also be extrapolated to other respiratory diseases like tuberculosis that also target these cells.

In response to the functional regulation of TNFα by Tpl2 and the low homology of Tpl2 with other MAP kinases, Wythe and Abbott laboratories started research into small molecule inhibitors of Tpl2 as a therapeutic approach to dampen inflammation from primary human cells and treatment of Rheumatoid Arthritis[414,415]. Currently a Tpl2 inhibitor drug called Tilpisertib (formerly GS-4875) has reached phase II clinical trials for treatment of Ulcerative Collitis[416]. However, collective assessment of various studies show that Tpl2 regulation of inflammation is actually more cell and stimulus specific than what can be generalized. For instance, in some cancers tpl2 can be a proto-oncogene (with overexpression associated with tumors) [417–419], but in others it can also act as a tumor suppressor, especially lung carcinomas (wherein reduced expression of Tpl2 is the cause of tumor progression)[420–423]. In two pulmonary models of allergy, both studies highlighted the role of Tpl2 deficiency causing exacerbated Type-2 inflammation. However in the house dust mite allergy model, the inflammation was a result of Tpl2 deficiency in the DCs[424], whereas in the ovalbumin model of allergy, the inflammation was attributed to the role of T cell regulation by

Tpl2, with the underlying cause being the polarization of Th2 cells [425]. Comparing between two studies examining the role of Tpl2 in diabetes, one study found higher Tpl2 expression associated with increased cytokine expression in the adipose tissue without any systemic differences in insulin resistance[426], thereby suggesting Tpl2 has more of an immune functionality. However the other study found that Tpl2 activity in macrophages induced inflammatory effects in adipocytes and developed insulin resistance leading to the development of diabetes[427]. In an intestinal model of Dextran Sodium Sulphate (DSS) induced colon tumorigenesis, Tpl2 suppressed the production of HGF from intestinal myfibroblasts to prevent tumorigesis[428]; however in a model where the DSS induced colitis, it was found that Tpl2 deficiency reduced inflammation and thereby reduced colitis[429]. Therefore, we see that even in similar diseases, the Tpl2 expression can have different impacts depending on the cells examined for Tpl2 function, the cause of the disease and even the output being considered (like inflammation, insulin resistance, etc).

In accordance with the above discussion of the intricate nature of Tpl2 regulation, the collective studies from our lab have shown[222,315](Wyatt, *et al.*, unpublished) that when responding to influenza, Tpl2 has a kinetic component spanning the duration of the infection. Cellular examination by culturing and stimulation[222,228], can only be done for limited hours, and does not account for stimulation by other interacting partners. Hence a systematic examination of silencing Tpl2 (conditional whole body knockout) using a cre recombinant system inducible by tetracycline (as tamoxifen induces unwanted side effects[430]) would make studying the kinetics much easier. Additionally, instead of interfering with the expression of Tpl2, it would be more beneficial to focus therapeutic interventions on the downstream effectors of the hypercytokinemia phenotype such as on CCL2 and IFN-λ. While we did not see improvements in survival with blocking of CCL2 (data not shown), it would be beneficial to examine the immune response in the *CCR2*$^{-/-}$

/*Tpl2*$^{-/-}$ mice to compare the impact of monocyte recruitment with internal regulation of Tpl2 within the monocytes. Blocking IFN-λ therapeutically in cases of hypercytokinemia might also be an interesting avenue to explore, as it may be more localized towards the pathological effects this late in the infection.

This influenza-infected *Tpl2*$^{-/-}$ mouse model that culminates in ARDS, could enable us to better understand this aggressive disease and assist in the design of better diagnostics and treatments. Of the inflammatory mediators that we have accessed, we observed increased NOS2 expression in the *Tpl2*$^{-/-}$ mice at 7 dpi[315]. Nitric oxide is expressed in lungs of humans[320,321], mice[137,283] and even chicken[322] on infection with highly pathogenic influenza viruses and mediate pulmonary damage. Additionally, pulmonary edema has been associated with the endogenous activity of NOS2 (Nitric Oxide synthase 2) in various models and clinical cases of lung injury, including hypercalcemia, endotoxin treatment, influenza, and ARDS[399–402]. NOS2 was also found to be required for pathologic vascular changes in the lungs[403] and generation of Reactive Nitrogen Species(RNS)[431] that in addition with free oxygen radicals could damage the epithelial/endothelial cells[403,432] to generate lung injury. The RNS generated by expression of inducible NOS2 was also found to increase stress markers in alveolar macrophages and epithelial cells in another model of lung injury[433].Thus collectively, NOS2 is involved in the immune response as well as in ARDS development, upregulated in conditions of Tpl2 as well as IFNAR1 ablation and equally expressed from monocytes as well as neutrophils. Such a multifactorial expression and functionality, as seen here, suggests that it is indispensable and potentially under Tpl2 regulation as well. Hence it would also be interesting to study the regulation of NOS2 by Tpl2 using *NOS2*$^{-/-}$/*Tpl2*$^{-/-}$ mice to evaluate the progress of the influenza infection. Furthermore, even in the influenza infected *Tpl2*$^{-/-}$ mice, if the NOS2 inhibitor Nomega-methyl-L-arginine (L-NMA)[277] was used, would it prevent all inflammation induced damage to prevent ARDS and allow the mice to recover is another point worth investigating. This would mean that therapeutics based on inhibition of NOS2 could be used to prevent severe infections from seasonal influenza, that result from a dysregulated immune response.

In a study that examined the peripheral blood mononuclear cells of patients suffering from various respiratory infections by transcriptional analysis, compared to healthy human controls, several genes were found to be differentially regulated at various timepoints following infection. Tpl2/MAP3K8 was one such gene upregulated at 4dpi and associated with recovery of the patients suffering from influenza infection[434]. Thus, blood transcriptional expression of Tpl2 is associated with recovery in influenza infected humans. On the other hand, this could also mean that lack of Tpl2 expression could have some association with poor prognosis post influenza infection in humans. Thus, another direction this work can take is to generate the 7dpi transcriptional profile of the infected *Tpl2*$^{-/-}$ mice to compare with that of the patients that are suffering with severe influenza infection, to predict the severity of the disease. We do not know yet, if a transient dysregulation in the expression of Tpl2 during a seasonal influenza infection could be a involved progression to a severe case. Furthermore, if Tpl2 expression were to transiently fluctuate patients with known interferonopathies, the result would be even more detrimental, similar to the case of the influenza infected *IFNAR1*$^{-/-}$*Tpl2*$^{-/-}$ mice. Hence having a viable diagnostic or prediction system would be invaluable as early antiviral treatment and early ARDS prevention would increase the odds of survival and speed up recovery. Unlike mice, human sampling sites are limited, so the best tissue for examination would be BALF or blood. If we could establish a transcriptional profile/ biomarker specific to Tpl2 ablation/inactivity with/without Interferon signaling from the BALF or Blood of the *Tpl2*$^{-/-}$ mice, we could then compare this to transcriptional profiles of patients in various stages of influenza infection and categorize based on underlying medical/physical conditions (along with healthy controls). If comparisons of these datasets yield correlation with the influenza infected *Tpl2*$^{-/-}$ mice, then this could be established as a diagnostic profile for severe influenza and simultaneously function as a model to develop therapeutics against such cases.

Tpl2 having a regulatory role in the immune response to influenza can also be extrapolated to other respiratory infections, especially since *Tpl2*$^{-/-}$ mice have already been shown to be more susceptible to tuberculosis infections[228]. This could be due to the underlying role of interferons in both infections or that they both involve the alveolar macrophages, however this merits further examination in both models. The lungs are subject to a lot more infectious agents including bacteria like *Streptococcus pneumoniae, Staphylococcus aureus,* S*treptococcus pyogenes, Haemophilus influenzae* and even viruses like respiratory syncytial virus (RSV), rhinovirus (RV), SARS, etc. Of these *Streptococcus pneumoniae* and *Staphylococcus aureus* are already notorious for co-infection or super-infection after influenza[435,436] and are likely nosocomial infections in older individuals hospitalized for influenza or given mechanical ventilation treatment for an extended period of time [235–237]. Moreover examination of the role of Tpl2 in mechanical ventilator induced ARDS yielded conflicting results[405,406], but there are other etiological agents like smoking, surgery, blood transfusion and so on that can be investigated in the context of how Tpl2 regulation of inflammation would influence the disease prognosis. Considering the ongoing worldwide disease burden, economic and mental health impact of SARS-CoV-2, in addition to being a respiratory virus that has been known to induce both excessive inflammation and ARDS, it is a very relevant and significant infectious agent to be considered here. Several studies have already shown the upregulation of MAP kinases[437] and specifically Tpl2[438,439] on infection of Airway Epithelial cells with SARS-CoV-2. This has raised the speculation of using the Tpl2 inhibitor as a therapeutic for

COVID-19. However, prior to this undertaking, the clinical and immune response should be examined in an in-vivo Tpl2 deficient system to examine the systemic, contiguous and longer-term impact of Tpl2 regulating the immune response to COVID-19. Moreover, such an examination would also have the benefit of yielding a larger set of druggable targets that could be targeted downstream, with more immediate relief and less off target side effects. Thus we can see that exploring the role of Tpl2 in regulating the immune response has a wide range of applications.

REFERENCES

1. Bouvier, Nicole M. xand Palese* P. THE BIOLOGY OF INFLUENZA VIRUSES. *Vaccine*. 2008;26(4):D49–D53. doi:10.1002/ejoc.201701499

2. ICTV. Virus Taxonomy: 2017 Release. Available online. https://talk.ictvonline.org/ictv-reports/ictv_9th_.

3. Kuchipudi S V., Nissly RH. Novel flu viruses in bats and cattle: "Pushing the envelope" of influenza infection. *Vet Sci*. 2018;5(3):1-10. doi:10.3390/vetsci5030071

4. Moeller A, Kirchdoerfer RN, Potter CS, Carragher B, Wilson IA. Organization of the influenza virus replication machinery. *Science*. 2012;338(6114):1631-1634. doi:10.1126/science.1227270

5. Resa-Infante P, Jorba N, Coloma R, Ortin J. The influenza virus RNA synthesis machine: advances in its structure and function. *RNA Biol*. 2011;8(2):207-215. doi:10.4161/rna.8.2.14513

6. Dawson WK, Lazniewski M, Plewczynski D. RNA structure interactions and ribonucleoprotein processes of the influenza A virus. *Brief Funct Genomics*. 2018;17(6):402-414. doi:10.1093/bfgp/elx028

7. Bui M, Wills EG, Helenius A, Whittaker GR. Role of the Influenza Virus M1 Protein in Nuclear Export of Viral Ribonucleoproteins. *J Virol*. 2000;74(4):1781-1786. doi:10.1128/jvi.74.4.1781-1786.2000

8. Gamblin SJ, Skehel JJ. Influenza hemagglutinin and neuraminidase membrane glycoproteins. *J Biol Chem*. 2010;285(37):28403-28409. doi:10.1074/jbc.R110.129809

9. Leung HSY, Li OTW, Chan RWY, Chan MCW, Nicholls JM, Poon LLM. Entry of Influenza A Virus with a 2,6-Linked Sialic Acid Binding Preference Requires Host Fibronectin. *J Virol*. 2012;86(19):10704-10713. doi:10.1128/jvi.01166-12

10. Yoshimura A, Ohnishi S. Uncoating of influenza virus in endosomes. *J Virol*. 1984;51(2):497-504. doi:10.1128/jvi.51.2.497-504.1984

11. Li S, Sieben C, Ludwig K, et al. PH-ontrolled two-step uncoating of influenza virus. *Biophys J*. 2014;106(7):1447-1456. doi:10.1016/j.bpj.2014.02.018

12. Terrier O, Carron C, De Chassey B, et al. Nucleolin interacts with influenza A nucleoprotein and contributes to viral ribonucleoprotein complexes nuclear trafficking and efficient influenza viral replication. *Sci Rep*. 2016;6(June):1-15. doi:10.1038/srep29006

13. Herold S, Becker C, Ridge KM, Budinger GRS. Influenza virus-induced lung injury: Pathogenesis and implications for treatment. *Eur Respir J*. 2015;45(5):1463-1478. doi:10.1183/09031936.00186214

14. Dou D, Revol R, Östbye H, Wang H, Daniels R. Influenza A virus cell entry, replication, virion assembly and movement. *Front Immunol*. 2018;9(JUL):1-17. doi:10.3389/fimmu.2018.01581

15. Influenza Type A viruses - CDC. https://www.cdc.gov/flu/avianflu/influenza-a-virus-subtypes.htm.

16. CDC. Influenza Type A Viruses. https://www.cdc.gov/flu/avianflu/influenza-a-virus-subtypes.htm.

17. Alexander DJ. A review of avian influenza in different bird species. *Vet Microbiol*. 2000;74(1-2):3-13. doi:10.1016/s0378-1135(00)00160-7

18. Lebarbenchon C, Feare CJ, Renaud F, Thomas F, Gauthier-Clerc M. Persistence of highly pathogenic avian influenza viruses in natural ecosystems. *Emerg Infect Dis*. 2010;16(7):1057-1062. doi:10.3201/eid1607.090389

19. Yoon SW, Webby RJ, Webster RG. Evolution and ecology of influenza a viruses. *Curr Top Microbiol Immunol*. 2014;385(1):359-375. doi:10.1007/82_2014_396

20. Wong SSY, Yuen KY. Avian influenza virus infections in humans. *Chest*. 2006;129(1):156-168. doi:10.1378/chest.129.1.156

21. Monne I, Fusaro A, Nelson MI, et al. Emergence of a Highly Pathogenic Avian Influenza Virus from a Low-Pathogenic Progenitor. *J Virol*. 2014;88(8):4375-4388. doi:10.1128/jvi.03181-13

22. Tellier R. Aerosol transmission of influenza A virus: A review of new studies. *J R Soc Interface*. 2009;6(SUPPL. 6). doi:10.1098/rsif.2009.0302.focus

23. Killingley B, Nguyen-Van-Tam J. Routes of influenza transmission. *Influenza Other Respi Viruses*. 2013;7(SUPPL.2):42-51. doi:10.1111/irv.12080

24. Yuan J, Zhang L, Kan X, et al. Origin and Molecular Characteristics of a Novel 2013 Avian Influenza A(H6N1) Virus Causing Human Infection in Taiwan. *Clin Infect Dis*. 2013;57(9):1367-1368. doi:10.1093/cid/cit479

25. McFee RB. Avian Influenza: The Next Pandemic? *Disease-a-Month*. 2007;53(7):348-387. doi:10.1016/j.disamonth.2007.05.006

26. WHO INFLUENZA fact sheet. https://www.who.int/news-room/fact-sheets/detail/influenza-(seasonal).

27. Kim H, Webster RG, Webby RJ. Influenza Virus: Dealing with a Drifting and Shifting Pathogen. *Viral Immunol*. 2018;31(2):174-183. doi:10.1089/vim.2017.0141

28. Flerlage T, Boyd DF, Meliopoulos V, Thomas PG, Schultz-Cherry S. Influenza virus and SARS-CoV-2: pathogenesis and host responses in the respiratory tract. *Nat Rev Microbiol*. 2021;19(7):425-441. doi:10.1038/s41579-021-00542-7

29. Monto AS, Gravenstein S, Elliott M, Colopy M, Schweinle J. Clinical signs and symptoms predicting influenza infection. *Arch Intern Med*. 2000;160(21):3243-3247. doi:10.1001/archinte.160.21.3243

30. Neuzil KM, Reed GW, Mitchel EF, Griffin MR. Influenza-associated morbidity and mortality in young and middle-aged women. *J Am Med Assoc*. 1999;281(10):901-907. doi:10.1001/jama.281.10.901

31. Martínez A, Soldevila N, Romero-Tamarit A, et al. Risk factors associated with severe outcomes in adult hospitalized patients according to influenza type and subtype. *PLoS One*. 2019;14(1):1-15. doi:10.1371/journal.pone.0210353

32. Walker TA, Waite B, Thompson MG, et al. Risk of Severe Influenza Among Adults With Chronic Medical Conditions. *J Infect Dis*. 2020;221(2):183-190. doi:10.1093/infdis/jiz570

33. Mertz D, Lo CKF, Lytvyn L, et al. Pregnancy as a risk factor for severe influenza infection: An individual participant data meta-analysis. *BMC Infect Dis*. 2019;19(1):1-10. doi:10.1186/s12879-019-4318-3

34. Miyashita K, Nakatani E, Hozumi H, Sato Y, Miyachi Y, Suda T. Risk Factors for Pneumonia and Death in Adult Patients with Seasonal Influenza and Establishment of Prediction Scores: A Population-Based Study. *Open Forum Infect Dis*. 2021;8(3):1-8. doi:10.1093/ofid/ofab068

35. Montalto NJ. An office-based approach to influenza: Clinical diagnosis and laboratory testing. *Am Fam Physician*. 2003;67(1):111-118.

36. Gaitonde DY, Moore CFC, Morgan MMK. Influenza : Diagnosis and Treatment. 2019.

37. Kalil AC, Thomas PG. Influenza virus-related critical illness: pathophysiology and epidemiology. *Crit Care*. 2019;23(258):1-7.

38. Taubenberger, Jeffery and Morens D. The Pathology of Influenza Virus Infections. *Ann Rev Pathol*. 2008;3(1):499-522. doi:10.1038/jid.2014.371

39. Li H, Weng H, Lan C, et al. Comparison of patients with avian in fl uenza A (H7N9) and in fl uenza A (H1N1) complicated by acute respiratory distress syndrome. 2018;12(February):5-10.

40. Salihefendic N, Zildzic M, Ahmetagic S. Acute Respiratory Distress Syndrome (ARDS) from Endemic Influenza A/H1N1: Prehospital Management. *Med Arch (Sarajevo, Bosnia Herzegovina)*. 2015;69(1):62-63. doi:10.5455/medarh.2015.69.62-63

41. Ventetuolo CE, Muratore CS. Extracorporeal life support in critically III adults. *Am J Respir Crit Care Med*. 2014;190(5):497-508. doi:10.1164/rccm.201404-0736CI

42. Yu WCL, Chan RWY, Wang J, et al. Viral replication and innate host responses in primary human alveolar epithelial cells and alveolar macrophages infected with influenza H5N1 and H1N1 viruses. *J Virol*. 2011;85(14):6844-6855. doi:10.1128/JVI.02200-10

43. Sakabe S, Iwatsuki-Horimoto K, Takano R, et al. Cytokine production by primary human macrophages infected with highly pathogenic H5N1 or pandemic H1N1 2009 influenza

viruses. *J Gen Virol*. 2011;92(6):1428-1434. doi:10.1099/vir.0.030346-0

44. Nain M, Hinder F, Gong JH, et al. Tumor necrosis factor-alpha production of influenza A virus-infected macrophages and potentiating effect of lipopolysaccharides. *J Immunol*. 1990;145(6):1921 LP - 1928.

45. Lamichhane PP, Samarasinghe AE. The Role of Innate Leukocytes during Influenza Virus Infection. *J Immunol Res*. 2019;2019:8028725. doi:10.1155/2019/8028725

46. Tripathi S, White MR, Hartshorn KL. The amazing innate immune response to influenza A virus infection. *Innate Immun*. 2015;21(1):73-98. doi:10.1177/1753425913508992

47. Bahadoran A, Lee SH, Wang SM, et al. Immune responses to influenza virus and its correlation to age and inherited factors. *Front Microbiol*. 2016;7(NOV):1-11. doi:10.3389/fmicb.2016.01841

48. Chen X, Liu S, Goraya MU, Maarouf M, Huang S, Chen JL. Host immune response to influenza A virus infection. *Front Immunol*. 2018;9(MAR):1-13. doi:10.3389/fimmu.2018.00320

49. Wang K, Lai C, Li T, et al. Basic fibroblast growth factor protects against influenza A virus-induced acute lung injury by recruiting neutrophils. *J Mol Cell Biol*. 2018;10(6):573-585. doi:10.1093/jmcb/mjx047

50. Ushakumary MG, Riccetti M, Perl AKT. Resident interstitial lung fibroblasts and their role in alveolar stem cell niche development, homeostasis, injury, and regeneration. *Stem Cells Transl Med*. 2021;10(7):1021-1032. doi:10.1002/sctm.20-0526

51. Van Riel D, Munster VJ, De Wit E, et al. Human and avian influenza viruses target different cells in the lower respiratory tract of humans and other mammals. *Am J Pathol*. 2007;171(4):1215-1223. doi:10.2353/ajpath.2007.070248

52. Schneider C, Nobs SP, Kurrer M, Rehrauer H, Thiele C, Kopf M. Induction of the nuclear receptor PPAR-γ 3 by the cytokine GM-CSF is critical for the differentiation of fetal monocytes into alveolar macrophages. *Nat Immunol*. 2014;15(11):1026-1037. doi:10.1038/ni.3005

53. Schulz C, Perdiguero EG, Chorro L, et al. A lineage of myeloid cells independent of myb and hematopoietic stem cells. *Science (80-)*. 2012;335(6077):86-90. doi:10.1126/science.1219179

54. Londrigan SL, Short KR, Ma J, et al. Infection of Mouse Macrophages by Seasonal Influenza Viruses Can Be Restricted at the Level of Virus Entry and at a Late Stage in the Virus Life Cycle. *J Virol*. 2015;89(24):12319-12329. doi:10.1128/jvi.01455-15

55. Marvin SA, Russier M, Huerta CT, Russell CJ, Schultz-Cherry S. Influenza Virus Overcomes Cellular Blocks To Productively Replicate, Impacting Macrophage Function. *J Virol*. 2017;91(2):1-18. doi:10.1128/jvi.01417-16

56. Ettensohn DB, Roberts Jr. NJ. Influenza Virus Infection of Human Alveolar and Blood-Derived Macrophages: Differences in Accessory Cell Function and Interferon Production. *J Infect Dis*. 1984;149(6):942-949. doi:10.1093/infdis/149.6.942

57. Yu WCL, Chan RWY, Wang J, et al. Viral Replication and Innate Host Responses in Primary Human Alveolar Epithelial Cells and Alveolar Macrophages Infected with Influenza H5N1 and H1N1 Viruses. *J Virol*. 2011;85(14):6844-6855. doi:10.1128/jvi.02200-10

58. Ardain A, Marakalala MJ, Leslie A. Tissue-resident innate immunity in the lung. *Immunology*. 2020;159(3):245-256. doi:10.1111/imm.13143

59. Sabatel C, Radermecker C, Fievez L, et al. Exposure to Bacterial CpG DNA Protects from Airway Allergic Inflammation by Expanding Regulatory Lung Interstitial Macrophages. *Immunity*. 2017;46(3):457-473. doi:10.1016/j.immuni.2017.02.016

60. Vercammen E, Staal J, Beyaert R. Sensing of viral infection and activation of innate immunity by toll-like receptor 3. *Clin Microbiol Rev*. 2008;21(1):13-25. doi:10.1128/CMR.00022-07

61. Guillot L, Le Goffic R, Bloch S, et al. Involvement of Toll-like receptor 3 in the immune response of lung epithelial cells to double-stranded RNA and influenza A virus. *J Biol Chem*. 2005;280(7):5571-5580. doi:10.1074/jbc.M410592200

62. Lund JM, Alexopoulou L, Sato A, et al. Recognition of single-stranded RNA viruses by

Toll-like receptor 7. *Proc Natl Acad Sci U S A*. 2004;101(15):5598-5603. doi:10.1073/pnas.0400937101

63. Lester SN, Li K. Toll-like receptors in antiviral innate immunity. *J Mol Biol*. 2014;426(6):1246-1264. doi:10.1016/j.jmb.2013.11.024

64. Saitoh SI, Abe F, Kanno A, et al. TLR7 mediated viral recognition results in focal type i interferon secretion by dendritic cells. *Nat Commun*. 2017;8(1). doi:10.1038/s41467-017-01687-x

65. GuanQun L, Yan Z, Billy T. Cytoplasm and Beyond: Dynamic Innate Immune Sensing of Influenza A Virus by RIG-I. *J Virol*. 2021;93(8):e02299-18. doi:10.1128/JVI.02299-18

66. Liu GQ, Lu Y, Thulasi Raman SN, et al. Nuclear-resident RIG-I senses viral replication inducing antiviral immunity. *Nat Commun*. 2018;9(1). doi:10.1038/s41467-018-05745-w

67. Wu B, Peisley A, Richards C, et al. Structural basis for dsRNA recognition, filament formation, and antiviral signal activation by MDA5. *Cell*. 2013;152(1-2):276-289. doi:10.1016/j.cell.2012.11.048

68. Dias Junior AG, Sampaio NG, Rehwinkel J. A Balancing Act: MDA5 in Antiviral Immunity and Autoinflammation. *Trends Microbiol*. 2019;27(1):75-85. doi:10.1016/j.tim.2018.08.007

69. Liu Y, Olagnier D, Lin R. Host and viral modulation of RIG-I-mediated antiviral immunity. *Front Immunol*. 2017;7(JAN):1-12. doi:10.3389/fimmu.2016.00662

70. Le Goffic R, Pothlichet J, Vitour D, et al. Cutting Edge: Influenza A Virus Activates TLR3-Dependent Inflammatory and RIG-I-Dependent Antiviral Responses in Human Lung Epithelial Cells. *J Immunol*. 2007;178(6):3368-3372. doi:10.4049/jimmunol.178.6.3368

71. Ichinohe T, Pang IK, Iwasaki A. Influenza virus activates inflammasomes via its intracellular M2 ion channel. *Nat Immunol*. 2010;11(5):404-410. doi:10.1038/ni.1861

72. Pothlichet J, Meunier I, Davis BK, et al. Type I IFN Triggers RIG-I/TLR3/NLRP3-dependent Inflammasome Activation in Influenza A Virus Infected Cells. *PLoS Pathog*.

2013;9(4). doi:10.1371/journal.ppat.1003256

73. Ichinohe T, Lee HK, Ogura Y, Flavell R, Iwasaki A. Inflammasome recognition of influenza virus is essential for adaptive immune responses. *J Exp Med*. 2009;206(1):79-87. doi:10.1084/jem.20081667

74. Thomas PG, Dash P, Aldridge JR, et al. The Intracellular Sensor NLRP3 Mediates Key Innate and Healing Responses to Influenza A Virus via the Regulation of Caspase-1. *Immunity*. 2009;30(4):566-575. doi:10.1016/j.immuni.2009.02.006

75. Lee S, Ishitsuka A, Noguchi M, et al. Influenza restriction factor MxA functions as inflammasome sensor in the respiratory epithelium. *Sci Immunol*. 2019;4(40). doi:10.1126/sciimmunol.aau4643

76. Teneema Kuriakose1, Si Ming Man1, R.K. Subbarao Malireddi1, Rajendra Karki1 S, Kesavardhana1, David E. Place1, Geoffrey Neale2, Peter Vogel3 and T-D, Kanneganti1. ZBP1/DAI is an innate sensor of influenza virus triggering the NLRP3 inflammasome and programmed cell death pathways. *Sci Immunol*. 2016;1(2). doi:10.1126/sciimmunol.aag2045.ZBP1/DAI

77. Tate MD, Ong JDH, Dowling JK, et al. Reassessing the role of the NLRP3 inflammasome during pathogenic influenza A virus infection via temporal inhibition. *Sci Rep*. 2016;6(February):1-8. doi:10.1038/srep27912

78. Cheong WC, Kang HR, Yoon H, Kang SJ, Ting JPY, Song MJ. Influenza A virus NS1 protein inhibits the NLRP3 inflammasome. *PLoS One*. 2015;10(5):1-16. doi:10.1371/journal.pone.0126456

79. Chan MCW, Cheung CY, Chui WH, et al. Proinflammatory cytokine responses induced by influenza A (H5N1) viruses in primary human alveolar and bronchial epithelial cells. *Respir Res*. 2005;6:1-13. doi:10.1186/1465-9921-6-135

80. Lam W, Yeung AC, Chu IM, Chan PKS. Profiles of cytokine and chemokine gene expression in human pulmonary epithelial cells induced by human and avian influenza viruses. *Virol J*. 2010;7(1):344. doi:10.1186/1743-422X-7-344

81. Veckman V, Österlund P, Fagerlund R, Melén K, Matikainen S, Julkunen I. TNF-α and

IFN-α enhance influenza-A-virus-induced chemokine gene expression in human A549 lung epithelial cells. *Virology*. 2006;345(1):96-104. doi:10.1016/j.virol.2005.09.043

82. Woo PCY, Tung ETK, Chan KH, Lau CCY, Lau SKP, Yuen KY. Cytokine profiles induced by the novel swine-origin influenza A/H1N1 virus: Implications for treatment strategies. *J Infect Dis*. 2010;201(3):346-353. doi:10.1086/649785

83. Aegerter H, Kulikauskaite J, Crotta S, et al. Influenza-induced monocyte-derived alveolar macrophages confer prolonged antibacterial protection. *Nat Immunol*. 2020;21(2):145-157. doi:10.1038/s41590-019-0568-x

84. Peteranderl C, Morales-Nebreda L, Selvakumar B, et al. Macrophage-epithelial paracrine crosstalk inhibits lung edema clearance during influenza infection. *J Clin Invest*. 2016;126(4):1566-1580. doi:10.1172/JCI83931

85. Lee H, Abston E, Zhang D, Rai A, Jin Y. Extracellular vesicle: An emerging mediator of intercellular crosstalk in lung inflammation and injury. *Front Immunol*. 2018;9(APR). doi:10.3389/fimmu.2018.00924

86. Moon HG, Cao Y, Yang J, Lee JH, Choi HS, Jin Y. Lung epithelial cell-derived extracellular vesicles activate macrophage-mediated inflammatory responses via ROCK1 pathway. *Cell Death Dis*. 2015;6(12):1-11. doi:10.1038/cddis.2015.282

87. Lee H, Zhang D, Zhu Z, Dela Cruz CS, Jin Y. Epithelial cell-derived microvesicles activate macrophages and promote inflammation via microvesicle-containing microRNAs. *Sci Rep*. 2016;6(July):1-11. doi:10.1038/srep35250

88. Soni S, Wilson MR, O'Dea KP, et al. Alveolar macrophage-derived microvesicles mediate acute lung injury. *Thorax*. 2016;71(11):1020-1029. doi:10.1136/thoraxjnl-2015-208032

89. Platanias LC. Mechanisms of type-I- and type-II-interferon-mediated signalling. *Nat Rev Immunol*. 2005;5(5):375-386. doi:10.1038/nri1604

90. Gibbert K, Schlaak JF, Yang D, Dittmer U. IFN-α subtypes: Distinct biological activities in anti-viral therapy. *Br J Pharmacol*. 2013;168(5):1048-1058. doi:10.1111/bph.12010

91. Pommerenke C, Wilk E, Srivastava B, et al. Global transcriptome analysis in influenza-infected mouse lungs reveals the kinetics of innate and adaptive host immune responses. *PLoS One*. 2012;7(7). doi:10.1371/journal.pone.0041169

92. Soto JA, Gálvez NMS, Andrade CA, et al. The Role of Dendritic Cells During Infections Caused by Highly Prevalent Viruses. *Front Immunol*. 2020;11(July):1-22. doi:10.3389/fimmu.2020.01513

93. Sato M, Hata N, Asagiri M, Nakaya T, Taniguchi T, Tanaka N. Positive feedback regulation of type I IFN genes by the IFN-inducible transcription factor IRF-7. *FEBS Lett*. 1998;441(1):106-110. doi:10.1016/S0014-5793(98)01514-2

94. Poddar S, Hyde JL, Gorman MJ, Farzan M, Diamond MS. The Interferon-Stimulated Gene IFITM3 Restricts Infection and Pathogenesis of Arthritogenic and Encephalitic Alphaviruses. *J Virol*. 2016;90(19):8780-8794. doi:10.1128/jvi.00655-16

95. Clemens MJ, Williams BR. Inhibition of cell-free protein synthesis by pppA2’p5’A2’p5’A: a novel oligonucleotide synthesized by interferon-treated L cell extracts. *Cell*. 1978;13(3):565-572. doi:10.1016/0092-8674(78)90329-x

96. Zhu J, Zhang Y, Ghosh A, et al. Antiviral activity of human OASL protein is mediated by enhancing signaling of the RIG-I RNA sensor. *Immunity*. 2014;40(6):936-948. doi:10.1016/j.immuni.2014.05.007

97. Lenschow DJ, Lai C, Frias-Staheli N, et al. IFN-stimulated gene 15 functions as a critical antiviral molecule against influenza, herpes, and Sindbis viruses. *Proc Natl Acad Sci U S A*. 2007;104(4):1371-1376. doi:10.1073/pnas.0607038104

98. Lee SMY, Gardy JL, Cheung CY, et al. Systems-level comparison of host-responses elicited by avian H5N1 and seasonal H1N1 influenza viruses in primary human macrophages. *PLoS One*. 2009;4(12). doi:10.1371/journal.pone.0008072

99. Stifter SA, Bhattacharyya N, Pillay R, et al. Functional Interplay between Type I and II Interferons Is Essential to Limit Influenza A Virus-Induced Tissue Inflammation. *PLoS Pathog*. 2016;12(1):1-20. doi:10.1371/journal.ppat.1005378

100. Seo SU, Kwon HJ, Ko HJ, et al. Type I interferon signaling regulates Ly6Chi monocytes

and neutrophils during acute viral pneumonia in mice. *PLoS Pathog*. 2011;7(2). doi:10.1371/journal.ppat.1001304

101. Lin SJ, Lo M, Kuo RL, et al. The pathological effects of CCR2+ inflammatory monocytes are amplified by an IFNAR1-triggered chemokine feedback loop in highly pathogenic influenza infection. *J Biomed Sci*. 2014;21(1):1-18. doi:10.1186/s12929-014-0099-6

102. Hamming OJ, Terczyńska-Dyla E, Vieyres G, et al. Interferon lambda 4 signals via the IFNλ receptor to regulate antiviral activity against HCV and coronaviruses. *EMBO J*. 2013;32(23):3055-3065. doi:10.1038/emboj.2013.232

103. Syedbasha M, Egli A. Interferon Lambda: Modulating immunity in infectious diseases. *Front Immunol*. 2017;8(FEB). doi:10.3389/fimmu.2017.00119

104. Sheppard P, Kindsvogel W, Xu W, et al. IL-28, IL-29 and their class II cytokine receptor IL-28R. *Nat Immunol*. 2003;4(1):63-68. doi:10.1038/ni873

105. Kotenko S V. IFN-λs. *Curr Opin Immunol*. 2011;23(5):583-590. doi:https://doi.org/10.1016/j.coi.2011.07.007

106. Davidson S, McCabe TM, Crotta S, et al. IFN λ is a potent anti-influenza therapeutic without the inflammatory side effects of IFN α treatment . *EMBO Mol Med*. 2016;8(9):1099-1112. doi:10.15252/emmm.201606413

107. Hemann EA, Green R, Turnbull JB, Langlois RA, Savan R, Gale M. Interferon-λ modulates dendritic cells to facilitate T cell immunity during infection with influenza A virus. *Nat Immunol*. 2019;20(8):1035-1045. doi:10.1038/s41590-019-0408-z

108. Yin Z, Dai J, Deng J, et al. Type III IFNs Are Produced by and Stimulate Human Plasmacytoid Dendritic Cells. *J Immunol*. 2012;189(6):2735-2745. doi:10.4049/jimmunol.1102038

109. Galani IE, Triantafyllia V, Eleminiadou EE, et al. Interferon-λ Mediates Non-redundant Front-Line Antiviral Protection against Influenza Virus Infection without Compromising Host Fitness. *Immunity*. 2017;46(5):875-890.e6. doi:10.1016/j.immuni.2017.04.025

110. Mordstein M, Neugebauer E, Ditt V, et al. Lambda Interferon Renders Epithelial Cells of

the Respiratory and Gastrointestinal Tracts Resistant to Viral Infections. *J Virol*. 2010;84(11):5670-5677. doi:10.1128/jvi.00272-10

111. Klinkhammer J, Schnepf D, Ye L, et al. IFN-λ prevents influenza virus spread from the upper airways to the lungs and limits virus transmission. *Elife*. 2018;7:1-18. doi:10.7554/eLife.33354

112. De Weerd NA, Nguyen T. The interferons and their receptors-distribution and regulation. *Immunol Cell Biol*. 2012;90(5):483-491. doi:10.1038/icb.2012.9

113. Nicol MQ, Campbell GM, Shaw DJ, et al. Lack of IFNγ signaling attenuates spread of influenza A virus in vivo and leads to reduced pathogenesis. *Virology*. 2019;526:155-164. doi:10.1016/j.virol.2018.10.017

114. Bot A, Bot S, Bona CA. Protective Role of Gamma Interferon during the Recall Response to Influenza Virus. *J Virol*. 1998;72(8):6637-6645. doi:10.1128/jvi.72.8.6637-6645.1998

115. Weiss ID, Wald O, Wald H, et al. IFN-γ treatment at early stages of influenza virus infection protects mice from death in a NK cell-dependent manner. *J Interf Cytokine Res*. 2010;30(6):439-449. doi:10.1089/jir.2009.0084

116. Indalao IL, Sawabuchi T, Takahashi E, Kido H. IL-1β is a key cytokine that induces trypsin upregulation in the influenza virus–cytokine–trypsin cycle. *Arch Virol*. 2017;162(1):201-211. doi:10.1007/s00705-016-3093-3

117. Schmitz N, Kurrer M, Bachmann MF, Kopf M. Interleukin-1 Is Responsible for Acute Lung Immunopathology but Increases Survival of Respiratory Influenza Virus Infection. *J Virol*. 2005;79(10):6441-6448. doi:10.1128/jvi.79.10.6441-6448.2005

118. Kim, Kwang S Jung, Hyemin Shin, In K Choi, Bo-Ra and Kim DH. Induction of Interleukin-1 Beta (IL-1b) is a Critical Component of Lung Inflammation During Influenza A (H1N1) Virus Infection. *J Med Virol*. 2015;87:1104–1112. doi:10.1002/jmv

119. Paquette SG, Banner D, Zhao Z, et al. Interleukin-6 is a potential biomarker for severe pandemic H1N1 influenza a infection. *PLoS One*. 2012;7(6):e38214. doi:10.1371/journal.pone.0038214

120. Yang ML, Wang CT, Yang SJ, et al. IL-6 ameliorates acute lung injury in influenza virus infection. *Sci Rep*. 2017;7(March):1-11. doi:10.1038/srep43829

121. Lauder SN, Jones E, Smart K, et al. Interleukin-6 limits influenza-induced inflammation and protects against fatal lung pathology. *Eur J Immunol*. 2013;43(10):2613-2625. doi:10.1002/eji.201243018

122. Radigan KA, Nicholson TT, Welch LC, et al. Influenza A Virus Infection Induces Muscle Wasting via IL-6 Regulation of the E3 Ubiquitin Ligase Atrogin-1. *J Immunol*. 2019;202(2):484-493. doi:10.4049/jimmunol.1701433

123. Liu S, Yan R, Chen B, et al. Influenza virus-induced robust expression of SOCS3 contributes to excessive production of IL-6. *Front Immunol*. 2019;10(AUG):1-15. doi:10.3389/fimmu.2019.01843

124. Ley K, Laudanna C, Cybulsky MI, Nourshargh S. Getting to the site of inflammation: the leukocyte adhesion cascade updated. *Nat Rev Immunol*. 2007;7(9):678-689. doi:10.1038/nri2156

125. Yamamoto K, Miyoshi-Koshio T, Utsuki Y, Mizuno S, Suzuki K. Virucidal activity and viral protein modification by myeloperoxidase: a candidate for defense factor of human polymorphonuclear leukocytes against influenza virus infection. *J Infect Dis*. 1991;164(1):8-14. doi:10.1093/infdis/164.1.8

126. Agraz-Cibrian JM, Giraldo DM, Mary F-M, Urcuqui-Inchima S. Understanding the molecular mechanisms of NETs and their role in antiviral innate immunity. *Virus Res*. 2017;228:124-133. doi:10.1016/j.virusres.2016.11.033

127. Abramson JS, Lewis JC, Lyles DS, Heller KA, Mills EL, Bass DA. Inhibition of neutrophil lysosome-phagosome fusion associated with influenza virus infection in vitro. Role in depressed bactericidal activity. *J Clin Invest*. 1982;69(6):1393-1397. doi:10.1172/JCI110580

128. Tate MD, Ioannidis LJ, Croker B, Brown LE, Brooks AG, Reading PC. The role of neutrophils during mild and severe influenza virus infections of mice. *PLoS One*. 2011;6(3):2-11. doi:10.1371/journal.pone.0017618

129. Vidy A, Maisonnasse P, Da Costa B, Delmas B, Chevalier C, Le Goffic R. The Influenza Virus Protein PB1-F2 Increases Viral Pathogenesis through Neutrophil Recruitment and NK Cells Inhibition. *PLoS One*. 2016;11(10):e0165361-e0165361. doi:10.1371/journal.pone.0165361

130. Narasaraju T, Yang E, Samy RP, et al. Excessive Neutrophils and Neutrophil Extracellular Traps Contribute to Acute Lung Injury of Influenza Pneumonitis. *Am J Pathol*. 2011;179(1):199-210. doi:https://doi.org/10.1016/j.ajpath.2011.03.013

131. Herold S, von Wulffen W, Steinmueller M, et al. Alveolar Epithelial Cells Direct Monocyte Transepithelial Migration upon Influenza Virus Infection: Impact of Chemokines and Adhesion Molecules. *J Immunol*. 2006;177(3):1817 LP - 1824. doi:10.4049/jimmunol.177.3.1817

132. Shi C, Pamer EG. Monocyte recruitment during infection and inflammation. *Nat Rev Immunol*. 2011;11(11):762-774. doi:10.1038/nri3070

133. Kurihara T, Warr G, Loy J, Bravo R. Defects in macrophage recruitment and host defense in mice lacking the CCR2 chemokine receptor. *J Exp Med*. 1997;186(10):1757-1762. doi:10.1084/jem.186.10.1757

134. Tsou CL, Peters W, Si Y, et al. Critical roles for CCR2 and MCP-3 in monocyte mobilization from bone marrow and recruitment to inflammatory sites. *J Clin Invest*. 2007;117(4):902-909. doi:10.1172/JCI29919

135. Serbina N V, Pamer EG. Monocyte emigration from bone marrow during bacterial infection requires signals mediated by chemokine receptor CCR2. *Nat Immunol*. 2006;7(3):311-317. doi:10.1038/ni1309

136. Kratofil RM, Kubes P, Deniset JF. Monocyte conversion during inflammation and injury. *Arterioscler Thromb Vasc Biol*. 2017;37(1):35-42. doi:10.1161/ATVBAHA.116.308198

137. Coates BM, Staricha KL, Koch CM, et al. Inflammatory Monocytes Drive Influenza A Virus–Mediated Lung Injury in Juvenile Mice. *J Immunol*. 2018;200(7):2391-2404. doi:10.4049/jimmunol.1701543

138. Ellis GT, Davidson S, Crotta S, Branzk N, Papayannopoulos V, Wack A. TRAIL +

monocytes and monocyte-related cells cause lung damage and thereby increase susceptibility to influenza– S treptococcus pneumoniae coinfection . *EMBO Rep*. 2015;16(9):1203-1218. doi:10.15252/embr.201540473

139. Ng SL, Teo YJ, Setiagani YA, Karjalainen K, Ruedl C. Type 1 Conventional CD103+ Dendritic Cells Control Effector CD8+ T Cell Migration, Survival, and Memory Responses During Influenza Infection . *Front Immunol* . 2018;9:3043.

140. M. JM, Holly B, Davide B, et al. Lung dendritic cells migrate to the spleen to prime long-lived TCF1hi memory CD8+ T cell precursors after influenza infection. *Sci Immunol*. 2021;6(63):eabg6895. doi:10.1126/sciimmunol.abg6895

141. Ho AWS, Prabhu N, Betts RJ, et al. Lung CD103^{+} Dendritic Cells Efficiently Transport Influenza Virus to the Lymph Node and Load Viral Antigen onto MHC Class I for Presentation to CD8 T Cells. *J Immunol*. 2011;187(11):6011 LP - 6021. doi:10.4049/jimmunol.1100987

142. Kim TS, Braciale TJ. Respiratory dendritic cell subsets differ in their capacity to support the induction of virus-specific cytotoxic CD8+ T cell responses. *PLoS One*. 2009;4(1):e4204. doi:10.1371/journal.pone.0004204

143. M. JM, Holly B, Davide B, et al. Lung dendritic cells migrate to the spleen to prime long-lived TCF1hi memory CD8+ T cell precursors after influenza infection. *Sci Immunol*. 2021;6(63):eabg6895. doi:10.1126/sciimmunol.abg6895

144. Ho AWS, Prabhu N, Betts RJ, et al. Lung CD103^{+} Dendritic Cells Efficiently Transport Influenza Virus to the Lymph Node and Load Viral Antigen onto MHC Class I for Presentation to CD8 T Cells. *J Immunol*. 2011;187(11):6011 LP - 6021. doi:10.4049/jimmunol.1100987

145. Smed-Sörensen A, Chalouni C, Chatterjee B, et al. Influenza a virus infection of human primary dendritic cells impairs their ability to cross-present antigen to CD8 T cells. *PLoS Pathog*. 2012;8(3). doi:10.1371/journal.ppat.1002572

146. GeurtsvanKessel CH, Willart MAM, van Rijt LS, et al. Clearance of influenza virus from the lung depends on migratory langerin+CD11b- but not plasmacytoid dendritic cells. *J*

Exp Med. 2008;205(7):1621-1634. doi:10.1084/jem.20071365

147. Belz GT, Smith CM, Kleinert L, et al. Distinct migrating and nonmigrating dendritic cell populations are involved in MHC class I-restricted antigen presentation after lung infection with virus. *Proc Natl Acad Sci U S A*. 2004;101(23):8670-8675. doi:10.1073/pnas.0402644101

148. Liu Y, Zheng J, Liu Y, et al. Uncompromised NK cell activation is essential for virus-specific CTL activity during acute influenza virus infection. *Cell Mol Immunol*. 2018;15(9):827-837. doi:10.1038/cmi.2017.10

149. Carlin LE, Hemann EA, Zacharias ZR, Heusel JW, Legge KL. Natural killer cell recruitment to the lung during influenza A virus infection is dependent on CXCR3, CCR5, and virus exposure dose. *Front Immunol*. 2018;9(APR):1-14. doi:10.3389/fimmu.2018.00781

150. Rédei GP. Missing Self Hypothesis. *Encycl Genet Genomics, Proteomics Informatics*. 2008;11(7):1225-1225. doi:10.1007/978-1-4020-6754-9_10515

151. Koutsakos M, McWilliam HEG, Aktepe TE, et al. Downregulation of MHC class I expression by influenza A and B viruses. *Front Immunol*. 2019;10(MAY). doi:10.3389/fimmu.2019.01158

152. Mahmoud AB, Tu MM, Wight A, et al. Influenza Virus Targets Class I MHC-Educated NK Cells for Immunoevasion. *PLoS Pathog*. 2016;12(2):1-22. doi:10.1371/journal.ppat.1005446

153. Guo H, Kumar P, Malarkannan S. Evasion of natural killer cells by influenza virus. *J Leukoc Biol*. 2011;89(2):189-194. doi:10.1189/jlb.0610319

154. Mandelboim O, Lieberman N, Lev M, et al. Recognition of haemagglutinins on virus-infected cells by NKp46 activates lysis by human NK cells. *Nature*. 2001;409(6823):1055-1060. doi:10.1038/35059110

155. Waffarn EE, Hastey CJ, Dixit N, et al. Infection-induced type I interferons activate CD11b on B-1 cells for subsequent lymph node accumulation. *Nat Commun*. 2015;6:8991. doi:10.1038/ncomms9991

156. Lam JH, Baumgarth N. The Multifaceted B Cell Response to Influenza Virus. *J Immunol*. 2019;202(2):351-359. doi:10.4049/jimmunol.1801208

157. Blanchard-Rohner G, Pulickal AS, Jol-van Der Zijde CM, Snape MD, Pollard AJ. Appearance of peripheral blood plasma cells and memory B cells in a primary and secondary immune response in humans. *Blood*. 2009;114(24):4998-5002. doi:10.1182/blood-2009-03-211052

158. Rothaeusler K, Baumgarth N. B-cell fate decisions following influenza virus infection. *Eur J Immunol*. 2010;40(2):366-377. doi:10.1002/eji.200939798

159. Turner JS, Zhou JQ, Han J, et al. Human germinal centres engage memory and naive B cells after influenza vaccination. *Nature*. 2020;586(7827):127-132. doi:10.1038/s41586-020-2711-0

160. Liu YJ, Malisan F, de Bouteiller O, et al. Within Germinal Centers, Isotype Switching of Immunoglobulin Genes Occurs after the Onset of Somatic Mutation. *Immunity*. 1996;4(3):241-250. doi:https://doi.org/10.1016/S1074-7613(00)80432-X

161. Hensley SE, Das SR, Bailey AL, et al. Hemagglutinin receptor binding avidity drives influenza A virus antigenic drift. *Science*. 2009;326(5953):734-736. doi:10.1126/science.1178258

162. Wrammert J, Smith K, Miller J, et al. Rapid cloning of high-affinity human monoclonal antibodies against influenza virus. *Nature*. 2008;453(7195):667-671. doi:10.1038/nature06890

163. Kirkpatrick E, Qiu X, Wilson PC, Bahl J, Krammer F. The influenza virus hemagglutinin head evolves faster than the stalk domain. *Sci Rep*. 2018;8(1):1-14. doi:10.1038/s41598-018-28706-1

164. Neu KE, Henry Dunand CJ, Wilson PC. Heads, stalks and everything else: how can antibodies eradicate influenza as a human disease? *Curr Opin Immunol*. 2016;42:48-55. doi:10.1016/j.coi.2016.05.012

165. Pica N, Hai R, Krammer F, et al. Hemagglutinin stalk antibodies elicited by the 2009 pandemic influenza virus as a mechanism for the extinction of seasonal H1N1 viruses.

Proc Natl Acad Sci U S A. 2012;109(7):2573-2578. doi:10.1073/pnas.1200039109

166. Grandea AG, Olsen OA, Cox TC, et al. Human antibodies reveal a protective epitope that is highly conserved among human and nonhuman influenza A viruses. *Proc Natl Acad Sci U S A*. 2010;107(28):12658-12663. doi:10.1073/pnas.0911806107

167. Liu W, Li H, Chen Y-H. N-terminus of M2 protein could induce antibodies with inhibitory activity against influenza virus replication. *FEMS Immunol Med Microbiol*. 2003;35(2):141-146. doi:10.1016/S0928-8244(03)00009-9

168. Feng J, Zhang M, Mozdzanowska K, et al. Influenza A virus infection engenders a poor antibody response against the ectodomain of matrix protein 2. *Virol J*. 2006;3(1):102. doi:10.1186/1743-422X-3-102

169. Guthmiller JJ, Utset HA, Wilson PC. B cell responses against influenza viruses: Short-lived humoral immunity against a life-long threat. *Viruses*. 2021;13(6):1-24. doi:10.3390/v13060965

170. Thathaisong U, Maneewatch S, Kulkeaw K, et al. Human monoclonal single chain antibodies (HuScFv) that bind to the polymerase proteins of influenza A virus. *Asian Pacific J allergy Immunol*. 2008;26(1):23-35.

171. Yodsheewan R, Maneewatch S, Srimanote P, et al. Human monoclonal ScFv specific to NS1 protein inhibits replication of influenza viruses across types and subtypes. *Antiviral Res*. 2013;100(1):226-237. doi:10.1016/j.antiviral.2013.07.019

172. Askonas BA, Taylor PM, Esquivel F. Cytotoxic T cells in influenza infection. *Ann N Y Acad Sci*. 1988;532:230-237. doi:10.1111/j.1749-6632.1988.tb36342.x

173. Eichelberger M, Allan W, Zijlstra M, Jaenisch R, Doherty PC. Clearance of influenza virus respiratory infection in mice lacking class I major histocompatibility complex-restricted CD8+ T cells. *J Exp Med*. 1991;174(4):875-880. doi:10.1084/jem.174.4.875

174. Bender BS, Croghan T, Zhang L, Small PAJ. Transgenic mice lacking class I major histocompatibility complex-restricted T cells have delayed viral clearance and increased mortality after influenza virus challenge. *J Exp Med*. 1992;175(4):1143-1145. doi:10.1084/jem.175.4.1143

175. Grant EJ, Quiñones-Parra SM, Clemens EB, Kedzierska K. Human influenza viruses and CD8(+) T cell responses. *Curr Opin Virol*. 2016;16:132-142. doi:10.1016/j.coviro.2016.01.016

176. Groscurth P, Filgueira L. Killing mechanisms of cytotoxic T lymphocytes. *News Physiol Sci*. 1998;13(1):17-21. doi:10.1152/physiologyonline.1998.13.1.17

177. Brehm MA, Daniels KA, Welsh RM. Rapid Production of TNF-α following TCR Engagement of Naive CD8 T Cells. *J Immunol*. 2005;175(8):5043 LP - 5049. doi:10.4049/jimmunol.175.8.5043

178. Topham DJ, Tripp RA, Doherty PC. CD8+ T cells clear influenza virus by perforin or Fas-dependent processes. *J Immunol*. 1997;159(11):5197-5200.

179. Mirandola P, Ponti C, Gobbi G, et al. Activated human NK and CD8+ T cells express both TNF-related apoptosis-inducing ligand (TRAIL) and TRAIL receptors but are resistant to TRAIL-mediated cytotoxicity. *Blood*. 2004;104(8):2418-2424. doi:10.1182/blood-2004-04-1294

180. Szabo SJ, Kim ST, Costa GL, Zhang X, Fathman CG, Glimcher LH. A novel transcription factor, T-bet, directs Th1 lineage commitment. *Cell*. 2000;100(6):655-669. doi:10.1016/s0092-8674(00)80702-3

181. Pape KA, Khoruts A, Mondino A, Jenkins MK. Inflammatory cytokines enhance the in vivo clonal expansion and differentiation of antigen-activated CD4+ T cells. *J Immunol*. 1997;159(2):591-598.

182. Longhi MP, Wright K, Lauder SN, et al. Interleukin-6 is crucial for recall of influenza-specific memory CD4 + T cells. *PLoS Pathog*. 2008;4(2):2-9. doi:10.1371/journal.ppat.1000006

183. Stripp BR, Reynolds SD. Maintenance and repair of the bronchiolar epithelium. *Proc Am Thorac Soc*. 2008;5(3):328-333. doi:10.1513/pats.200711-167DR

184. Zahm JM, Kaplan H, Hérard AL, et al. Cell migration and proliferation during the in vitro wound repair of the respiratory epithelium. *Cell Motil Cytoskeleton*. 1997;37(1):33-43. doi:10.1002/(SICI)1097-0169(1997)37:1<33::AID-CM4>3.0.CO;2-I

185. Crosby LM, Waters CM. Epithelial repair mechanisms in the lung. *Am J Physiol Lung Cell Mol Physiol*. 2010;298(6):L715-L731. doi:10.1152/ajplung.00361.2009

186. Katsura H, Kobayashi Y, Tata PR, Hogan BLM. IL-1 and TNFα Contribute to the Inflammatory Niche to Enhance Alveolar Regeneration. *Stem Cell Reports*. 2019;12(4):657-666. doi:10.1016/j.stemcr.2019.02.013

187. Budinger GRS, Chandel NS, Donnelly HK, Eisenbart J, Oberoi M, Jain M. Active transforming growth factor-β1 activates the procollagen I promoter in patients with acute lung injury. *Intensive Care Med*. 2005;31(1):121-128. doi:10.1007/s00134-004-2503-2

188. Fahy RJ, Lichtenberger F, McKeegan CB, Nuovo GJ, Marsh CB, Wewers MD. The acute respiratory distress syndrome: A role for transforming growth factor-β1. *Am J Respir Cell Mol Biol*. 2003;28(4):499-503. doi:10.1165/rcmb.2002-0092OC

189. Guo H, Topham DJ. Interleukin-22 (IL-22) Production by Pulmonary Natural Killer Cells and the Potential Role of IL-22 during Primary Influenza Virus Infection. *J Virol*. 2010;84(15):7750-7759. doi:10.1128/jvi.00187-10

190. Ivanov S, Renneson J, Fontaine J, et al. Interleukin-22 Reduces Lung Inflammation during Influenza A Virus Infection and Protects against Secondary Bacterial Infection. *J Virol*. 2013;87(12):6911-6924. doi:10.1128/jvi.02943-12

191. Pociask DA, Scheller E V., Mandalapu S, et al. IL-22 is essential for lung epithelial repair following influenza infection. *Am J Pathol*. 2013;182(4):1286-1296. doi:10.1016/j.ajpath.2012.12.007

192. Chang Y, Kim HY, Albacker L a, Baumgarth N, Andrew NJ. Reactivity Independently of Adaptive Immunity. *Nat Immunol*. 2012;12(7):631-638. doi:10.1038/ni.2045.Innate

193. Le Goffic R, Arshad MI, Rauch M, et al. Infection with influenza virus induces IL-33 in murine lungs. *Am J Respir Cell Mol Biol*. 2011;45(6):1125-1132. doi:10.1165/rcmb.2010-0516OC

194. Monticelli LA, Sonnenberg GF, Abt MC, et al. Innate lymphoid cells promote lung-tissue homeostasis after infection with influenza virus. *Nat Immunol*. 2011;12(11):1045-1054. doi:10.1038/ni.2131

195. Anikina AG, Shkurupii VA, Potapova O V., Kovner A V., Shestopalov AM. Expression of profibrotic growth factors and their receptors by mouse lung macrophages and fibroblasts under conditions of acute viral inflammation in influenza A/H5N1 virus. *Bull Exp Biol Med*. 2014;156(6):833-837. doi:10.1007/s10517-014-2463-7

196. Carlson CM, Turpin EA, Moser LA, et al. Transforming growth factor-β: Activation by neuraminidase and role in highly pathogenic H5N1 influenza pathogenesis. *PLoS Pathog*. 2010;6(10). doi:10.1371/journal.ppat.1001136

197. Narasaraju T, Ng HH, Phoon MC, Chow VTK. MCP-1 antibody treatment enhances damage and impedes repair of the alveolar epithelium in influenza pneumonitis. *Am J Respir Cell Mol Biol*. 2010;42(6):732-743. doi:10.1165/rcmb.2008-0423OC

198. Major J, Crotta S, Llorian M, et al. Repair During Recovery From Viral Infection. *Science (80-)*. 2020;369(6504):712-717.

199. Miyoshi J, Higashi T, Mukai H, Ohuchi T, Kakunaga T. Structure and transforming potential of the human cot oncogene encoding a putative protein kinase. *Mol Cell Biol*. 1991;11(8):4088-4096. doi:10.1128/mcb.11.8.4088-4096.1991

200. Hedl, Matija and Abraham C. A TPL2 (MAP3K8) disease-risk polymorphism increases TPL2 expression thereby leading to increased pattern recognition receptor-initiated caspase-1 and caspase-8 activation, signalling and cytokine secretion. *Gut*. 2017;65(11):1799–1811. doi:10.1016/j.physbeh.2017.03.040

201. Makris A, Patriotis C, Bear SE, Tsichlis PN. Genomic organization and expression of Tpl-2 in normal cells and Moloney murine leukemia virus-induced rat T-cell lymphomas: activation by provirus insertion. *J Virol*. 1993;67(7):4283-4289. doi:10.1128/jvi.67.7.4283-4289.1993

202. Decicco-Skinner KL, Trovato EL, Simmons JK, Lepage PK, Wiest JS. Loss of tumor progression locus 2 (tpl2) enhances tumorigenesis and inflammation in two-stage skin carcinogenesis. *Oncogene*. 2011;30(4):389-397. doi:10.1038/onc.2010.447

203. Patriotis C, Makris A, Bear SE, Tsichlis PN. Tumor progression locus 2 (Tpl-2) encodes a protein kinase involved in the progression of rodent T-cell lymphomas and in T-cell

activation. *Proc Natl Acad Sci U S A*. 1993;90(6):2251-2255. doi:10.1073/pnas.90.6.2251

204. Ceci JD, Patriotis CP, Tsatsanis C, et al. activated by carboxy-terminal truncation. 1997:688-700.

205. Gándara ML, López P, Hernando R, Castaño JG, Alemany S. The COOH-Terminal Domain of Wild-Type Cot Regulates Its Stability and Kinase Specific Activity. *Mol Cell Biol*. 2003;23(20):7377-7390. doi:10.1128/mcb.23.20.7377-7390.2003

206. Dumitru CD, Ceci JD, Tsatsanis C, et al. TNF-α induction by LPS is regulated posttranscriptionally via a Tpl2/ERK-dependent pathway. *Cell*. 2000;103(7):1071-1083. doi:10.1016/S0092-8674(00)00210-5

207. Kate S, C. PV, Eugene V, et al. The kinase TPL2 activates ERK and p38 signaling to promote neutrophilic inflammation. *Sci Signal*. 2017;10(475):eaah4273. doi:10.1126/scisignal.aah4273

208. Pattison MJ, Mitchell O, Flynn HR, et al. TLR and TNF-R1 activation of the MKK3/MKK6-p38α axis in macrophages is mediated by TPL-2 kinase. *Biochem J*. 2016;473(18):2845-2861. doi:10.1042/BCJ20160502

209. Eliopoulos AG, Wang CC, Dumitru CD, Tsichlis PN. Tpl2 transduces CD40 and TNF signals that activate ERK and regulates IgE induction by CD40. *EMBO J*. 2003;22(15):3855-3864. doi:10.1093/emboj/cdg386

210. Stafford M, Morrice N, Peggie M, Cohen P. Interleukin-1 stimulated activation of the cot catalytic subunit through the phosphorylation of THR290 and SER62. *FEBS Lett*. 2006;580:4010-4014. doi:10.1016/j.febslet.2006.06.004

211. Maria H, Georgios K, Christos P, et al. Tumor Progression Locus 2 Mediates Signal-Induced Increases in Cytoplasmic Calcium and Cell Migration. *Sci Signal*. 2011;4(187):ra55-ra55. doi:10.1126/scisignal.2002006

212. Israël A. The IKK complex, a central regulator of NF-kappaB activation. *Cold Spring Harb Perspect Biol*. 2010;2(3):1-14. doi:10.1101/cshperspect.a000158

213. Gantke T, Sriskantharajah S, Ley SC. Regulation and function of TPL-2, an IB kinase-

regulated MAP kinase kinase kinase. *Cell Res*. 2011;21(1):131-145. doi:10.1038/cr.2010.173

214. Waterfield M, Jin W, Reiley W, Zhang M, Sun S-C. IκB Kinase Is an Essential Component of the Tpl2 Signaling Pathway. *Mol Cell Biol*. 2004;24(13):6040-6048. doi:10.1128/mcb.24.13.6040-6048.2004

215. Cho J, Melnick M, Solidakis GP, Tsichlis PN. Tpl2 (tumor progression locus 2) phosphorylation at Thr 290 is induced by lipopolysaccharide via an Iκ-B kinase-β-dependent pathway and is required for Tpl2 activation by external signals. *J Biol Chem*. 2005;280(21):20442-20448. doi:10.1074/jbc.M413554200

216. Luciano BS, Hsu S, Channavajhala PL, Lin LL, Cuozzo JW. Phosphorylation of threonine 290 in the Activation Loop of Tp12/Cot is necessary but not sufficient for kinase activity. *J Biol Chem*. 2004;279(50):52117-52123. doi:10.1074/jbc.M403716200

217. Ben-Addi A, Mambole-Dema A, Brender C, et al. IκB kinase-induced interaction of TPL-2 kinase with 14-3-3 is essential for Toll-like receptor activation of ERK-1 and -2 MAP kinases. *Proc Natl Acad Sci U S A*. 2014;111(23). doi:10.1073/pnas.1320440111

218. Robinson MJ, Beinke S, Kouroumalis A, Tsichlis PN, Ley SC. Phosphorylation of TPL-2 on Serine 400 Is Essential for Lipopolysaccharide Activation of Extracellular Signal-Regulated Kinase in Macrophages. *Mol Cell Biol*. 2007;27(21):7355-7364. doi:10.1128/mcb.00301-07

219. Roget K, Ben-Addi A, Mambole-Dema A, et al. IκB Kinase 2 Regulates TPL-2 Activation of Extracellular Signal-Regulated Kinases 1 and 2 by Direct Phosphorylation of TPL-2 Serine 400. *Mol Cell Biol*. 2012;32(22):4684-4690. doi:10.1128/mcb.01065-12

220. Xie X, Zhu L, Jie Z, et al. TRAF2 regulates T cell immunity by maintaining a Tpl2-ERK survival signaling axis in effector and memory CD8 T cells. *Cell Mol Immunol*. 2021;18(9):2262-2274. doi:10.1038/s41423-020-00583-7

221. Tsatsanis C, Vaporidi K, Zacharioudaki V, et al. Tpl2 and ERK transduce antiproliferative T cell receptor signals and inhibit transformation of chronically stimulated T cells. *Proc Natl Acad Sci U S A*. 2008;105(8):2987-2992. doi:10.1073/pnas.0708381104

222. Kuriakose T, Tripp RA, Watford WT. Tumor Progression Locus 2 Promotes Induction of IFNλ, Interferon Stimulated Genes and Antigen-Specific CD8^{+} T Cell Responses and Protects against Influenza Virus. *PLoS Pathog*. 2015;11(8):1-22. doi:10.1371/journal.ppat.1005038

223. Banerjee A, Gugasyan R, McMahon M, Gerondakis S. Diverse Toll-like receptors utilize Tpl2 to activate extracellular signal-regulated kinase (ERK) in hemopoietic cells. *Proc Natl Acad Sci U S A*. 2006;103(9):3274-3279. doi:10.1073/pnas.0511113103

224. Acuff N V., Li X, Elmore J, Rada B, Watford WT. Tpl2 promotes neutrophil trafficking, oxidative burst, and bacterial killing. *J Leukoc Biol*. 2017;101(6):1325-1333. doi:10.1189/jlb.3a0316-146r

225. Rowley SM, Kuriakose T, Dockery LM, et al. Tumor progression locus 2 (Tpl2) kinase promotes chemokine receptor expression and macrophage migration during acute inflammation. *J Biol Chem*. 2014;289(22):15788-15797. doi:10.1074/jbc.M114.559344

226. Kuriakose T, Rada B, Watford WT. Tumor progression locus 2-dependent oxidative burst drives phosphorylation of extracellular signal-regulated kinase during TLR3 and 9 signaling. *J Biol Chem*. 2014;289(52):36089-36100. doi:10.1074/jbc.M114.587121

227. Mielke LA, Elkins KL, Wei L, et al. Tumor Progression Locus 2 (Map3k8) Is Critical for Host Defense against Listeria monocytogenes and IL-1β Production . *J Immunol*. 2009;183(12):7984-7993. doi:10.4049/jimmunol.0901336

228. McNab FW, Ewbank J, Rajsbaum R, et al. TPL-2–ERK1/2 Signaling Promotes Host Resistance against Intracellular Bacterial Infection by Negative Regulation of Type I IFN Production. *J Immunol*. 2013;191(4):1732-1743. doi:10.4049/jimmunol.1300146

229. Kaiser F, Cook D, Papoutsopoulou S, et al. TPL-2 negatively regulates interferon-β production in macrophages and myeloid dendritic cells. *J Exp Med*. 2009;206(9):1863-1871. doi:10.1084/jem.20091059

230. Soria-Castro I, Krzyzanowska A, Pelaéz ML, et al. Cot/tpl2 (MAP3K8) mediates myeloperoxidase activity and hypernociception following peripheral inflammation. *J Biol Chem*. 2010;285(44):33805-33815. doi:10.1074/jbc.M110.169409

231. Perfield JW, Lee Y, Shulman GI, et al. Tumor progression locus 2 (TPL2) regulates obesity-associated inflammation and insulin resistance. *Diabetes*. 2011;60(4):1168-1176. doi:10.2337/db10-0715

232. Watford WT, Hissong BD, Durant LR, et al. Tpl2 kinase regulates T cell interferon-γ production and host resistance to toxoplasma gondii. *J Exp Med*. 2008;205(12):2803-2812. doi:10.1084/jem.20081461

233. Acuff, NV, Li, X, Latha, K, Nagy, T, Watford W. Tpl2 Promotes Innate Cell Recruitment and Effector T Cell Differentiation To Limit Citrobacter rodentium Burden and Dissemination. *Infect Immun*. 2017;85(10):1-13.

234. https://www.cdc.gov/flu/weekly/index.htm. No Title. https://www.cdc.gov/flu/weekly/index.htm.

235. Chertow DS, Memoli MJ. Bacterial Coinfection in Influenza: A Grand Rounds Review. *JAMA*. 2013;309(3):275-282. doi:10.1001/jama.2012.194139

236. Palacios G, Hornig M, Cisterna D, et al. Streptococcus pneumoniae coinfection is correlated with the severity of H1N1 pandemic influenza. *PLoS One*. 2009;4(12):1-5. doi:10.1371/journal.pone.0008540

237. Rice TW, Rubinson L, Uyeki TM, et al. Critical illness from 2009 pandemic influenza A virus and bacterial coinfection in the United States. *Crit Care Med*. 2012;40(5):1487-1498. doi:10.1097/CCM.0b013e3182416f23

238. J. SK, Shivaprakash G, A. BJ, et al. Early Control of H5N1 Influenza Virus Replication by the Type I Interferon Response in Mice. *J Virol*. 2009;83(11):5825-5834. doi:10.1128/JVI.02144-08

239. Fukushi M, Ito T, Oka T, et al. Serial histopathological examination of the lungs of mice infected with influenza A virus PR8 strain. *PLoS One*. 2011;6(6):1-7. doi:10.1371/journal.pone.0021207

240. O’Brien KB, Vogel P, Duan S, et al. Impaired wound healing predisposes obese mice to severe influenza virus infection. *J Infect Dis*. 2012;205(2):252-261. doi:10.1093/infdis/jir729

241. Wu H, Haist V, Baumgärtner W, Schughart K. Sustained viral load and late death in Rag2-/- mice after influenza A virus infection. *Virol J*. 2010;7:172. doi:10.1186/1743-422X-7-172

242. Tate MD, Deng Y-M, Jones JE, Anderson GP, Brooks AG, Reading PC. Neutrophils Ameliorate Lung Injury and the Development of Severe Disease during Influenza Infection. *J Immunol*. 2009;183(11):7441-7450. doi:10.4049/jimmunol.0902497

243. Putri WCWS, Muscatello DJ, Stockwell MS, Newall AT. Economic burden of seasonal influenza in the United States. *Vaccine*. 2018;36(27):3960-3966. doi:10.1016/j.vaccine.2018.05.057

244. Houser K and SK. Influenza Vaccines: Challenges and Solutions. *Cell Host Microbe*. 2015;17(3):295-300. doi:10.1016/j.physbeh.2017.03.040

245. Hussain M, Galvin HD, Haw TY, Nutsford AN, Husain M. Drug resistance in influenza a virus: The epidemiology and management. *Infect Drug Resist*. 2017;10:121-134. doi:10.2147/IDR.S105473

246. Dong G, Peng C, Luo J, et al. Adamantane-resistant influenza a viruses in the world (1902-2013): Frequency and distribution of M2 gene mutations. *PLoS One*. 2015;10(3):1-20. doi:10.1371/journal.pone.0119115

247. Zaraket H, Saito R, Suzuki Y, et al. Genetic makeup of amantadine-resistant and oseltamivir-resistant human influenza A/H1N1 viruses. *J Clin Microbiol*. 2010;48(4):1085-1092. doi:10.1128/JCM.01532-09

248. Ortiz JR, Neuzil KM, Shay DK, et al. The burden of influenza-associated critical illness hospitalizations. *Crit Care Med*. 2014;42(11):2325-2332. doi:10.1097/CCM.0000000000000545

249. Ichiyama T, Isumi H, Ozawa H, Matsubara T, Morishima T, Furukawa S. Cerebrospinal fluid and serum levels of cytokines and soluble tumor necrosis factor receptor in influenza virus-associated encephalopathy. *Scand J Infect Dis*. 2003;35(1):59-61. doi:10.1080/0036554021000026986

250. Gao R, Bhatnagar J, Blau DM, et al. Cytokine and chemokine profiles in lung tissues from

fatal cases of 2009 pandemic influenza A (H1N1): Role of the host immune response in pathogenesis. *Am J Pathol*. 2013;183(4):1258-1268. doi:10.1016/j.ajpath.2013.06.023

251. Perrone LA, Plowden JK, García-Sastre A, Katz JM, Tumpey TM. H5N1 and 1918 pandemic influenza virus infection results in early and excessive infiltration of macrophages and neutrophils in the lungs of mice. *PLoS Pathog*. 2008;4(8). doi:10.1371/journal.ppat.1000115

252. Chang ST, Tchitchek N, Ghosh D, Benecke A, Katze MG. A chemokine gene expression signature derived from meta-analysis predicts the pathogenicity of viral respiratory infections. *BMC Syst Biol*. 2011;5. doi:10.1186/1752-0509-5-202

253. Cheung CY, Poon LLM, Lau AS, et al. Induction of proinflammatory cytokines in human macrophages by influenza A (H5N1) viruses: A mechanism for the unusual severity of human disease? *Lancet*. 2002;360(9348):1831-1837. doi:10.1016/S0140-6736(02)11772-7

254. De Jong MD, Simmons CP, Thanh TT, et al. Fatal outcome of human influenza A (H5N1) is associated with high viral load and hypercytokinemia. *Nat Med*. 2006;12(10):1203-1207. doi:10.1038/nm1477

255. Iwasaki A. A virological view of innate immune recognition. *Annu Rev Microbiol*. 2012;66:177-196. doi:10.1146/annurev-micro-092611-150203

256. Duan M, Hibbs ML, Chen W. The contributions of lung macrophage and monocyte heterogeneity to influenza pathogenesis. *Immunol Cell Biol*. 2017;95(3):225-235. doi:10.1038/icb.2016.97

257. Kaplanski G, Marin V, Montero-Julian F, Mantovani A, Farnarier C. IL-6: A regulator of the transition from neutrophil to monocyte recruitment during inflammation. *Trends Immunol*. 2003;24(1):25-29. doi:10.1016/S1471-4906(02)00013-3

258. Lin KL, Sweeney S, Kang BD, Ramsburg E, Gunn MD. CCR2-Antagonist Prophylaxis Reduces Pulmonary Immune Pathology and Markedly Improves Survival during Influenza Infection. *J Immunol*. 2011;186(1):508-515. doi:10.4049/jimmunol.1001002

259. Short KR, Kroeze EJBV, Fouchier RAM, Kuiken T. Pathogenesis of influenza-induced acute respiratory distress syndrome. *Lancet Infect Dis*. 2014;14(1):57-69.

doi:10.1016/S1473-3099(13)70286-X

260. Yang H-T, Papoutsopoulou S, Belich M, et al. Coordinate Regulation of TPL-2 and NF- B Signaling in Macrophages by NF- B1 p105. *Mol Cell Biol*. 2012;32(17):3438-3451. doi:10.1128/mcb.00564-12

261. Farias R, Rousseau S. The TAK1→IKKβ→TPL2→MKK1/MKK2 signaling cascade regulates IL-33 expression in cystic fibrosis airway epithelial cells following infection by Pseudomonas aeruginosa. *Front Cell Dev Biol*. 2016;3(JAN):1-10. doi:10.3389/fcell.2015.00087

262. Papoutsopoulou S, Symons A, Tharmalingham T, et al. ABIN-2 is required for optimal activation of Erk MAP kinase in innate immune responses. *Nat Immunol*. 2006;7(6):606-615. doi:10.1038/ni1334

263. Beinke S, Robinson MJ, Hugunin M, Ley SC. Lipopolysaccharide activation of the TPL-2/MEK/extracellular signal-regulated kinase mitogen-activated protein kinase cascade is regulated by IkappaB kinase-induced proteolysis of NF-kappaB1 p105. *Mol Cell Biol*. 2004;24(21):9658-9667. doi:10.1128/MCB.24.21.9658-9667.2004

264. Senger K, Pham VC, Varfolomeev E, et al. The kinase TPL2 activates ERK and p38 signaling to promote neutrophilic inflammation. *Sci Signal*. 2017;10(475). doi:10.1126/scisignal.aah4273

265. Lang V, Symons A, Watton SJ, et al. ABIN-2 forms a ternary complex with TPL-2 and NF-kappa B1 p105 and is essential for TPL-2 protein stability. *Mol Cell Biol*. 2004;24(12):5235-5248. doi:10.1128/MCB.24.12.5235-5248.2004

266. Belich MP, Salmerón A, Johnston LH, Ley SC. TPL-2 kinase regulates the proteolysis of the NF-κB-inhibitory protein NF-κB1 p105. *Nature*. 1999;397(6717):363-368. doi:10.1038/16946

267. Sanz-Garcia C, Nagy LE, Lasunción MA, Fernandez M, Alemany S. Cot/tpl2 participates in the activation of macrophages by adiponectin. *J Leukoc Biol*. 2014;95(6):917-930. doi:10.1189/jlb.0913486

268. Mielke LA, Elkins KL, Wei L, et al. Tumor Progression Locus 2 (Map3k8) Is Critical for

Host Defense against Listeria monocytogenes and IL-1β Production . *J Immunol*. 2009;183(12):7984-7993. doi:10.4049/jimmunol.0901336

269. Schmid S, Sachs D, Ten Oever BR. Mitogen-activated protein kinase-mediated licensing of interferon regulatory factor 3/7 reinforces the cell response to virus. *J Biol Chem*. 2014;289(1):299-311. doi:10.1074/jbc.M113.519934

270. Lamichhane PP, Samarasinghe AE. The Role of Innate Leukocytes during Influenza Virus Infection. *J Immunol Res*. 2019;2019. doi:10.1155/2019/8028725

271. Sánchez Á, Relaño C, Carrasco A, et al. Map3k8 controls granulocyte colony-stimulating factor production and neutrophil precursor proliferation in lipopolysaccharide-induced emergency granulopoiesis. *Sci Rep*. 2017;7(1):1-14. doi:10.1038/s41598-017-04538-3

272. Sugamata R, Dobashi H, Nagao T, et al. Contribution of neutrophil-derived myeloperoxidase in the early phase of fulminant acute respiratory distress syndrome induced by influenza virus infection. *Microbiol Immunol*. 2012;56(3):171-182. doi:10.1111/j.1348-0421.2011.00424.x

273. Foong RE, Sly PD, Larcombe AN, Zosky GR. No role for neutrophil elastase in influenza-induced cellular recruitment, cytokine production or airway hyperresponsiveness in mice. *Respir Physiol Neurobiol*. 2010;173(2):164-170. doi:10.1016/j.resp.2010.08.003

274. Zhu L, Liu L, Zhang Y, et al. High Level of Neutrophil Extracellular Traps Correlates with Poor Prognosis of Severe Influenza A Infection. *J Infect Dis*. 2018;217(3):428-437. doi:10.1093/infdis/jix475

275. Kodama T, Yukioka H, Kato T, Kato N, Hato F, Kitagawa S. Neutrophil elastase as a predicting factor for development of acute lung injury. *Intern Med*. 2007;46(11):699-704. doi:10.2169/internalmedicine.46.6182

276. Kulkarni U, Zemans RL, Smith CA, Wood S, Deng JC, Goldstein DR. Excessive neutrophil levels in the lung underlie the ageassociated increase in influenza mortality. *Mucosal Immunol*. 2019;12(2):545-554. doi:10.1038/s41385-018-0115-3.Excessive

277. Karupiah G, Chen JH, Mahalingam S, Nathan CF, MacMicking JD. Rapid interferon gamma-dependent clearance of influenza A virus and protection from consolidating

pneumonitis in nitric oxide synthase 2-deficient mice. *J Exp Med*. 1998;188(8):1541—1546. doi:10.1084/jem.188.8.1541

278. Rauch I, Müller M, Decker T. The regulation of inflammation by interferons and their STATs. *Jak-Stat*. 2013;2(1):e23820. doi:10.4161/jkst.23820

279. Lehmann MH, Torres-Domínguez LE, Price PJR, Brandmüller C, Kirschning CJ, Sutter G. CCL2 expression is mediated by type I IFN receptor and recruits NK and T cells to the lung during MVA infection. *J Leukoc Biol*. 2016;99(6):1057-1064. doi:10.1189/jlb.4ma0815-376rr

280. Pothlichet J, Chignard M, Si-Tahar M. Cutting Edge: Innate Immune Response Triggered by Influenza A Virus Is Negatively Regulated by SOCS1 and SOCS3 through a RIG-I/IFNAR1-Dependent Pathway. *J Immunol*. 2008;180(4):2034-2038. doi:10.4049/jimmunol.180.4.2034

281. Khatri M, Saif YM. Influenza virus infects bone marrow mesenchymal stromal cells in vitro: implications for bone marrow transplantation. *Cell Transplant*. 2013;22(3):461-468. doi:10.3727/096368912X656063

282. Sawyer RT, Strausbauch PH, Volkman A. Resident macrophage proliferation in mice depleted of blood monocytes by strontium-89. *Lab Invest*. 1982;46(2):165-170.

283. Perrone LA, Belser JA, Wadford DA, Katz JM, Tumpey TM. Inducible nitric oxide contributes to viral pathogenesis following highly pathogenic influenza virus infection in mice. *J Infect Dis*. 2013;207(10):1576-1584. doi:10.1093/infdis/jit062

284. Ottonello L, Montecucco F, Bertolotto M, et al. CCL3 (MIP-1alpha) induces in vitro migration of GM-CSF-primed human neutrophils via CCR5-dependent activation of ERK 1/2. *Cell Signal*. 2005;17(3):355-363. doi:10.1016/j.cellsig.2004.08.002

285. Ishiguro N, Takada A, Yoshioka M, et al. Induction of interferon-inducible protein-10 and monokine induced by interferon-γ from human endothelial cells infected with Influenza A virus. *Arch Virol*. 2004;149(1):17-34. doi:10.1007/s00705-003-0208-4

286. Lukacs NW, Strieter RM, Warmington K, Lincoln P, Chensue SW, Kunkel SL. Differential recruitment of leukocyte populations and alteration of airway hyperreactivity

by C-C family chemokines in allergic airway inflammation. *J Immunol*. 1997;158(9):4398-4404.

287. Van Acker GJD, Perides G, Weiss ER, Das S, Tsichlis PN, Steer ML. Tumor progression locus-2 is a critical regulator of pancreatic and lung inflammation during acute pancreatitis. *J Biol Chem*. 2007;282(30):22140-22149. doi:10.1074/jbc.M702225200

288. Sanz-Garcia C, Ferrer-Mayorga G, González-Rodríguez Á, et al. Sterile inflammation in acetaminophen-induced liver injury is mediated by Cot/tpl2. *J Biol Chem*. 2013;288(21):15342-15351. doi:10.1074/jbc.M112.439547

289. Roulis M, Nikolaou C, Kotsaki E, et al. Intestinal myofibroblast-specific Tpl2-Cox-2-PGE2 pathway links innate sensing to epithelial homeostasis. *Proc Natl Acad Sci U S A*. 2014;111(43):E4658-67. doi:10.1073/pnas.1415762111

290. Martel G, Bérubé J, Rousseau S. The Protein Kinase TPL2 Is Essential for ERK1/ERK2 Activation and Cytokine Gene Expression in Airway Epithelial Cells Exposed to Pathogen-Associated Molecular Patterns (PAMPs). *PLoS One*. 2013;8(3):1-9. doi:10.1371/journal.pone.0059116

291. Moltedo B, Li W, Yount JS, Moran TM. Unique type I interferon responses determine the functional fate of migratory lung dendritic cells during influenza virus infection. *PLoS Pathog*. 2011;7(11). doi:10.1371/journal.ppat.1002345

292. Tisoncik JR, Billharz R, Burmakina S, et al. The NS1 protein of influenza A virus suppresses interferon-regulated activation of antigenpresentation and immune-proteasome pathways. *J Gen Virol*. 2011;92(9):2093-2104. doi:10.1099/vir.0.032060-0

293. Du Y, Yang F, Wang Q, et al. Influenza a virus antagonizes type i and type II interferon responses via SOCS1-dependent ubiquitination and degradation of JAK1. *Virol J*. 2020;17(1):1-10. doi:10.1186/s12985-020-01348-4

294. Pauli EK, Schmolke M, Wolff T, et al. Influenza A virus inhibits type I IFN signaling via NF-κB-dependent induction of SOCS-3 expression. *PLoS Pathog*. 2008;4(11):1-15. doi:10.1371/journal.ppat.1000196

295. Kedzierski L, Linossi EM, Kolesnik TB, et al. Suppressor of Cytokine Signaling 4

(SOCS4) Protects against Severe Cytokine Storm and Enhances Viral Clearance during Influenza Infection. *PLoS Pathog*. 2014;10(5). doi:10.1371/journal.ppat.1004134

296. Uetani K, Thomassen MJ, Erzurum SC. Nitric oxide synthase 2 through an autocrine loop via respiratory epithelial cell-derived mediator. *Am J Physiol Lung Cell Mol Physiol*. 2001;280(6):L1179-88. doi:10.1152/ajplung.2001.280.6.L1179

297. Tripathi P, Tripathi P, Kashyap L, Singh V. The role of nitric oxide in inflammatory reactions. *FEMS Immunol Med Microbiol*. 2007;51(3):443-452. doi:10.1111/j.1574-695X.2007.00329.x

298. Fielding CA, McLoughlin RM, McLeod L, et al. IL-6 Regulates Neutrophil Trafficking during Acute Inflammation via STAT3. *J Immunol*. 2008;181(3):2189-2195. doi:10.4049/jimmunol.181.3.2189

299. Oliver Dienz, Jonathan G. Rud, Sheri M. Eaton, Paula A. Lanthier, Elianne Burg, Angela Drew, Janice Bunn, Benjamin T. Suratt, Laura Haynes and MR. Essential role of IL-6 in protection against H1N1 influenza virus by promoting neutrophil survival in the lung. *Mucosal Immunol*. 2012;5(3):258-266. doi:10.1016/j.physbeh.2017.03.040

300. Zhai Y, Franco LM, Atmar RL, et al. Host Transcriptional Response to Influenza and Other Acute Respiratory Viral Infections – A Prospective Cohort Study. *PLoS Pathog*. 2015;11(6):1-29. doi:10.1371/journal.ppat.1004869

301. Liu JW, Lin SH, Wang LC, Chiu HY, Lee JA. Comparison of Antiviral Agents for Seasonal Influenza Outcomes in Healthy Adults and Children: A Systematic Review and Network Meta-analysis. *JAMA Netw Open*. 2021;4(8):1-14. doi:10.1001/jamanetworkopen.2021.19151

302. Malone L, Cm MBA, Grigorenko E, Stalons D. Id Week 2015. 2017;2(September):2633851. doi:10.1093/o

303. Fowlkes AL, Steffens A, Reed C, Temte JL, Campbell AP, Rubino H. Influenza antiviral prescribing practices and the influence of rapid testing among primary care providers in the US, 2009-2016. *Open Forum Infect Dis*. 2019;6(6):2009-2016. doi:10.1093/ofid/ofz192

304. C. GC, J. MA. Current Best Practices for Respiratory Virus Testing. *J Clin Microbiol*. 2011;49(9_Supplement):S44-S48. doi:10.1128/JCM.00698-11

305. Cheng PKC, Leung TWC, Ho ECM, et al. Oseltamivir-and amantadine-resistant influenza viruses A (H1N1). *Emerg Infect Dis*. 2009;15(6):966-968. doi:10.3201/eid1506.081357

306. Goldhill DH, te Velthuis AJW, Fletcher RA, et al. The mechanism of resistance to favipiravir in influenza. *Proc Natl Acad Sci*. 2018;115(45):11613 LP - 11618. doi:10.1073/pnas.1811345115

307. Belshe RB, Smith MH, Hall CB, Betts R, Hay AJ. Genetic basis of resistance to rimantadine emerging during treatment of influenza virus infection. *J Virol*. 1988;62(5):1508-1512. doi:10.1128/jvi.62.5.1508-1512.1988

308. Shi T, Nie Z, Huang L, et al. Mortality risk factors in children with severe influenza virus infection admitted to the pediatric intensive care unit. *Medicine (Baltimore)*. 2019;98(35):e16861. doi:10.1097/MD.0000000000016861

309. Areechokchai D, Jiraphongsa C, Laosiritaworn Y, Hanshaoworakul W, O'Reilly M. Investigation of avian influenza (H5N1) outbreak in humans--Thailand, 2004. *MMWR Suppl*. 2006;55(1):3-6.

310. Kusznierz G, Carolina C, Manuel RJ, et al. Impact of influenza in the post-pandemic phase: Clinical features in hospitalized patients with influenza A (H1N1) pdm09 and H3N2 viruses, during 2013 in Santa Fe, Argentina. *J Med Virol*. 2017;89(7):1186-1191. doi:10.1002/jmv.24758

311. Chaves SS, Aragon D, Bennett N, et al. Patients hospitalized with laboratory-confirmed influenza during the 2010-2011 influenza season: exploring disease severity by virus type and subtype. *J Infect Dis*. 2013;208(8):1305-1314. doi:10.1093/infdis/jit316

312. Kaji M, Watanabe A, Aizawa H. Differences in clinical features between influenza A H1N1, A H3N2, and B in adult patients. *Respirology*. 2003;8(2):231-233. doi:10.1046/j.1440-1843.2003.00457.x

313. Honda K, Takaoka A, Taniguchi T. Type I Inteferon Gene Induction by the Interferon Regulatory Factor Family of Transcription Factors. *Immunity*. 2006;25(3):349-360.

doi:10.1016/j.immuni.2006.08.009

314. Xiao N, Eidenschenk C, Krebs P, et al. The Tpl2 Mutation Sluggish Impairs Type I IFN Production and Increases Susceptibility to Group B Streptococcal Disease . *J Immunol*. 2009;183(12):7975-7983. doi:10.4049/jimmunol.0902718

315. Latha K, Jamison KF, Watford WT. Tpl2 Ablation Leads to Hypercytokinemia and Excessive Cellular Infiltration to the Lungs During Late Stages of Influenza Infection . *Front Immunol* . 2021;12:3919.

316. Rodriguez AE, Bogart C, Gilbert CM, et al. Enhanced IL-1β production is mediated by a TLR2-MYD88-NLRP3 signaling axis during coinfection with influenza A virus and Streptococcus pneumoniae. *PLoS One*. 2019;14(2):10-13. doi:10.1371/journal.pone.0212236

317. Ishikawa H, Fukui T, Ino S, et al. Influenza virus infection causes neutrophil dysfunction through reduced G-CSF production and an increased risk of secondary bacteria infection in the lung. *Virology*. 2016;499:23-29. doi:10.1016/j.virol.2016.08.025

318. Tate MD, Brooks AG, Reading PC. The role of neutrophils in the upper and lower respiratory tract during influenza virus infection of mice. *Respir Res*. 2008;9:1-13. doi:10.1186/1465-9921-9-57

319. Jewell NA, Cline T, Mertz SE, et al. Lambda Interferon Is the Predominant Interferon Induced by Influenza A Virus Infection In Vivo . *J Virol*. 2010;84(21):11515-11522. doi:10.1128/jvi.01703-09

320. I. Mian A. Nitric Oxide Metabolites as Biomarkers for Influenza-Like Acute Respiratory Infections Presenting to the Emergency Room. *Open Respir Med J*. 2012;6(1):127-134. doi:10.2174/1874306401206010127

321. Nin N, Sánchez-Rodríguez C, Ver LS, et al. Lung histopathological findings in fatal pandemic influenza A (H1N1). *Med Intensiva*. 2012;36(1):24-31. doi:https://doi.org/10.1016/j.medin.2011.10.005

322. Burggraaf S, Bingham J, Payne J, Kimpton WG, Lowenthal JW, Bean AGD. Increased inducible nitric oxide synthase expression in organs is associated with a higher severity of

H5N1 influenza virus infection. *PLoS One*. 2011;6(1):1-12. doi:10.1371/journal.pone.0014561

323. Saini R, Patel S, Saluja R, et al. Nitric oxide synthase localization in the rat neutrophils: immunocytochemical, molecular, and biochemical studies. *J Leukoc Biol*. 2006;79(3):519-528. doi:10.1189/jlb.0605320

324. Wang L, Taneja R, Razavi HM, Law C, Gillis C, Mehta S. Specific role of neutrophil inducible nitric oxide synthase in murine sepsis-induced lung injury in vivo. *Shock*. 2012;37(5):539-547. doi:10.1097/SHK.0b013e31824dcb5a

325. Redford PS, Mayer-Barber KD, McNab FW, et al. Influenza A virus impairs control of mycobacterium tuberculosis coinfection through a type i interferon receptor-dependent pathway. *J Infect Dis*. 2014;209(2):270-274. doi:10.1093/infdis/jit424

326. Sato M, Suemori H, Hata N, et al. Distinct and essential roles of transcription factors IRF-3 and IRF-7 in response to viruses for IFN-α/β gene induction. *Immunity*. 2000;13(4):539-548. doi:10.1016/S1074-7613(00)00053-4

327. Taniguchi T, Takaoka A. The interferon-α/β system in antiviral responses: A multimodal machinery of gene regulation by the IRF family of transcription factors. *Curr Opin Immunol*. 2002;14(1):111-116. doi:10.1016/S0952-7915(01)00305-3

328. Wang Y, Li T, Chen Y, Wei H, Sun R, Tian Z. Involvement of NK Cells in IL-28B–Mediated Immunity against Influenza Virus Infection. *J Immunol*. 2017;199(3):1012-1020. doi:10.4049/jimmunol.1601430

329. Crotta S, Davidson S, Mahlakoiv T, et al. Type I and Type III Interferons Drive Redundant Amplification Loops to Induce a Transcriptional Signature in Influenza-Infected Airway Epithelia. *PLoS Pathog*. 2013;9(11). doi:10.1371/journal.ppat.1003773

330. Helft J, Manicassamy B, Guermonprez P, et al. Cross-presenting CD103+ dendritic cells are protected from influenza virus infection. *J Clin Invest*. 2012;122(11):4037-4047. doi:10.1172/JCI60659

331. Kallet RH, Haas CF. Acute respiratory distress syndrome. *Respir Care Clin N Am*. 2003;9(3):315-322. doi:10.1016/S1078-5337(03)00038-8

332. Matthay MA, Zemans RL. The acute respiratory distress syndrome: pathogenesis and treatment. *Annu Rev Pathol*. 2011;6:147-163. doi:10.1146/annurev-pathol-011110-130158

333. Matthay MA, Zemans RL, Zimmerman GA, et al. Acute respiratory distress syndrome. *Nat Rev Dis Prim*. 2018;5(1). doi:10.1038/s41572-019-0069-0

334. Bein T, Weber-Carstens S, Apfelbacher C. Long-term outcome after the acute respiratory distress syndrome: Different from general critical illness? *Curr Opin Crit Care*. 2018;24(1):35-40. doi:10.1097/MCC.0000000000000476

335. Heyland DK, Groll D, Caeser M. Survivors of acute respiratory distress syndrome: relationship between pulmonary dysfunction and long-term health-related quality of life. *Crit Care Med*. 2005;33(7):1549-1556. doi:10.1097/01.ccm.0000168609.98847.50

336. Wang A, Gao G, Wang S, et al. Clinical characteristics and risk factors of acute respiratory distress syndrome (ARDS) in COVID-19 patients in Beijing, China: A retrospective study. *Med Sci Monit*. 2020;26:1-9. doi:10.12659/MSM.925974

337. Brown R, McKelvey MC, Ryan S, et al. The Impact of Aging in Acute Respiratory Distress Syndrome: A Clinical and Mechanistic Overview. *Front Med*. 2020;7(October):1-8. doi:10.3389/fmed.2020.589553

338. Wu C, Chen X, Cai Y, et al. Risk Factors Associated with Acute Respiratory Distress Syndrome and Death in Patients with Coronavirus Disease 2019 Pneumonia in Wuhan, China. *JAMA Intern Med*. 2020;180(7):934-943. doi:10.1001/jamainternmed.2020.0994

339. McNicholas BA, Madotto F, Pham T, et al. Demographics, management and outcome of females and males with acute respiratory distress syndrome in the LUNG SAFE prospective cohort study. *Eur Respir J*. 2019;54(4). doi:10.1183/13993003.00609-2019

340. Park PK, Cannon JW, Ye W, et al. Incidence, risk factors, and mortality associated with acute respiratory distress syndrome in combat casualty care. *J Trauma Acute Care Surg*. 2016;81(5 Suppl 2 Proceedings of the 2015 Military Health System Research Symposium):S150-S156. doi:10.1097/TA.0000000000001183

341. Heffernan DS, Dossett LA, Lightfoot MA, et al. Gender and ARDS in Critically Injured Adults: A Prospective Study. *J Trauma*. 2011;71(4):878-885.

doi:10.1097/TA.0b013e31822c0d31

342. Xu B, Ge Y, Lu Y, Chen Q, Zhang H. Risk factors and prognosis of acute respiratory distress syndrome following abdominal surgery. *Exp Ther Med*. 2019;17(1):159-164. doi:10.3892/etm.2018.6928

343. Su IL, Wu VCC, Chou AH, et al. Risk factor analysis of postoperative acute respiratory distress syndrome after type A aortic dissection repair surgery. *Medicine (Baltimore)*. 2019;98(29):e16303. doi:10.1097/MD.0000000000016303

344. Ranieri VM, Rubenfeld GD, Thompson BT, et al. Acute respiratory distress syndrome: The Berlin definition. *JAMA - J Am Med Assoc*. 2012;307(23):2526-2533. doi:10.1001/jama.2012.5669

345. Bellani G, Laffey JG, Pham T, et al. Epidemiology, patterns of care, and mortality for patients with acute respiratory distress syndrome in intensive care units in 50 countries. *JAMA - J Am Med Assoc*. 2016;315(8):788-800. doi:10.1001/jama.2016.0291

346. Villar J, Pérez-Méndez L, Blanco J, et al. A universal definition of ARDS: The PaO2/FiO2 ratio under a standard ventilatory setting - A prospective, multicenter validation study. *Intensive Care Med*. 2013;39(4):583-592. doi:10.1007/s00134-012-2803-x

347. Aboab J, Louis B, Jonson B, Brochard L. Relation between PaO2/FIO2 ratio and FIO2: A mathematical description. *Intensive Care Med*. 2006;32(10):1494-1497. doi:10.1007/s00134-006-0337-9

348. Bellingan GJ. The pulmonary physician in critical care • 6: The pathogenesis of ALI/ARDS. *Thorax*. 2002;57(6):540 LP - 546. doi:10.1136/thorax.57.6.540

349. Tomashefski JFJ. Pulmonary pathology of the adult respiratory distress syndrome. *Clin Chest Med*. 1990;11(4):593-619.

350. Olajuyin AM, Zhang X, Ji HL. Alveolar type 2 progenitor cells for lung injury repair. *Cell Death Discov*. 2019;5(1). doi:10.1038/s41420-019-0147-9

351. Villar J, Blanco J, Añón JM, et al. The ALIEN study: Incidence and outcome of acute

respiratory distress syndrome in the era of lung protective ventilation. *Intensive Care Med*. 2011;37(12):1932-1941. doi:10.1007/s00134-011-2380-4

352. Rubenfeld GD, Caldwell E, Peabody E, et al. Incidence and Outcomes of Acute Lung Injury. *N Engl J Med*. 2005;353(16):1685-1693. doi:10.1056/NEJMoa050333

353. Esteban A, Anzueto A, Frutos F, et al. Characteristics and outcomes in adult patients receiving mechanical ventilation: A 28-day international study. *J Am Med Assoc*. 2002;287(3):345-355. doi:10.1001/jama.287.3.345

354. Esteban A, Frutos-Vivar F, Muriel A, et al. Evolution of mortality over time in patients receiving mechanical ventilation. *Am J Respir Crit Care Med*. 2013;188(2):220-230. doi:10.1164/rccm.201212-2169OC

355. Wang CY, Calfee CS, Paul DW, et al. One-year mortality and predictors of death among hospital survivors of acute respiratory distress syndrome. *Intensive Care Med*. 2014;40(3):388-396. doi:10.1007/s00134-013-3186-3

356. Töpfer L, Menk M, Weber-Carstens S, et al. Influenza A (H1N1) vs non-H1N1 ARDS: analysis of clinical course. *J Crit Care*. 2014;29(3):340-346. doi:10.1016/j.jcrc.2013.12.013

357. Homsi S, Milojkovic N, Homsi Y. Clinical pathological characteristics and management of acute respiratory distress syndrome resulting from influenza A (H1N1) virus. *South Med J*. 2010;103(8):782-786. doi:10.1097/SMJ.0b013e3181e6ca0c

358. Hagau N, Slavcovici A, Gonganau DN, et al. Clinical aspects and cytokine response in severe H1N1 influenza A virus infection. *Crit Care*. 2010;14(6):R203. doi:10.1186/cc9324

359. Fiore-Gartland A, Panoskaltsis-Mortari A, Agan AA, et al. Cytokine profiles of severe influenza virus-related complications in children. *Front Immunol*. 2017;8(NOV):1-12. doi:10.3389/fimmu.2017.01423

360. Li C, Yang P, Sun Y, et al. IL-17 response mediates acute lung injury induced by the 2009 Pandemic Influenza A (H1N1) Virus. *Cell Res*. 2012;22(3):528-538. doi:10.1038/cr.2011.165

361. Shinya K, Gao Y, Cilloniz C, et al. Integrated Clinical, Pathologic, Virologic, and Transcriptomic Analysis of H5N1 Influenza Virus-Induced Viral Pneumonia in the Rhesus Macaque. *J Virol*. 2012;86(11):6055-6066. doi:10.1128/jvi.00365-12

362. Laufe MD, Simon RH, Flint A, Keller JB. Adult respiratory distress syndrome in neutropenic patients. *Am J Med*. 1986;80(6):1022-1026. doi:10.1016/0002-9343(86)90659-5

363. Grunwell JR, Giacalone VD, Stephenson S, et al. Neutrophil Dysfunction in the Airways of Children with Acute Respiratory Failure Due to Lower Respiratory Tract Viral and Bacterial Coinfections. *Sci Rep*. 2019;9(1):1-13. doi:10.1038/s41598-019-39726-w

364. Yang L, Gao C, Li F, et al. Monocyte-to-lymphocyte ratio is associated with 28-day mortality in patients with acute respiratory distress syndrome: a retrospective study. *J Intensive Care*. 2021;9(1):1-11. doi:10.1186/s40560-021-00564-6

365. Ghoneim HE, Thomas PG, McCullers JA. Depletion of Alveolar Macrophages during Influenza Infection Facilitates Bacterial Superinfections. *J Immunol*. 2013;191(3):1250-1259. doi:10.4049/jimmunol.1300014

366. Kim EA, Lee KS, Primack SL, et al. Viral pneumonias in adults: Radiologic and pathologic findings. *Radiographics*. 2002;22(SPEC. ISS):137-149. doi:10.1148/radiographics.22.suppl_1.g02oc15s137

367. Xu T, Qiao J, Zhao L, et al. Acute respiratory distress syndrome induced by avian influenza A (H5N1) virus in mice. *Am J Respir Crit Care Med*. 2006;174(9):1011-1017. doi:10.1164/rccm.200511-1751OC

368. Deng G, Bi J, Kong F, et al. Acute respiratory distress syndrome induced by H9N2 virus in mice. *Arch Virol*. 2010;155(2):187-195. doi:10.1007/s00705-009-0560-0

369. Blondonnet R, Constantin JM, Sapin V, Jabaudon M. A Pathophysiologic Approach to Biomarkers in Acute Respiratory Distress Syndrome. *Dis Markers*. 2016;2016. doi:10.1155/2016/3501373

370. van der Zee P, Rietdijk W, Somhorst P, Endeman H, Gommers D. A systematic review of biomarkers multivariately associated with acute respiratory distress syndrome

development and mortality. *Crit Care*. 2020;24(1):243. doi:10.1186/s13054-020-02913-7

371. Isabel García-Laorden M, Lorente JA, Flores C, Slutsky AS, Villar J. Biomarkers for the acute respiratory distress syndrome: How to make the diagnosis more precise. *Ann Transl Med*. 2017;5(14):1-10. doi:10.21037/atm.2017.06.49

372. Spadaro S, Park M, Turrini C, et al. Biomarkers for Acute Respiratory Distress syndrome and prospects for personalised medicine. *J Inflamm (United Kingdom)*. 2019;16(1):1-11. doi:10.1186/s12950-018-0202-y

373. Zimmerman GA, Albertine KH, Carveth HJ, et al. Endothelial activation in ARDS. *Chest*. 1999;116(SUPPL.):18S-24S. doi:10.1378/chest.116.suppl_1.18S

374. Park S, DiMaio TA, Scheef EA, Sorenson CM, Sheibani N. PECAM-1 regulates proangiogenic properties of endothelial cells through modulation of cell-cell and cell-matrix interactions. *Am J Physiol Cell Physiol*. 2010;299(6):C1468-C1484. doi:10.1152/ajpcell.00246.2010

375. Imaizumi TA, Albertine KH, Jicha DL, McIntyre TM, Prescott SM, Zimmerman GA. Human Endothelial Cells Synthesize ENA-78: Relationship to IL-8 and to Signaling of PMN Adhesion. *Am J Respir Cell Mol Biol*. 1997;17(2):181-192. doi:10.1165/ajrcmb.17.2.2818

376. Hiratsuka S, Kataoka Y, Nakao K, et al. Vascular Endothelial Growth Factor A (VEGF-A) Is Involved in Guidance of VEGF Receptor-Positive Cells to the Anterior Portion of Early Embryos. *Mol Cell Biol*. 2005;25(1):355-363. doi:10.1128/mcb.25.1.355-363.2005

377. Koltsova EK, Ley K. The mysterious ways of the chemokine cxcl5. *Immunity*. 2010;33(1):7-9. doi:10.1016/j.immuni.2010.07.012

378. Walz A, Schmutz P, Mueller C, Schnyder-Candrian S. Regulation and function of the CXC chemokine ENA-78 in monocytes and its role in disease. *J Leukoc Biol*. 1997;62(5):604-611. doi:10.1002/jlb.62.5.604

379. Woodfin A, Voisin MB, Nourshargh S. PECAM-1: A multi-functional molecule in inflammation and vascular biology. *Arterioscler Thromb Vasc Biol*. 2007;27(12):2514-2523. doi:10.1161/ATVBAHA.107.151456

380. Nag S, Eskandarian MR, Davis J, Eubanks JH. Differential expression of vascular endothelial growth factor-A (VEGF-A) and VEGF-B after brain injury. *J Neuropathol Exp Neurol*. 2002;61(9):778-788. doi:10.1093/jnen/61.9.778

381. Mushimiyimana I, Tomas Bosch V, Niskanen H, et al. Genomic Landscapes of Noncoding RNAs Regulating VEGFA and VEGFC Expression in Endothelial Cells . *Mol Cell Biol*. 2021;41(7). doi:10.1128/mcb.00594-20

382. Snelgrove RJ, Goulding J, Didierlaurent AM, et al. A critical function for CD200 in lung immune homeostasis and the severity of influenza infection. *Nat Immunol*. 2008;9(9):1074-1083. doi:10.1038/ni.1637

383. Yue X, Guidry JJ. Differential protein expression profiles of bronchoalveolar lavage fluid following lipopolysaccharide-induced direct and indirect lung injury in mice. *Int J Mol Sci*. 2019;20(14). doi:10.3390/ijms20143401

384. Okada M, Fang Yan S, Pinsky DJ. Peroxisome proliferator-activated receptor-γ (PPAR-γ) activation suppresses ischemic induction of Egr-1 and its inflammatory gene targets. *FASEB J*. 2002;16(14):1861-1868. doi:10.1096/fj.02-0503com

385. Cuzzocrea S, Pisano B, Dugo L, et al. Rosiglitazone, a ligand of the peroxisome proliferator-activated receptor-γ, reduces acute inflammation. *Eur J Pharmacol*. 2004;483(1):79-93. doi:10.1016/j.ejphar.2003.10.056

386. Synenki L, Chandel NS, Budinger GRS, et al. Bronchoalveolar lavage fluid from patients with acute lung injury/acute respiratory distress syndrome induces myofibroblast differentiation. *Crit Care Med*. 2007;35(3):842-848. doi:10.1097/01.CCM.0000257254.87984.69

387. Buttignol M, Pires-Neto RC, Rossi e Silva RC, Albino MB, Dolhnikoff M, Mauad T. Airway and parenchyma immune cells in influenza A(H1N1)pdm09 viral and non-viral diffuse alveolar damage. *Respir Res*. 2017;18(1):1-10. doi:10.1186/s12931-017-0630-x

388. Kuiken T, Rimmelzwaan GF, Van Amerongen G, Osterhaus ADME. Pathology of human influenza A (H5N1) virus infection in cynomolgus macaques (Macaca fascicularis). *Vet Pathol*. 2003;40(3):304-310. doi:10.1354/vp.40-3-304

389. Gye YP, Christman JW. Involvement of cyclooxygenase-2 and prostaglandins in the molecular pathogenesis of inflammatory lung diseases. *Am J Physiol - Lung Cell Mol Physiol*. 2006;290(5). doi:10.1152/ajplung.00513.2005

390. Fukunaga K, Kohli P, Bonnans C, Fredenburgh LE, Levy BD. Cyclooxygenase 2 Plays a Pivotal Role in the Resolution of Acute Lung Injury. *J Immunol*. 2005;174(8):5033-5039. doi:10.4049/jimmunol.174.8.5033

391. Zannikou M, Barbayianni I, Fanidis D, et al. MAP3K8 Regulates Cox-2–Mediated Prostaglandin E 2 Production in the Lung and Suppresses Pulmonary Inflammation and Fibrosis . *J Immunol*. 2021;206(3):607-620. doi:10.4049/jimmunol.2000862

392. Shizuma T. Autoimmune Hemolytic Anemia Following Influenza Virus Infection or Administration of Influenza Vaccine. *J Blood Disord Transfus*. 2014;05(03):3-5. doi:10.4172/2155-9864.1000200

393. Uchide N, Ohyama K, Bessho T, Toyoda H. Lactate dehydrogenase leakage as a marker for apoptotic cell degradation induced by influenza virus infection in human fetal membrane cells. *Intervirology*. 2009;52(3):164-173. doi:10.1159/000224644

394. Wu MY, Yao L, Wang Y, et al. Clinical evaluation of potential usefulness of serum lactate dehydrogenase (LDH) in 2019 novel coronavirus (COVID-19) pneumonia. *Respir Res*. 2020;21(1):1-6. doi:10.1186/s12931-020-01427-8

395. Legrand C, Bour JM, Jacob C, et al. Lactate dehydrogenase (LDH) activity of the number of dead cells in the medium of cultured eukaryotic cells as marker. *J Biotechnol*. 1992;25(3):231-243. doi:10.1016/0168-1656(92)90158-6

396. Meyer NJ, Gattinoni L, Calfee CS. Acute respiratory distress syndrome. *Lancet*. 2021;398(10300):622-637. doi:10.1016/S0140-6736(21)00439-6

397. Roch A, Guervilly C, Papazian L. Fluid management in acute lung injury and ards. *Ann Intensive Care*. 2011;1(1):16. doi:10.1186/2110-5820-1-16

398. Kuiken T, Taubenberger JK. Pathology of human influenza revisited. *Vaccine*. 2008;26(SUPPL. 4). doi:10.1016/j.vaccine.2008.07.025

399. Baldus S, Castro L, Eiserich JP, Freeman BA. Is ·NO news bad news in acute respiratory distress syndrome? *Am J Respir Crit Care Med*. 2001;163(2):308-310. doi:10.1164/ajrccm.163.2.ed2000c

400. Agorreta J, Garayoa M, Montuenga LM, Zulueta JJ. Effects of acute hypoxia and lipopolysaccharide on nitric oxide synthase-2 expression in acute lung injury. *Am J Respir Crit Care Med*. 2003;168(3):287-296. doi:10.1164/rccm.200209-1027OC

401. Kristof AS, Goldberg P, Laubach V, Hussain SNA. Role of inducible nitric oxide synthase in endotoxin-induced acute lung injury. *Am J Respir Crit Care Med*. 1998;158(6):1883-1889. doi:10.1164/ajrccm.158.6.9802100

402. Chen HI, Yeh DY, Kao SJ. The detrimental role of inducible nitric oxide synthase in the pulmonary edema caused by hypercalcemia in conscious rats and isolated lungs. *J Biomed Sci*. 2008;15(2):227-238. doi:10.1007/s11373-007-9211-1

403. Syed MA, Choo-Wing R, Homer RJ, Bhandari V. Role of nitric oxide isoforms in vascular and alveolar development and lung injury in vascular endothelial growth factor overexpressing neonatal mice lungs. *PLoS One*. 2016;11(1):1-19. doi:10.1371/journal.pone.0147588

404. Chiang CC, Korinek M, Cheng WJ, Hwang TL. Targeting Neutrophils to Treat Acute Respiratory Distress Syndrome in Coronavirus Disease. *Front Pharmacol*. 2020;11(October). doi:10.3389/fphar.2020.572009

405. Kaniaris E, Vaporidi K, Vergadi E, et al. Genetic and pharmacologic inhibition of Tpl2 kinase is protective in a mouse model of ventilator-induced lung injury. *Intensive Care Med Exp*. 2014;2(1):15. doi:10.1186/2197-425X-2-15

406. Manitsopoulos N, Aidinis V, Perreas K, Orfanos S, Kotanidou A. The effects of tpl2 inhibition in Ventilator-induced lung injury. *Eur Respir J*. 2017;50(suppl 61):PA349. doi:10.1183/1393003.congress-2017.PA349

407. Han T, Lai Y, Jiang Y, Liu X, Li D. Influenza A virus infects pulmonary microvascular endothelial cells leading to microvascular leakage and release of pro-inflammatory cytokines. *PeerJ*. 2021;9:1-20. doi:10.7717/peerj.11892

408. Teijaro JR, Walsh KB, Cahalan S, et al. Endothelial cells are central orchestrators of cytokine amplification during influenza virus infection. *Cell*. 2011;146(6):980-991. doi:10.1016/j.cell.2011.08.015

409. Hingorani AD, Cross J, Kharbanda RK, et al. Acute systemic inflammation impairs endothelium-dependent dilatation in humans. *Circulation*. 2000;102(9):994-999. doi:10.1161/01.CIR.102.9.994

410. Daiber A, Xia N, Steven S, et al. *New Therapeutic Implications of Endothelial Nitric Oxide Synthase (ENOS) Function/Dysfunction in Cardiovascular Disease*. Vol 20.; 2019. doi:10.3390/ijms20010187

411. The Jaxon Laboratory. C.129(Cg)-Siglecftm1.2Avrk/J. https://www.jax.org/strain/025869.

412. Jung S, Unutmaz D, Wong P, et al. In Vivo Depletion of $CD11c^+$ Dendritic Cells Abrogates Priming of $CD8^+$ T Cells by Exogenous Cell-Associated Antigens. *Immunity*. 2002;17(2):211-220. doi:10.1016/S1074-7613(02)00365-5

413. Landsman L, Jung S. Lung Macrophages Serve as Obligatory Intermediate between Blood Monocytes and Alveolar Macrophages. *J Immunol*. 2007;179(6):3488 LP - 3494. doi:10.4049/jimmunol.179.6.3488

414. Hall JP, Kurdi Y, Hsu S, et al. Pharmacologic inhibition of Tpl2 blocks inflammatory responses in primary human monocytes, synoviocytes, and blood. *J Biol Chem*. 2007;282(46):33295-33304. doi:10.1074/jbc.M703694200

415. Cusack K, Allen H, Bischoff A, et al. Identification of a selective thieno[2,3-c]pyridine inhibitor of COT kinase and TNF-α production. *Bioorganic Med Chem Lett*. 2009;19(6):1722-1725. doi:10.1016/j.bmcl.2009.01.088

416. Sciences G. Study to Evaluate the Efficacy and Safety of Tilpisertib in Adults With Moderately to Severely Active Ulcerative Colitis (Falcon). https://clinicaltrials.gov/ct2/show/NCT04130919.

417. Ohara R, Hirota S, Onoue H, Nomura S, Kitamura Y, Toyoshima K. Identification of the cells expressing cot proto-oncogene mRNA. *J Cell Sci*. 1995;108(1):97-103. doi:10.1242/jcs.108.1.97

418. Christoforidou A V, Papadaki HA, Margioris AN, Eliopoulos GD, Tsatsanis C. Expression of the Tpl2/Cot oncogene in human T-cell neoplasias. *Mol Cancer*. 2004;3(1):34. doi:10.1186/1476-4598-3-34

419. Sourvinos G, Tsatsanis C, Spandidos DA. Overexpression of the Tpl-2/Cot oncogene in human breast cancer. *Oncogene*. 1999;18(35):4968-4973. doi:10.1038/sj.onc.1202891

420. Gkirtzimanaki K, Gkouskou KK, Oleksiewicz U, et al. TPL2 kinase is a suppressor of lung carcinogenesis. *Proc Natl Acad Sci U S A*. 2013;110(16). doi:10.1073/pnas.1215938110

421. Lee J, Kotliarova S, Kotliarov Y, et al. Tumor stem cells derived from glioblastomas cultured in bFGF and EGF more closely mirror the phenotype and genotype of primary tumors than do serum-cultured cell lines. *Cancer Cell*. 2006;9(5):391-403. doi:https://doi.org/10.1016/j.ccr.2006.03.030

422. Beer DG, Kardia SLR, Huang C-C, et al. Gene-expression profiles predict survival of patients with lung adenocarcinoma. *Nat Med*. 2002;8(8):816-824. doi:10.1038/nm733

423. Basso K, Margolin AA, Stolovitzky G, Klein U, Dalla-Favera R, Califano A. Reverse engineering of regulatory networks in human B cells. *Nat Genet*. 2005;37(4):382-390. doi:10.1038/ng1532

424. Kannan Y, Li Y, Coomes SM, et al. Tumor progression locus 2 reduces severe allergic airway inflammation by inhibiting Ccl24 production in dendritic cells. *J Allergy Clin Immunol*. 2017;139(2):655-666.e7. doi:10.1016/j.jaci.2016.05.031

425. Watford WT, Wang C-C, Tsatsanis C, et al. Ablation of Tumor Progression Locus 2 Promotes a Type 2 Th Cell Response in Ovalbumin-Immunized Mice. *J Immunol*. 2010;184(1):105-113. doi:10.4049/jimmunol.0803730

426. Ballak DB, Van Essen P, Van Diepen JA, et al. MAP3K8 (TPL2/COT) affects obesity-induced adipose tissue inflammation without systemic effects in humans and in mice. *PLoS One*. 2014;9(2):2-9. doi:10.1371/journal.pone.0089615

427. Ceppo F, Berthou F, Jager J, Dumas K, Cormont M, Tanti JF. Implication of the Tpl2 kinase in inflammatory changes and insulin resistance induced by the interaction between

adipocytes and macrophages. *Endocrinology*. 2014;155(3):951-964. doi:10.1210/en.2013-1815

428. Koliaraki V, Roulis M, Kollias G. Tpl2 regulates intestinal myofibroblast HGF release to suppress colitis-associated tumorigenesis. *J Clin Invest*. 2012;122(11):4231-4242. doi:10.1172/JCI63917

429. Lawrenz M, Visekruna A, Kühl A, Schmidt N, Kaufmann SHE, Steinhoff U. Genetic and pharmacological targeting of TPL-2 kinase ameliorates experimental colitis: a potential target for the treatment of Crohn's disease? *Mucosal Immunol*. 2012;5(2):129-139. doi:10.1038/mi.2011.57

430. Wyatt KD, Sakamoto K, Watford WT. Tamoxifen administration induces histopathologic changes within the lungs of Cre-recombinase-negative mice: A case report. *Lab Anim*. September 2021:00236772211042968. doi:10.1177/00236772211042968

431. van der Vliet A, Eiserich JP, Cross CE. Nitric oxide: a pro-inflammatory mediator in lung disease? *Respir Res*. 2000;1(2):1. doi:10.1186/rr14

432. Persinger RL, Blay WM, Heintz NH, Hemenway DR, Janssen-Heininger YM. Nitrogen dioxide induces death in lung epithelial cells in a density-dependent manner. *Am J Respir Cell Mol Biol*. 2001;24(5):583-590. doi:10.1165/ajrcmb.24.5.4340

433. Sunil VR, Shen J, Patel-Vayas K, Gow AJ, Laskin JD, Laskin DL. Role of reactive nitrogen species generated via inducible nitric oxide synthase in vesicant-induced lung injury, inflammation and altered lung functioning. *Toxicol Appl Pharmacol*. 2012;261(1):22-30. doi:10.1016/j.taap.2012.03.004

434. Zhai Y, Franco LM, Atmar RL, et al. Host Transcriptional Response to Influenza and Other Acute Respiratory Viral Infections – A Prospective Cohort Study. *PLOS Pathog*. 2015;11(6):e1004869.

435. Bakaletz LO. Viral-bacterial co-infections in the respiratory tract. *Curr Opin Microbiol*. 2017;35:30-35. doi:10.1016/j.mib.2016.11.003

436. Jia L, Zhao J, Yang C, et al. Severe Pneumonia Caused by Coinfection With Influenza Virus Followed by Methicillin-Resistant Staphylococcus aureus Induces Higher Mortality

in Mice . *Front Immunol* . 2019;9:3189.

437. Yingyun C, Yin L, Xuming Z. Suppression of Coronavirus Replication by Inhibition of the MEK Signaling Pathway. *J Virol*. 2007;81(2):446-456. doi:10.1128/JVI.01705-06

438. Islam T, Rahman MR, Aydin B, Beklen H, Arga KY, Shahjaman M. Integrative transcriptomics analysis of lung epithelial cells and identification of repurposable drug candidates for COVID-19. *Eur J Pharmacol*. 2020;887:173594. doi:10.1016/j.ejphar.2020.173594

439. Goel S, Saheb Sharif-Askari F, Saheb Sharif Askari N, et al. SARS-CoV-2 Switches ‘on’ MAPK and NFκB Signaling via the Reduction of Nuclear DUSP1 and DUSP5 Expression . *Front Pharmacol* . 2021;12:404.